Ecological impacts of groundwater discharge to Mediterranean coastal lagoons

Aladin Andrisoa

AIX-MARSEILLE UNIVERSITÉ

Ecole Doctorale des Sciences de l'Environnement (ED251)

Centre Européen de Recherche et d'Enseignement des Géosciences de l'Environnement (CEREGE)

Thesis presented for the degree of:

Docteur d'Aix-Marseille Université

Ecological impacts of groundwater discharge to Mediterranean coastal lagoons

Aladin ANDRISOA

Supervisors: Thomas STIEGLITZ and Patrick RAIMBAULT

Date of defense: 26 March 2019

JURY

Luc LAMBS	EcoLab, Université Toulouse III	Rapporteur
Rutger DE WIT	MARBEC Montpellier	Rapporteur
Jaye CABLE	University of North Carolina	Examinateur
Pieter VAN BEEK	LEGOS, Toulouse	Examinateur
Paul TRÉGUER	Université de Bretagne Occidentale	Examinateur
Bruno HAMELIN	CEREGE, Aix-Marseille Université	Examinateur
Franck LARTAUD	Sorbonne Université, LECOB, Banyuls-sur-Mer	Invité
Thomas STIEGLITZ	CEREGE, Aix-en-Provence	Directeur
Patrick RAIMBAULT	Institut Méditerranéen d'Océanologie, Marseille	Co-Directeur

ABSTRACT

Whilst the role of groundwater discharge and porewater fluxes (recirculation) as important pathways for nutrient delivery to coastal systems is increasingly being recognized, there remains limited evidence of its "downstream" ecological implications. This thesis aims at investigating the ecological role that groundwater flows play in some aspects of the functioning and vulnerability of coastal lagoonal ecosystems. Two contrasting lagoons on the French Mediterranean coastline were studied (La Palme and Salses-Leucate lagoons). Firstly, using concurrent water and radon mass balances, a comparison between the main nutrient sources for La Palme lagoon (karstic groundwater, recirculation, diffusion from sediments, inputs from a sewage treatment plant and atmospheric deposition) revealed that the recirculation of lagoon water through the lagoon sediments is the main source of both dissolved inorganic nitrogen (DIN) and phosphorous (DIP) to this lagoon. Secondly, the ecological impact of groundwater discharge and porewater recirculation fluxes was assessed by investigating their role in supporting primary production using nitrogen and carbon isotopes signatures. The nitrogen isotopic signatures in primary producers reflect predominantly the nitrogen isotopic signatures of the terrestrial (karstic) groundwater and porewater source in both La Palme and Salses-Leucate lagoons, demonstrating the important role of these sources in supporting primary production. The carbon isotope signatures indicate groundwater discharge as a significant source also of dissolved inorganic carbon to primary producers. Finally, in a different approach, the influence of terrestrial groundwater discharge on the growth of the Mediterranean mussel *Mytilus galloprovincialis* is documented. Variations in growth rate and condition index (tissue weight / shell weight) of mussels growing in and outside groundwater-influence in Salses-Leucate lagoon were examined. Mussels from the groundwater-influenced sites have higher growth rate and condition index compared to those from the control site, likely as consequence of both the higher winter temperatures and the groundwater-driven nutrient supply that increase the food availability to support mussel growth. Estimated growth rates from the groundwater-influenced sites are amongst the highest rates recorded in the Mediterranean region. The

results of this thesis demonstrate the important role groundwater processes can play in coastal ecosystems.

Keywords: coastal lagoons, groundwater discharge, nutrient cycles, primary production, mussel growth

Extended abstract in French

Etat de l'Art

Les lagunes côtières sont des écosystèmes littoraux hautement productifs et jouent un rôle primordial dans la dynamique biogéochimique des océans (Anthony et al. 2002; Newton et al. 2014). Elles soutiennent et procurent un grand nombre de services écosystémiques comme l'aquaculture, la pêche et le tourisme qui sont d'une grande importance socio-économique. Situées à l'interface des domaines continentaux et océaniques, les lagunes sont très dynamiques et directement soumises aux influences terrestre et marine (Kjerfve 1994), subissant à de multiples pressions anthropiques et naturelles qui les rendent fragiles et vulnérables. Les lagunes côtières sont considérées comme l'un des écosystèmes les plus fortement impactés et particulièrement par le processus d'eutrophisation lié à l'apport excessif de nutriments (Caumette et al. 1996; De Wit 2011). Suite à une augmentation rapide de la population, l'apport en éléments nutritifs ayant pour principale origine les engrais agricoles et les eaux usées domestiques et industrielles a doublé durant les cinq dernières décennies (Caumette et al. 1996).

Au cours des dernières décennies, les eaux souterraines et le eaux porales (recirculation) ont été reconnues en tant que voies d'apports de nutriments vers les écosystèmes côtiers (Burnett et al. 2003; Slomp and Van Cappellen 2004). Les apports de nutriments associés aux eaux souterraines et aux eaux porales peuvent parfois rivaliser avec ceux fournis par les rivières (Dorsett et al. 2011; Tovar-Sánchez et al. 2014). Ces apports en nutriments par les eaux souterraines et les eaux porales peuvent ainsi avoir une conséquence sur la production primaire et le fonctionnement écologique des écosystèmes côtiers (Valiela et al. 1992; Cole et al. 2006). Bien que le rôle écologique des eaux souterraines et eaux porales soit de plus en plus reconnu, les études antérieures reposent sur des mesures indirectes et il y a encore peu d'information sur le réel impact écologique en milieu lagunaire.

Les impacts écologiques des eaux souterraines et des eaux porales dans les écosystèmes côtiers ne se limitent pas seulement sur les producteurs primaires, mais aussi sur les autres organismes qui peuvent réagir aux variations de la salinité, température, lumière et la turbulence (Troccoli-Ghinaglia et al. 2010; Lee

et al. 2017). Des études ont montré que les eaux souterraines augmentent la diversité de la méiofaune sur la plage d'Olhos de Agua au Portugal (Encarnação et al. 2015) et augmentent la richesse spécifique et la biomasse des poissons et d'invertébrés dans les eaux côtières japonaises (Hata et al. 2016; Utsunomiya et al. 2017). Malgré ces études, les effets des eaux souterraines sur les niveaux trophiques supérieurs comme les huîtres et les moules demeurent peu documentés (Miller and Ullman 2004; Utsunomiya et al. 2017).

Objectif

L'objectif de cette thèse est alors d'évaluer les effets écologiques des eaux souterraines et des eaux porales dans les écosystèmes lagunaires. Pour ce faire, cette thèse s'articule autour de trois axes majeurs:

i) Quantification des flux de nutriments associés aux eaux souterraines et eaux porales;
ii) Evaluation du rôle des eaux souterraines et eaux porales dans le soutien production primaire dans les lagunes côtières;
iii) Evaluation de l'influence des eaux souterraines sur la croissance des moules méditerranéennes en milieu lagunaire.

Site d'étude

Cette thèse a été réalisée dans les étangs de La Palme et de Salses-Leucate situés dans le sud-ouest de la France sur la façade méditerranéenne. L'étang de La Palme est relativement petit (superficie 500 ha; profondeur moyenne 0.5 m; volume d'eau $\sim 3\times10^3$ m^3) (Wilke and Boutière 2000) et très connu par sa haute biodiversité et haute valeur écologique. Il est alimenté en eaux douces grâce à plusieurs résurgences karstiques localisées dans la partie nord-ouest avec un débit moyen de 10^4 m^3 j^{-1} (Wilke and Boutière 2000; Stieglitz et al. 2013). Une station d'épuration d'eaux usées déverse des eaux usées traitées dans la partie nord de l'étang avec un débit moyen de 10^2 m^3 j^{-1}. La recirculation d'eau de la lagune est estimée de 3×10^4 à 2×10^5 m^3 j^{-1} selon étude récente (Stieglitz et al. 2013).

L'étang de Salses-Leucate est plus grand (5600 ha) et plus profond (profondeur moyenne: 1.5 m). Il est connecté avec la Mer Méditerranée par trois ouvertures dans la partie Est de l'étang. La principale zone d'étude est la partie ouest qui est alimentée en eau douce par deux résurgences karstiques Font Dame et Font Estramar qui ont des débits de 3.0×10^5 m^3 j^{-1} et 2.0×10^5 m^3 j^{-1} respectivement. Une station d'épuration d'eau déverse aussi d'eau douce sur la partie de sud-ouest de l'étang.

- Quantification des flux de nutriments associés aux eaux souterraines et eaux porales

Cette étude a pour objectif de quantifier les flux des nutriments apportés par les eaux souterraines et la recirculation (eaux porales) dans l'étang de La Palme. L'étude a été effectuée sur le bassin nord de l'étang qui représente 85% de la superficie et 95% du volume d'eau de l'étang, et reçoit tous les apports en eau souterraine de la résurgence karstique. L'approche consiste à utiliser le radon (^{222}Rn) qui est un traceur radioactif naturel à courte période, utilisé globalement pour tracer et quantifier la décharge d'eau souterraine dans les zones côtières (Burnett and Dulaiova 2003; Stieglitz et al. 2010). Des bilans de masse de masse d'eau et de radon ont été effectués pour quantifier les flux des eaux souterraines karstiques et la circulation à travers le sédiment en supposant un état stationnaire, c'est-à-dire un équilibre entre les termes sources et les termes puits. Des campagnes de terrain ont été réalisées en Juin 2016, Novembre 2016, Avril 2017 et Juin 2017 pour effectuer une mesure continue de la distribution spatiale du radon à l'aide des compteurs RAD7 (Durridge) branchés en parallèle et connectés avec une membrane (Dulaiova et al. 2005; Stieglitz 2005). La salinité et la température de l'eau ont été également mesurées en continue avec une sonde WTW multiparamètre. Parralèlement des échantillons ont été collectés pour la détermination des concentrations en radon et en éléments nutritifs (NO_3^-, NH_4^+ et PO_4^{3-}) dans la résurgence, les eaux usées et à trois points de l'étang. Des échantillons d'eau porale ont été aussi prélevés à différentes profondeurs dans les trois stations de la lagune pour les analyses de radon, salinité et nutriments dans les eaux interstitielles.

Nos résultats montrent que la salinité des eaux porales augmente avec la profondeur, reflètant un mélange d'eau de la lagune avec une eau porale profonde hypersalée (salinité jusqu'à 80). Les eaux porales sont enrichies en radon avec des concentrations maximales de 6800 ± 600, 4600 ± 400 et 8000 ± 900 Bq m^{-3} pour les trois stations étudiées alors que les concentrations dans les eaux de surface sont relativement faibles (20-200 Bq m^{-3}). Les concentrations en NH_4^+ et PO_4^{3-} sont également très élevées dans les eaux porales comparées à celles des eaux de surface et augmentent avec la profondeur dans le sédiment. Cependant, les concentrations en NO_3^- dans les eaux porales sont comparables voire inférieures à celles des eaux de surface.

Pour les échantillons de surface, des fortes concentrations en radon (jusqu'à 300 Bq m^{-3} en juin 2016) et de faible salinité (jusqu'à 17 en Avril 2017) sont observées dans la partie nord de l 'étang proche de la source karstique, avec une diminution des concentrations en radon et augmentation de la salinité vers le sud de la lagune. Dans la résurgence, la salinité varie de 5.0 à 9.4 selon la saison, indiquant une interaction entre eaux souterraines douces et eaux de mer dans l'aquifère. Les concentrations en radon dans la source sont relativement constantes tout au long de l'année et considérablement enrichies par rapport aux concentrations de la lagune, avec des valeurs de 2290 ± 90 à 2600 ± 110 Bq m^{-3}. Les concentrations en NO_3^- sont considérablement élevées dans la résurgence (50-62 µmol L^{-1}) et les eaux usées (100-520 µmol L^{-1}) comparées à celles de la lagune (0.1-7.8 µmol L^{-1}), entrainant un important gradient de concentrations corrélé à la valeur de salinité. Les concentrations en NH_4^+ dans la résurgence (0.1-0.5 µmol L^{-1}) et les eaux usées (2.6-16 µmol L^{-1}) sont comparables voire inférieures à celles de la lagune (0.8 – 36 µmol L^{-1}) alors que celles en PO_4^{3-} sont largement plus élevées dans les eaux usées (22-71 µmol L^{-1}) que dans la résurgence (0.1-0.4 µmol L^{-1}) et la lagune (0.1-2.5 µmol L^{-1}). Par conséquent, la résurgence et les eaux usées ne sont pas des sources importantes de ces éléments nutritifs pour la lagune et les fortes concentrations observées dans l'étang suggèrent l'existence d'autres sources qui peuvent être la diffusion et/ou la recirculation.

Le bilan de masse d'eau révèle des flux d'eau souterraine de 3 ± 15 × 10^3 m^3 j^{-1} en Juin 2016 à 25 ± 9 × 10^3 m^3 j^{-1} en Novembre 2016. Ces flux sont comparables avec

des estimations antérieures menées à l'étang de La Palme (Wilke and Boutière 2000; Stieglitz et al. 2013). Le bilan de masse de radon révèle par contre des flux de recirculation de 42 ± 33 × 10^3 à 89 ± 44 × 10^3 m^3 j^{-1}.

En multipliant ces flux d'eau avec les concentrations dans les endmembers (source karstique et eaux interstitielles), les flux de nutriments ont pu être estimés. La recirculation représente une importante source de NH_4^+ (1900-5500 mol j^{-1}) et de PO_4^{3-} (27-71 mol j^{-1}) et la résurgence karstique constitue une importante source de NO_3^- (200-1200 mol j^{-1}), en comparaison avec les autres sources (diffusion, eaux usées et déposition atmosphérique). En somme, la recirculation représente plus de 80% de l'apport total en azote inorganique dissous et plus de 50% de l'apport total en phosphore inorganique dissous dans la lagune de La Palme.

Cette étude permet alors de mettre en exergue le rôle des eaux souterraines et la recirculation comme une importante source de nutriments dans l'étang de La Palme et qu'il est nécessaire d'évaluer les effets écologiques de ces eaux souterraines pour une bonne gestion des écosystèmes lagunaires.

- Rôle des eaux souterraines et des eaux porales dans le soutien de la production primaire

Cette étude a pour objectif d'évaluer le rôle des eaux souterraines karstiques et des eaux porales (recirculation) dans le soutien de la production primaire dans les lagunes de La Palme et de Salses-Leucate. Le transfert de l'azote et du carbone inorganique dissous des eaux souterraines et des eaux porales vers les macrophytes et phytoplancton a été examiné à l'aide de variations d'abondance naturelle des isotopes de l'azote ($\delta^{15}N$) et du carbone ($\delta^{13}C$).

Des campagnes de terrain ont étaient menées sur les deux lagunes en Juin 2016, Novembre 2016 et Juin 2017 et en Avril 2017 (pour l'étang de La Palme uniquement). Des échantillons d'eau de surface ont été collectés dans plusieurs stations des lagunes, les résurgences karstiques et les stations d'épuration d'eaux usées pour quantifier les signatures isotopiques de l'azote inorganique (sous forme de nitrate $\delta^{15}N\text{-}NO_3^-$) et du carbone inorganique ($\delta^{13}C$-DIC). Les signatures isotopiques en azote (NO_3^- + NH_4^+) des eaux porales ont été également mesurées

(δ^{15}N-DIN). En outre, des macrophytes et des matières particulaires (assimilées la population phytoplanctonique) ont été collectés dans les lagunes, les résurgences karstiques et dans les stations d'épuration pour la quantification des isotopes de l'azote (δ^{15}N) et du carbone (δ^{13}C).

Les résultats montrent que les sources étudiées d'azote inorganiques des deux lagunes (résurgences karstiques, eaux porales et les eaux usées) ont des δ^{15}N distinctement différentes, permettant ainsi l'identification de l'origine de l'azote dans différentes zones des étangs. Les sources karstiques ont une valeur moyenne de δ^{15}N-NO_3^- de 3.1 ± 2.1‰ (=n=4) à l'étang de La Palme et 1.0 ± 1.2‰ (n=5) à Salses-Leucate. Les δ^{15}N-DIN (NO_3^- + NH_4^+) des eaux porales sont significativement plus élevées (7.1 ± 3.3‰; n=12) et 6.4 ± 2.1‰ (n=3) dans les lagunes La Palme et Salses-Leucate respectivement. Par ailleurs, les NO_3^- des eaux usées sont beaucoup plus enrichies en δ^{15}N avec des valeurs moyennes de 16.4 ± 4.5‰ (n=3) dans l'étang de La Palme et 17.6 ± 3.7‰ (n=2) dans l'étang de Salses-Leucate. Les δ^{15}N dans les macrophytes et des matières en suspension sont en générale plus proches de celles des résurgences karstiques et des eaux porales, avec quelques exceptions. Ce constat tend à indiquer que l'azote apporté par les eaux usées ne supporterait qu'une faible part de la croissance des organismes végétaux des étangs qui obtiennent la majorité de leur azote inorganique des résurgences karstiques et/ou des eaux porales. Une élévation exceptionnelle des valeurs de δ^{15}N des producteurs primaires a été enregistrée pendant l'été et ceci est attribué à l'augmentation de flux d'eaux usées pendant cette période. A noter qu'à l'étang de La Palme, les signatures isotopiques de l'azote des eaux souterraines et des eaux porales sont relativement proches et c'est difficile de les séparer. Par contre à l'étang de Salses-Leucate, les signatures sont distinctes et les influences des eaux souterraines karstiques se limitent seulement aux endroits proches des résurgences et les eaux porales semblent être la principale source d'azote inorganique pour les producteurs primaires.

Les signatures isotopiques du DIC (δ^{13}C-DIC) dans les étangs de La Palme et Salses-Leucate augmentent généralement avec la salinité et montrent un mélange conservatif entre les eaux souterraines karstiques et l'eau de mer. Ce qui indique que les eaux souterraines et les eaux marines sont des importantes sources de DIC

dans les lagunes. Le flux important de DIC provenant du sédiment ((20-120) × 10^3 mol j^{-1}) nous montre aussi que les eaux porales sont aussi des sources non-négligeables de DIC.

Les macrophytes et les matières en suspension (phytoplankton) se trouvant proche des résurgences karstiques ont des faibles $\delta^{13}C$ alors que ceux qui sont dans la partie marine ont des signatures élevées indiquant que les producteurs primaires se trouvant proches des résurgences karstiques obtiennent la majorité de leur carbone inorganique de ces résurgences tandis que ceux qui se trouvent dans la partie marine dépendent du carbone inorganique qui est en équilibre avec le CO_2 atmosphérique. Avec un important flux de DIC des eaux porales, les eaux porales constituent également une importante source de DIC pour ces producteurs primaires.

Pour conclure, cette étude met en évidence le rôle des eaux souterraines karstiques et des eaux porales dans le soutien de la production primaire dans les lagunes de La Palme et Salses-Leucate. Le traçage de l'azote montre que les résurgences karstiques et les eaux porales sont les principales sources de d'azote inorganique pour les producteurs primaires. Les résurgences karstiques, les eaux porales et l'eau de mer en échange avec l'atmosphère sont les principales sources de carbone inorganique pour les producteurs primaires dans les lagunes de La Palme et Salses-Leucate.

- Rôle des eaux souterraines sur la croissance des moules méditerranéennes

L'objectif de cette étude est d'évaluer l'influence des eaux souterraines sur la croissance des moules méditerranéennes (*Mytilus galloprovincialis)* dans la lagune côtière de Salses-Leucate (France). Le taux de croissance et l'indice de condition (poids des tissus / poids de la coquille) des moules se développant dans les sites influencés par les eaux souterraines et dans un site témoin hors influence des eaux souterraines ont été examinés.

Des individus de *Mytilus galloprovincialis* ont été récoltés à l'état sauvage dans l'étang de Salses-Leucate dans deux stations influencées par les résurgences de

Font Dame et Font Estramar et dans un site témoin hors influence des eaux souterraines. Les moules collectées ont été marquées avec de la calcéine qui est un colorant fluorescent, permettant de situer temporellement une strie de croissance donnée. Les moules marquées ont été placées dans des cages et remises dans leurs habitats originaux. Deux cages ont été utilisées (à 20 et 50 cm du fond) dans les sites influencés par les résurgences et une seule cage dans le site témoin (pas de stratification de la colonne d'eau). Des sondes CTDs ont été installées sur chaque cage pour enregistrer les données horaires de salinité, température et profondeur. Les autres données environnementales ont été récupérées au niveau de la station météorologique Météo-France à Leucate. L'étude a été réalisée sur une période de 20 mois avec une première mise en cage le 10/10/2016 sur les sites influencés par les résurgences et le 17/02/2017 pour le site témoin. Des collectes ont été ainsi organisées le 14/01/2017, le 27/03/2017, le 29/11/2017 et le 29/01/2018.

Le taux de croissance de chaque individu a été calculé à partir de la distance mesurée entre la position du marquage et le bord de la coquille lors du jour de la collecte. Le nombre de stries entre le marquage et la collecte de chaque individu a été également compté pour estimer le nombre d'incréments fabriqués sur une échelle de temps régulière. Les courbes de croissance des moules *Mytilus galloprovincialis* ont été reconstruites en utilisant le modèle de Von Bertalanffy décrit dans Nedoncelle et al. (2013). Les résultats de nos modèles ont été également comparés avec les modèles obtenus pour la même espèce dans la région méditerranéenne.

Les résultats montrent que les moules *Mytilus galloprovincialis* de l'étang de Salses-Leucate ont tendance à suivre un rythme diurne pour la fabrication de leur incrément de croissance. L'effet de marée est insignifiant dans la lagune de Salses-Leucate due une faible influence de la marée en Mer Méditerranée. Ceci s'oppose généralement aux croissances des moules en milieu marin sous influence de la marée, qui suivent un cycle semi-diurne (deux incréments de croissance par jour). La périodicité journalière de la formation d'incrément de croissance des moules dans l'étang de Salses-Leucate est liée l'horloge biologique de l'animal (Schöne 2008; Connor and Gracey 2011). La biologie de beaucoup d'organismes est liée aux

variations des conditions environnementales qui présentent d'une manière générale un cycle journalier, particulièrement pour la température et la lumière.

Les courbes de croissance de Von Bertalanffy démontrent que les taux de croissance des *Mytilus galloprovincialis* dans la lagune de Salses-Leucate comptent parmi les taux les plus élevés enregistrés dans la région méditerranéenne, particulièrement dans les sites influencés par les résurgences. Les moules à Salses-Leucate montrent une forte croissance juvénile et les tailles maximales sont atteintes dans les jeunes âges, ce qui indique que la lagune de Salses-Leucate est favorable pour la croissance de ces moules. Les analyses de croissance révèlent que les moules provenant des sites influencés par les résurgences ont un taux de croissance (41.9 ± 1.9 µm j^{-1}) et un indice de condition élevés (9.1 ± 0.4) comparé à ceux du site témoin hors influence des eaux souterraines (taux de croissance: 27.7 ± 2.0 µm d^{-1}; indice de condition: 5.8 ± 0.4). Ce développement plus efficace est probablement dû aux températures hivernales plus élevées dans les sites influencés par les eaux souterraines (Page and Hubbard 1987; Schöne et al. 2003a). Ce taux de croissance élevé peut être aussi expliqué par la disponibilité en nourriture dans ces sites. Les résurgences sont reconnues comme une importante source de nutriments en milieu lagunaire, favorisant ainsi une grande productivité primaire (Tamborski et al. 2018; Rodellas et al. 2018). Bien que l'apport d'eau douce par les résurgences puisse avoir des effets négatifs sur la croissance des *Mytilus galloprovincialis* (His et al. 1989; Vuorinen et al. 2002), nos résultats montrent une forte croissance dans les sites influencés par ces résurgences. Ce qui suggère que les moules sont peut-être acclimatées à la dessalure ou bien que les effets de la salinité sont négligeable comparés à ceux de la température et de la disponibilité en nourriture.

Une baisse de la production en moule est actuellement observée, due au manque de sites favorables pour la mytiliculture, liée à une forte pression anthropique. Identifier des sites appropriés pour la mytiliculture demeure un grand défi pour les producteurs de moules. Nos résultats montrent que les sites influencés par les résurgences sont des sites potentiels pour l'élevage de moules, en particulier au voisinage des eaux oligotrophes telles que la Mer Méditerranée. Donc outre son

rôle écologique, les eaux souterraines peuvent aussi avoir des effets économiques non négligeable en milieux lagunaires.

Conclusion

Pour conclure, cette thèse montre que les eaux souterraines et la recirculation (eaux porales), sont des importantes sources de nutriments dans les lagunes de La Palme et Salses-Leucate. Nos résultats mettent en évidence que la recirculation d'eau salée de la lagune à travers les sédiments est la principale source d'azote (essentiellement sous forme d'ammonium) et de phosphore inorganiques dissous dans les lagunes côtières. Cet important apport en éléments nutritifs a un effet sur le fonctionnement écologique de ces écosystèmes lagunaires. Dans un premier temps, les variations d'abondance naturelle des isotopes de l'azote et du carbone montrent que les macrophytes et phytoplancton des lagunes de La Palme et Salses-Leucate obtiennent la majorité de leur azote à partir des eaux souterraines karstiques et des eaux porales (recirculation) et la majorité de leur carbone à partir des résurgences karstiques, des eaux porales et l'eau de mer en échange avec l'atmosphère. Dans un deuxième temps, les moules des sites influencés par les eaux souterraines ont un taux de croissance et un indice de condition plus élevés que celles du site témoin hors influence des eaux souterraines. Les taux de croissance estimés pour les sites influencés par les eaux souterraines comptent parmi les taux les plus élevés enregistrés dans la région méditerranéenne. Ces résultats démontrent le rôle important que peuvent jouer les apports d'eaux souterraines dans le fonctionnement des écosystèmes lagunaires côtiers.

Acknowledgements

We used to say that it's not the destination but the journey that truly matters. I enjoy the road but I never took such a long and a bumpy one, so it feels good to finally reach the end of it. This PhD was not only a scientific adventure but a human one as well. I met many people along the way and would never made it without their support and help.

First and foremost, I would like to sincerely thank my supervisors Thomas Stieglitz and Patrick Raimbault for giving me the chance to carry out such an interesting study and for their guidance, help and constructive feedback during my PhD. I would like to especially express my gratitude to Thomas Stieglitz for encouraging my research and allowing me to grow as a research scientist.

I would like to express my gratitude to Valentí Rodellas, for always being there to help, for always sharing his knowledge and for all the good moments during the field campaigns. Your friendly advice made my journey much more enjoyable. I would like to acknowledge Franck Lartaud (LECOB) for the warm welcome in his lab, the training on sclerochronology and the immense scientific support. I would like to thank my PhD thesis committee (Peter Cook, Rutger de Wit, Florence Sylvestre, Dominique Munaron and Vincent Bailly-Comte) for their guidance throughout the progress of this work. Many thanks for Nicole Garcia (MIO) for the help with the nutrient analysis. I would like to thank Marine David, Simon Benjannin, Joe Tamborski, Camille Fleger (Parc Naturel Narbonnaise) and Laurence Fonbonne (Rivage Leucate), Henry Comte and Michel for their support during field campaigns. A big thank to Christophe Monnin for sharing the carbon data from La Palme lagoon. I would also like to thank Ingrid Neuveu for the help with the sclerochronological analysis.

Big thanks for my office mates Chloe Poulin and Wuhib Tamrat for the warm welcome at the office 109. Their kindness, constant good mood and good jokes made these three years great moments. I would like to thank the administrative and technical staff of CEREGE. I would also like to thank everyone that I had close contact with at CEREGE: Ross, Ricardo, Maureen, Julie, Eléonore, Noémie, Patricia, Christian, Manon, Sébastien, Pierre, William, Frida, Emmeline, Hamed, Nicolas,

Franck, Jesus, they made that three years pass like three months. I would also like to thank Céline, Amandine, Nicolas L., Benjamin, Brina, Rachid, Abdallah, Kevin, Agathe, Clémént O., Marie, Jonathan, Daniele, Abel and Claire for their time and friendship. Thanks a lot for Jérome, Clément, Vlad, Yoann and Vincent for the Thursday football.

Funding for this PhD research was provided by the French National Research Agency (ANR) through ANR @RAction chair medLOC (ANR-14-ACHN-0007-01) which is hereby acknowledged.

I would also like to thank my family for supporting me endlessly through my PhD journey. Special gratitude and thanks to my mother, your prayers have sustained me this far. My older Brother Tsiry, you inspired and encouraged me to undertake my PhD, your effective advice and support have always led me towards my goals. To Larissa, thank you for always being there for me and bringing a smile to my face during the ups and downs that come with undertaking a PhD degree. I would also like to thank Colin and Iphigénie for their constant support.

Last but not least, I would like to thank all my friends and family from Madagascar, Marseille, Aix-en-Provence, Paris, Brussels or somewhere else for the tremendous help and support during all these years.

MISAOTRA BETSAKA!

Table of contents

List of figures

List of tables

PREFACE

Coastal lagoons are highly dynamic transitional (brackish) water bodies, which are controlled by physical processes of both marine and terrestrial origin. They are among the most productive ecosystems on Earth, and support a wide range of ecosystem services that are relied upon by coastal communities, including aquaculture, fishery, tourism and others. Their high ecological value is recognized by European legislation through the application of the EU Habitats Directive and Natura 2000 network (Loureiro et al. 2006; De Wit 2011; Brito et al. 2012). Because of their restricted exchange with the ocean and terrestrial influence, there is an important accumulation of compounds (e.g. nutrients) in coastal lagoons, which supports high primary production. Due to their high primary productivity, they provide habitats and serve as nursery areas and feeding grounds for many fish, crustaceans, invertebrates, macrophytes, seagrass and birds (Kennish and Paerl 2010; Pérez-Ruzafa et al. 2011).

Whilst coastal lagoons are ecologically and economically important for coastal communities, their strong terrestrial influence makes these ecosystems vulnerable to anthropogenic and climate change impacts, and they are considered as among the most heavily impacted aquatic ecosystems (Kennish and Paerl 2010). Most of the anthropogenic pressures are related to rapid population growth and intensification of urbanization. Harbor and marine development, recreational and commercial fishing, aquaculture, and agriculture are among the anthropogenic activities threatening coastal lagoons. Well-known consequences of climate change in coastal ecosystems include sea level rise, increase in water temperature, and changes in precipitation intensity and volume (Brochier and Ramieri 2001). Nutrient loading from agricultural activities and sewage effluents are major issues in coastal lagoons and often cause eutrophication (Anthony et al. 2009; Pérez-Ruzafa et al. 2011). While the importance of surface water discharge as source of human-induced pollution to coastal ecosystems has been well documented for decades, the role of groundwater discharge is often overlooked.

Over the past decades, groundwater discharge and porewater fluxes (recirculation), have been recognized as an important source of nutrient to coastal

ecosystems (Burnett et al. 2003; Slomp and Van Cappellen 2004; Kroeger et al. 2007). Inputs of nutrients associated with groundwater discharge and porewater fluxes can sometimes rival those fluxes supplied by rivers (Dorsett et al. 2011; Cyronak et al. 2013; Tovar-Sánchez et al. 2014). A considerable and a growing body of evidence suggests important ecological implications linked to groundwater discharge and porewater fluxes in coastal systems e.g. eutrophication, algal blooms, hypoxia events (e.g. Valiela et al. 1992; Wang et al. 2016). Most of these studies are based on indirect evidence, i.e. by measuring nutrient fluxes to coastal sites and subsequent inference that these nutrients are taken up by primary producers. Indeed, to date, only a comparatively small number of studies have directly addressed the transfer of dissolved nutrients originated from groundwater discharge and porewater fluxes into primary producers (Herrera-Silveira 1998; McClelland and Valiela 1998; Hwang et al. 2005).

The ecological implications of groundwater discharge to coastal ecosystems are not limited to nutrient loading, and thus primary production. In some regions with substantial groundwater loading, organisms may respond to changes in salinity, light penetration into water column, pH and turbulence (Short and Burdick 1996; Troccoli-Ghinaglia et al. 2010; Lee et al. 2017). Groundwater input has been demonstrated to increase meiofauna diversity in Olhos de Agua beach in Portugal (Encarnação et al. 2015) and enhance species richness, abundance and biomass of fishes and invertebrates in Japanese coastal waters, where high groundwater-borne nutrient concentrations have been reported (Hata et al. 2016; Utsunomiya et al. 2017). Despite these very few studies, there is limited information on the effects of groundwater discharge on animals at higher trophic levels such as oyster and mussels, particularly in coastal lagoons (Miller and Ullman 2004; Utsunomiya et al. 2017).

The ANR (French National Research Agency) @RAction chair MedLOC project "Rethinking Land-Ocean Connectivity – an Integrated Approach to Understanding the Effects of Groundwater on Coastal Ecosystems" (project leader T Stieglitz) aimed at closing the gap of fundamental understanding of the role groundwater flows play in the functioning and vulnerability of the French Mediterranean coastal lagoonal ecosystems. While a great amount of works has been and continuous to

be undertaken on many aspects of ecosystem functioning, anthropogenic and climate impacts on these French Mediterranean coastal lagoons, the role groundwater plays in the ecosystem functioning has not been investigated to date. Coastal lagoon ecology is traditionally biological disciplines, while groundwater studies are traditionally geological and hydrological disciplines. Hence, coupling hydrology and ecology crosses well established disciplinary borders, often resulting in studies lacking either the hydrological inputs or the ecological response (Zalewski 2002). Thus, there is a need to link physical and ecological processes in these coastal lagoonal ecosystems.

As part of this ANR project, my PhD research focuses on the ecological impacts of groundwater discharge in two French Mediterranean coastal lagoons (La Palme and Salses-Leucate lagoons). La Palme lagoon is a reference lagoon for the European Framework Directive for Water Quality Protection and Salses-Leucate lagoon is characterized by large groundwater inputs. The main objectives of this thesis were to:

i) Identify groundwater sources and quantification of groundwater-borne nutrients fluxes.
ii) Assess the role of groundwater discharge in supporting primary production in coastal lagoons.
iii) Quantify groundwater effects on the growth of Mediterranean mussels in a coastal lagoon.

To address these objectives, my PhD thesis is structured in 5 chapters:

Chapter 1 is an introduction to coastal lagoons, groundwater processes and the study site. This chapter includes a detailed overview of coastal lagoons, including the definition, classification, and the ecological and biogeochemical characteristics of lagoons. A general description of terrestrial groundwater and porewater fluxes (recirculation), their quantification techniques, and their biogeochemical and ecological implications in coastal lagoons are presented. This chapter includes also a description of French Mediterranean coastal lagoons and the two studied lagoons: La Palme and Salses-Leucate lagoons.

In **Chapter 2,** groundwater-driven nutrient inputs to coastal lagoons are quantified, and the relevance of lagoon water recirculation as a conveyor of dissolved nutrients discussed. Nutrient fluxes driven by terrestrial groundwater discharge are contrasted against those of lagoon water recirculation through sediments, sewage input and other sources, using concurrent water and radon mass balances in La Palme lagoon. The recirculation through sediments is shown to be the main source of dissolved inorganic nitrogen and phosphorus to the lagoon. This study highlights the important role of groundwater processes as a major conveyor of dissolved nutrients to coastal lagoons and their possible ecological implications to lagoonal ecosystems. This chapter is published in:

(1) Valentí Rodellas, Thomas C Stieglitz, Aladin Andrisoa, Peter G Cook, Patrick Raimbault, Joseph J Tamborski, Pieter Van Beek, Olivier Radakovitch (2018). Groundwater-driven nutrient inputs to coastal lagoons: the relevance of lagoon water recirculation as a conveyor of dissolved nutrients. *Science of the Total Environment 642, 764-780.*

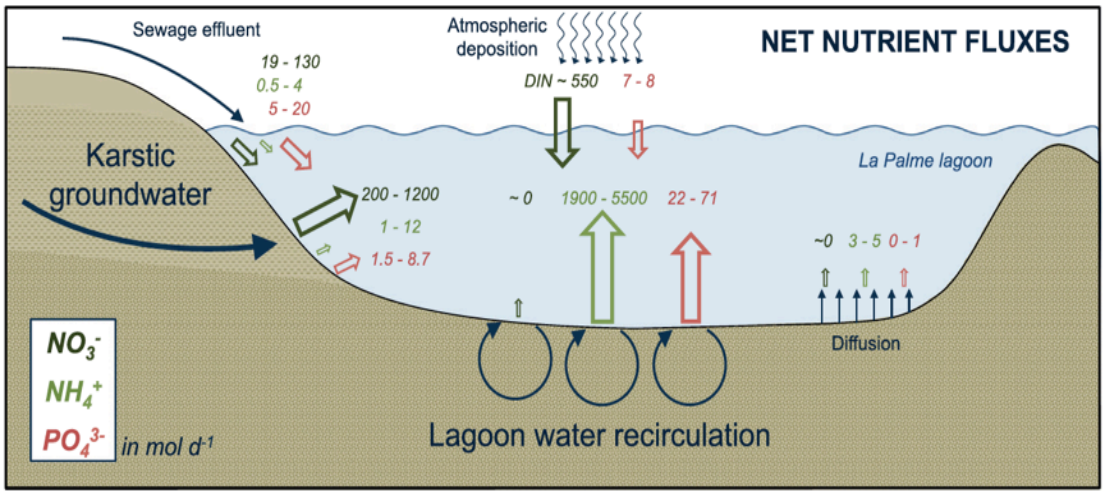

In **Chapter 3,** the uptake of these nutrients delivered by groundwater discharge and porewater fluxes (recirculation) by primary producers is investigated using nitrogen ($\delta^{15}N$) and carbon isotopes signatures ($\delta^{13}C$). We demonstrate a direct impact on lagoon ecological processes by documenting the transfer of groundwater and porewater derived nutrients into primary producers, thereby linking physical (nutrient delivery) and ecological (nutrient uptake) processes in

La Palme and Salses-Leucate lagoons. The $\delta^{15}N$ signatures in primary producers reflect predominantly the $\delta^{15}N$ signatures of the terrestrial (karstic) groundwater and porewater source, indicating the important role of these sources in fuelling primary production. The $\delta^{13}C$ signatures also show the contribution of karstic groundwater discharge and porewater fluxes as a significant source of dissolved inorganic carbon to primary producers. One publication related to this chapter is:

(2) Aladin Andrisoa, Thomas C. Stieglitz, Valentí Rodellas, Patrick Raimbault. Primary production in coastal lagoons supported by groundwater discharge and porewater fluxes inferred from nitrogen and carbon isotope signatures. *Marine Chemistry 210, 48-60*.

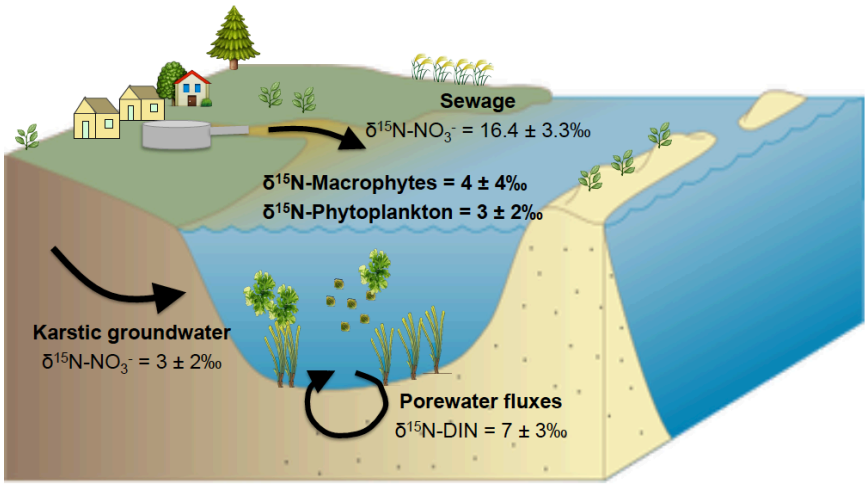

In **Chapter 4,** the influence of fresh (terrestrial) groundwater discharge on the growth of the Mediterranean mussel *Mytilus galloprovincialis* in Salses-Leucate lagoon is investigated. Variations in growth rate and condition index (ratio between the tissue dry weight and shell weight) of mussels growing in and outside groundwater influence are examined, and the role of environmental parameters in mussel growth in this natural environment is investigated. Mussels from the groundwater-influenced sites have higher growth rate and condition index compared to those from the control site, as consequence of both the higher winter temperatures and the groundwater-driven nutrient supply that increase the food availability to support mussel growth. Importantly, growth rates from groundwater-influenced sites are amongst the highest rates recorded in the Mediterranean region. This work forms part of a accepted manuscript:

(3) Aladin Andrisoa, Franck Lartaud, Ingrid Neveu, Valentí Rodellas, Thomas C. Stieglitz. Enhanced growth rates of the Mediterranean mussels in a coastal lagoon driven by groundwater inflow. Accepted in *Frontiers in Marine Science*, Special Issue 'Submarine Groundwater Discharge: Impacts on Coastal Ecosystem by Hidden Water and Dissolved Materials'.

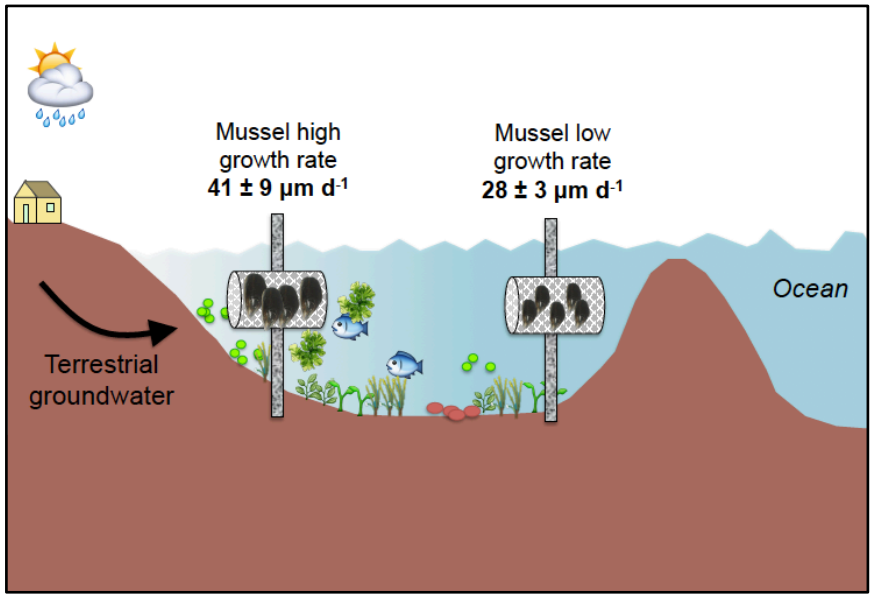

In **Chapter 5**, the conclusions of this PhD thesis are summarized, and some future research perspectives are explored.

Additional publications that this thesis is not directly based on but to which I have contributed as a co-author are:

(4) P G Cook, V Rodellas, A Andrisoa, TC Stieglitz (2018). Exchange across the sediment-water interface quantified from porewater radon profiles. *Journal of Hydrology 559, 873-883*.

(5) Joseph Tamborski, Simon Bejannin, Jordi Garcia-Orellana, Marc Souhaut, Céline Charbonnier, Pierre Anschutz, Mireille Pujo-Pay, Pascal Conan, Olivier Crispi, Christophe Monnin, Thomas Stieglitz, Valentí Rodellas, Aladin Andrisoa, Christelle Claude, Pieter van Beek (2018). A comparison between water recirculation and terrestrially-driven dissolved silica fluxes to the Mediterranean Sea traced using radium isotopes. *Geochimica et Cosmochimica Acta 238, 496-515.*

(6) Valentí Rodellas, Peter G. Cook, Aladin Andrisoa, Samuel Meulé, Thomas C. Stieglitz. Porewater fluxes into a coastal lagoon driven by wind waves and water level oscillations. Submitted in *Journal of Hydrology.*

My contributions to the three papers forming a chapter in this thesis were:

Chapter 2: Contributing to sample collection, sample analysis and the writing of the manuscript.

Chapter 3: Contributing to the design of the study, leading the field investigations in La Palme and Salses-Leucate lagoons and the sample analyses at the Mediterranean Institute of Oceanography (France), and taking the lead in writing the manuscript.

Chapter 4: Contributing to the design of the study, leading the field investigations in Salses-Leucate lagoon and the sample analyses at the Observatoire Oceanologique de Banyuls-sur-Mer (France), co-supervision an M2 student and taking the lead in writing the manuscript.

– Chapter 1 –

Introduction

1.1 Coastal lagoons

1.1.1 General characteristics

Coastal lagoons are shallow coastal water bodies separated from the ocean by a barrier, connected at least intermittently to the ocean by one or more restricted inlets (Kjerfve 1994). They are a particular type of estuary where seawater mixes with freshwater from their catchments (De Wit 2011). Coastal lagoons occupy about 13% of the world coastlines and are present on almost every continent (Fig. 1.1). They are most extensive along the African coast (17.9%) and the coasts of North America (17.6%), and less along the coasts of Asia (13.3%), South America (12.2%), Australia (11.4%), and Europe (5.3%) (Kennish and Paerl 2010). The most extensive stretch of coastal lagoons is along the Atlantic and Gulf coasts of the United States, covering 2800 km of shorelines (Miththapala 2013). Coastal lagoons can have different sizes ranging from 2 to 900.000 ha such as the Lagoa dos Patos in Brazil (Kennish and Paerl 2010). They differ significantly in hydrological and morphology characteristics.

Mediterranean coastal lagoons are relatively young ecosystems mostly formed during the Holocene (5000 - 1000 years ago) as a result of sea level rise (Cataudella et al. 2015). The Mediterranean region hosts around 400 coastal lagoons, covering a surface of about 641.000 ha (Kennish and Paerl 2010). For instance, in Italy alone, there are at least 194 coastal lagoons covering 168.000 ha. In France, there are 35 coastal lagoons, which cover a total surface area of 52.164 ha (Pérez-Ruzafa et al. 2011; IFREMER 2014). Mediterranean coastal lagoons greatly vary in size, ranging from 2 ha (e.g. the Chalikiopoulou lagoon, Greece) to 78 000 ha (Manzala lake, Egypt) (Cataudella et al. 2015). Like in many coastal areas, land use and land reclamation for agriculture, industry, and urban development have greatly contributed to the contraction of the overall coastal lagoon surface in Mediterranean region.

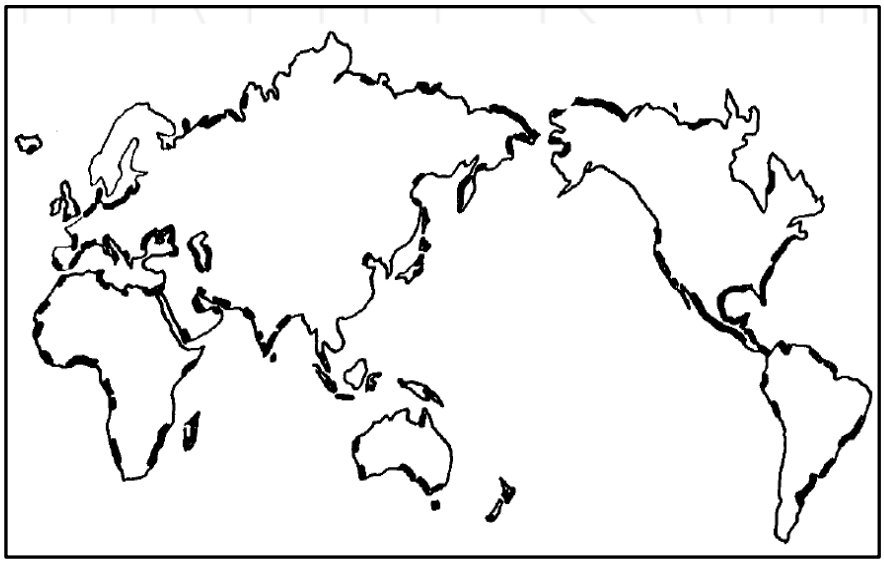

Figure 1.1| World distribution of coastal lagoons (De Wit 2011). Black areas represent coastal lagoons.

1.1.2 Classification

Coastal lagoons can be classified according to different parameters. A common classification is based on their salinity. Lagoons with salinities below 5 are oligohalines, mesohaline lagoons have salinity between 5 and 18, polyhaline lagoons have salinity ranging from 18 to 30 and lagoons with salinity above 30 are mixoeuhaline (De Wit 2011). However, several coastal lagoons exhibit considerable variations of salinity during the year, which may prevent their classification in one of these salinity-dependent categories.

Coastal lagoons can also be classified according their geomorphology and the water exchange with the coastal ocean (Fig. 1.2) (Kjerfve 1994; Kennish and Paerl 2010; Duck and da Silva 2012):

i) Choked lagoons

Choked lagoons usually have narrow channel connected to the ocean and are often located along coasts with high wave energy and important littoral drift (Niencheski et al. 2007; Bruno and Acha 2015). Although the lagoons may experience tidal fluctuations, the narrow channel inhibits the tide from entering the lagoon and prevents the variations of water level. Tidal fluctuations in choked lagoons are often reduced to 5% compared to adjacent coastal tide (Kjerfve 1994). Due to

limited exchange with the open ocean and high evaporation, choked lagoons in arid or semi-arid areas are often permanently or temporary hypersaline.

ii) Restricted lagoons

Restricted lagoons are connected to the ocean by multiple channels, which temporarily restrict the exchange between lagoon and ocean (e.g. Lakhdar et al. 2006). However, they usually have efficient water exchange and are generally influenced by tidal variations. Restricted coastal lagoons are often affected by winds and thus vertically well mixed. Salinity is highly variable ranging from brackish to saline water. The water residence time is usually shorter than in choked lagoons.

iii) Leaky lagoons

Leaky lagoons have wide channels to the open ocean, allowing water exchange between lagoon and the sea (Kjerfve 1994; Duck and da Silva 2012). They are often strongly influenced by tides and have salinity close to that of the adjacent sea.

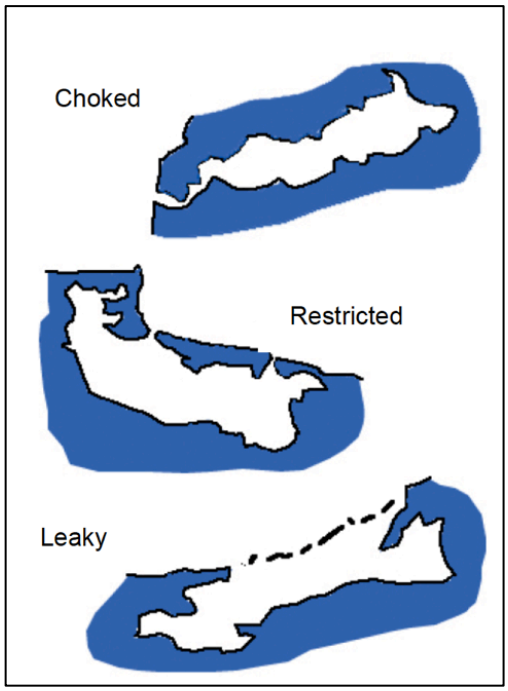

Figure 1.2| Geomorphic types of coastal lagoons (chocked, restricted and leaky) based on water exchange with the coastal ocean (Kjerfve 1994; Duck and Silva 2012). In this thesis, a choked (La Palme) and a restricted (Salses-Leucate) lagoons were studied.

1.1.3 Ecological characteristics

Coastal lagoons are among the most productive ecosystems on Earth, and support a wide range of ecosystem services that are valued by coastal communities (Danovaro and Pusceddu 2007; Anthony et al. 2009). Their high ecological value is recognized by European legislation through the application of the EU Habitats Directive and Natura 2000 network (Loureiro et al. 2006; Brito et al. 2012). Because of their restricted exchange with the ocean and terrestrial influence, there is an important accumulation of compounds (e.g. nutrients) in coastal lagoons, which supports high biological productivity. Many coastal lagoons fall within the range of eutrophic conditions (300 to 500 g C m^{-2} $year^{-1}$) (Nixon 1995; Caumette et al. 1996), and few are oligotrophic (< 100 g C m^{-2} $year^{-1}$). Nutrient availability is a limiting factor for primary producers in the ocean but it is often available is coastal lagoons (Fig. 1.3). This nutrient availability supports high primary production in coastal lagoons and thereby support the entire food web (Nixon 1995). However, excessive inputs of nutrients may result in eutrophication, which is characterized generally by phytoplankton bloom, hypoxia, reduced light availability, subsequent reduced seagrass beds, and fish kills (Valiela and Costa 1988; Nixon 1995; Caumette et al. 1996). In highly eutrophic ecosystems, phytoplankton can be in very high abundance and dominate the entire primary production (Nixon 1995).

Due to their high primary productivity, coastal lagoons support abundant communities of animal and play a significant role in coastal ecosystems by providing habitats and serving as nursery areas and feeding grounds for large number of species (Kennish and Paerl 2010; Pérez-Ruzafa et al. 2011). They provide essential habitat for many fish, crustaceans, small invertebrates, macrophytes, seagrass and birds. In the Mediterranean coastal lagoons host more than 620 species of macrophytes and 200 species of fish (Pérez-Ruzafa et al. 2011). Seagrass species in coastal lagoons provide not only physical habitat for many animal species but also play important role in biogeochemical processes contributing to lagoon water quality. For oligotrophic lagoons, *Zostera* and *Ruppia* are the dominant macrophytes in coastal lagoons. In contrast, opportunistic species such *Ulva*, *Gracillaria* and *Cladophora* dominate for eutrophic lagoons (Viaroli et al. 2008). Due to the high productivity in coastal lagoons, numerous

species are generally permanent resident and dominate the biotic communities (Barnes 1980). Many fish and invertebrate species also evolve for at least a part of their life cycle in coastal lagoons, generally spawning in the open ocean where salinity is more constant and migrating as juveniles in the lagoon (De Wit 2011). Coastal lagoons are thus considered as nursery and feeding grounds for many species and thus support high biodiversity. For instance, the relatively small Thau lagoon in South of France (75 km^2) is home to 100 mollusc species of the 500 found in the Mediterranean Sea (De Wit 2011).

Coastal lagoons provide goods and services for coastal communities by supporting important fisheries, aquaculture, tourist and recreational services. Fisheries represent likely the most extensive exploitation of biological resources in coastal lagoons yielding in average 100 kg $year^{-1}$ of fishes (Macintosh 1994; Pérez-Ruzafa et al. 2011). The total catch in Mediterranean coastal lagoons exceed 49,000 tons $year^{-1}$ of fishes, averaging 90 (±14) kg ha^{-1} $year^{-1}$ (Pérez-Ruzafa et al. 2011). Aquaculture from coastal lagoons produces nearly 5.7% of the world aquaculture production. In 2008, the global aquaculture production reached 67,000 tons (500,000 US $) and 133,000 tons (719,000 US $) for sea bass (*Dicentrarchus labrax*) and sea bream (*Sparus auratus*), respectively (Pérez-Ruzafa et al. 2011). In the Mediterranean region, the growth and survival of important Mediterranean seafood such as mullets, seabream and seabass in coastal lagoons are significantly higher than in other coastal waters chiefly due to higher nutrient concentrations and primary productivity in coastal lagoons (Chauvet 1988). The farming of suitable species of fish (e.g. tilapia, milksfish, and sea perch), shellfish (e.g. shrimps, oysters, and mussels), and macrophytes (e.g. Cymodocea, Gracilaria, and Laminaria) have increased natural fishery yields in coastal lagoons (Macintosh 1994).

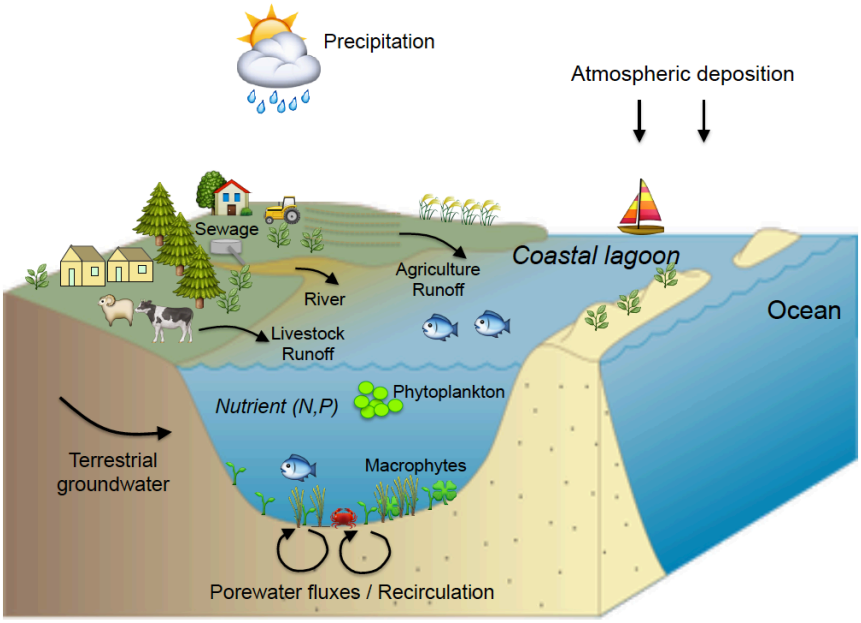

Figure 1.3| Coastal lagoon with associated ecological characters and potential environmental impacts (Adapted from SUPAGRO 2016).

1.1.4 Threats to coastal lagoons

1.1.4.1 Human impacts

Whilst coastal lagoons are ecologically and economically important for coastal communities, their strong terrestrial influence makes these ecosystems vulnerable to anthropogenic impact, and terrestrial and freshwater inputs, and considered as among the most heavily impacted aquatic ecosystems (Fig. 1.3) (Kennish and Paerl 2010). Most of the anthropogenic pressures are related to rapid population growth and intensification of urbanization. For instance in the Mediterranean region, the coastal population is about one third of the total population of the bordering countries and could reach 220 million by the year 2025 (Brochier and Ramieri 2001). Coastal watershed development often result in water quality problems, contamination, and habitat alteration (Pérez-Ruzafa et al. 2011). Harbor and marine development, recreational and commercial fishing, aquaculture, and agriculture are among the anthropogenic activities threatening coastal lagoons. Nutrient loading from agricultural activities and sewage effluents are major issues in coastal lagoons and often cause eutrophication (Fig. 1.3) (Caumette et al. 1996; De Wit 2011). Eutrophication of coastal surface waters may lead to phytoplankton

bloom, hypoxia, loss of seagrass beds and change of community structure, loss of biodiversity, and therefore severe economic impacts (Valiela et al. 1992; Castel et al. 1996; Anthony et al. 2009). While the importance of surface water discharge as source of human-induced pollution to coastal ecosystems has been well documented for decades, the role of groundwater discharge is often overlooked.

Because of their importance for coastal communities and their vulnerability, there is an increasing need to protect and manage coastal lagoons. Best management strategies are often implemented as part of integrated coastal zone management strategies to reduce anthropogenic impacts threatening the conservation and sustainability of coastal lagoon habitat (Kennish and Paerl 2010).

1.1.4.2 Climate change impacts

Well-known consequences of climate change include sea level rise, increase in water temperature, and changes in precipitation intensity and volume.

Sea level rise is one of the most important effects of climate change in the coastal zone, particularly in semi-enclosed basin such as the Mediterranean Sea (Brochier and Ramieri 2001). Satellite observations since 1993 showed that sea level increases at a rate of approximately 3 mm $year^{-1}$, which is significantly higher than the rate reported during the previous half-century (1.7 ± 0.3 mm $year^{-1}$; Church and White 2006). Low-lying and shallow-gradient coastal lagoons are more vulnerable to sea level rise as it narrows the barrier islands and may result in complete disappearance of lagoon, as the lagoon may be converted to an open bay. Sea level rise increases also exchange between lagoon and the open sea and thus increase lagoon water salinity, which may alter species composition in the lagoon (Anthony et al. 2009).

Water temperature increase is also a well-recognized consequence of climate change. The temperature of the world's ocean has increased by 0.3°C and will likely continue to increase for the next century (Anthony et al. 2009). Changes in air temperature significantly influence the water temperature of slow-moving, shallow water bodies such as coastal lagoons (Anthony et al. 2009; Dailidienė et al. 2011). Water temperature has great influence on dissolved oxygen concentrations

and the physiology of living organisms in coastal lagoons. Increasing water temperature tend to reduce the dissolved oxygen concentrations (Bopp et al. 2002), which may affect considerably aerobic species and may even cause hypoxia. Chronic hypoxia in coastal waters is often associated with long-term change in benthic community structure dominated by hypoxia-tolerant species and thus decreases the lagoonal biodiversity (Conley et al. 2007). Furthermore, small change in water temperature may have large impacts on the distribution pattern and migration of lagoonal species (Tomanek and Somero 1999) as increase in water temperature may increase the colonization of allochthonus species that are adapted to the new climatic conditions (Stachowicz et al. 2002).

It is widely recognized that climate change has significant impact on precipitation intensity, timing and volume (Dore 2005; Tabari and Willems 2018). Enhanced precipitation events increase freshwater input to coastal lagoons and thus decrease the salinity. Decreased salinity may have significant negative impacts on marine species living in coastal lagoons and increase the colonization of euryhaline or freshwater species (Kennish and Paerl 2010). Another effect of increased precipitation includes increased surface runoff, which increases the delivery of sediment and nutrients to coastal lagoons (Orpin et al. 1999). Conversely, lower precipitation reduces freshwater inputs and potentially cause hypersaline environment (Anthony et al. 2009). In coastal lagoons with low precipitation, terrestrial groundwater discharges can play an important role in maintaining the brackish conditions and thus preventing hypersalinity of a lagoon during the dry season in a seasonal environment (Stieglitz et al. 2013).

1.2 Groundwater processes

While the ecosystem functioning and the impacts of human activities and climate on coastal lagoons have been well studied, the role of groundwater process has only been recently recognized. Indeed, recent investigations demonstrated that groundwater discharge and porewater fluxes (recirculation), are important sources of nutrients to coastal lagoons (Tait et al. 2014; Malta et al. 2017; Rodellas et al. 2018).

1.2.1 Terrestrial groundwater and porewater fluxes (recirculation)

Terrestrial groundwater is defined as low salinity groundwater originated from inland recharge driven by terrestrial hydraulic gradient and includes point source discharge from springs, and diffuse seepage from coastal aquifers (Taniguchi et al. 2002; Burnett et al. 2003) (Fig. 1.3). Distinctly different from groundwater inflow, porewater fluxes or recirculation refer to both short- and long-scale recirculation of saline lagoon water through sediments, which are driven by pressure gradients forced by tides, waves, bottom currents, benthic organisms and porewater density changes (Burnett et al. 2003; Santos et al. 2012a; Huettel et al. 2014) (Fig. 1.3). A part of the marine community uses the term SGD (submarine groundwater discharge) to include both processes and describes SGD as "flow of water through continental margins from seabed to the coastal ocean, with scale lengths of meters to kilometres, regardless of fluid composition or driving forces" (Moore 2010).

1.2.2 Quantification techniques

Quantifying groundwater discharge and porewater fluxes is a challenging task due to the inherent complexity of the discharge process (Burnett et al. 2006). Groundwater inputs are temporally and spatially variable and occur below the sea surface, where direct measurement and observation are complicated. Quantification of groundwater and porewater fluxes depends on the hydrogeological conditions, climate variability and human management of coastal ecosystem (McCoy and Corbett 2009). Groundwater discharge and porewater fluxes (recirculation) can be detected and quantified by a numbers of method

including chiefly (1) direct measurements, (2) piezometers, (3) tracer techniques, (4) water balances, (5) thermal imaging, (6) electromagnetic techniques and (7) eddy correlation approach. Whatever the quantification method, groundwater-derived solute flux to coastal systems is most often determined by multiplying the concentration of that solute in the coastal aquifer by the calculated groundwater flux.

- Seepage meters are the most common method of direct measurement as they are relatively simple and inexpensive. They are recognized for providing accurate estimations on small spatial scales (ca. 1 m^2) (Corbett and Cable 2003; Burnett et al. 2006). The main disadvantage of the seepage meter method is that it is labour intensive and time consuming (Corbett and Cable 2003). Therefore, automated seepage meters were developed based on heat pulse (Taniguchi and Fukuo 1993), acoustic Doppler technologies (Paulsen et al. 2001) and dye dilution technologies (Sholkovitz et al. 2003).

- The use of piezometers (often multi-level piezometer nests) is another method for quantifying groundwater discharge and porewater fluxes in coastal systems. With this technique, groundwater potential in the sediments can be measured at multiple depths (Povinec et al. 2008). The method is based on the measurements of the hydraulic conductivity and gradient of porewater combined with the Darcy Law. The drawback of the method is the natural variability in the seepage fluxes because of the heterogeneity in the local geology (Burnett et al. 2006). Hydraulic conductivity varies within the aquifer and it is thus difficult to obtain representative value.

- Natural tracer approaches are widely applied to estimate groundwater inputs in costal systems. The main advantage of the method is that natural tracers present an integrated signal when entering the system via different pathways in the aquifer, allowing smoothing out small-scale spatial and temporal variability. However, natural tracers require that all other sources (e.g. river discharge, sediment inputs, precipitation, in situ production) and sinks (e.g. export offshore, in situ consumption, radioactive decay, atmospheric evasion) are evaluated, which is often a difficult task. Among different tracers, naturally

occurring radionuclides (radium isotopes and radon) have been extensively used in groundwater studies (Charette et al. 2001; Beck et al. 2007; Burnett et al. 2008; Rodellas et al. 2012; Stieglitz et al. 2013). Radium isotopes (^{223}Ra, ^{224}Ra, ^{226}Ra and ^{228}Ra) and radon (^{222}Rn) are highly enriched in groundwater relative to surface waters (typically 1-2 orders of magnitude), (quasi) conservative, and easy to measure, making them suitable tracers for estimating groundwater discharge and porewater fluxes in coastal systems.

- The water balance approach has been useful in some situations as an estimate of groundwater discharge (Sekulic 1996; Stieglitz et al. 2013; Prakash et al. 2018). The method is based on the quantification of the inputs (e.g. precipitation) and the outputs (e.g. evapotranspiration, surface runoff, and groundwater discharge) of freshwater into a system (Burnett et al. 2006). By constraining all other terms, groundwater discharge can be estimated. The method is relatively simple but it has some limitations. The input and output terms need to be precisely determined for an accurate estimation of the groundwater discharge. Fresh groundwater estimation is often imprecise due to large uncertainties associated with the values used in the calculation.

- Thermal imaging has been used to detect the location and spatial variability of groundwater discharge (Johnson et al. 2008; Bejannin et al. 2017). The method allows detecting cold or warm groundwater inputs in coastal areas due to the thermal contrast between groundwater and the surrounding waters. Whilst discrete temperature measurements are feasible, airborne thermal infrared (TIR) remote sensing is frequently used because it allows covering larger areas. TIR technique is often effective because of its combined used with in-situ measurements, including salinity and geochemical tracers (Wilson and Rocha 2012; Kelly et al. 2013; Tamborski et al. 2015).

- The electromagnetic technique is based on the measurement of the electrical resistivity of the sediments, which is a function of porosity and fluid conductivity (Moore 2010). The technique is based on stationary or streaming electrodes attached to an electric generator to allow rapid data acquisition

across relatively long distances from beach or coastal waters (Stieglitz et al. 2008).

- The eddy correlation approach is based on measuring continuously and simultaneously the fluctuation vertical velocity above the sediment-water interface using acoustic Doppler velocimeters (ADCP) and the variations on salinity or temperature. If the groundwater salinity or temperature differs from that of the water column, the groundwater flow can thus be estimated from heat or salt balance (Crusius et al. 2008).

1.2.3 Groundwater- and recirculation-driven nutrient in coastal ecosystems

Nutrient such as nitrogen, phosphorus, silica and carbon are elements essential for primary production in coastal ecosystems. During the past decade, terrestrial groundwater and porewater fluxes (recirculation) are recognized as an important conveyor of these elements to coastal ecosystems (Santos et al. 2012b; Maher et al. 2013; Rodellas et al. 2014b; Tovar-Sánchez et al. 2014; Tamborski et al. 2018).

1.2.3.1 Nitrogen sources and biogeochemistry

Nitrogen is the most important element in coastal systems such as lagoons as it is often a limiting factor for primary producers' growth and thus evaluating its input and biogeochemical cycling is particularly important (Castel et al. 1996; Caumette et al. 1996). Groundwater typically has higher dissolved nitrogen concentrations than surface water, making it an important contributor to the biogeochemical budgets in coastal ecosystems (Table 1.1) (Johannes 1980; Null et al. 2012). For instance, groundwater discharge delivers over 85% of the nitrogen into Buttermilk Bay, Massachusetts USA (Valiela and Costa 1988). In the Mediterranean Sea, which is an oligotrophic basin characterized by limited surface water inputs, numerous studies have demonstrated that the flux of dissolved inorganic nitrogen via groundwater inputs is equal or greater than that from other sources (Garcia-Solsona et al. 2010a; Weinstein et al. 2011; Tovar-Sánchez et al. 2014; Rodellas et al. 2015).

Table 1.1| Dissolved nitrogen (NO_3^- + NH_4^+) concentrations in groundwater and surface seawater in coastal systems.

Sites		DIN (μM)	References
Yeoja Bay, South Korea	Groundwater	31 - 250	Hwang et al. 2005
	Surface	0 - 5	
Dor Bay, Mediterranean Sea	Groundwater	150 - 325	Weinstein et al. 2011
	Surface	0 - 5	
Buttermilk Bay, USA	Groundwater	24 - 145	Valiela and Coasta 1988
	Surface	0 - 6	

Such large nitrogen input driven by groundwater processes may have biogeochemical impacts on coastal ecosystems. Nitrogen originated from terrestrial groundwater and porewater fluxes are generally subject to active biogeochemical processes in coastal sediments (Slomp and Van Cappellen 2004). Once delivered into a coastal lagoon, the cycle of nitrogen cycle in coastal lagoons includes many processes that are mostly mediated by bacteria, which are summaries in Fig. 1.4 and briefly here.

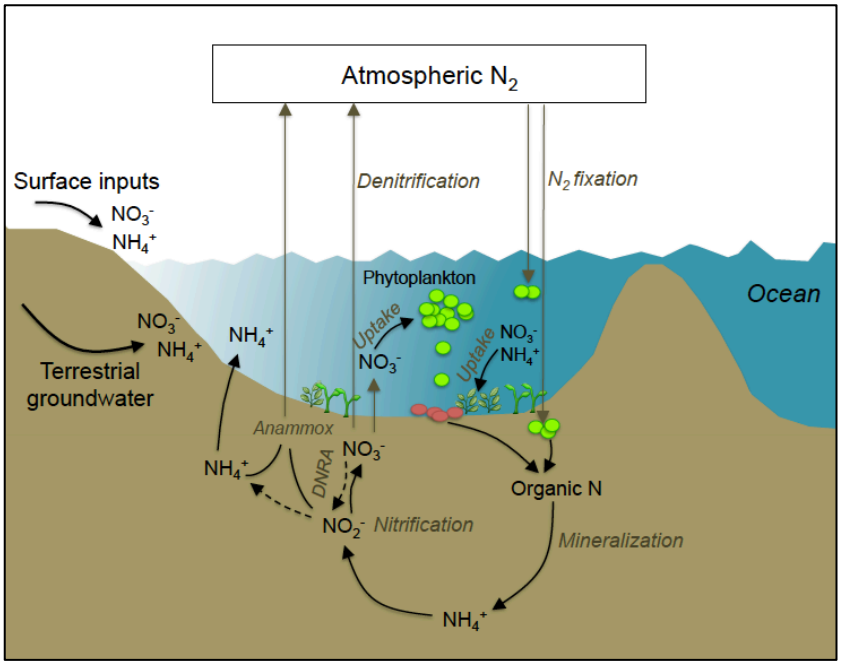

Figure 1.4| Diagram summarizing the major N cycle pathways in coastal lagoons

- **Uptake** of dissolved inorganic nitrogen (NO_3^- and NH_4^+) by the primary producers (phytoplankton and macrophytes) from the water column or porewaters is an important process of the nitrogen cycle in coastal lagoons (Capone 2008). In aquatic ecosystems, the main pathway of nitrogen uptake is through the leaves (Madsen and Cedergreen 2002; De Brabandere et al. 2007), accounting for about the 80% of the total nitrogen acquisition (Lee and Dunton 1999). Uptake through roots is often negligible (De Brabandere et al. 2007). NH_4^+ is preferentially taken up by primary producers over NO_3^- due to reduced energetic costs for its uptake (Middelburg and Nieuwenhuize 2000; Cohen and Fong 2005). Assimilation of NO_3^- is more energetically demanding, because it requires the synthesis of NO_3^- and NO_2^- reductases and associative active transport systems (Syrett 1981).

- **Nitrogen fixation** is the biological reduction of N_2 to reactive nitrogen by diverse arrays of Eubacteria and Archaea called diazotrophs that have the enzyme nitrogenase (Purvaja et al. 2008). It is a crucial process in oligotrophic ecosystems because it can provide potential N in usable form to primary producers. N_2 fixation can contribute to more than 50% of the nitrogen required for seagrass growth in tropical zones (Capone 1988) and between 5 and 30% in temperate areas (McGlathery et al. 1998; Welsh 2000). Lower N_2 fixation rates were reported in coastal lagoons with high denitrification rates because of the competition between diazotrophs and denitrifiers (Hernández-López et al. 2017).

- The **mineralization** of organic nitrogen (also called ammonification) converts organic nitrogen to ammonium (Herbert 1999). The process is the result of the breakdown of organic matter such as dead macrophytes and animals or waste materials like excrement, and is carried out by bacteria. The rate of mineralization varies with soil temperature, moisture and the oxygen concentration in the sediments.

- **Nitrification** is the biological oxidation of ammonium to NO_3^- via nitrite (NO_2^-). Nitrification is a two-stage process with the oxidation of NH_4^+ to NO_2^- mediated by ammonia oxidizing bacteria and preceding NO_2^- conversion to NO_3^- by nitrite

oxidizers. Nitrification can occur in water column as well as in oxygenated sediment layers (Voss et al. 2011). Nitrification rates in macrophytes colonized sediment were 20-fold higher than in uncolonized sediment (Kemp et al. 1982). In addition, borrowing activity increases nitrification rate due to higher ammonium concentrations in the deeper sediment layers (Herbert 1999). Nitrate generated by the oxygenated sediment layers can either diffuse into the overlying water column as a source of regenerated nitrogen or enter the anoxic sediment where it can be denitrified or reduced to NH_4^+ via dissimilatory nitrate reduction to ammonium (DNRA).

- Under anaerobic condition, nitrate in anoxic sediment and water column layers is reduced to N_2 during bacterial **denitrification**. Nitrate derived from terrestrial groundwater and porewater fluxes can thus be denitrified in anoxic conditions. Denitrification is the major process that permanently removes reactive nitrogen from coastal ecosystems (Koike and Hattori 1978; Deutsch et al. 2010; Voss et al. 2011). It is also a key process in the sediment nitrogen cycle because it reduces the available nitrogen for primary producers and thus helps to control the rate of eutrophication. Like for nitrification, denitrification rate is higher in macrophytes colonized sediment than in uncolonized sediment since macrophytes increase the organic content of the sediment by trapping detritus and/or excrete organic carbon from the roots (Christensen and Sørensen 1986, 1988).

- In addition to denitrification, **dissimilatory nitrate reduction to ammonium** (DNRA) is a further important process of nitrate reduction in coastal ecosystems (An and Gardner 2002). DNRA is a two-step process with the first step consisting of reducing NO_3^- to NO_2^- and the second step converts the NO_2^- to NH_4^+. Whilst the final product of denitrification (N_2 gas) is lost from the systems, the nitrogen produced from DNRA is conserved in a form that is available to organisms (Koike and Hattori 1978; Omnes et al. 1996). Previous studies showed that DNRA rates may be as high as denitrification in coastal sediments (Koike and Hattori 1978; An and Gardner 2002) and water column (Lam et al. 2009). Terrestrial groundwater-derived NO_3^- may convert to NH_4^+ via DNRA when passing through anoxic sediments.

- Finally, **anammox** is the anaerobic oxidation of ammonium that utilizes the pools of NH_4^+ and NO_2^- to form N_2 via the intermediates nitric oxide (NO) and hydrazine. Anammox is responsible for the production of more than 50% of the oceanic N_2 and plays a significant role in nitrogen cycles (Hong et al. 2009).

1.2.3.2 Phosphorus

Like nitrogen, phosphorus can be a limiting factor for primary producer growth in coastal ecosystems (Sundareshwar et al. 2003; Trommer et al. 2013). Groundwater inputs can be an important source of dissolved phosphorus to coastal systems (Null et al. 2012; Rodellas et al. 2014b). Phosphorus concentrations in groundwater are highly variable and depend on the inputs and the aquifer type and permeability. Anthropogenic activities are the main source of phosphorus in groundwater mainly commercial fertilizer, manure and wastewater (Slomp and Van Cappellen 2004). Groundwater has often higher dissolved phosphorus concentrations than surface water and thus an important conveyor of dissolved phosphorus in coastal ecosystems (Null et al. 2012). The phosphorus flux from groundwater input is often greater than that from other sources (e.g. Rodellas et al. 2018). Phosphorus in groundwater is mainly in form of inorganic dissolved PO_4^{3-}. Under oxic conditions, dissolved PO_4^{3-} is rapidly removed from groundwater through sorption to Fe-oxides or co-precipitation with metal into mineral phases (Slomp and Van Cappellen 2004).

Phosphorus in coastal ecosystems, mainly in form of phosphate, originates mainly from rock weathering, fertilizers and sewages, which are delivered by groundwater inputs and surface runoffs (Fig. 1.5). In the water column, dissolved phosphorus is taken up by phytoplankton and macrophytes to support their growth, whereas particulate phosphorus can sink to the bottom and accumulate as sediments. In lagoon water, low phosphate concentrations are often related to adsorption by particulate matter and the sediments (Caumette et al. 1996). In sediments, organic phosphorus is mineralized to produce phosphate, which is immediately available for primary producers by direct root uptake or porewater fluxes to the lagoon water (Fig. 1.5).

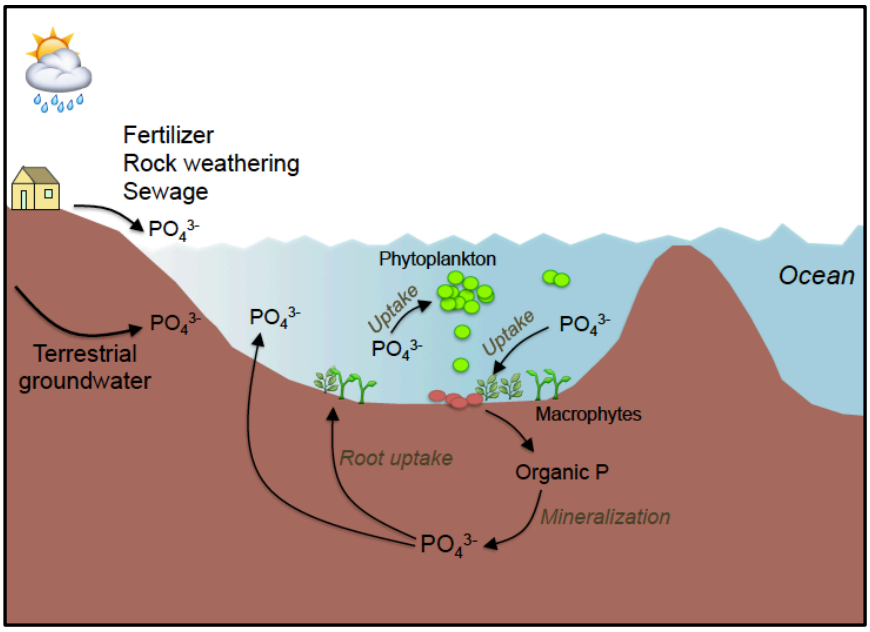

Figure 1.5| Diagram summarizing the major P cycle pathways in coastal lagoons

1.2.3.3 Silica

Dissolved silica is a major nutrient which partly support diatom primary productivity in coastal ecosystems (Tréguer and De La Rocha 2013). Like nitrogen and phosphorus, silica is also generally enriched in terrestrial groundwater (Tovar-Sánchez et al. 2014; Rahman et al. 2019) and porewater (Anschutz et al. 2016; Tamborski et al. 2018; Cho et al. 2018), making dissolved silica useful tracer of groundwater discharge (Garcia-Solsona et al. 2010a). In the Mediterranean coasts, groundwater-derived silica inputs are comparable or higher than surface inputs (e.g. Tovar-Sánchez et al. 2014; Rodellas et al. 2015). The major external source of dissolved silica is the weathering of continental rocks, and especially basalts as they are easily weathered (Allègre et al. 2010; Morin et al. 2015).

The conceptual model presented in Fig. 1.6 shows silicate flux associated with groundwater discharge in coastal systems. The terrestrial groundwater (**F1**) with low salinity and enriched in dissolved Si mixes with the recirculated coastal waters (**F3**), which have high salinity but low dissolved Si concentrations, and they advance toward the sea, resulting in a conservative mixing process (Niencheski et al. 2007; Sospedra et al. 2018). Dissolved silica in the coastal zone is thus supplied by both terrestrial groundwater (**F2**) and the seawater water recirculation (**F3**).

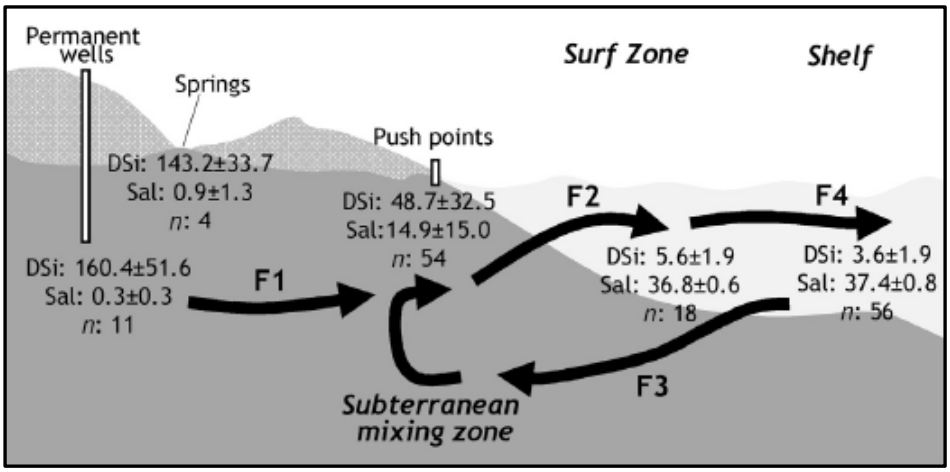

Figure 1.6| Conceptual model (not to scale) of silicate flux in a coastal surface water-groundwater system. The average and standard deviation of dissolved silica (in μM), salinity and number of samples are shown for each compartment. **F1:** terrestrial groundwater, **F2:** groundwater entering the ocean, **F3:** recirculation and **F4:** the flux to the ocean (Sospedra et al. 2018).

1.2.3.4 Carbon

Groundwater discharge has been shown to be an important source of both dissolved inorganic carbon (DIC) (Cai et al. 2003; Dorsett et al. 2011; Santos et al. 2012b; Maher et al. 2013; Atkins et al. 2013) and dissolved organic carbon (DOC) (Goñi and Gardner 2003; Santos et al. 2009; Maher et al. 2013). For instance, Atkins et al. (2013) demonstrated that dissolved inorganic carbon concentration in a coastal floodplain creek in South Wales, Australia increases significantly with increasing groundwater inputs (Fig. 1.7). Like DIC, DOC associated with groundwater discharge is also an important component of the carbon budget in coastal ecosystems. DOC inputs to coastal ocean associated with groundwater discharge result chiefly from the decomposition of organic matter (Goñi and Gardner 2003). Previous studies showed that between 25 and 90% of the DOC inputs to coastal systems are groundwater-derived (Santos et al. 2009; Maher et al. 2013).

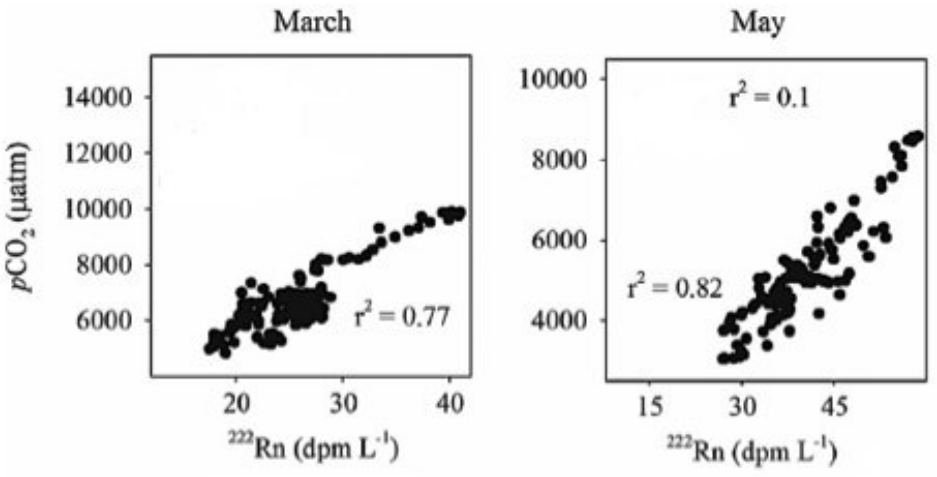

Figure 1.7| Relationship between pCO_2 and ^{222}Rn (natural groundwater tracer) in March and May 2012 in a coastal floodplain creek in South Wales, Australia (Atkins et al. 2013).

In coastal ecosystems, carbon delivered by surface inputs are mainly in form of particulate organic carbon (POC), dissolved organic carbon (DOC) and dissolved inorganic carbon (DIC) (Alin et al. 2012) while groundwater-derived carbon are mainly in form of DIC (mostly CO_2 and HCO_3^-) and DOC (Maher et al. 2013; Atkins et al. 2013). Dissolved and particulate organic carbons in water column are mineralized to DIC, which can be in form of CO_2 or HCO_3^- depending on the pH (Fig. 1.8). Photosynthetic uptake of DIC by primary producers consumes CO_2 ultimately derived from the atmosphere and yields POC, which fuel respiration. Respiration may occur in water column and produce CO_2 available for primary producers or for gas exchange with the atmosphere. Furthermore, POC may sink to the sediment and can undergo long-term burial (Alin and Johnson 2007). POC may also undergo diagenesis and yields CO_2, which can be delivered to the water column through porewater fluxes (Fig. 1.8) (Hammond et al. 1999).

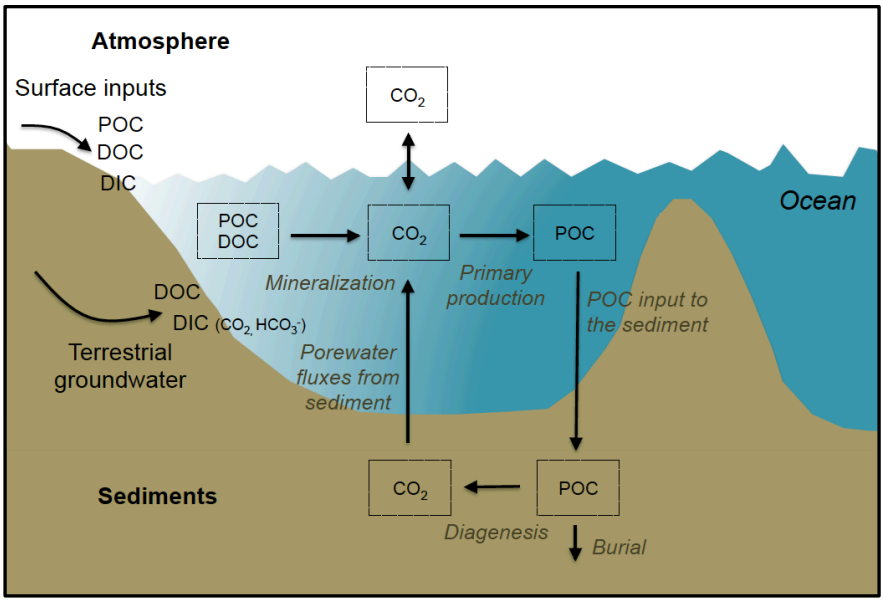

Figure 1.8| Diagram summarizing the major C cycle pathways in coastal lagoons. Based on Alin et al. (2012).

1.2.3.5 Ecological implications

Despite the role of terrestrial groundwater and porewater fluxes of as pathways nutrients to coastal ecosystems, there remains limited evidence of its direct downstream ecological implications (Valiela et al. 1990a; Null et al. 2012; Rodellas et al. 2014b). Few studies have attempted to show the ecological role of groundwater processes in coastal ecosystems. For instance, Valiela et al. (1990) showed that nutrients derived from contaminated groundwater cause an increased growth of macroalgae and phytoplankton, reduction of seagrass beds, and reductions of the associated fauna in coastal waters. Some authors also showed direct correlation between groundwater discharge and increased primary production in coastal waters (Fig. 1.9) (Herrera-Silveira 1998; Rodellas et al. 2014b). In some regions, eutrophication has been directly linked to nutrient inputs via direct groundwater discharge (Valiela et al. 1990a; McClelland et al. 1997; Kwon et al. 2017).

The ecological effects of groundwater inputs to coastal ecosystems are not limited to nutrient loading, and thus the primary production. In some regions with substantial groundwater loading, organisms may respond to changes in salinity, light penetration into water column, pH and turbulence (Short and Burdick 1996;

Troccoli-Ghinaglia et al. 2010; Lee et al. 2017). Groundwater discharge has been shown to reduce coral cover and coral species diversity in coastal ecosystems due mainly to lower salinity (Lirman et al. 2003; Amato et al. 2016) and also the change of carbon chemistry of the coastal waters (Crook et al. 2012). The decrease in abundance of meiofaunal and macrofaunal communities in groundwater-impacted sites in some coastal region results from lower salinity that most meiofauna and macrofauna could not tolerate (Ouisse et al. 2011; Kotwicki et al. 2014). Recent investigations demonstrated also that groundwater discharge enhances species richness, abundance and biomass of fishes and invertebrates in Japanese coastal waters, where high groundwater-borne nutrient concentrations have been reported (Hata et al. 2016; Utsunomiya et al. 2017; Piló et al. 2018). Despite the studies that assessed the ecological effect of groundwater discharge on coastal ecosystems, they are greatly outnumbered by studies solely determining nutrient flux via groundwater processes in coastal systems and very few are conducted in coastal lagoons.

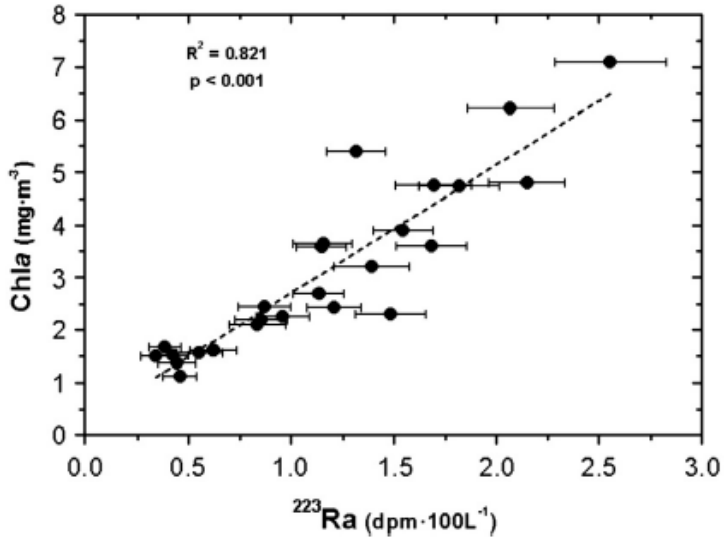

Figure 1.9| Relations between Chl-a (primary production proxy) and ^{223}Ra (a natural groundwater tracer). Dashed line represents the best linear fit to the data (Rodellas et al. 2014b).

1.3 Study site description

1.3.1 French Mediterranean coastal lagoons

The French Mediterranean coast includes 35 coastal lagoons, which cover a total surface area of 52.160 ha (Fig. 1.10) (Cataudella et al. 2015). The surfaces of the French Mediterranean coastal lagoons vary from 15.000 ha (Berre lagoon) to 86 ha (Perols lagoon). The region is overall cold during winters and hot and dry during summers. It experiences rainfall during fall and spring and little rain during summer with a total annual precipitation of 400 mm (Rodellas et al. 2018). It is also generally characterized by strong northwesterly winds, regularly exceeding 10 m s^{-1}. The lagoon water depths are generally low with a maximum depth of 2 m for most of the lagoons. The water salinity differs from one lagoon to another and is highly variable across seasons. The water temperature and the dissolved oxygen concentrations are also highly variable because of the low water depth of these lagoons. Indeed, they follow the variations of air temperature with low temperature in winter and high temperature in summer. The oxygen concentrations are often close to saturation except in summer where the biodegradation of organic matter causes subsequent anoxic conditions. The wind regime often controls the temperature variations which can reach 10°C of daily variations (Cataudella et al. 2015).

My PhD focused on two groundwater-fed coastal lagoons: La Palme and Salses-Leucate lagoons (Fig. 1.10). La Palme lagoon is a reference lagoon for the European Framework Directive for Water Quality Protection and Salses-Leucate lagoon is characterized by large groundwater inputs.

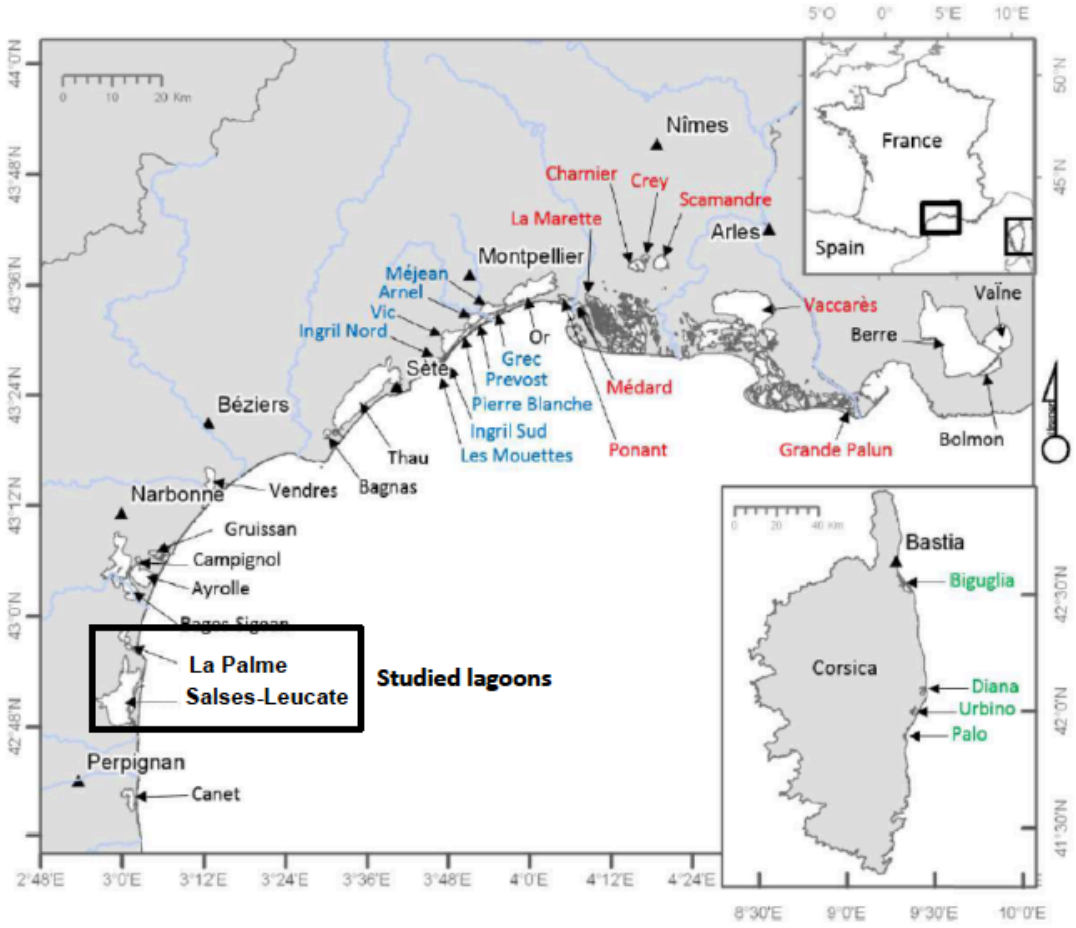

Figure 1.10| Geographical situation of the French Mediterranean coastal lagoons (Le Fur et al. 2019).

Table 1.2| General characteristics of La Palme and Salses-Leucate lagoons

Lagoon	Catchment area (km^2)	Surface (ha)	Mean water depth (m)	Groundwater fluxes ($m^3\ d^{-1}$)
La Palme	65	500	0.5	$\sim 10^4$
Salses-Leucate	160	5600	1.5	$\sim 5 \times 10^5$

1.3.2 La Palme lagoon

1.3.2.1 Geomorphology and bathymetry

La Palme lagoon is a relatively small lagoon with a surface area of 500 ha and a catchment area of 65 km^2 (Table 1.2). The mean and maximum water depths are 0.5 m and 1.5 m, respectively. This chocked lagoon (see section 1.1.2) is seasonally connected with the Mediterranean Sea via a small opening, which is usually closed during summer and periodically opens between fall and spring (Fig. 1.11). Exchange with the Mediterranean Sea is further restricted by a road dike and a railway dike, which are intersected by a small bridge each, allowing water exchange (Fig. 1.11). The southern part of the lagoon is relatively shallow (mean depth: 0.2 m), and is partially dry during summer months. Strong north-westerly winds, regularly exceeding 10 m s^{-1}, play an important role in the hydrodynamics of the lagoon. They regulate the lagoon connection with the open sea and drive porewater fluxes (Stieglitz et al. 2013; Cook et al. 2018a).

1.3.2.2 Hydrology and groundwater inputs

The opening in the southern part of the lagoon allow temporarily water exchange with the Mediterranean Sea, which is primarily driven by strong northwesterly winds called “Tramontane” characteristic of the region. Winds are the main driver of the lagoon hydrodynamics with the “Tramontane” pushing the lagoon water towards offshore and limiting marine influence while sporadic wind from the sea enhances seawater inputs into the lagoon. Tidal forcing plays minor role in the hydrodynamic functioning of the lagoon due low tidal variation in the Mediterranean Sea (<0.4 m) and the restricted exchange between the lagoon and the sea (Fig. 1.11a). Karstified Jurassic and lower Cretaceous limestones constitute the main aquifer of the area (Wilke and Boutière 2000). Throughout the year, the lagoon receives freshwater from a limestone aquifer (3 - 25 × 10^3 m^3 d^{-1}; Rodellas et al. 2018), mainly through a karstic spring (~50%), connected to the lagoon via a small, short stream in the northwestern part of the lagoon (Fig. 1.11) (Wilke and Boutière 2000). This karstic groundwater input has been demonstrated to contribute to maintaining transitional (brackish) ecosystem functioning of the

lagoon (Stieglitz et al. 2013). Few small streams also drain freshwater into the lagoon from a relatively small catchment area mainly composed by Quaternary alluvial deposits, but they flow only during strong rainfall events. Total water inputs from these streams are estimated to be significantly smaller (more than one order of magnitude smaller) than inflows from karstic groundwater (Wilke and Boutière 2000). A sewage treatment plant intermittently discharges treated wastewater into the north part of the lagoon from La Palme village (1700 inhabitants) with a mean water flow of 2.6×10^2 m^3 d^{-1} (Fig. 1.11a) (PNRNM 2016). Estimated recirculation flows are estimated to be on the order of 3×10^4 - 2×10^5 m^3 d^{-1}, which is the equivalent of the volume of entire lagoon recirculating through the sediment every ca. 25 days (Stieglitz et al. 2013). The sediments throughout most of the lagoon are fine-to-coarse grained sands (100-500 μm) with the northern part dominated by fine-grained sediments (ca. 50 μm) (IFREMER 2003).

In La Palme lagoon, the lagoon water temperatures show overall seasonal variations with maximum temperature recorded in August (25.5°C) and minimum in January (8.5°C) (IFREMER 2014). The salinity in the lagoon is highly variable in space and time. The salinity is generally lower during winter and higher during summer periods due to evaporation and little rainfall. The salinity distributions show also strong spatial gradient with low salinity observed in the northern part of the lagoon due to discharge of low-salinity groundwater and treated wastewater from La Palme village (Stieglitz et al. 2013; Tamborski et al. 2018). Conversely, hypersaline conditions persist in southern part of the lagoon due to limited exchange with the northern part and evaporation. The dissolved oxygen concentrations in the lagoon are generally close to saturation (IFREMER 2014).

1.3.2.3 Ecology

La Palme lagoon is one of the rare remaining pristine systems in the region (Derolez et al. 2015). The lagoon has a high ecological diversity and is recognized as RAMSAR site. It is listed in the French environmental protection program Natura 2000 as a site of outstanding ecological value and listed as reference site for the European Framework Directive for Water Quality Protection. La Palme

lagoon is home to large number of fishes, invertebrates and diverse macrophyte species; the lagoon is mostly covered by seagrass meadows (DREAL 2010). The lagoon hosts also a large number of bird species that are sedentary or migratory.

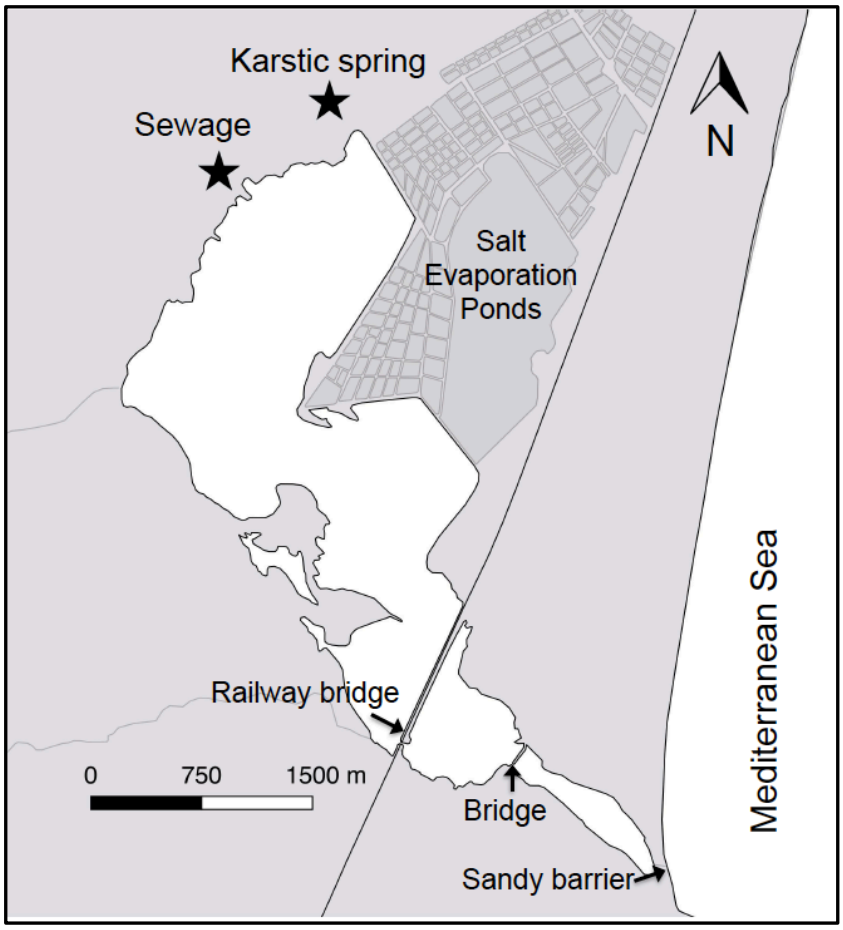

Figure 1.11| Map of La Palme lagoon. Locations of sewage treatment plant and groundwater springs are shown.

1.3.3 Salses-Leucate lagoon

1.3.3.1 Geomorphology and bathymetry

Salses-Leucate lagoon is relatively large with a volume of 90 millions m^3, a surface area of 5600 ha and a catchment area of 160 km^2 (Fig. 1.12). The mean and maximum depths of the lagoon are 1.5 m and 3.5 m, respectively (Table 1.2). The lagoon is divided in two basins: northern and southern basins. The northern basin

is smaller (1540 ha) and shallower (mean depth=1.5 m) than the southern basin (3860 ha; mean depth=2.1 m).

Four distinct geological features characterize the geology of Salses-Leucate (Ladagnous and Le Bec 1997):

- In the north, a Pliocene plateau formed by marls and limestone
- In the east, a quaternary sandy barrier separating the lagoon from the sea
- In the south, a plio-quaternary plain formed by clay and molasses
- In the west, the Corbières formed by secondary limestone.

This restricted lagoon (see section 1.1.2) is permanently connected with the Mediterranean Sea by three large artificial openings in the eastern part of the lagoon, through which lagoon water efficiently exchanges on a continuous basis (Fig. 1.12).

1.3.3.2 Hydrology and groundwater inputs

Like in La Palme lagoon, tidal variations are also negligible in Salses-Leucate lagoon. Karstic groundwater discharges directly to the southern basin through two karstic springs, Font Estramar and Font Dame. The spring Font Estramar is the main outlet of the karst formation of the eastern Corbières and is visible in form of a basin of 25 m of diameter (Fig. 1.12) (Fleury et al. 2007). It has a mean water flow of 3.0×10^5 m^3 d^{-1} and its water flows toward the lagoon by a channel of about 500 m. The spring Font Dame originates in the middle of a large swamp and is formed of several sources, close to each other. The water is also delivered to the lagoon through a channel with a flow of 2.0×10^5 m^3 d^{-1} (Fleury et al. 2007). A sewage treatment plant discharges treated wastewater into the basin from Salses-le-Château village (3500 inhabitants) (Fig. 1.12). A few small streams also drain freshwater into the lagoon from the catchment area but they flow only during rainfall periods. The western part of the lagoon (close to karstic springs) is dominated by fine-grained sediments (<20 μm) while most of the lagoon is dominated by fine-to-coarse grained sands (100-500 μm) (IFREMER 2005).

The lagoon water temperatures show overall seasonal variations with maximum recorded in July (23°C) and minimum in January (8°C) (Ladagnous and Le Bec 1997; IFREMER 2014). The water column is well-mixed because of low water depth and wind-driven mixing. The salinity shows also seasonal variability with lower salinities in winter and higher salinities in summer. The lagoon salinity ranges overall between 25 and 37 and lower salinities are observed in western parts of the lagoon because of fresh terrestrial groundwater inputs from the springs Font Estramar and Font Dame (Fig. 1.12) (Stieglitz et al. 2013). The dissolved oxygen concentrations in the lagoon are generally close to saturation. Lower concentrations can be, however, recorded during eutrophication events (IFREMER 2014).

1.3.3.3 Ecology

Salses-Leucate lagoon supports a wide range of habitats and has a remarkable diversity that is explained by its large size and relatively low pollution. The lagoon is listed as a Site of Community Importance under the European Habitat Directive and a Special Protection Area under the EU Bird Directives, and thus a part of the Natura 2000 network. Salses-Leucate lagoon functions as feeding and nursery grounds for several Mediterranean fish species (e.g. mullets, seabream and seabass). The lagoon hosts more than 70 species of macrophytes and 15% have been introduced (Boudouresque and Verlaque 2002). Macrophytes in the lagoon are dominated by seagrass, particularly the species *Zostera noltii* (Ladagnous and Le Bec 1997). Salses-Leucate lagoon is also home to many molluscs and constitutes an important site for mussel and oyster farming in the region.

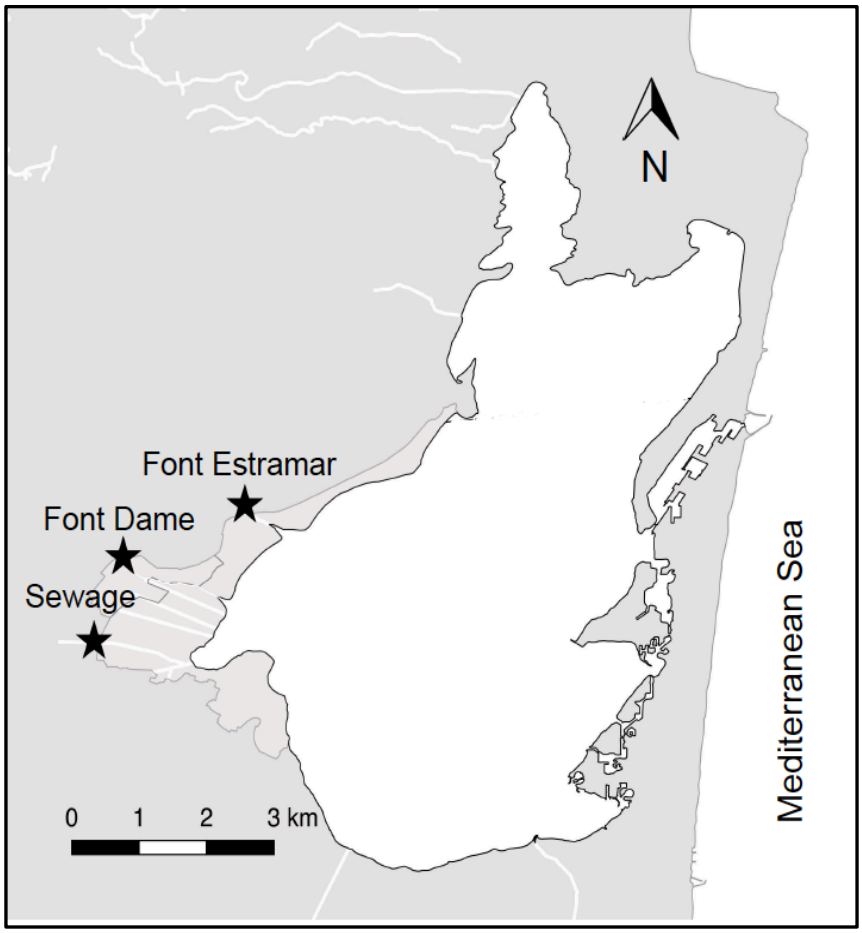

Figure 1.12| Map of Salses-Leucate lagoon. Locations of sewage treatment plant and groundwater springs are shown.

– Chapter 2 –

Groundwater-driven nutrient inputs to coastal lagoons: the relevance of lagoon water recirculation as a conveyor of dissolved nutrients

This chapter is based on:

Valentí Rodellas, Thomas C Stieglitz, Aladin Andrisoa, Peter G Cook, Patrick Raimbault, Joseph J Tamborski, Pieter Van Beek, Olivier Radakovitch (2018). Groundwater-driven nutrient inputs to coastal lagoons: the relevance of lagoon water recirculation as a conveyor of dissolved nutrients. *Science of the Total Environment 642, 764-780.*

2.1 Introduction

Groundwater processes are increasingly recognized as an important source of nutrients to coastal wetlands and lagoons, bays and coves, salt marshes, coral reefs or entire ocean basins, and sometimes rivaling loads from riverine inputs (Slomp and Van Cappellen 2004; Beusen et al. 2005; Rodellas et al. 2015; Szymczycha and Pempkowiak 2015; Sadat-Noori et al. 2016; Adyasari et al. 2018). These evaluations usually incorporate nutrient inputs associated with the discharge of fresh terrestrial groundwater from coastal aquifers, but also to the recirculation of seawater or lagoon water (porewater fluxes) through permeable sediments. These two disparate processes are commonly incorporated within the definition of Submarine Groundwater Discharge (SGD), mainly because both processes represent advective water flows across the sediment-water interface that can supply chemical loads to coastal and lagoonal waters (Burnett et al. 2006; Moore 2010). Terrestrial groundwater discharge is a source of new nutrients to coastal systems, derived from natural (e.g. vegetation, rocks, microorganisms) and anthropogenic (e.g. agriculture, industrial and domestic wastewaters) sources to coastal aquifers (Slomp and Van Cappellen 2004; Knee and Paytan 2011). Whilst seawater recirculation does not represent a net input of water, it can also result in a significant net flux of nutrients to coastal waters mainly as a consequence of i) the biogeochemical transformations occurring when fresh groundwater mixes with seawater in coastal aquifers and permeable coastal sediments (Moore 1999; Santos et al. 2008); ii) the continuous supply of oxidants and fine particulate and dissolved matter into sediment porewaters that fuel biological and chemical reactions within sediments (Anschutz et al. 2009; Huettel et al. 2014); and iii) the remobilization of nutrients stored in sediments as a consequence of past regimes or anthropogenic activities (Trezzi et al. 2016; Martínez-Soto et al. 2016). Therefore, the biogeochemical composition of terrestrial groundwater discharge and saline recirculation flows may be considerably different, requiring the separation of both processes to better understand and characterize fluxes of dissolved nutrients to coastal lagoons and their ecological implications (Weinstein et al. 2011; Sadat-Noori et al. 2016). However, there are still limited studies that have attempted to distinguish nutrient fluxes driven by terrestrial groundwater

and recirculation inputs (Kroeger and Charette 2008; Santos et al. 2009; Weinstein et al. 2011; Sadat-Noori et al. 2016; Tamborski et al. 2017), and these are rarely focused on lagoonal ecosystems. Most studies conducted in coastal lagoons are based on nutrient fluxes supplied by terrestrial groundwater (Ji et al. 2013; Tait et al. 2014; Malta et al. 2017) and neglect the potential role of water recirculation through sediments as a pathway for dissolved nutrients loads.

In this study, we assess the relative significance of terrestrial groundwater discharge from a karst origin (referred hereinafter as karstic groundwater) and saline water recirculation through sediments in conveying dissolved nutrients to a coastal lagoon. This study was conducted in La Palme lagoon (France, Mediterranean Sea), a small shallow coastal lagoon where both the discharge of karstic groundwater and the recirculation of lagoon water through permeable sediments have been documented previously (Stieglitz et al. 2013; Bejannin et al. 2017). In this study, detailed estimations of fluxes of dissolved inorganic nutrients (NO_3^-, NH_4^+ and PO_4^{3-}) driven by karstic groundwater discharge and lagoon water recirculation are conducted via concurrent water and radon mass balances. The present study is focused on the northern basin of La Palme Lagoon, which represents the main water body (~85% of the total lagoon area; >95% of the total lagoon water volume) and receives all of the groundwater inputs from karstic springs.

***Terminology**:* Advective fluxes occurring over small spatial scales (mm to cm) are often excluded from the current definition of SGD and referred to as "porewater exchange" (Moore 2010; Santos et al. 2012a). For the purpose of this study, we prefer distinguishing exchange processes depending on their origin, composition and driving force, rather than differentiating them according to their length-scale. Therefore, the term karstic groundwater discharge is used for low-salinity groundwater driven by the terrestrial hydraulic gradient, whereas recirculation fluxes refer to both short- and long-scale recirculation of saline water through sediments, which is driven by pressure gradients forced by tides, waves, bottom currents, benthic organisms, or bottom water / porewater density changes (Santos et al. 2012a; Huettel et al. 2014).

2.2 Theory

The magnitude of karstic groundwater- and recirculation-driven nutrient fluxes was estimated through a radon-based approach. Radon (^{222}Rn) is a natural environmental tracer that has been widely used for quantifying groundwater inflows (both terrestrial and recirculation flows, usually in combination) (Burnett and Dulaiova 2003; Cook et al. 2006; Stieglitz et al. 2010; Rodellas et al. 2012). Radon is a radioactive (half-life of 3.8 days) inert gas that is produced from the decay of ^{226}Ra, mainly associated with sediment and aquifer solids. Radon tends to be depleted in surface waters due to gaseous exchange with the atmosphere and radioactive decay, so that radon concentrations in groundwater and sediment porewaters are elevated relative to surface waters by 2-3 orders of magnitude.

2.2.1 Concurrent water and radon mass balances for surface waters

Following Stieglitz et al (2013), mass balances for water and radon were constructed to simultaneously estimate karstic groundwater discharge and saline recirculation water flows to the northern basin of La Palme lagoon.

The surface water mass balance for the northern basin of La Palme lagoon is:

$$\frac{\partial V_N}{\partial t} = Q_g + PA_N - EA_N - Q_{NC} \qquad (2.1)$$

where V_N and A_N are the water volume [m^3] and surface area [m^2] of the northern basin, respectively, Q_g is the karstic groundwater discharge [m^3 d^{-1}], P and E are the precipitation and evaporation rates [m d^{-1}], respectively, Q_{NC} is the water flow from the northern to the central basin of the lagoon [m^3 d^{-1}] (negative flows indicate inputs from the central basin) and t is time [d].

The radon mass balance for the northern basin of La Palme lagoon is:

$$\frac{\partial CV_N}{\partial t} = Q_g C_g + \lambda V_N C_{Ra} + \left(F_{diff} + F_{recir}\right)A_N - kA_N(C - \alpha C_{air}) - \lambda V_N C - Q_{NC} C - D_{NC}\Delta C \quad (2.2)$$

where C and C_g are the mean concentration of radon in the northern basin and in karstic groundwater [Bq m^{-3}], respectively, C_{Ra} is the mean concentration of ^{226}Ra

in the northern basin [Bq m^{-3}], F_{diff} and F_{recir} are the net fluxes of radon per unit area from underlying lagoon sediments due to molecular diffusion and lagoon water recirculation [Bq m^{-2} d^{-1}], respectively, λ is the radioactive decay constant of radon [d^{-1}], k is the gas transfer velocity [m d^{-1}], C_{air} the radon concentration in air [Bq m^{-3}] and α the air-water partitioning of radon corrected for salinity and temperature (Schubert et al. 2012b), D_{NC} is the dispersive exchange flux of radon between the northern and the central basins of the lagoon [m^3 d^{-1}], and ΔC is the difference in radon concentrations at the boundary between northern and central basins [Bq m^{-3}]. Notice that if Q_{NC} is negative, the mean radon concentration from the central basin should be used as C in the term $Q_{NC}C$. The term αC_{air} can be neglected in comparison to C. Stieglitz et al. (2013) showed that radon exchange fluxes between the northern and central basins (including advective and dispersive fluxes) account for less than 1% of total radon outputs, and thus the terms $Q_{NC}C$ and $D_{NC}\Delta C$ are neglected for the radon mass balance. The simplified equation used in this study is thus:

$$\frac{\partial CV_N}{\partial t} = Q_g C_g + \lambda V_N C_{Ra} + \left(F_{diff} + F_{recir}\right)A_N - kA_N C - \lambda V_N C \qquad (2.3)$$

2.3 Methods

2.3.1 Porewater collection and analysis

Seasonal surveys were conducted in June 2016, November 2016, April 2017 and June 2017. During each survey, porewater samples for radon, salinity and nutrient analysis were collected at 3 different locations (Pz1, Pz2 and Pz3; Fig. 2.1) using a direct-push, shielded-screen well-point piezometer (2.2a) (Charette and Allen 2006). These locations were chosen to be representative of the different types of sediments in the lagoon. Whereas Pz2 is not located in the northern section of the lagoon, sediments from Pz2 have the same characteristics as sediments from the southern part of the northern basin, and thus this location is considered as representative of this area. A fourth location (Pz4; Fig. 2.1) was also selected as representative of fine-grained sediment areas, but porewater samples could not be collected due to the low hydraulic conductivities of the clay sediments. At each one of the three locations, porewater samples were collected at depths of 5, 10, 15, 20,

30, 50 and 80 cm below the sediment–water interface. For radon analysis, 10-mL of filtered (0.8 μm) porewater was collected at each depth using a gas-tight syringe coupled to the piezometer tubing and directly transferred to 20-mL vials prefilled with a 10-mL high-efficiency mineral oil scintillation cocktail, while minimizing water-air contact (Cable and Martin 2008). Concentrations of radon were analyzed by liquid scintillation counting on a Quantulus 1220 with alpha-beta discrimination counting (background of 0.2-0.4 cpm; efficiency of 1.6-2.2, depending on the quenching factor of the sample). Samples for salinity analysis (10 mL) were also collected at each depth and measured using a pre-calibrated WTW multiparameter sonde (WTW Multi 3430 meter with TetraCon® 925 probe for conductivity and temperature measurements). For nutrient analysis (ammonium (NH_4^+), nitrate (NO_3^-) and phosphate (PO_4^{3-})), 20 mL of filtered (0.7 μm) porewater was collected at each depth in acid-clean vials. Nutrient samples were preserved with $HgCl_2$ (6 g l^{-1}) to prevent bacterial activity (Kirkwood 1992). NO_3^- and PO_4^{3-} concentrations were measured by colorimetric methods using a Technicon AutoAnalyser® II with detection limits of 0.05 μmol L^{-1} and 0.02 μmol L^{-1} for NO_3^- and PO_4^{3-}, respectively (Aminot and Kérouel 2007). NH_4^+ concentrations were determined on dilute samples (4 to 10 times) with a Turner Designs TD-700 Fluorometer (detection limit: 0.05 μmol L^{-1}) (Holmes et al. 1999).

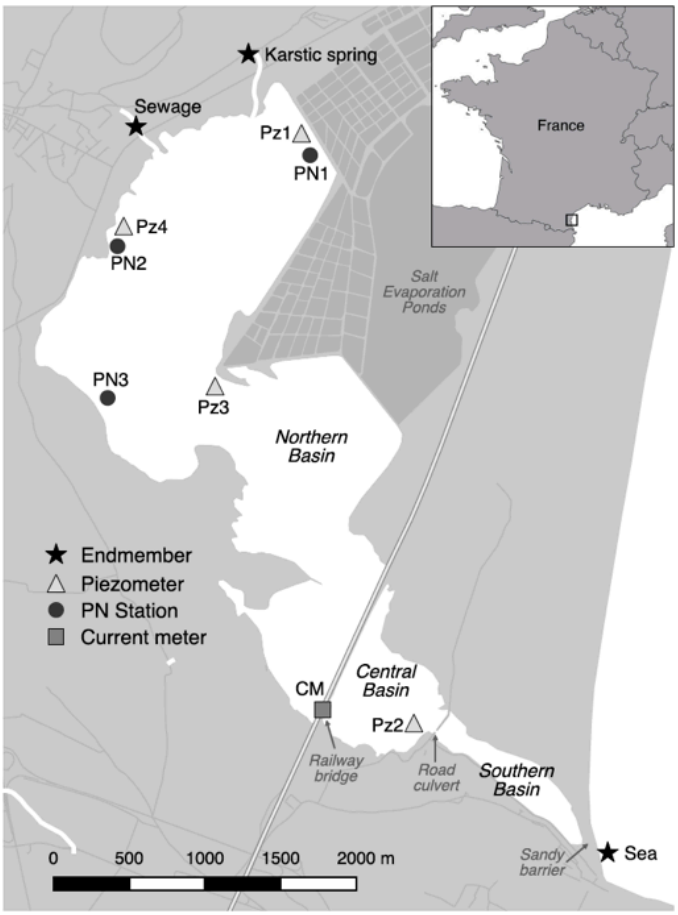

Figure 2.1| Study site (La Palme lagoon) location on the French Mediterranean coastline. Sampling locations for endmembers (karstic spring, sewage effluent and seawater) and porewaters (piezometer) are shown, as well as the position of monitoring stations from the "Parc Naturel Régional de la Narbonaisse en Méditerranée" (PN station) and the site where the current meter was installed.

2.3.2 Surface water collection and analysis

During each sampling campaign, the spatial distribution of radon and salinity in lagoon waters from the northern section of the lagoon was investigated by continuously measuring these parameters from a moving boat (Fig. 2.2b). For radon counting, two electronic radon-in-air monitors RAD7 (Durridge) were connected in parallel and coupled to a gas exchange membrane (Fig. 2.2c) (Liqui-Cel MiniModule; (Dulaiova et al. 2005; Schubert et al. 2012a). Surface water was pumped with a submersible pump directly to the membrane, where equilibrium was established between the dissolved radon in continuously pumped lagoon water and radon in a closed air loop that circulates through the monitors. Radon

concentration in water was determined from the measured concentration in air, by using the air-water partitioning of radon corrected for water salinity and temperature (Schubert et al. 2012b). The small lag time produced by radon extraction and radioactive counting was corrected following (Stieglitz et al. 2010). Surface water salinity and temperature were measured using the WTW multiparameter sonde (Multi 3430 meter and TetraCon® 925 probe). Measured radon concentrations and salinities were interpolated by kriging at 50 m spatial resolution to obtain distribution grids and weighted-average concentrations. For radon, the analytical uncertainty (1σ) was also taken into account to derive grids of minimum and maximum radon concentrations, which were used to estimate the uncertainties associated with average radon concentrations. Radon data points (n > 40 for each survey) were spatially well distributed in the northern basin of the lagoon and thus we assume that uncertainties derived from spatial interpolation are smaller than analytical uncertainties (relative uncertainties for C of 20-30%, depending on the survey). The application of different interpolation methods (Inverse Distance Weighted and Triangulated Irregular Network) resulted in similar average radon concentrations to those obtained by kriging (< 10% of difference between interpolation methods).

Radon and nutrient samples were also collected from the sewage effluent, the main karstic groundwater spring and from surface waters (Fig. 2.2d) (~10 cm above the sediment-water interface) at the three piezometer locations (Pz1, Pz2 and Pz3; Fig. 2.1). Additional nutrient samples were collected throughout the lagoon (5-10 samples/survey) to obtain a qualitative distribution of nutrients in surface waters. Radon samples (2 L) were collected using a small submersible pump to minimize gas loss (Fig. 2.2e) and analyzed using the radon-in-air monitor RAD7 coupled to a gas extraction accessory for bottles (Durridge Inc) (Fig. 2.2f). Radon samples in surface waters were counted twice: just after sample collection to determine dissolved radon and after aging for a minimum of 4 weeks to estimate the ^{226}Ra dissolved in surface waters. Nutrient samples were collected with a 1-L acid-clean Nalgene bottle and analysed as described above. Temperatures and salinities were measured *in situ* in groundwater, sewage effluent and surface waters using the

WTW multiparameter sonde (Multi 3430 meter and TetraCon® 925 probe) (Fig. 2.2b).

Figure 2.2| Sampling campaign in La Palme lagoon. (a) Porewater sampling using a direct-push, shielded-screen well-point piezometer, (b) radon and salinity mapping, (c) two RAD7 monitors connected in parallel, (d) karstic groundwater spring, (e) radon sampling in the lagoon with submersible pump, and (f) counting of radon samples.

2.3.3 Ancillary measurements and analysis

A detailed bathymetry map for the northern section of the lagoon was constructed by interpolating echosounder/DGPS data collected in December 2016 to 50 m spatial resolutions. To estimate the water volumes of the lagoon for the different campaigns, the bathymetry grid was corrected for changes in water level estimated from water depth measurements throughout the lagoon at each sampling ($n > 20$ for each sampling). The corrected bathymetry grids for each campaign, together with the radon concentration and salinity grids, were used to obtain volume-weighted average radon concentration and salinity values for the northern section of the lagoon.

Lagoon water level was recorded continuously at 10 min intervals using HOBO pressure transducers installed at 3 sites of the northern part of the lagoon (Pz1, Pz3 and Pz4) from 1 April 2017 to 28 April 2017 and from 9 June 2017 to 4 July 2017. Recorded pressures were corrected for atmospheric variation and used to estimate the variation of lagoon water depth over time for the April 2017 and June 2017 campaigns. Additionally, a drag-tilt current meter (Marotte HS) was installed under the railway bridge in June 2017 to estimate the magnitude of water flows exchanged between northern and central basins. Exchanged daily water flows were obtained from current measurements recorded every 5 minutes and the exchange section of the bridge (17 m^2; Fiandrino et al. 2012). Hourly rainfall, temperature and wind data at the nearby meteorological station "Leucate" was extracted from the database of the French meteorological service (Météo France). Monthly data on lagoon water levels and salinity at three sites in the northern lagoon (PN stations in Fig. 2.1), as well as water estimated inflows from the sewage treatment plant, were obtained from the database of the "Parc Naturel Régional de la Narbonnaise en Méditerranée" (PNRNM) (Fig. 2.3).

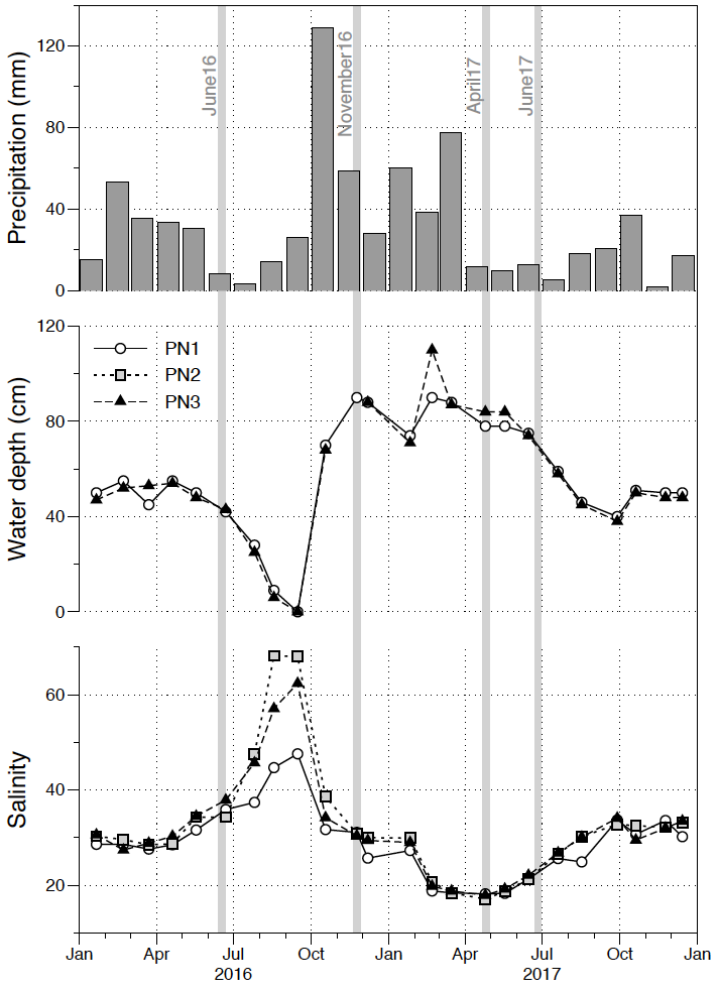

Figure 2.3| Precipitation surface water level and salinity in La Palme lagoon during 2016 and 2017 (Precipitation data from "Météo France"; surface water depth and salinity data from the three monitoring stations of PNRNM, see Fig. 2.1). Periods of the surveys are indicated.

2.3.4 Radon equilibration experiment

Four sediment cores of ~30 cm length were collected at sites Pz1, Pz2, Pz3 and Pz4 (Fig. 2.1) to estimate the production of radon from sediments. The cores were sliced at 5 cm intervals and the sections of 5-10, 15-20 and 25-30 cm from each site were used for sediment equilibration experiments (Corbett et al. 1998). Ca. 200 g of dry sediment was put into 500 mL bottles and the remaining volume was filled with Ra-free lagoon water (Ra removed by using acrylic fiber impregnated with MnO_2; (Moore and Reid 1973). The bottles containing the sediments (hermetically sealed) were stored for more than 1 month and periodically shaken.

The radon concentration in water was directly measured using the RAD7 coupled to the gas extraction accessory for bottles and the results were corrected to the specific ratio porewater/solids in sediments (Stieglitz et al. 2013). The average radon concentration from the three sections at each site is used to represent the porewater radon concentration in equilibrium with sediments.

2.4 Results

2.4.1 Porewater profiles

Porewater could be easily sampled with a push-point piezometer from most of the depths at the locations Pz1, Pz2 and Pz3, indicating a relatively high hydraulic permeability for the sandy sediments at these locations. The only exception was a relatively impermeable layer found at Pz3, extending from ~30 to ~40 cm below the sediment-water interface. Porewater samples could not be collected from Pz4 due to the low hydraulic conductivities of the clay sediments from this location.

Porewater salinity depth profiles reflected mixing between two endmembers: i) lagoon water with varying salinities depending on the season and the location (e.g. Fig. 2.2), and ii) deep, evaporative, hypersaline (salinity up to 80) porewater (Fig. 2.4). Most of the vertical porewater profiles displayed an increase in salinities downward, showing different trends in different locations and seasons depending on the dynamics of the mixing between these two endmembers. Porewaters were significantly enriched in radon (maximum concentration of 6800 ± 600, 4600 ± 400 and 8000 ± 900 Bq m^{-3} in Pz1, Pz2 and Pz3, respectively) relative to surface waters (20-200 Bq m^{-3}), mainly as a consequence of radon production from ^{226}Ra in sediments and the lack of atmospheric evasion (Fig. 2.4). A deficit of *in situ* porewater radon concentrations relative to radon in equilibrium with sediments (derived from sediment equilibration experiments; Fig. 2.4) was generally observed for the upper sediments, indicating radon exchange between porewaters and overlying lagoon waters due to radon diffusion or/and water advection (i.e. water recirculation).

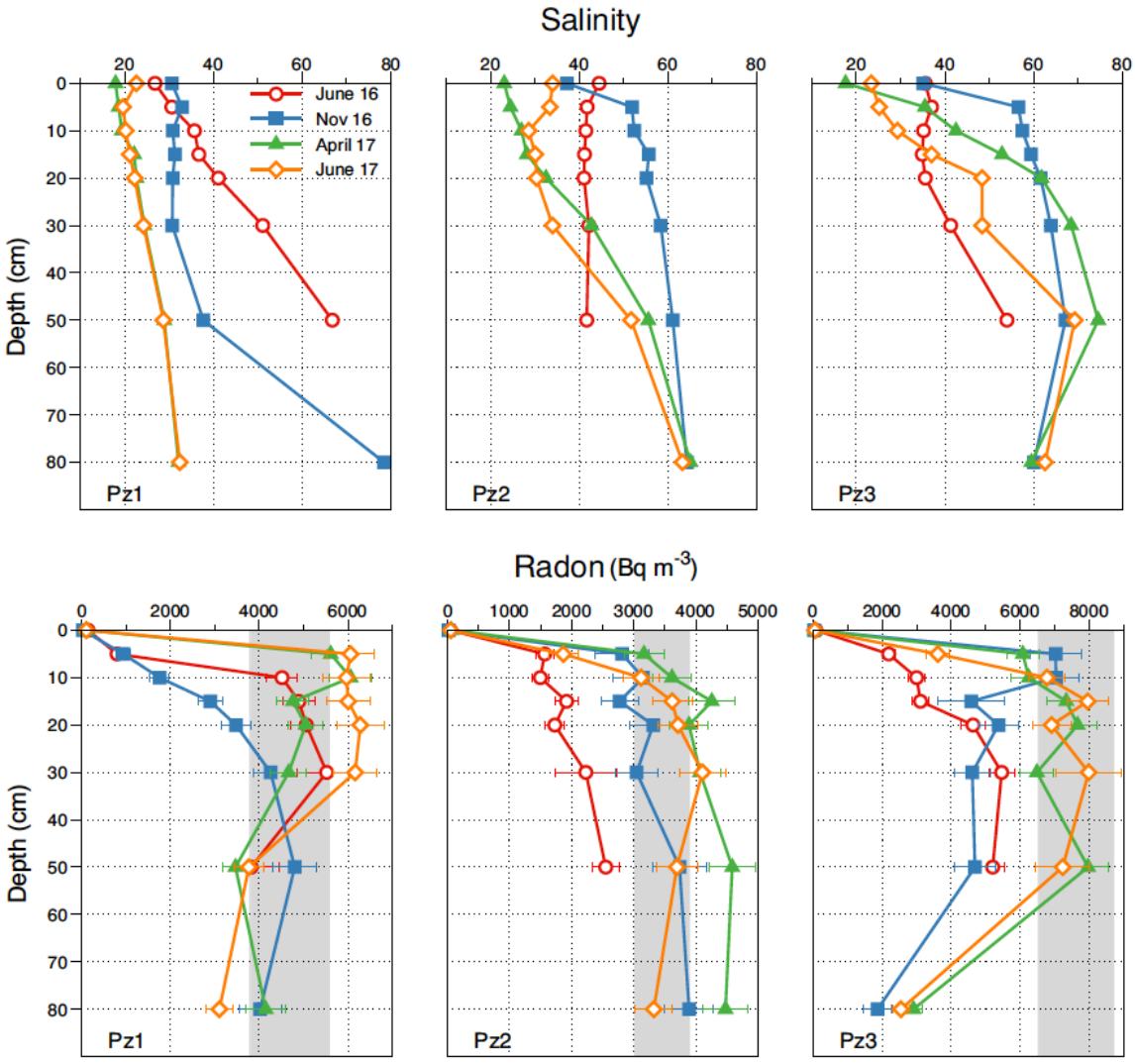

Figure 2.4| Depth profiles (in cm below the sediment-water interface) of salinity and radon concentration in porewater for the three piezometers collected at each campaign. Reported values at a depth of 0 cm corresponds to the samples collected in surface waters (~10 cm above the sediment-water interface). The gray area represents radon concentration in equilibrium with sediments estimated from equilibration experiments.

Porewater concentrations of NH_4^+ and, to a lesser extent, PO_4^{3-} were significantly enriched relative to lagoon waters (20- and 5-fold on average, respectively), with concentrations generally increasing with depth (Fig. 2.5). In contrast, concentrations of NO_3^- in porewaters were comparable or even lower than those measured in overlying waters. No clear seasonal patterns were observed for any of the analyzed dissolved nutrients in porewaters.

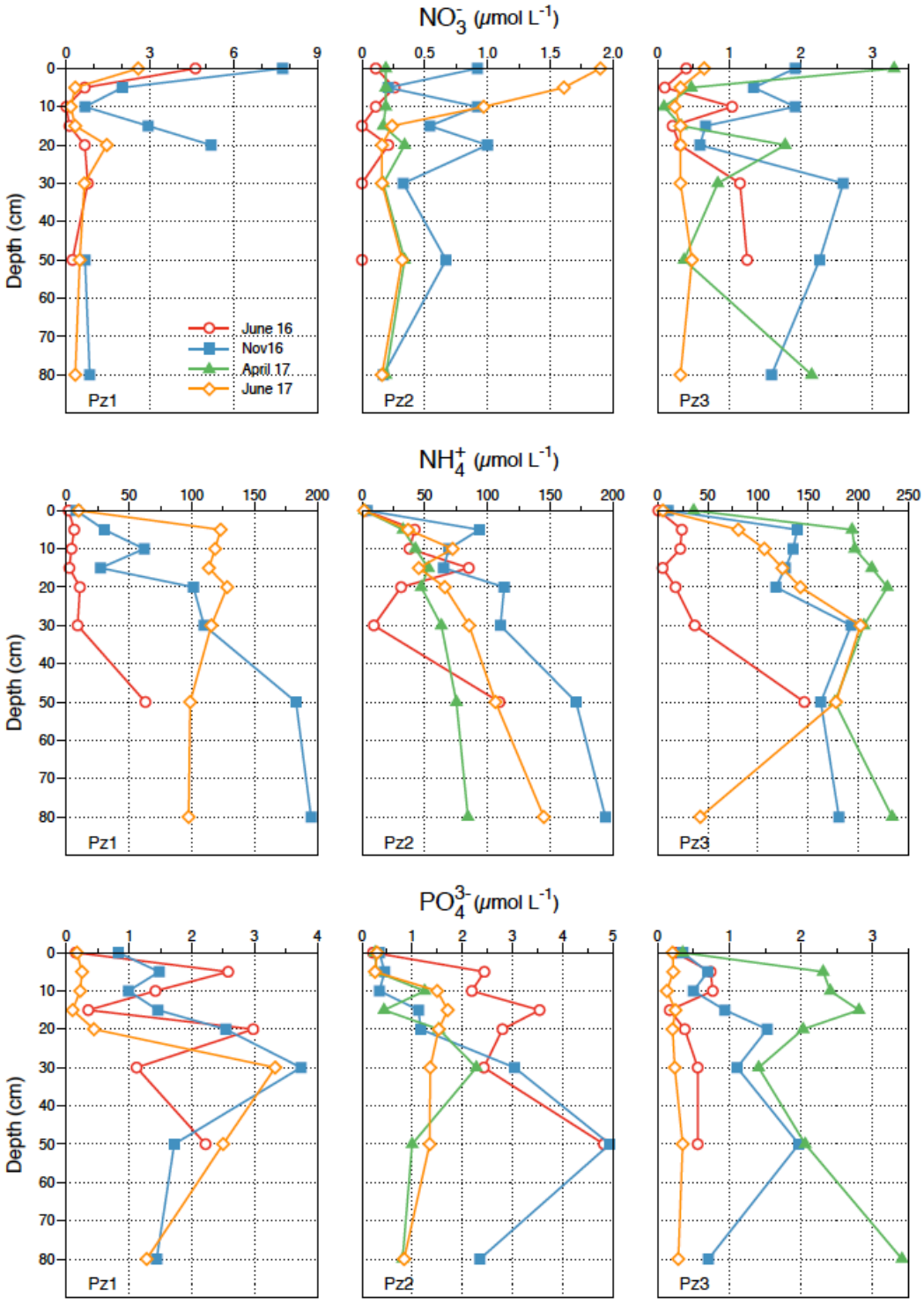

Figure 2.5| Depth profiles (in cm below the sediment-water interface) of dissolved inorganic nutrient (NO_3^-, NH_4^+ and PO_4^{3-}) concentrations in porewater for the three piezometers collected at each campaign. Reported values at a depth of 0 cm corresponds to the samples collected in surface waters (~10 cm above the sediment-water interface). Note that nutrient samples at Pz1 were not analyzed for the April 2017 survey.

2.4.2 Radon and salinity distributions in lagoon surface waters

The highest radon concentrations (higher than 300 Bq m^{-3} in June 2016) and lowest salinities (down to 17, in April 2017) occurred in the far north of the lagoon, with radon concentrations decreasing and salinities increasing southwards (Fig. 2.6). This distribution indicates the presence of low-salinity, high-radon sources in the north of the lagoon, coinciding with the main karstic spring, and agrees well with previous observations from (Stieglitz et al. 2013). The lagoon water volume (i.e. water depth) varied significantly through the year, with lower water volumes in summer when evaporative loss exceeded water input (e.g. estimated water volume of $2.5 \cdot 10^6$ m^3 in June 2016) and maximum values in the wet season (e.g. $5.3 \cdot 10^6$ m^3 in November 2016) (Fig. 2.2; Fig 2.6; Table 2.1). The seasonal evolution of salinity also reflected the annual variations on low-salinity water inputs and evaporation rates (Fig. 2.2; Fig. 2.6). Salinity was at a maximum in summer 2016 (average salinity of 37 in June 2016), decreasing significantly during the wet season (salinities of 32 and 18 in November 2016 and April 2017, respectively), and increasing again at the end of spring due to a reduction in low-salinity inputs and an increase in evaporation rates (average salinity of 23 in June 2017) (Fig. 2.2; Fig. 2.6). Radon concentrations were also maximal in summer campaigns (average concentrations of 120 ± 20 and 93 ± 24 Bq m^{-3} for June 2016 and June 2017, respectively), whereas the lowest concentrations were measured in November 2016 (23 ± 7 Bq m^{-3}) (Table 2.1). While the salinity of the lagoon largely represents a balance between the rate of freshwater inputs and evaporation, the radon concentration is highly influenced by recirculation inputs (which do not affect salinity, as they do not represent a net water flux) and the wind speed (which affects the gas exchange rate). For these reasons, the seasonal variability of salinity and radon concentrations do not necessarily coincide. Additionally, while the radon activity reflects the water balance over the few days prior to sampling, salinity reflects lagoon dynamics over a much longer time period (see section 2.4.4).

Groundwater discharging from the main karstic spring was brackish (salinity 5.0 to 9.4, depending on the season), presumably reflecting some degree of interaction between fresh groundwater and seawater in the coastal aquifer. Radon

concentration in the karstic spring was constant throughout the year and significantly enriched relative to lagoon waters, with values ranging from 2290 ± 90 to 2600 ± 110 Bq m^{-3}. Radon concentrations measured in the sewage effluent were on the order of 20 Bq m^{-3}, and thus this source is hereafter neglected.

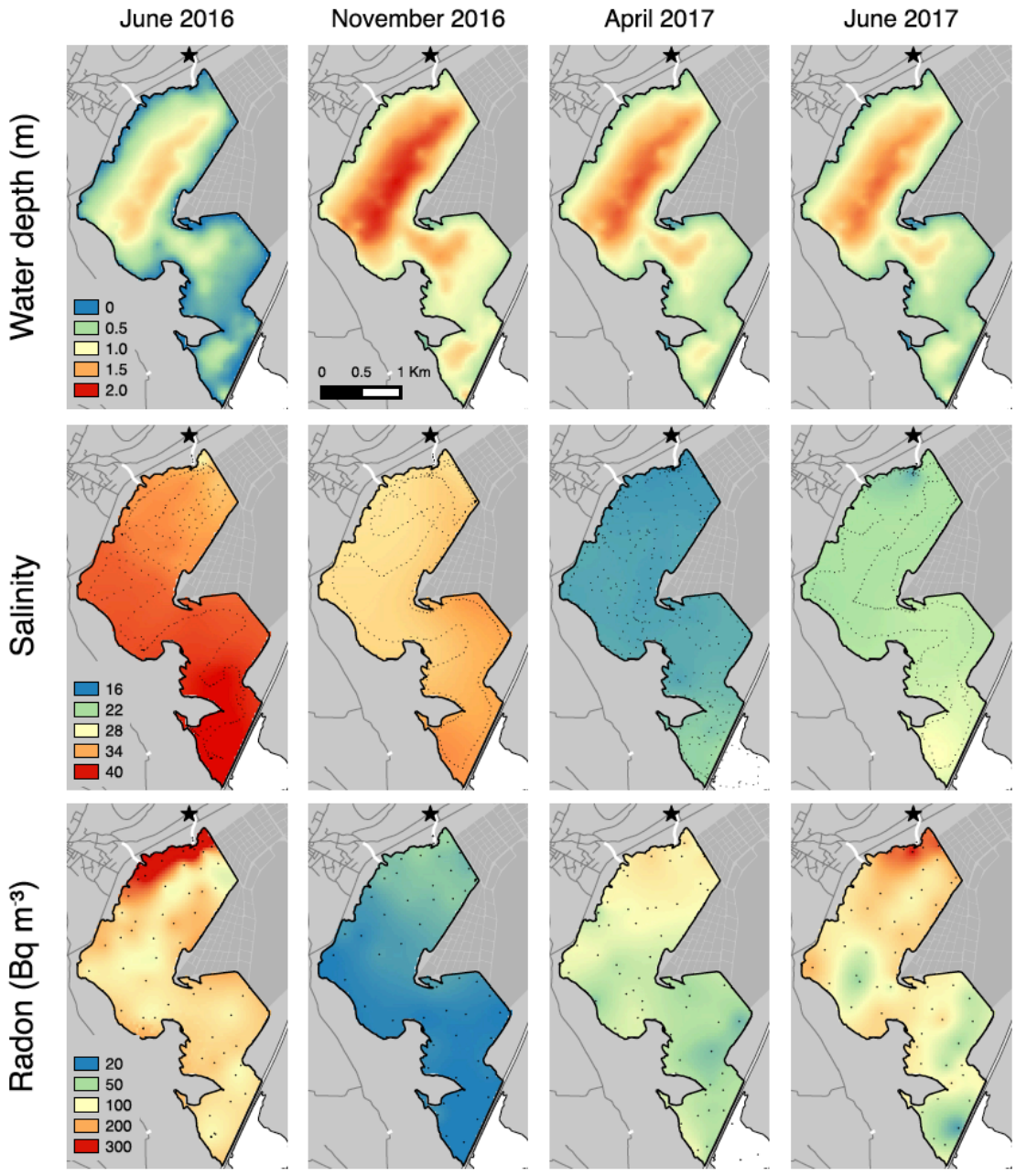

Figure 2.6| Seasonal distribution of radon and salinity and water levels in the northern basin of La Palme lagoon. Points used to derive the interpolation for salinity and radon grids are shown. The main karstic spring is indicated with a black star.

Table 2.1| Definition of the terms and values used in the mass balances for water and radon based on Equations 2.1 and 2.2. The terms estimated from the mass balance are highlighted in bold.

Term	Definition	June 16		November 16		April 16		June 17		Unit
		Value	Uncert.	Value	Uncert.	Value	Uncert.	Value	Uncert.	
Water balance										
A_N	Area Northern lagoon	4.1	0.4	4.4	0.4	4.4	0.4	4.4	0.4	$\cdot 10^6$ m^2
V_N	Volume Northern lagoon	2.5	0.2	5.3	0.5	4.4	0.4	4.0	0.4	$\cdot 10^6$ m^3
dV_N/dt	Change volume over time	-26	13	16	8	−15	7	−24	12	$\cdot 10^3$ m^3 d^{-1}
P	Precipitation	0.54	0.11	1.41	0.28	0.09	0.02	0.29	0.06	$\cdot 10^{-3}$ m^3 m^{-2} d^{-1}
E	Evaporation	6.9	1.7	3.3	0.8	6.0	1.6	6.5	1.8	$\cdot 10^{-3}$ m^3 m^{-2} d^{-1}
Q_{NC}	Water flow from N to S	3.9	1.9	1.3	0.6	3.9	2.0	4.1	2.0	$\cdot 10^3$ m^3 d^{-1}
Summary water flows										
$P \cdot A_N$	Total precipitation	2.2	0.5	6.3	1.4	0.4	0.1	1.3	0.3	$\cdot 10^3$ m^3 d^{-1}
$E \cdot A_N$	Total evaporation	28	7	15	4	27	8	29	8	$\cdot 10^3$ m^3 d^{-1}
Q_{NC}	Water flow from N to S	3.9	1.9	1.3	0.6	3.9	2.0	4.1	2.0	$\cdot 10^3$ m^3 d^{-1}
dV_N/dt	Change volume over time	−26	13	16	8	−15	7	−24	12	$\cdot 10^3$ m^3 d^{-1}
Q_g	**Karstic groundwater flow**	**3**	**15**	**25**	**9**	**15**	**11**	**7**	**15**	**$\cdot 10^3$ m^3 d^{-1}**
Radon balance										
dC/dt	Change radon concentration over time	0		0		0		0		Bq d^{-1}
C_g	Radon concentration groundwater	2600	110	2290	90	2570	90	2430	60	Bq m^{-3}
C_{Ra}	Ra226 concentration	30	20	30	20	30	20	30	20	Bq m^{-3}
C	Rn concentration in lagoon waters	120	20	23	7	65	17	93	24	Bq m^{-3}
λ	Rn decay constant	0.181		0.181		0.181		0.181		d^{-1}
k	Gas transfer velocity	0.3	0.1	3.1	1.0	1.1	0.5	0.6	0.4	m d^{-1}
F_{diff}	Radon diffusion flux from sediments	12.5	1.6	11.4	1.4	12.3	1.5	13.5	1.6	Bq m^{-2} d^{-1}
Summary radon fluxes										
dCV_N/dt	Change radon inventory over time	0		0		0		0		$\cdot 10^6$ Bq d^{-1}
$Q_g \cdot C_g$	Radon flux from karstic groundwater	9	39	57	20	39	28	18	36	$\cdot 10^6$ Bq d^{-1}
$\lambda \cdot V_N \cdot C_{Ra}$	Radon production from Ra decay	13	9	29	19	24	16	22	15	$\cdot 10^6$ Bq d^{-1}
$k \cdot A_N \cdot C$	Radon gas loss	130	50	310	140	320	170	250	160	$\cdot 10^6$ Bq d^{-1}
$\lambda \cdot V_N \cdot C$	Radon decay	85	20	18	6	52	14	75	21	$\cdot 10^6$ Bq d^{-1}
$F_{diff} \cdot A_N$	Total radon diffusion from sediments	51	8	51	8	55	9	60	9	$\cdot 10^6$ Bq d^{-1}
$F_{recirc} \cdot A_N$	**Total radon inputs from recirculation**	**140**	**70**	**190**	**140**	**250**	**170**	**220**	**170**	**$\cdot 10^6$ Bq d^{-1}**
F_{recirc}	**Rn inputs from recirculation**	**35**	**16**	**43**	**33**	**57**	**39**	**51**	**38**	**Bq m^{-2} d^{-1}**

2.4.3 Nutrients in lagoon surface waters

NO_3^- concentrations were significantly higher in the karstic groundwater spring (50 – 62 μmol L^{-1}) and in the sewage effluent (100 – 520 μmol L^{-1}) than in lagoon waters (0.1 – 65 μmol L^{-1}) (Fig. 2.7). The decrease of NO_3^- concentrations with increasing salinity observed in lagoon waters (Fig. 2.7) clearly indicates a low-salinity source of NO_3^- (sewage effluent and/or groundwater spring) and a diminution of concentrations due to mixing with NO_3^--poor lagoon waters and NO_3^- removal chiefly due to biological uptake (Capone 2008). No clear nutrient patterns were observed for NH_4^+ and PO_4^{3-} vs salinity (Fig. 2.7). Concentrations of NH_4^+ in the karstic groundwater spring (0.1 – 0.5 μmol L^{-1}) and in the sewage effluent (2.6 – 16 μmol L^{-1}) were lower or comparable to concentrations in lagoon waters (0.8 – 36 μmol L^{-1}), whereas PO_4^{3-} concentrations in the sewage effluent (22 – 71 μmol L^{-1}) were significantly higher than concentrations in both karstic groundwaters (0.1 – 0.4 μmol L^{-1}) and lagoon waters (0.1 – 2.5 μmol L^{-1}). The low NH_4^+ and PO_4^{3-} concentrations measured in karstic groundwater and in the sewage effluent (only for NH_4^+), together with the lack of any clear nutrient-salinity pattern (Fig. 2.7), suggest that neither the karstic spring nor the sewage effluent are significant sources of these nutrients to lagoon waters. Relatively high concentrations for both NH_4^+ and PO_4^{3-} were indeed measured at mid to high salinity lagoon waters, corresponding to areas far from both the sewage and karstic groundwater inputs. This distribution suggests that there is either production of NH_4^+ and PO_4^{3-} in the water column, which is unlikely given its aerobic nature (Christensen et al. 2000), or an additional source of these nutrients, most likely inputs from sediments due to diffusion and/or lagoon water recirculation.

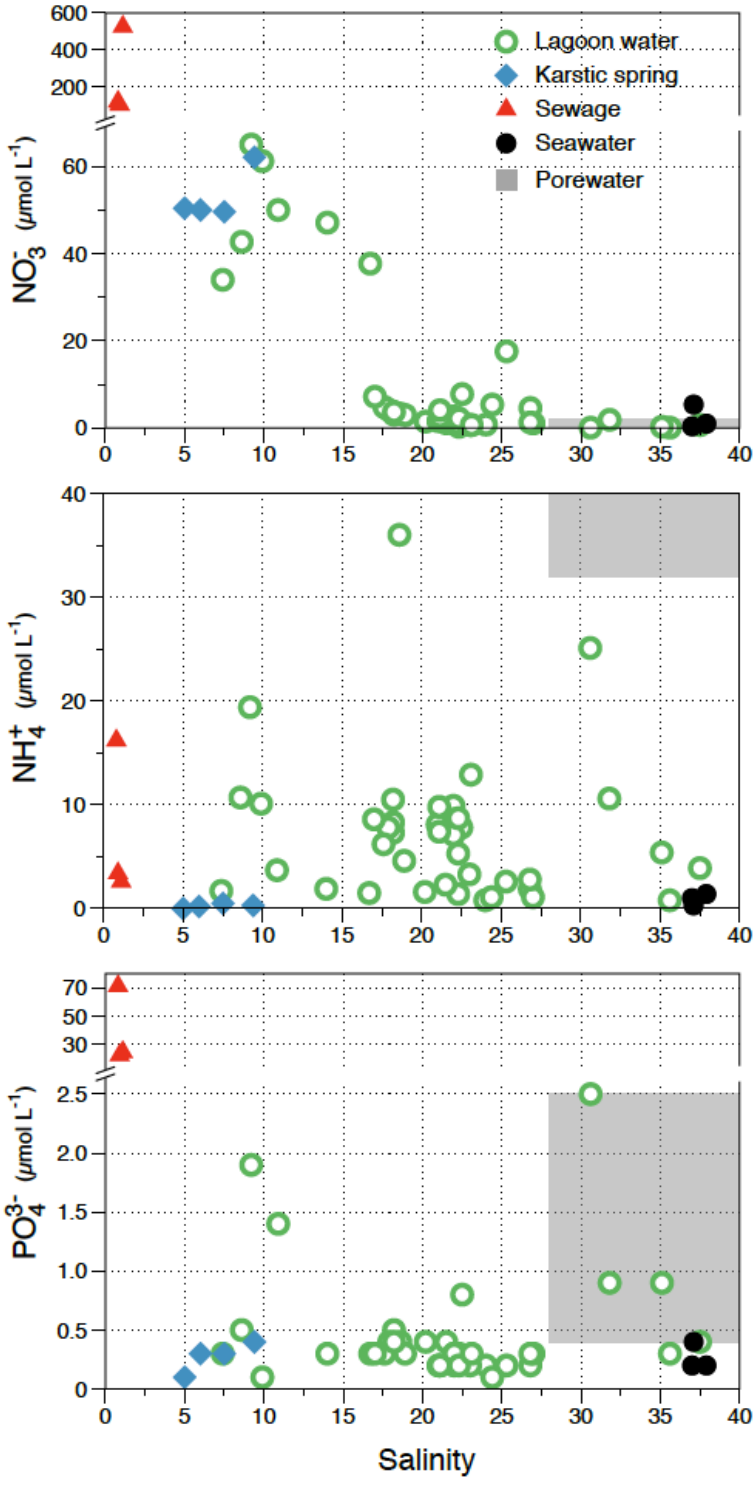

Figure 2.7| Dissolved inorganic nutrient (NO_3^-, NH_4^+ and PO_4^{3-}) concentrations in lagoon waters, the karstic spring, the sewage effluent and seawater endmembers, as a function of water salinity. The gray area represents the range of nutrient concentrations and salinities covering 66% of porewater samples (it extends to a salinity of 61 and to a NH_4^+ concentration of 180 µmol L^{-1}).

2.4.4 Estimation of karstic groundwater and recirculation inputs from water and radon mass balances

Water (Eq. 2.1) and radon (Eq. 2.3) mass balance equations were solved analytically for the four seasonal samplings, and uncertainties were propagated throughout each term. The values used and the approach followed to estimate all terms in the water (Eq. 2.1) and radon (Eq. 2.3) mass balances are described in the following sections (2.4.4.1 – 2.4.4.2) and summarized in Table 2.1 and Table 2.2.

2.4.4.1 Water mass balance

The terms in the water mass balance were estimated for a period of 30 days prior to the surveys, and thus karstic groundwater estimates represent average water flows for the same period of time. Water levels measured continuously for ~1 month in April 2017 and June 2017 (Fig. 2.8) were used to estimate the water volume change over time ($\frac{\partial V_N}{\partial t}$) for April 2017 and June 2017 campaigns. The trend derived from monthly measurements of water level at 2 different stations in the northern lagoon (PN1 and PN3; Fig. 2.2) was used as estimate for $\frac{\partial V_N}{\partial t}$ for June 2016 and November 2016 campaigns. The Penman equation was used to estimate evaporation rates (E) from air temperature, wind speed, relative humidity and net solar irradiance (Penman 1948). This equation has already been tested and applied in similar lagoons on the French Mediterranean coastline (IFREMER 2010). Following Stieglitz et al. (2013) and assuming that the exchange between the lagoon and the sea is negligible and the volume of the southern and central basins is relatively constant over time, the water flow from the northern section of La Palme lagoon to the central basin (Q_{NC}) equals the total evaporative loss minus precipitation in the central and southern basins ($Q_{NC} = (E\text{-}P)\cdot A_{C+S}$). Estimated Q_{NC} water flows are on the order of $(1 - 4)\cdot 10^3$ m^3 d^{-1}, which are in relatively good agreement with the estimated water flows for June 2017 using the drag-tilt current meter installed under the railway bridge (average of $(1 \pm 7)\cdot 10^3$ m^3 d^{-1}).

By solving Eq. 1.1 for each survey, karstic groundwater flow to La Palme lagoon (Q_g) is estimated to range from $(3 \pm 15)\cdot 10^3$ m^3 d^{-1} in June 2016 to $(25 \pm 9)\cdot 10^3$ m^3 d^{-1} in November 2016 (Table 1.1). These flows are in good agreement with

previous estimates of karstic groundwater flows into La Palme lagoon (Wilke and Boutière 2000; Stieglitz et al. 2013). The estimated groundwater flows have large uncertainties (relative uncertainties sometimes higher than 100%), which are mainly derived from the assumed uncertainty of 50% associated with $\frac{\partial V_N}{\partial t}$, and make difficult to evaluate the seasonal variability of groundwater inputs. However, as previously observed by Wilke and Boutière (2000), karstic groundwater inputs into La Palme lagoon during the wet season (November 16 and April 17) are consistently higher than during the dry season (June 16 and June 17). This seasonal variability in karstic groundwater inputs is likely linked to variations on the terrestrial hydraulic gradient, as commonly observed in groundwater studies in coastal systems (Holliday et al. 2007; Smith et al. 2008; Garcia-Solsona et al. 2010b; Rodellas et al. 2012).

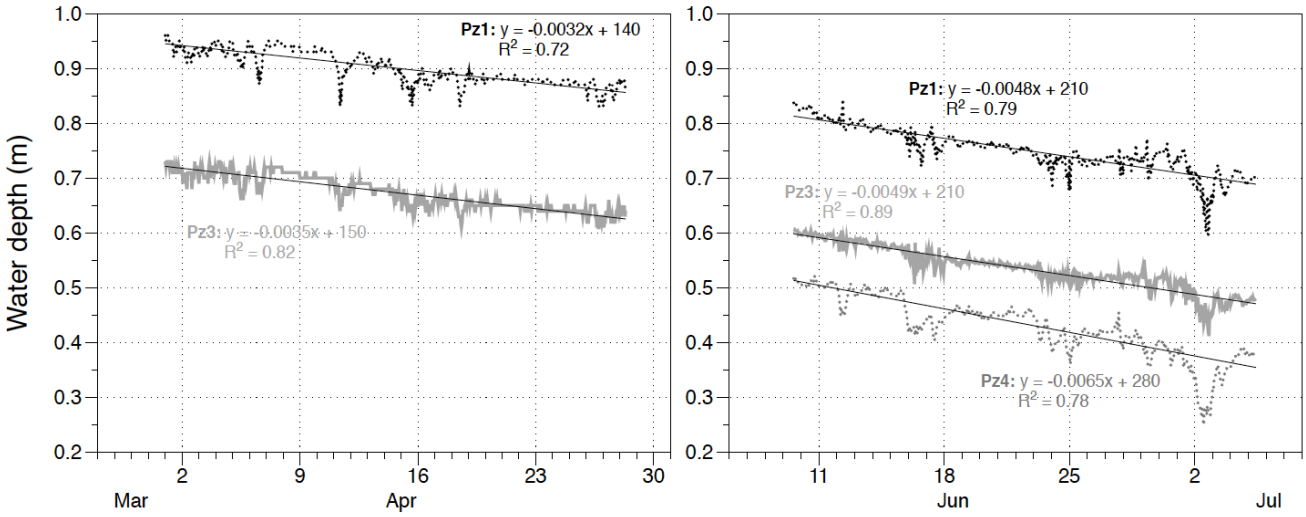

Figure 2.8| Evolution of water depths in the northern basin of La Palme lagoon in April and June 2017. Average changes in lagoon water level over time derived from linear regressions (-0.0034 and -0.0054 m d^{-1} for April and June 2017, respectively) were used to estimate $\frac{\partial V_N}{\partial t}$ for April 2017 and June 2017 campaigns. The short-term variations on water depth are likely produced by rapidly changing wind conditions and are expected to have a minor influence on the water mass balance.

2.4.4.2 Radon mass balance

In a system with reduced exchange with offshore waters, the rate of radon decrease from the water column will follow $e^{-(\lambda t+\frac{k}{h}t)}$, where λ is the radon decay constant (0.181 d^{-1}), t is the time, k is the radon gas transfer velocity and h the water depth. Considering an average k and h of 1.3 m d^{-1} and 0.9 m for La Palme lagoon, respectively (Table 2.1), less than 5% of the initial radon inventory would remain in the system after 2 days. Therefore, unlike the water mass balance, radon concentrations measured in the lagoon during the different surveys mainly reflected the dynamics of radon inputs and outputs during the 48 hours previous to the sampling. Provided that there are no abrupt changes in wind regimes during these previous hours, it is thus reasonable to assume relatively constant radon inventories during these 2-day periods (i.e. $\frac{\partial CV_N}{\partial t} = 0$) (see section 2.5.2. for further discussion).

Q_{gw} was estimated in the water mass balance as the average karstic groundwater flow for the month previous to the survey. By using these estimates in the radon mass balance we are implicitly assuming that Q_{gw} is constant during these periods and thus representative of groundwater inputs during the 48 hours previous to the sampling.

The diffusive flux of radon from sediments (F_{diff}) was estimated from a depth-independent approach following (Martens et al. 1980; Cook et al. 2008):

$$F_{diff} = (c_{eq} - c_L)\sqrt{\lambda\theta D_s} \qquad (2.4)$$

where θ is sediment porosity, D_s is the diffusion coefficient of radon in sediments and c_{eq} and c_L are radon concentration in equilibrium with sediments and in lagoon water, respectively. D_s was estimated as a function of temperature (T) and corrected for tortuosity ($D_s = \theta(10^{-[(980/T)+1.59]}$; (Peng et al. 1974; Ullman and Aller 1982). A sediment porosity of 0.47, 0.43, 0.39 and 0.71 was used or Pz1, Pz2, Pz3 and Pz4, respectively, as estimated in a concurrent study in La Palme lagoon (Tamborski et al. 2018). c_{eq} was derived from equilibration experiments (depth-averaged radon equilibrium concentration of 4700 ± 900, 3400 ± 500, 7600 ± 1100 and 5500 ± 900 Bq m^{-3} for Pz1, Pz2, Pz3 and Pz4, respectively) and c_L was

considered negligible in comparison with c_{eq}. According to the distribution of surficial sediments in La Palme lagoon (IFREMER 2003), we assumed that results obtained from Pz1, Pz2, Pz3 and Pz4 are representative of 20%, 15%, 40% and 25% (assumed absolute uncertainty of ± 5%), respectively, of the total sediment surface area of the northern basin of La Palme lagoon, resulting in average radon diffusion fluxes on the order of 10 - 15 Bq m^{-2} d^{-1}. Dissolved ^{226}Ra concentration measured in lagoon waters ranged from 10 to 50 Bq m^{-3}, in good agreement with previous estimates for La Palme lagoon (Stieglitz et al. 2013).

Wind-dependent gas transfer velocities (k) were estimated from the empirical equation of (MacIntyre et al. 1995), normalized for radon in seawater and the specific water temperature at each sampling (Wanninkhof 2014):

$$k_{(cm/h)} = 0.45u^{1.6}\left(\frac{Sc}{660}\right)^{-0.5} \qquad (2.5)$$

where u is the wind speed [m s^{-1}], Sc is the Schmidt number for radon at a given temperature (Wanninkhof 2014), and $k_{(cm/h)}$ is the gas transfer velocity in [cm h^{-1}]. To obtain a representative k value for each seasonal sampling, we used the wind speed (± its uncertainty) that covers the range comprised between the 1st and 3rd quartiles of all the hourly wind measurements during the 48-h previous to the sampling. Wind speeds ranged from 2.0 ± 0.3 m s^{-1} in June 2017 to 9.9 ± 2.1 m s^{-1} in November 2016, resulting in estimates of k ranging from 0.3 ± 0.1 to 3.1 ± 1.0 m d^{-1} (Table 1.1). The uncertainties associated with these estimates are derived from the variation of wind speeds, and thus, they do not take into account uncertainties associated with the empirical equation to estimate k (see section 2.5.2).

The net flux of radon driven by recirculation of lagoon water through sediments (F_{recirc}) can be estimated by solving Eq. 2.3, resulting in radon fluxes ranging from 35 ± 16 to 57 ± 39 Bq m^{-2} d^{-1}. These radon fluxes are in good agreement with the previous estimates for La Palme lagoon in summer of 17-66 Bq m^{-2} d^{-1} (Stieglitz et al. 2013). Net fluxes of radon driven by recirculation of lagoon water through sediment for the different samplings are similar and do not show any seasonal pattern, partially due to the large relative uncertainties associated with these estimates.

2.4.4.3 Recirculation water flows to La Palme lagoon

Volumetric flows of lagoon water recirculating through sediments can be obtained by dividing the radon flux by the radon concentration in porewaters inflowing to the lagoon, i.e. the recirculation endmember. The radon concentration of the recirculation endmember is the concentration in porewaters immediately below the sediment-water interface (subtracting the concentration in overlying waters) (Cook et al. 2018a; b). We thus used the radon concentration from the shallowest porewater sample from each piezometer, which was collected at 5 cm from the sediment-water interface. An average radon concentration for the recirculation endmember was obtained for each sampling period by area-weighting the concentrations in the different piezometers according to their spatial representativeness.

The estimated water flows of lagoon water recirculating through sediments derived from the radon mass balance to the northern section of La Palme lagoon range from $(42 \pm 33) \cdot 10^3$ to $(89 \pm 44) \cdot 10^3$ m^3 d^{-1} and are summarized in Table 2.3. These flows are in good agreement with previous estimates of recirculation flows in La Palme lagoon from tracer-derived approaches (Stieglitz et al. 2013; Tamborski et al. 2018), which were only focused on the summer season. Recirculation flows estimated here are significantly higher than karstic groundwater inputs (Table 2.3) and are equivalent to 0.5 - 5% of lagoon water volume recirculating through bottom-sediments every day.

Table 2.2| Summary of the approaches used to estimate values and uncertainties of all the terms used on Equations 2.1-2.4.

Term	Definition	Estimation of value	Estimation of uncertainty
Water balance			
A_N	Area Northern lagoon	Digitalization from GoogleEarth images + bathymetry grids	Relative unc. of 10% assumed
A_{C+S}	Area Central and Southern lagoon	Digitalization from GoogleEarth images + bathymetry grids	Relative unc. of 10% assumed
V_N	Volume Northern lagoon	A_N * average depth from bathymetry grids	Relative unc. of 10% assumed
dV_N/dt	Change volume over time	Water level change from PN monthly measurements (June 16, November 16) and water level loggers (April 17, June 17)	Relative unc. of 50% assumed
P	Precipitation	Average precipitation 30 days before surveys (MétéoFrance)	Relative unc. of 20% assumed
E	Evaporation	Average evaporation 30 days before surveys, derived from Penman equation and weather data (MétéoFrance)	Standard deviation
Q_{NC}	Water flow from N to S	$(P - E) * A_{C+S}$	Propagation uncertainties
Q_g	Karstic groundwater flow	Water mass balance (Eq. (1))	Propagation uncertainties
Radon balance			
dC/dt	Change radon concentration over time	Assumed to be 0	–
C_g	Radon concentration groundwater	Radon measured in karstic spring	Analytical uncertainty
C_{Ra226}	Ra226 concentration	Average ^{226}Ra concentration in surface waters (n = 10)	Range covering all values
C	Rn concentration in lagoon waters	Weighted-average radon (from radon distribution grid)	Range covering distribution grids of min and max radon
λ	Rn decay constant	Known	–
θ	Porosity	Calculated in Tamborski et al. (submitted)	–
D_s	Radon diffusion coefficient	After Peng et al. (1974) and Ullman and Aller (1982)	–
c_{eq}	Radon in equilibrium with sediments	Equilibration experiments (average of 3 samples at each piezometer)	Standard deviation
$A_{sed\text{-}pz}$	Sediment area representative of each Pz	Estimated from sediment distribution maps (IFREMER, 2003)	Absolute unc. of 5% assumed
F_{diff}	Radon diffusion flux from sediments	Depth-independent approach (Eq. (4))	Propagation uncertainties
u	Wind speed	Average hourly wind speed from 48 h before the survey	Range covering 50% of hourly wind speeds (Q1-Q3)
k	Gas transfer velocity	After MacIntyre equation (Eq. (5))	Propagation uncertainties
F_{recirc}	Rn inputs from recirculation	Radon mass balance (Eq. (3))	Propagation uncertainties

2.4.5 Nutrient fluxes from karstic groundwater and recirculation

The most commonly applied approach to estimate groundwater-driven nutrient fluxes to a surface water body is to multiply the water flow by the representative concentration in the groundwater endmember (Charette1 and Buesseler 2004; Santos et al. 2009; Liu et al. 2012; Tovar-Sánchez et al. 2014). The karstic spring inflowing to La Palme lagoon can be directly sampled and therefore the nutrient fluxes driven by karstic groundwater discharge can be accurately estimated (Table 2.3). Given that the nutrient concentrations in the spring were relatively constant throughout the year, these fluxes follow the same seasonal pattern as groundwater flows, with maximum fluxes of NO_3^-, NH_4^+ and PO_4^{3-} of 1200 ± 400, 12 ± 4 and 8.7 ± 3.0 mol d^{-1} in November 2016 (Table 2.3).

The recirculation-driven nutrient inputs were estimated from the recirculation-driven radon flux and the excess (in relation to overlying water) ratio of nutrient over radon concentrations in porewaters. Excess ratios from samples collected at 5 cm below the sediment-water interface at each piezometer were averaged considering their spatial representativeness to obtain an average excess ratio for each sampling period. Estimated net nutrient fluxes driven by lagoon water recirculation to La Palme lagoon (Table 2.3) are on the order of 1900 – 5500 mol d^{-1} for NH_4^+ and 22 – 71 mol d^{-1} for PO_4^{3-}. NO_3^- concentrations in porewaters are comparable or lower than in overlying waters, suggesting that recirculation of lagoon water in La Palme lagoon is not a relevant source of NO_3^- and it could act mainly as a sink.

Table 2.3| Water flows, endmember nutrient concentrations and nutrient fluxes from karstic groundwater and lagoon water recirculation to the northern basin of La Palme lagoon for the different surveys. The recirculation nutrient endmember refers to weighted-average excess nutrient concentrations (samples collected at 5 cm below the sediment-water interface at each piezometer) for each survey.

	Water flow		Nutrient endmember			Nutrient flux					
			NO_3^-	NH_4^+	PO_4^{3-}	NO_3^-		NH_4^+		PO_4^{3-}	
	$\cdot 10^3$ m^3 d^{-1}	Δ	µmol L^{-1}	µmol L^{-1}	µmol L^{-1}	mol d^{-1}	Δ	mol d^{-1}	Δ	mol d^{-1}	Δ
June 2016											
Karstic groundwater	**3**	15	62	0.28	0.43	**220**	900	**1.0**	4.3	**1.5**	6.5
Recirculation	**89**	44	−2.7	21	0.79	**−240**	130	**1900**	900	**71**	36
November 2016											
Karstic groundwater	**25**	9	48	0.49	0.35	**1200**	400	**12**	4	**8.7**	3.0
Recirculation	**42**	33	−8.1	103	1.0	**−340**	280	**4400**	3400	**43**	34
April 2017											
Karstic groundwater	**15**	11	51	0.12	0.10	**780**	540	**1.7**	1.2	**1.5**	1.0
Recirculation	**48**	32	−1.8	115	1.3	**−87**	59	**5500**	3800	**60**	41
June 2017											
Karstic groundwater	**7**	15	50	0.17	0.25	**360**	730	**1.2**	2.4	**1.8**	3.7
Recirculation	**55**	43	−0.6	87	0.39	**−35**	27	**4900**	3700	**22**	17

2.5 Discussion

2.5.1 Uncertainties on estimated radon, water and nutrient fluxes from recirculation

2.5.1.1 Net radon fluxes from recirculation

The uncertainties associated with net radon fluxes via recirculation derived from the mass balance approach (Table 2.1, Table 2.2) largely depend on the accuracy of determining those input and output terms with a high relative contribution to the mass balance. Lagoon water recirculation is the largest source of radon to La Palme lagoon (accounting for > 60% of total inputs; Table 2.1). The second most relevant source is radon diffusion from sediments, which accounts for 15-25% of total inputs. Estimated radon diffusive fluxes are in good agreement with previous estimates in La Palme obtained via alternative approaches (Stieglitz et al. 2013), suggesting that this input term is relatively well constrained. Potential errors in estimating the other radon source terms (karstic groundwater inputs and production from ^{226}Ra decay) have a small influence on final radon budget estimates and uncertainties.

Radon evasion to the atmosphere (60-90% of total outputs) and radon decay (5-40%) are the main radon output terms. Recirculation-driven radon flux estimates are thus highly sensitive to k and C, and thus, on the uncertainties associated with these terms. By selecting wide uncertainties of wind speeds (u covering the values between 1st and 3rd quartiles of wind data during the 48-h prior to sampling) and radon concentration in lagoon waters (covering the range between maximum and minimum C estimates), we are likely accounting for the real variability and covering the representative u and C for each sampling period. However, these estimates only take into account those uncertainties associated with the different parameters, and do not consider those structural uncertainties related to the approach assumptions, which are difficult to accurately constrain.

The most critical assumption of the radon mass balance is that the empirical McIntyre equation (MacIntyre et al. 1995) provides accurate estimates of k from measured wind speeds (as commonly done in the literature; (Burnett and Dulaiova 2003; Dimova and Burnett 2011). Recent studies have suggested that

this equation might not be appropriate for shallow environments like coastal lagoons (Cockenpot et al. 2015). Had we used other empirical equations we would have obtained significantly different results, but most likely within the uncertainties of the current estimates: e.g. using an equation derived from Kremer et al. (2003) for shallow environments, we would have estimated recirculation-driven radon fluxes from 30% lower (in June 2016) to 60% higher (in November 2016) than those obtained using the MacIntyre et al. (1995) gas-exchange equation.

Another critical assumption of the radon mass balance is assuming constant radon inventories during the 2-day period before surveys (i.e. $\frac{\partial CV_N}{\partial t} = 0$). Radon concentrations might be highly variable over short temporal scales as a consequence of temporally variable wind-dependent radon evasion to the atmosphere, and thus dynamic modelling is often more appropriate than steady state mass balances (Dimova and Burnett 2011; Stieglitz et al. 2013; Gilfedder et al. 2015). During a 1-month time series, (Gilfedder et al. 2015) found that radon concentrations in surface water from a shallow (1-2 m) wetland could decrease up to ~20% as consequence of wind speeds exceeding 5 m s^{-1}. A daily decrease in radon concentrations by ~20% in La Palme lagoon (i.e. $\frac{\partial CV_N}{\partial t}$ = $-2 \cdot 10^7$ - $8 \cdot 10^7$ Bq d^{-1}, depending on the survey) would result on estimated radon fluxes from recirculation 10% – 40% smaller than those estimated assuming constant radon inventories. Given that the surveys were conducted in periods with relatively constant wind conditions (for the 48 hours before sampling), we expect changes on radon concentrations and inventories over time not to be higher than the example above.

2.5.1.2 Estimation of recirculation-driven water flows and net nutrient fluxes

In addition to the uncertainties associated with radon fluxes (Discussed above), the appropriate characterization of the radon concentration in the recirculation endmember is also a critical component of the final radon-derived water flow estimates (Gonneea et al. 2013; Cerdà-Domènech et al. 2017; Cook et al. 2018a;

b). Whereas it is clear that the radon concentration of porewater that should be used as recirculation endmember is the concentration immediately below the sediment-water interface, the depth at which a porewater concentration should be measured depends upon the hydrodynamic dispersivity (Cook et al. 2018a; b).

In a concurrent study conducted in La Palme lagoon by Cook et al. (2018a), the vertical porewater radon profiles were simulated using water recirculation model (advection cycling model) that allows estimating recirculation fluxes. The shape of the radon profiles collected at Pz1 suggests that recirculation fluxes are driven by pressure gradients reversing at short temporal scales (< 0.5 h). Winds forcing appears to be the main driver of recirculation, as already suggested by Stieglitz et al. (2013). The study demonstrated that for solute transport on the order of 0.5 – 1 m, the endmember concentration should be measured within 1 cm of the sediment surface. Collecting porewaters at such shallow depths for radon analysis is virtually impossible. In this study, we acknowledge that by using radon concentrations from porewaters at 5 cm as endmembers rather than at 1 cm we are underestimating the water flow, and thus the flows provided here are conservative estimates.

Estimating the recirculation-driven nutrient flux also requires an accurate estimation of the excess ratio of nutrient over radon concentrations in the recirculation endmember. Whereas this approach also requires characterizing the ratio in discharging porewaters (i.e. within 1 cm below the sediment-water interface), the excess nutrient-radon concentration ratios of those nutrients produced in sediments (such as NH_4^+ and PO_4^{3-}; Fig. 2.9) vary significantly less with depth than absolute radon and nutrient concentrations do. Therefore, using the excess concentration ratios from the shallowest porewater sample (at 5 cm below the sediment-water interface) may provide a better constraint on the recirculation endmember, compared to absolute concentrations alone.

The estimation of recirculation water flows and net nutrient fluxes also relies on the assumption that the three piezometers used are representative of large specific sediment areas. This assumption alone can potentially introduce much

larger uncertainties than those associated to parameter determination. Although the number of profiles is small, the relative similitude of radon concentrations and radon-nutrient ratios from the different profiles provides some level of confidence in the extrapolation.

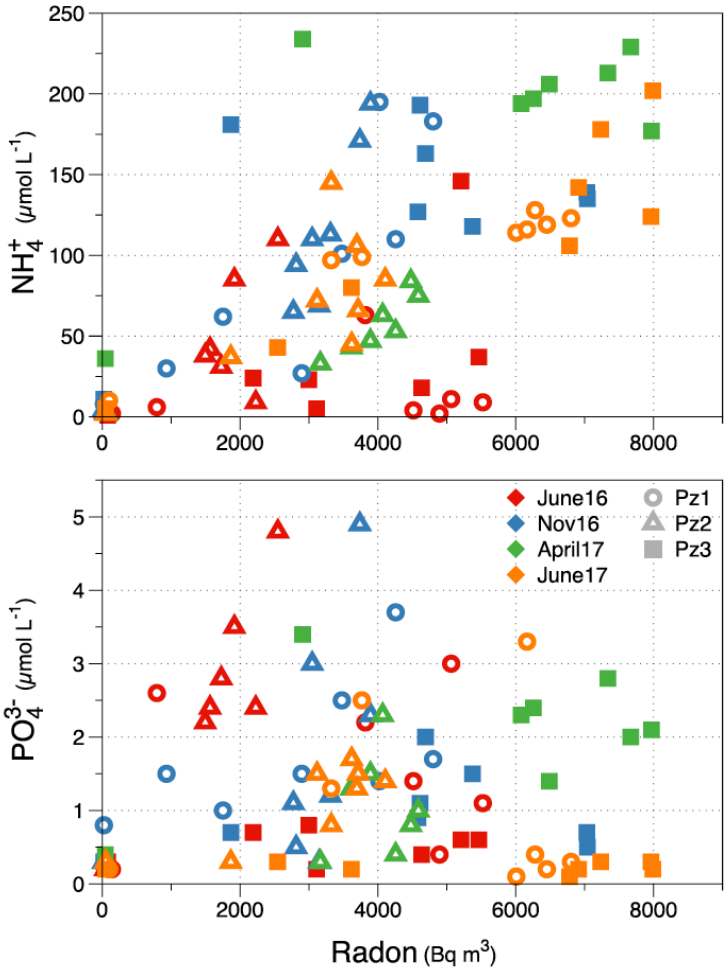

Figure 2.9| Concentration of NH_4^+ and PO_4^{3-} plotted against radon concentrations in porewaters, arranged by piezometer and sampling campaign.

2.5.2 Nutrient fluxes to La Palme lagoon

2.5.2.1 Nutrient fluxes from karstic groundwater and lagoon water recirculation

As commonly observed in other carbonate systems, groundwater-driven fluxes of dissolved inorganic nitrogen (DIN, mainly in the form of NO_3^- because highly oxic groundwater conditions limit denitrification) are significantly higher than those of dissolved inorganic phosphorous (DIP = PO_4^{3-}) (Table 2.3; Fig. 2.10). Whereas P is rapidly removed from groundwater through co-precipitation with dissolved Ca (Slomp and Van Cappellen 2004; Hernández-Terrones et al. 2011; Weinstein et al. 2011), high DIN concentrations are commonly found in fast-flowing groundwater systems, such as karsts, mainly as a consequence of anthropogenic N inputs (e.g. fertilizers, manure, wastewater) and the lack of major removal processes (Slomp and Van Cappellen 2004; Weinstein et al. 2011; Tovar-Sánchez et al. 2014).

Estimated nutrient fluxes from recirculation in La Palme lagoon reveal that sediments constitute a source of NH_4^+ and PO_4^{3-}, and a sink of NO_3^- (Table 2.3; Fig. 2.10). The cycling and transformation of nutrients in sediments is governed by several factors, such as the content of organic matter, dissolved oxygen, the type of sediments, as well as the processes and conditions in the overlying water column (Middelburg and Levin 2009; Rigaud et al. 2013; Ni et al. 2017). Biogeochemical nutrient cycling in permeable sediments has been studied extensively (Slomp and Van Cappellen 2004; Kroeger and Charette 2008; Anschutz et al. 2009; Huettel et al. 2014; Devol 2015). Mechanisms of NO_3^- production/consumption in sediment largely depend on oxygen conditions, generally resulting in NO_3^- production from sediments under oxic conditions due to nitrification and in NO_3^- consumption in sediments with low oxygen content, mainly due to denitrification or dissimilatory nitrate reduction to ammonium (DNRA) (Slomp and Van Cappellen 2004; Rigaud et al. 2013; Devol 2015). NO_3^- reduction processes and organic matter mineralization during early diagenesis, in particular under low oxygen conditions, result in the formation of various remineralization products, such as NH_4^+ and, to a lesser extent, PO_4^{3-} (Middelburg and Levin 2009; Rigaud et al. 2013; Devol 2015). Whereas under

slow diffusion-dominated nutrient fluxes most of the produced NH_4^+ is nitrified in surface oxic sediments, rapid recirculation fluxes in permeable sediments (which allow for a continuous supply of NO_3^- and organic compounds from the water column) favor the release of NH_4^+ from the sediment, bypassing the nitrification zone (Rao et al. 2008; Kessler et al. 2012; Huettel et al. 2014). Lagoon sediments can sequester and bury PO_4^{3-} dissolved in lagoon waters, which can later be released to porewater mainly due to the aerobic and anaerobic mineralization of organic matter during early diagenesis (Mesnage and Picot 1995; Anschutz et al. 2007; De Vittor et al. 2016). Thus, advective flushing of sediments under slightly oxic or anoxic conditions could explain recirculation-driven inputs of NH_4^+ and PO_4^{3-}, as well as the removal of NO_3^-.

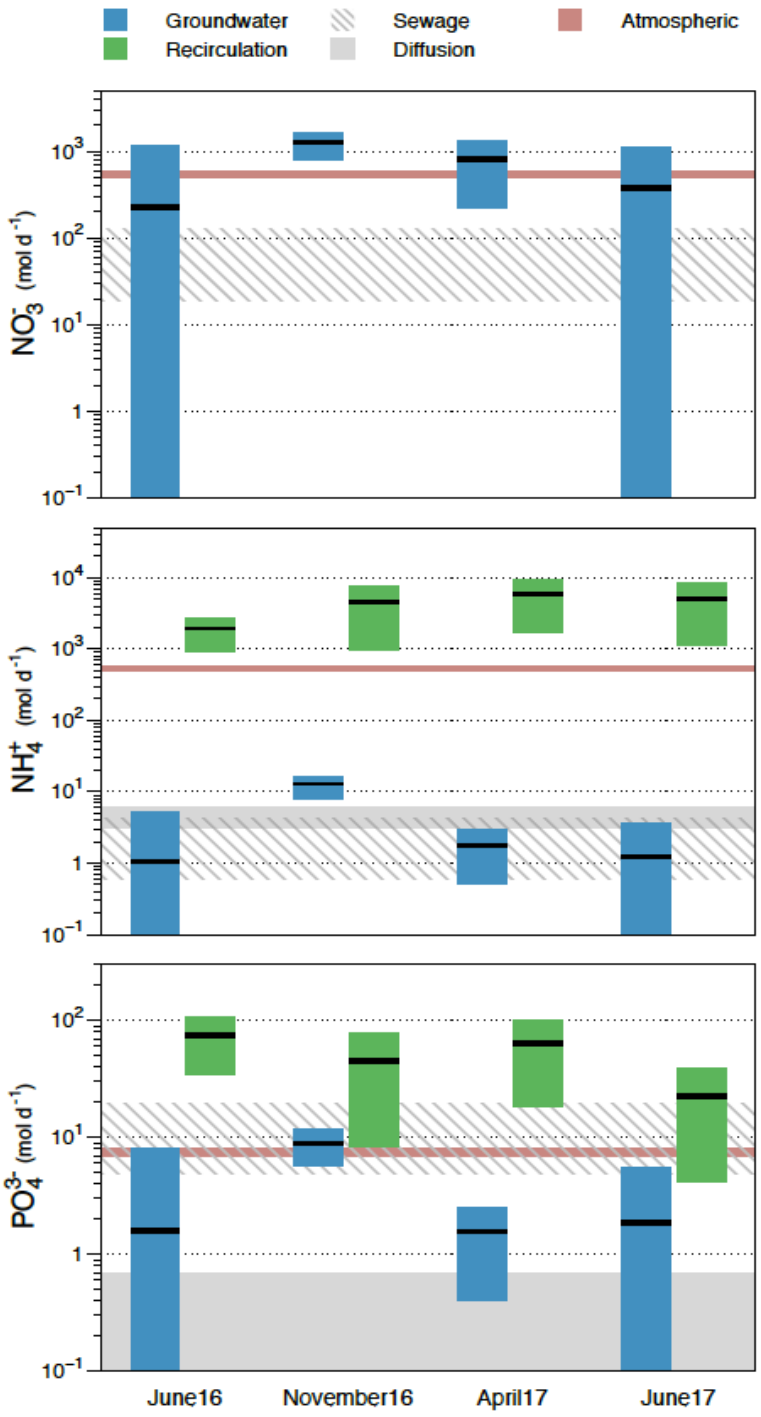

Figure 2.10| Fluxes of dissolved inorganic nutrients to the northern basin of La Palme lagoon driven by terrestrial groundwater discharge, lagoon water recirculation, diffusion, inputs from the sewage treatment plant and atmospheric deposition estimated for the different surveys. Boxes cover the range between minimum and maximum estimates (negative values not included), and black lines represent the average value. Inputs from atmospheric deposition on NO_3^- and NH_4^+ panels refer to total DIN fluxes.

2.5.2.2 Comparison of potential sources of nutrient to the lagoon

To evaluate the significance of groundwater processes as conveyors of dissolved inorganic nutrients to La Palme lagoon, the estimated fluxes can be compared to the other potential sources of nutrients to the lagoon, including discharges from the sewage treatment plant, diffusion from sediments and atmospheric deposition.

Inputs of NO_3^-, NH_4^+ and PO_4^{3-} from the sewage treatment plant are on the order of 70 ± 50, 2.4 ± 1.9 and 12 ± 7 mol d^{-1}, respectively, as estimated from the water flows from the sewage treatment plant and the average nutrient concentrations measured in the effluent (Fig. 2.10). Inputs of nutrients from atmospheric deposition are derived from reported atmospheric DIN (120 – 130 µmol m^{-2} d^{-1}) and DIP fluxes (1.5 – 1.8 µmol m^{-2} d^{-1}) in the nearby "Cap Bear" station (~50 km south of La Palme lagoon) (Markaki et al. 2010), resulting in atmospheric fluxes of 550 – 580 mol d^{-1} for DIN and 7 – 8 mol d^{-1} for DIP.

Diffusive fluxes of nutrients from sediments were calculated by applying Fick's first law (De Vittor et al. 2016). The specific diffusion coefficients of the evaluated nutrients were derived from (Schwarzenbach et al. 2002) and corrected for water temperature at each survey following (Li and Gregory 1974). Diffusion fluxes were estimated using the measured nutrient gradients in shallow porewaters (from 0 to 5 cm below the sediment-water interface). Considering all the surveys and piezometers, estimated fluxes of nutrients driven by molecular diffusion from sediments are on the order of 3 - 5 mol d^{-1} for NH_4^+ and 0.01 – 0.7 mol d^{-1} for PO_4^{3-} (negative fluxes are obtained for NO_3^- given the higher concentrations in overlying waters than in porewaters) (Fig. 2.10).

Despite the large uncertainties of these estimates, a comparison between all the potential nutrient sources (Fig. 2.10) reveals that karstic groundwater represents the main source of NO_3^- to La Palme lagoon. Inputs of DIN from atmospheric deposition are likely comparable to karstic groundwater-driven fluxes of NO_3^-. However, for NH_4^+ and PO_4^{3-}, the recirculation of lagoon water through sediments is the most important nutrient source, accounting on average for >80% and > 50% of total NH_4^+ and PO_4^{3-} inputs to La Palme lagoon,

respectively. The estimated nutrient contribution from karstic groundwater and recirculation inputs is indeed in good agreement with the distribution of nutrients in lagoon waters of La Palme (Fig. 2.7): highest concentrations of NO_3^- were measured in low-salinity waters, indicating a low-salinity high-NO_3^- source (i.e. karstic groundwater discharge), and concentrations decreased with distance from this source. In contrast, concentrations of NH_4^+ and PO_4^{3-} did not show any clear pattern with salinity, with maximum concentrations found in mid-salinity waters located far from sewage and karstic groundwater inflows, which is consistent with inputs of NH_4^+ and PO_4^{3-} from recirculation of lagoon water through sediments (Fig. 2.7).

2.5.2.3 Water recirculation and terrestrially-driven dissolved silica fluxes

In a concurrent study in Palme lagoon by Tamborski et al. (2018) that I contributed (but not part of this thesis), we estimated the fluxes of dissolved silica into the lagoon using Ra isotope mass balance. Dissolved silica is a major nutrient which partly supports diatom primary productivity in coastal ecosystems (Tréguer and De La Rocha 2013). Like nitrogen and phosphorus, silica is also generally enriched in terrestrial groundwater (Tovar-Sánchez et al. 2014; Rahman et al. 2019) and porewater (Weinstein et al. 2011; Anschutz et al. 2016; Cho et al. 2018), making dissolved silica useful tracer of groundwater discharge (Garcia-Solsona et al. 2010b). In this study, Ra mass balance was constructed to assess the relative importance of dissolved silica inputs from the karstic groundwater spring compared to lagoon water recirculation during June 2016. The results showed that dissolved silica flux driven by lagoon water recirculation was approximately one order of magnitude greater (1900 ± 1700 mol d^{-1}) than the flux driven by karstic groundwater (250 ± 50 mol d^{-1}) and significantly greater than the molecular diffusion (970 ± 750 mol d^{-1}), suggesting that the lagoon water recirculation through sediments is also the main source of dissolved silica (in addition to DIN and DIP) to La Palme lagoon. These large inputs of dissolved silica driven by lagoon water recirculation may thus play an important role in sustaining primary production in La Palme lagoon.

2.5.3 The role of lagoon water recirculation as nutrient source

Groundwater inputs from karstic springs represent the main source of freshwater to La Palme lagoon, contributing to maintain the lagoon under non-hypersaline conditions for most of the year and thus playing a relevant role for lagoon ecosystem functioning (Stieglitz et al. 2013). Despite the volumetric importance of karstic groundwater inputs to La Palme lagoon, nutrient fluxes estimated in this work indicate that the recirculation of lagoon water through sediments is likely the main source of both dissolved inorganic nitrogen (DIN) and phosphorous (DIP) to La Palme lagoon. These results are in contrast with most of the studies conducted in systems influenced by fresh groundwater inputs that have attempted to differentiate nutrient fluxes from terrestrial groundwater and recirculation flows. In the only other study conducted in the Mediterranean Sea, Weinstein et al. (2011) found that the nutrient loads regenerated in coastal sediments during seawater recirculation were relatively low, resulting in nutrient-poor recirculated seawater inputs, whereas terrestrial, fresh groundwater was the main source of nutrients. Other studies, most of them conducted in the Atlantic shoreline of the USA, suggested that recirculated saline water might deliver significant loads of nutrients, although the nitrogen fluxes from terrestrial groundwater discharge were significantly higher (Kroeger and Charette 2008; Santos et al. 2009; Bernard et al. 2014) or comparable (Kroeger and Charette 2008; Sadat-Noori et al. 2016; Bejannin et al. 2017) than those supplied by saline water recirculation.

Unlike most of the previous sites where groundwater inputs occur via diffusive (non-point source) discharge processes, groundwater discharge in La Palme lagoon is via point-sourced, karstic springs. The influence of karstic groundwater inputs is thus restricted to areas close to the springs. In contrast, recirculation fluxes are essentially ubiquitous in areas with permeable sediments. Therefore, the relative significance of recirculation fluxes as a source of nutrients may be even higher for most of the areas not influenced by karstic groundwater inputs. The important role of recirculation fluxes in La Palme lagoon is also partially enhanced by the shallow water column of the site (< 2 m), which may favor the recirculation of water through sediments (e.g. the interaction between wave-

driven oscillatory flows and seabed morphology increases in shallow waters; (Precht and Huettel 2003) and the accumulation of compounds in lagoon waters. The relative importance of recirculation-driven nutrient inputs might thus be particularly relevant in shallow systems covered by permeable sediments.

Solute inputs from lagoon water recirculation may have a critical impact on the primary production of this system. Fluxes of nutrients to La Palme lagoon from karstic groundwater discharge and water recirculation have DIN/DIP ratios above the Redfield ratio (DIN/DIP of 140-500 in the karstic spring and 30-230 in recirculation fluxes). Surfaces waters from most of the lagoon appear to be N-limited (DIN/DIP < 10), with the exception of fresher areas highly influenced by karstic groundwater inputs, which are P-limited. Therefore, recirculation-driven nutrient fluxes may represent a relevant source of dissolved inorganic nitrogen to support phytoplankton growth in areas not influenced by karstic inputs. Nitrogen inputs from recirculation of lagoon waters through sediments are largely supplied in the form of NH_4^+, whose uptake by primary producers is preferred over NO_3^- uptake due to reduced energetic costs associated with its utilization (Middelburg and Nieuwenhuize 2000; Cohen and Fong 2005; Jauzein et al. 2017). Nutrient inputs supplied by lagoon water recirculation are thus expected to play a relevant role in the ecological functioning of the lagoon.

It is beyond the scope of this study to evaluate the physical or biological mechanisms driving the recirculation of these large amounts of lagoon water through sediments. A number of different mechanisms have been identified to force flow across the sediment-water interface, including wave and tidal pumping, interaction of bottom currents and seafloor topography, density instabilities or pumping activities of benthic fauna (Santos et al. 2012a; Huettel et al. 2014). In the case of La Palme lagoon, Stieglitz et al (2013) suggested that wind-driven variations of lagoon water levels could represent the main mechanism inducing recirculation flows. More recently, Cook et al. (2018a) indicated that the shape of radon porewater depth profiles in La Palme lagoon is consistent with porewater exchange driven by pressure gradients reversing at short temporal scales, such as those produced by the action of wind-driven waves. Other studies in lagoonal embayments have also suggested that the

burrowing activities of benthic fauna (bioturbation and bioirrigation) can drive the exchange of significant amounts of water between sediments and overlying water, in similar magnitudes than those observed in La Palme lagoon (0.01-0.03 $m^3\ m^{-2}\ d^{-1}$) (Martin et al. 2006; Roskosch et al. 2012; Rodellas et al. 2017).

2.6 Conclusions

The significant contribution of recirculated lagoon waters to the studied lagoon highlights the importance of this often-overlooked process as a conveyor of dissolved inorganic nutrients to coastal and lagoonal ecosystems. These findings emphasize the need for a sound understanding of these recirculation-driven nutrient fluxes and their ecological implications to properly understand the functioning and vulnerability of coastal lagoonal ecosystems. Future studies on the nutrient biogeochemical cycling in coastal lagoons, as well as management strategies towards the mitigation of the negative impacts of eutrophication in these ecosystems, should thus properly evaluate the loads of nutrients and other solutes supplied by lagoon water recirculation through sediments.

– Chapter 3 –

Primary production in coastal lagoons supported by groundwater discharge and porewater fluxes inferred from nitrogen and carbon isotope signatures

This Chapter is based on:

Aladin Andrisoa, Thomas C. Stieglitz, Valentí Rodellas, Patrick Raimbault. Primary production in coastal lagoons supported by groundwater discharge and porewater fluxes inferred from nitrogen and carbon isotope signatures. *Marine Chemistry 210, 48-60.*

3.1 Introduction

Nitrogen and carbon inputs from terrestrial and sedimentary sources are key drivers of primary production in coastal ecosystems (Zheng 2009; Chappuis Eglantine et al. 2017). The contribution of surface water fluxes (rivers, streams, runoff…) to coastal nitrogen and carbon budgets have been extensively documented (Middelburg and Nieuwenhuize 2001; Brunet et al. 2005). In recent years, it has also been recognised that dissolved inorganic nitrogen and carbon are significantly supplied by both groundwater discharge and porewater fluxes (sometimes referred as recirculation processes) (Burnett et al. 2003; Slomp and Van Cappellen 2004; Kroeger et al. 2007; Deborde et al. 2008; Knee et al. 2010; Santos et al. 2012a; Atkins et al. 2013; Anschutz et al. 2016). Inputs of dissolved inorganic nitrogen and carbon associated with groundwater discharge and porewater fluxes can sometimes rival those fluxes supplied by surface runoff (Dorsett et al. 2011; Cyronak et al. 2013; Tovar-Sánchez et al. 2014). For the purpose of this study, we use the term karstic groundwater for low-salinity groundwater driven by the terrestrial hydraulic gradient and porewater fluxes to refer to the total efflux of saline water across the sediment-water interface (Burnett et al. 2003; Santos et al. 2012a). Unlike other studies that distinguish benthic fluxes into Submarine Groundwater Discharge or porewater exchange depending on the spatial scale of the recirculation process (Moore 2010; Santos et al. 2012a, 2014), here we use the term porewater fluxes to include all benthic fluxes, regardless of their spatial scale.

A considerable and growing body of work suggests important ecological implications linked to groundwater and porewater fluxes in coastal systems, e.g. eutrophication, algal blooms, hypoxia events (Valiela et al. 1992; Rodellas et al. 2014b; Wang et al. 2016). Most of these studies are based on indirect evidence, i.e. by measuring nutrient fluxes to coastal sites and subsequent inference that these nutrients are taken up by primary producers. Indeed, to date, only a comparatively small number of studies have directly addressed the transfer of dissolved nitrogen and carbon originated from groundwater discharge and porewater fluxes into primary producers (Herrera-Silveira 1998; McClelland and Valiela 1998; Valiela and Costa 1988; Hwang et al. 2005). This study aims at

demonstrating the direct impact on lagoon ecological processes by documenting the transfer of groundwater and porewater derived nutrients into primary producers, thereby linking physical (nutrient delivery) and ecological (nutrient uptake) processes.

Inputs of nitrogen (mainly NO_3^- and NH_4^+) to the coastal zone supplied by groundwater and porewater fluxes can be derived from natural (e.g. vegetation, rocks, microorganisms cycling) or anthropogenic sources (e.g. fertilizers, sewage, mining waste) (Valiela et al. 1992; Slomp and Van Cappellen 2004; Cole et al. 2006). Additional sources of dissolved inorganic nitrogen to coastal environments are the disposal of wastewater and atmospheric deposition directly to the aquatic system (Valiela et al. 1992; Cole et al. 2005). In the case of carbon, aside from groundwater and porewater-driven inputs, dissolved inorganic carbon (mainly dissolved CO_2 and HCO_3^-) originates also from atmospheric CO_2, mineralisation of organic matter in surface waters, respiration and rock weathering (Brunet et al. 2005; Hansen et al. 2006). In order to fully evaluate nutrient budgets of a coastal water body, a distinction of 'new' external and 'old' regenerated or recycled nutrients is required. Nitrogen and carbon inputs supplied by external sources (e.g. karstic groundwater, atmospheric deposition or direct wastewater discharge) represent inputs of new nutrients to the lagoonal system, but this is not necessarily the case for porewater fluxes. Net nitrogen and carbon fluxes driven by porewater inputs may originate from the remineralization of organic matter or the recycling of inorganic nutrients within the sediment (Weinstein et al. 2011; Sadat-Noori et al. 2016). Thus, whilst referred to as porewater-driven nitrogen and carbon inputs, they could be originally supplied by other sources. In other words, groundwater and (in particular) porewater can represent any combination of these 'original' source terms, and it may perhaps be more appropriate to use the term 'pathway' rather than 'source'. This is particularly the case for porewater-derived inputs. However, we will use the term 'source' to refer to groundwater and porewater inputs, as commonly done in coastal groundwater studies. Whilst the application of stable isotopes of species of interest (here N & C) can help with these investigations, they alone do not allow for the full distinction of new versus old

(regenerated) sources. We suggest that this limitation is common to almost all studies of chemical fluxes associated with porewater exchange, and that this issue will require further investigations if a full nutrient (or solute) budget was to be obtained.

In order to establish the sources that supply nitrogen and carbon for the growth of primary producers, natural abundance ratios of stable nitrogen and carbon isotopes ($\delta^{15}N$ and $\delta^{13}C$) are widely used (Zieman et al. 1984; Lassauque et al. 2010). Primary producers integrate the isotopic signature of their nitrogen and carbon sources over their lifetime and thus provide an insight into the potential sources at that time scale (e.g. Derse et al. 2007; Santiago et al. 2017). Isotope fractionation during nutrient uptake may induce variations in the $\delta^{15}N$ and $\delta^{13}C$ in the primary producers and needs to be taken into account for an appropriate evaluation (Hemminga & Mateo, 1996; Lepoint et al., 2004).

Typical ranges of $\delta^{15}N$ in source terms are +2 to +5‰ for nitrogen in soil, -3 to +3‰ for fertilizers, +2 to +8‰ for groundwater from natural soils and +10 to +20‰ for sewage effluent (Kendall et al. 2007; Kendall 2015). Provided that different sources supplying an ecosystem have distinguishable signatures, their relative contributions can be identified by comparing the $\delta^{15}N$ signatures in primary producers with those of the sources (Derse et al. 2007; Benson et al. 2008).

Similarly, carbon stable isotopes incorporated in the primary producer's biomass can be used to trace the source of inorganic carbon and provide insight into the carbon cycling processes and the environmental conditions during growth (Vizzini et al. 2005; Inglett and Reddy 2006). The isotopic signature of dissolved inorganic carbon ($\delta^{13}C$-DIC) available for photosynthesis chiefly determines the isotopic signatures in primary producers (Boschker et al., 2005; Hemminga & Mateo, 1996). In seawater, $\delta^{13}C$-DIC is around 0‰ (Hemminga and Mateo 1996; Raven et al. 2002), $\delta^{13}C$-DIC ranges between -11 and -8‰ in groundwater (Atekwana and Krishnamurthy 1998), and is around -11‰ in sewage effluent (Barros et al. 2010).

The objective of this study is to assess the role of groundwater discharge and porewater fluxes in supporting primary production of groundwater-fed coastal lagoons. We studied the transfer of dissolved nitrogen and carbon originated from groundwater and advective porewater fluxes to macrophytes and phytoplankton in two lagoons on the French Mediterranean coastline (Fig. 3.1). The smaller La Palme lagoon receives relatively large amounts of groundwater, significantly diluting lagoon salinity, whereas the larger Salses-Leucate lagoon experiences only partial fresh groundwater exposure (Stieglitz et al. 2013).

3.2 Materials and Methods

3.2.1 Nutrient sources

Nutrient fluxes from the potential sources in La Palme lagoon were determined in a concurrent study (Rodellas et al. 2018). Estimated NO_3^- fluxes were 220 - 1200 mol d^{-1} for karstic groundwater discharge and 19 - 130 mol d^{-1} for sewage effluent, whereas NO_3^- inputs from porewater fluxes and diffusion were shown to be negligible. NH_4^+ fluxes were 1 - 12 mol d^{-1}, 1900 - 5500 mol d^{-1}, 0.5 - 4 mol d^{-1} and 3 – 5 mol d^{-1} for karstic groundwater, porewater fluxes, sewage effluent and diffusion, respectively. Karstic groundwater represents thus a major source of NO_3^-, while porewater fluxes are the main source of NH_4^+ to La Palme lagoon (by > three orders of magnitude). Nitrogen inputs from diffusion were negligible compared to advective porewater fluxes, and thus the porewater source is assumed to represent chiefly advective porewater input.

In addition, we do not consider atmospheric nitrogen fixation in this study because it is a minor process in temperate systems (McGlathery et al. 1998; Welsh 2000), in contrast to the (sub)tropics where fixation plays a major role (Patriquin and Knowles 1972; Hansen et al. 2000). Whilst seawater can be a source of nitrogen in some cases (Capone 2008; Voss et al. 2011), the inputs of nitrogen from seawater are negligible in this study due to the reduced concentration in Mediterranean seawater (0 - 2 μmol L^{-1}) (Siokou-Frangou et al. 2010; Pasqueron De Fommervault et al. 2015) and the limited exchange between

the lagoon and the sea. However, seawater inflow is a pathway for external carbon.

3.2.2 Sample collection and analysis

3.2.2.1 Water

Fieldwork was conducted in June 2016, November 2016 and June 2017 in both lagoons, and additionally in April 2017 in La Palme lagoon. Temperature and salinity data were measured with a pre-calibrated WTW Multi 3430 probe (precision, ± 0.5 %). Lagoon surface water samples were collected with a 1-L widemouth Nalgene bottle along the salinity gradient (Fig. 3.1a and b). A push-point piezometer was used to collect 20 mL of porewater samples in the lagoon at 5, 10, 15 and 20 cm depth (e.g. Niencheski et al. 2007). Samples were preserved with $HgCl_2$ (6 g l^{-1}) to prevent bacterial activity for ammonium (NH_4^+), nitrate + nitrite (NO_x = NO_3^- + NO_2^-) and phosphate (PO_4^{3-}) analyses (Kirkwood 1992). Nitrate and nitrite were not separately quantified and defined here as nitrate (NO_3^-).

NO_3^- and PO_4^{3-} concentrations were measured by colorimetric method on a Technicon AutoAnalyser® II with detection limits of 0.05 µmol L^{-1} and 0.02 µmol L^{-1} for NO_3^- and PO_4^{3-}, respectively (Aminot and Kérouel 2007). NH_4^+ concentrations were determined on diluted samples (4 to 10 times) with a Turner Designs TD-700 Fluorometer (detection limit: 0.01 µmol L^{-1}) (Holmes et al. 1999). In the springs and sewage effluents, the $\delta^{15}N$-NO_3^- in water column was analysed. In the sediment porewater, NO_3^- concentrations were very low, and therefore the measured $\delta^{15}N$ of total DIN (NH_4^+ + NO_3^-) is taken to represent NH_4^+. The $\delta^{15}N$ of NO_3^- and DIN were determined following the reduction / diffusion method (Fig. 3.2a) (Sigman et al. 1997; Holmes et al. 1998; Raimbault et al. 1999). The method involves the conversion of nitrate to ammonium using Devarda's alloy and the diffusion of ammonia gas onto an acidified filter. The lack of ^{15}N fractionation during diffusion was checked using nitrate reference. Note that due low nutrient concentrations in the lagoon water and seawater samples, nitrogen isotopic signatures were not measured.

Lagoon surface water samples for δ^{13}C-DIC analyses were collected along the salinity gradient with a 100 mL glass vial. Samples were collected underwater to prevent atmospheric exchange, and the vials were immediately crimp-sealed with rubber serum stoppers and open top aluminium caps and then poisoned with $HgCl_2$ to prevent bacterial activity. The δ^{13}C of DIC was measured following the procedure of Miyajima et al. (1995). A headspace of 3 mL is created inside each airtight glass vials with pure helium gas and each sample is then acidified with 10N H_2SO_4. After the original DIC has equilibrated with the headspace gas, a portion of this headspace gas is collected with a glass syringe for injection into a mass spectrometer.

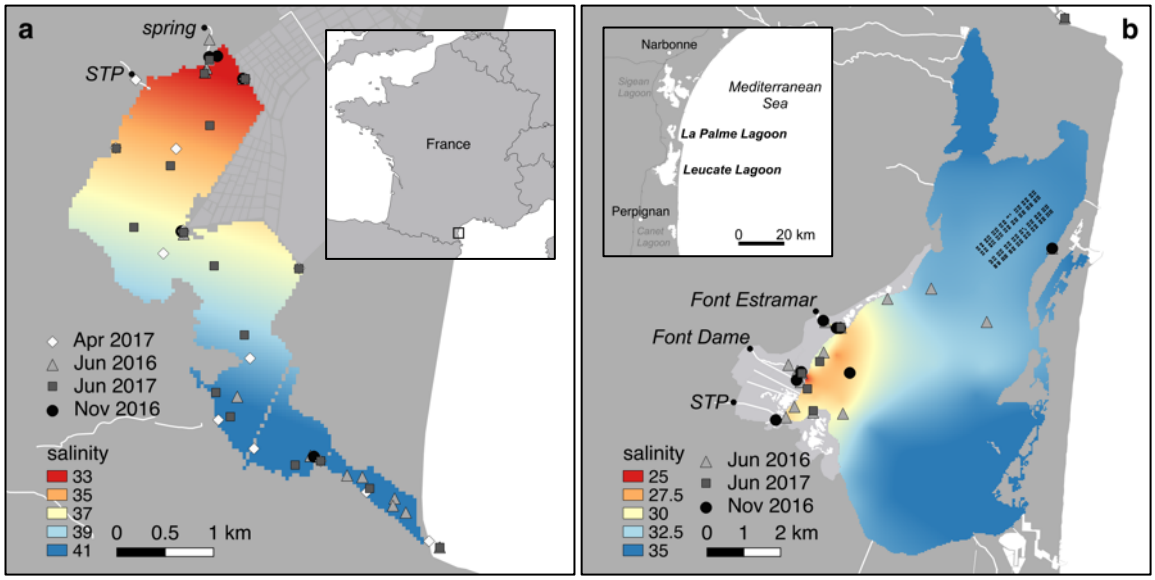

Figure 3.1| Sampling locations overlaid on the surface salinity distribution (June 2016) in (a) La Palme and (b) Salses-Leucate lagoons (modified from Rodellas et al 2018). Locations of sewage treatment plants (STP) and groundwater springs are shown.

3.2.2.2 Primary producers

During each campaign, dominant macrophytes were collected in the springs, at the outlets of the sewage treatment facilities and at multiple sites in the lagoons along the salinity gradient (Fig. 3.1 and Fig. 3.2b). Leaves were sampled non-discriminately from the dominant species observed (*Zostera noltii, Ruppia cirrhosa, Ulva sp, Phragmites communis*). Samples were rinsed with deionised water, bagged and transported on ice to the laboratory, where they were oven-

dried at 60°C, ground and homogenized with a mortar and pestle (Fig. 3.2c). Approximately 1 mg of the ground samples was analysed for $\delta^{15}N$ and $\delta^{13}C$. Each sample was acidified with 50 µL of 0.25N H_2SO_4 to eliminate carbonates, which may interfere with $\delta^{13}C$ measurements. To assess if variability in the signatures is linked to species differences, signatures in different species collected at the same location were compared. Particulate organic matter (POM), predominantly representing phytoplankton (Carlier et al. 2007, 2009), was sampled in the springs, sewage and the lagoons. 0.4 to 1 L of water samples were filtered through GF/F filters (0.7 µm) under moderate vacuum until clogging. Filters were kept frozen until analyses on mass spectrometry.

All isotope analyses (in primary producers and water column) were carried out at the Mediterranean Institute of Oceanography (Marseille) using elemental analyzer mass spectrometer Integra CN Sercon (Fig. 3.2d) (Raimbault et al. 2008; Lacoste et al. 2016). Following common notion, the isotopic composition ($\delta^{15}N$ or $\delta^{13}C$) was expressed as relative difference between isotopic ratios in sample and in conventional standards (atmospheric N_2 for nitrogen and Vienna Pee Dee Belemnite for carbon):

$$\delta^{15}\text{N or } \delta^{13}\text{C (‰)} = \left(R_{sample}/R_{standard} - 1\right) \times 1000 \quad (3.1)$$

where R is the ratio $^{15}N/^{14}N$ or $^{13}C/^{12}C$. The precisions of replicate analyses were 0.5‰ and 0.3‰ for $\delta^{15}N$ and $\delta^{13}C$, respectively.

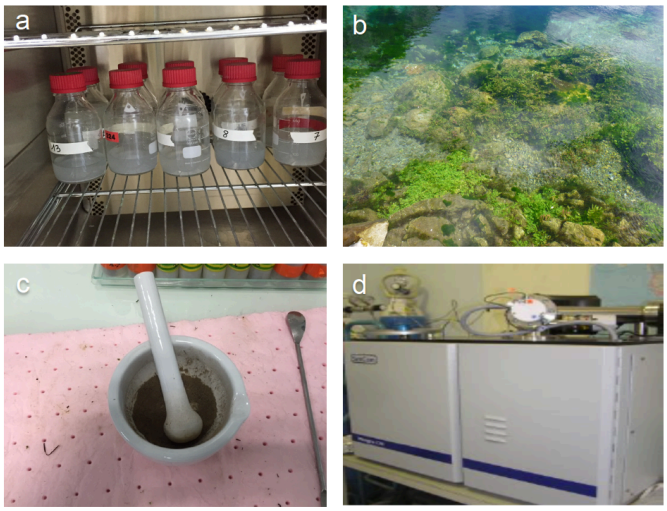

Figure 3.2| (a) Reduction / diffusion method for measurement of the $\delta^{15}N$ of NO_3^- and DIN, (b) macrophyte samples in karstic spring, (c) grounded macrophyte samples for stable isotope analyses and (d) stable isotope analyses on elemental analyzer mass spectrometer Integra CN Sercon.

3.3 Results

3.3.1 NO_3^- and NH_4^+ concentrations

Overall, NO_3^- concentrations in the lagoon systems decreased with increasing salinity, and highest concentrations were observed in the springs and the sewage outlets (Fig. 3.3). Surface water NO_3^- concentrations in the lagoons ranged from below the detection limit (0.05 µmol L^{-1}) to 7.8 µmol L^{-1} and between 0.1 and 54.5 µmol L^{-1} in La Palme lagoon and Salses-Leucate lagoon, respectively (Fig. 3.3a and b). In the streams draining the springs and downstream of the sewage treatment facilities, the concentrations were significantly elevated over lagoon values (34.0 - 65.0 µmol L^{-1} La Palme lagoon; 0.3 - 41.7 µmol L^{-1} Salses-Leucate lagoon). In June 2017, the NO_3^- concentration measured at the outlet of the sewage in La Palme lagoon was exceptionally high at 522 µmol L^{-1}.

Unlike NO_3^-, the NH_4^+ concentrations did not show any clear spatial pattern in either lagoon. The concentrations ranged from 0.8 to 36 µmol L^{-1} in La Palme lagoon and from 0.2 to 30.4 µmol L^{-1} in Salses-Leucate lagoon and in the streams (creeks) (Fig. 3.3c and d). The springs showed significantly lower NH_4^+

concentrations, while the concentrations in the sewage and the porewaters were markedly higher, particularly in Salses-Leucate lagoon.

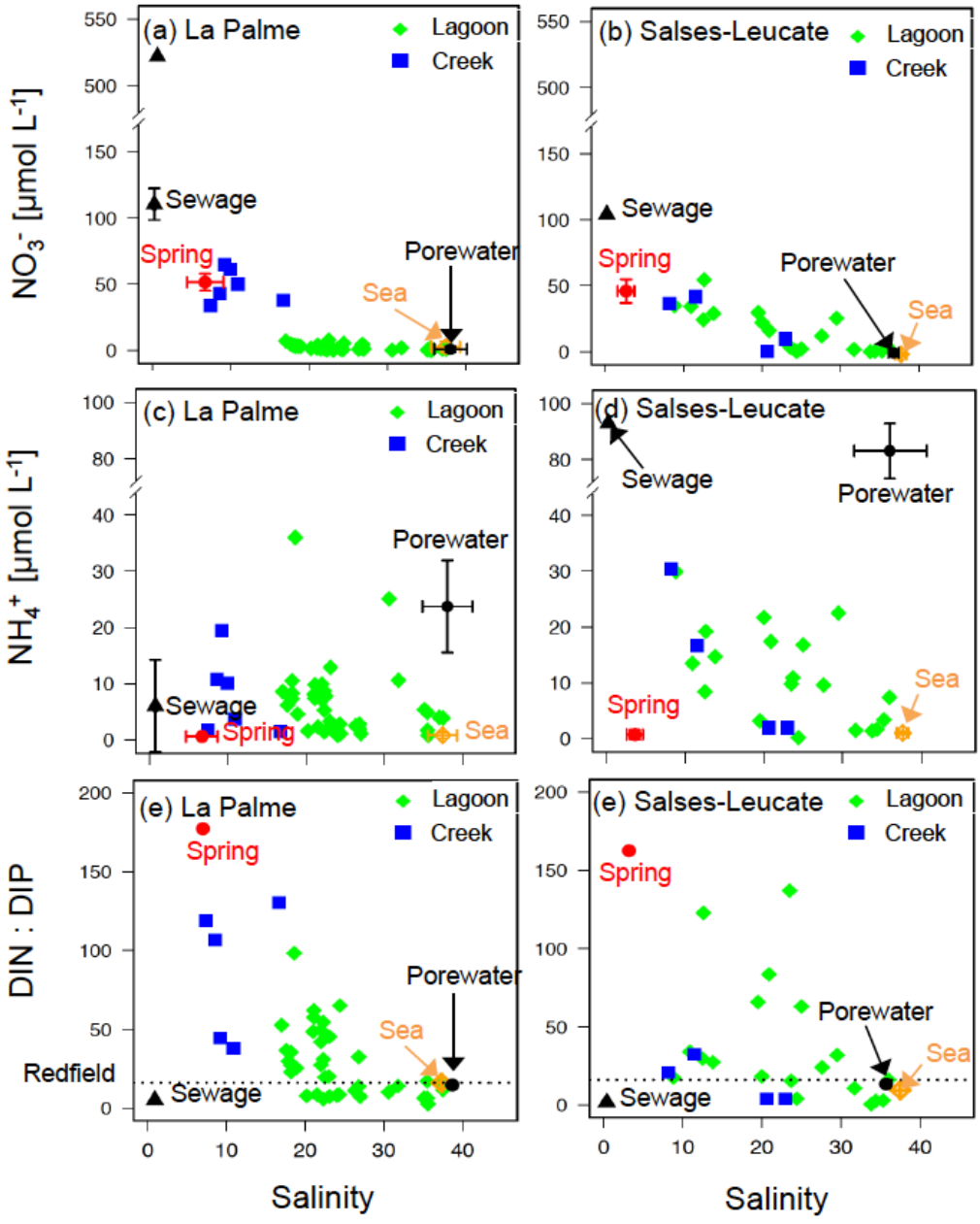

Figure 3.3| (a, b) Variation of NO_3^-, (c, d) NH_4^+ concentrations and (e, f) the stoichiometric ratios of DIN:DIP along the salinity gradient in La Palme and Salses-Leucate lagoons, respectively. The dashed lines represent the DIN:DIP Redfield ratio of 16:1. Endmembers indicate the average NO_3^- and NH_4^+ concentrations and the DIN:DIP ratios in the sewage effluents (black triangle), springs (red circle) and seawater (orange diamond). NO_3^- and NH_4^+ concentrations and DIN:DIP data in the lagoons (green diamond) and the creeks (blue square) are not differentiated for the four sampling campaigns. Note the scale differences on the y-axes and the axis breaks.

3.3.2 Source isotopic signatures

Karstic groundwater $\delta^{15}N\text{-}NO_3^-$ were 3.1 ± 2.1‰ (n=4) and 1.0 ± 1.2‰ (n=5) in La Palme and Salses-Leucate lagoons, respectively. NO_3^- samples from sewage effluents were enriched in ^{15}N with a mean $\delta^{15}N\text{-}NO_3^-$ of 16.4 ± 4.5‰ (n=3) in La Palme lagoon and 17.6 ± 3.7‰ (n=2) in Salses-Leucate lagoon. Porewater $\delta^{15}N$-DIN (NO_3^- + NH_4^+) values were depleted compared to those of sewage with mean values of 7.1 ± 3.3‰ (n=12) and 6.4 ± 2.1‰ (n=3) in La Palme and Salses-Leucate lagoons, respectively. With exception of a small overlap of groundwater and lagoon porewater in La Palme lagoon, in general the signatures of the sources (karstic groundwater, porewater and sewage) are sufficiently different to identify the nitrogen source used for primary producers to support their growth (Fig. 3.4a). Nitrogen isotopic signatures of lagoon waters and seawater were below detection limit of our methods due to the low nitrogen concentrations in these surface waters.

The observed nitrogen isotopic signatures in the different sources are in good agreement with previously reported ranges: $\delta^{15}N$ commonly ranges between +10 and +20‰ for sewage effluents, between +2 and +5‰ for porewater, and between +2 and +8 ‰ for groundwater from natural soils (Fig. 3.4a) (Cole et al., 2005; Kendall et al., 2007). Processes such as NH_4^+ volatilization and denitrification have been identified previously as the main reason for the elevated signatures of $\delta^{15}N$ in sewage effluents (Aravena et al., 1993). The nitrogen signatures in porewaters are strongly affected by the drainage, vegetation, plant litter, land use and climate (Kendall and Aravena 2000). The $\delta^{15}N\text{-}NO_3^-$ signatures of the karstic groundwater, which is lower than the other sources in both lagoons, depend strongly on the land use and the nitrogen delivery (Cole et al. 2006). For instance, groundwater heavily influenced by septic system or wastewater can become enriched in $\delta^{15}N$ (between +10 and +20‰), whereas the $\delta^{15}N$ signature can be lower (between -3 and +3‰) for groundwater NO_3^- derived from fertilizers (Kendall et al. 2007). The relatively low $\delta^{15}N\text{-}NO_3^-$ of the karstic groundwater (1-3‰) reflects the negligible influence of wastewater in the watershed due to the central sewage system (as

opposed to septic tanks) not affecting groundwater loading on one hand and a low population pressure in general on the other.

Similar to nitrogen isotopes, the carbon signatures of the three analyzed DIC sources were distinct from another (Fig. 3.4b). Karstic groundwater had average $\delta^{13}C$ values of -8.5 ± 1.0‰ (n=4) and -8.0 ± 0.4‰ (n=5) in La Palme and Salses-Leucate lagoons, respectively, which agree with literature values (e.g. -13.5 to -6.9‰ karstic catchment Changjiang River, China; Li et al. 2010). Sewage $\delta^{13}C$-DIC was depleted with an average value of -12.5 ± 1.7‰ (n=3) in La Palme lagoon and -10.5‰ (n=1) in Salses-Leucate lagoon, again comparable to previously reported values e.g. for sewage-influenced estuaries (-15 to -11‰; Hellings et al. 2001; Barros et al. 2010). Porewater samples for $\delta^{13}C$-DIC analyses could not be collected due to CO_2 volatility; previous studies reported $\delta^{13}C$-DIC values between -18 and -9‰ in marine and coastal porewaters (Yang et al. 2008). Seawater had a $\delta^{13}C$-DIC of 0.6 ± 0.5‰ (n=3) in La Palme and 0.9‰ in Salses-Leucate lagoon, which agrees with previously reported values (ca. 0‰; Raven et al. 2002). The lighter $\delta^{13}C$-DIC of groundwater reflects mineralisation of organic matter combined with the weathering of carbonate minerals, while the seawater DIC is in isotopic equilibrium with the atmospheric CO_2 (Chanton and Lewis 1999).

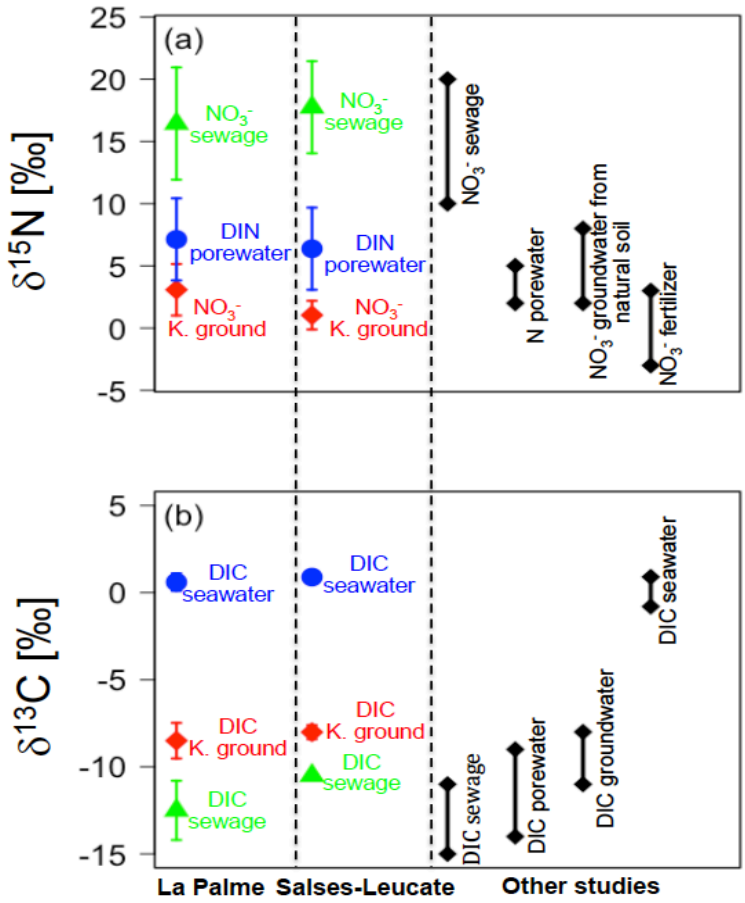

Figure 3.4| (a) The $\delta^{15}N$ of nitrogen ($\delta^{15}N$-NO_3^- for sewage and groundwater samples; $\delta^{15}N$-DIN for porewater samples) and (b) the $\delta^{13}C$ of DIC sources measured in La Palme and Salses-Leucate lagoons compared with nitrogen sources in literature. The isotopic signatures of the nitrogen sources (sewage, porewater and springs) and carbon sources (sewage, groundwater and seawater in equilibrium with the atmospheric CO_2) measured in this study are in good agreement with values reported in the literature (Atekwana and Krishnamurthy 1998; Chanton and Lewis 1999; Cole et al. 2005; Kendall et al. 2007; Yang et al. 2008; Barros et al. 2010).

The $\delta^{13}C$-DIC signatures measured in lagoon waters increase with increasing salinity in both lagoons (Fig. 3.5a and b), ranging from -8.5 to 0.2‰ in La Palme lagoon and -7.5 to 1.7‰ in Salses-Leucate lagoon, similar to previous observations (e.g. -12 to 0‰ in Apalachicola Bay, Florida (Chanton and Lewis 1999) or in estuaries (Gillikin et al. 2006) and coastal bays (Barros et al. 2010). $\delta^{13}C$-DIC in lagoon waters seemed to be explained by the mixing of freshwater (karstic groundwater) and marine sources (see section 3.4.2.1).

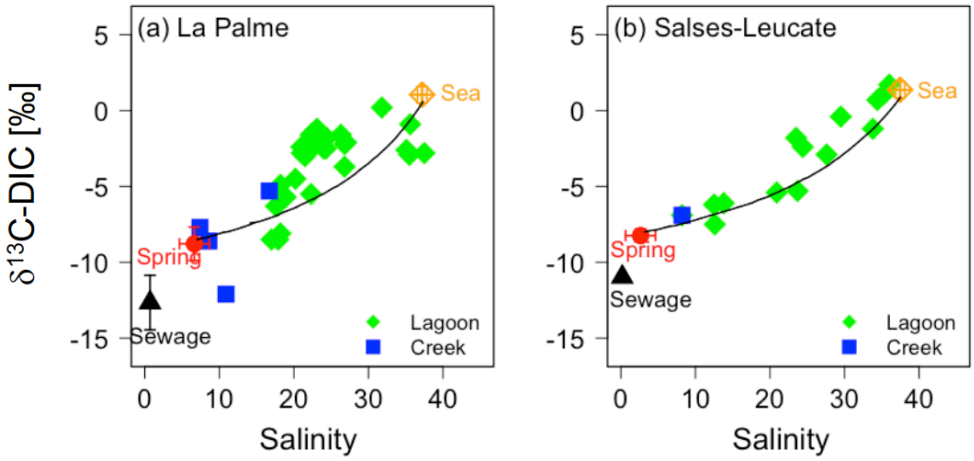

Figure 3.5| $\delta^{13}C$ of DIC in water along the salinity gradient in (a) La Palme and (b) Salses-Leucate lagoons. Endmembers indicate the average $\delta^{13}C$-DIC in the sewage effluents (black triangle), springs (red circle) and seawater (orange diamond). $\delta^{13}C$-DIC samples are not differentiated for the four sampling campaigns. The black lines represent the conservative binary isotopic mixing line between $\delta^{13}C$-DIC in karstic groundwater and seawater endmembers, derived using the DIC concentrations in groundwater (5900 ± 800 µmol L^{-1}) and in seawater (2300 ± 200 µmol L^{-1}) (C. Monnin, unpublished data) (Chanton and Lewis 1999).

3.3.3 $\delta^{15}N$ in macrophytes and POM

Macrophyte $\delta^{15}N$ signatures ranged from -3.0 to 12.6‰ in La Palme lagoon and from -1.8 to 9.9‰ in Salses-Leucate lagoon, but did not show a clear pattern with respect to salinity in either lagoon (Fig. 3.6a and b). In La Palme lagoon, macrophytes collected in June 2017 at the northern part of the lagoon and close to the sewage and spring sources showed significantly elevated isotopic signatures over otherwise generally stable values (Fig. 3.6a). Macrophytes sampled in the karstic springs had lower $\delta^{15}N$ in La Palme lagoon (mean: 0.0 ± 2.3‰; n=4) and in Salses-Leucate lagoon (mean: 0.4 ± 1.6‰; n=6) while higher signatures were measured at the sewage outlets (11.4 ± 2.5‰ in La Palme lagoon and 18.1‰; n=1 in Salses-Leucate lagoon).

Overall, the $\delta^{15}N$ of POM showed larger variability compared to that of macrophytes, but like in macrophytes, no clear spatial pattern was observed in the distribution of $\delta^{15}N$-POM (representing phytoplankton) in either lagoon (Fig. 3.6c and d). The $\delta^{15}N$ in POM collected at the karstic springs were lower (0.9 ±

3.9‰ (n=3) in La Palme lagoon and 1.7 ± 5.2‰ in Salses-Leucate lagoon) while the signatures from the sewage treatment plants were markedly high (11.7 ± 4.2‰ (n=3) in La Palme lagoon and 10.9‰ (n=1) in Salses-Leucate lagoon).

Overall, the $\delta^{15}N$ in macrophytes and POM measured in this study were in very good agreement with previous measurements from the same lagoons (Carlier et al. 2007, 2009).

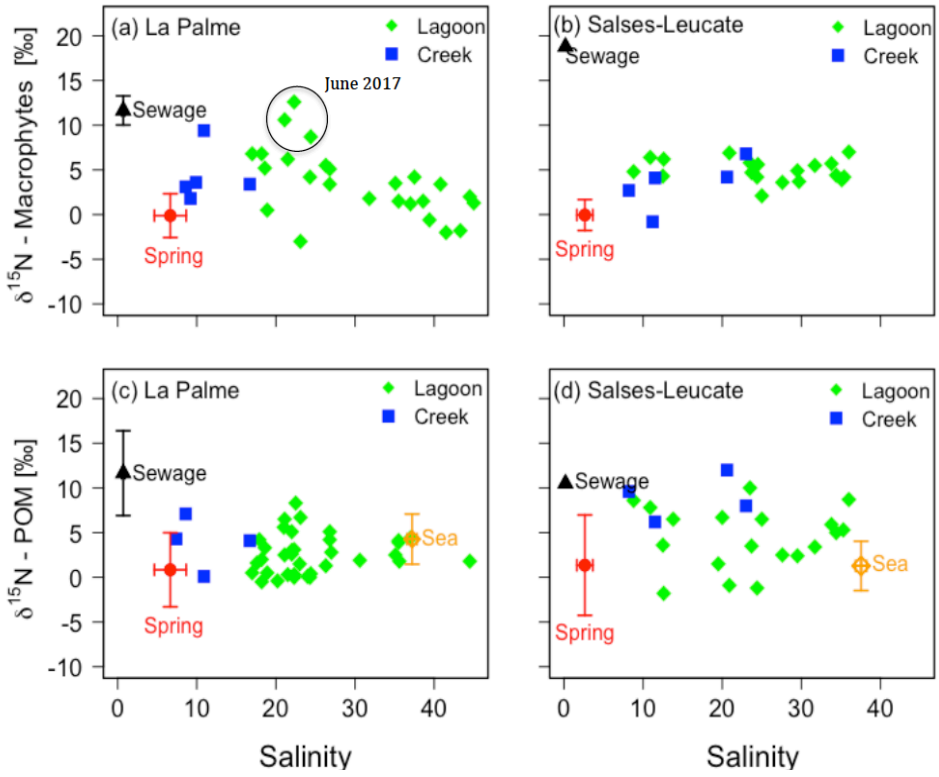

Figure 3.6| The $\delta^{15}N$ of (a, b) macrophytes and (c, d) POM along the salinity gradient in La Palme and Salses-Leucate lagoons, respectively. Endmembers indicate the average $\delta^{15}N$ of primary producers sampled close to the sewage outlet (black triangle), springs (red circle) and seawater (orange diamond). The $\delta^{15}N$ data from primary producers are shown together for the four sampling campaigns.

3.3.4 $\delta^{13}C$ in macrophytes and POM

The $\delta^{13}C$ in macrophytes showed an overall increase with increasing salinity in both lagoons (Fig. 3.7a and b), similar to the trend shown by $\delta^{13}C$-DIC signatures in lagoon waters. $\delta^{13}C$ was markedly lower in macrophytes collected in springs (-33.6 ± 2.0‰ (n=4) in La Palme lagoon and -34.4 ± 2.5‰ (n=5) in Salses-Leucate

lagoon) and at the outlet of the sewage treatment plants (-26.7 to -10.4‰ La Palme lagoon; -16.6 to -7.5‰ Salses-Leucate lagoon).

In La Palme lagoon, δ^{13}C-POM showed also an increase with increasing salinity (Fig. 3.7c). In the spring and sewage respectively, δ^{13}C-POM was -29.4 ± 2.9‰ and -26.5 ± 2.6‰. In Salses-Leucate lagoon, the δ^{13}C-POM values showed minor increase along the salinity gradient compared to the values in La Palme lagoon (Fig. 3.7d). Lower signatures were however observed in the springs (mean: -29.7 ± 3.6‰; n=6) and sewage (-26.9‰).

Similar to nitrogen isotopes, carbon isotope ratios measured in macrophytes and POM in this study are consistent with previous observations in the same lagoons (Carlier et al., 2007, 2009) and at other Mediterranean sites (Lepoint et al. 2000; Vizzini and Mazzola 2003).

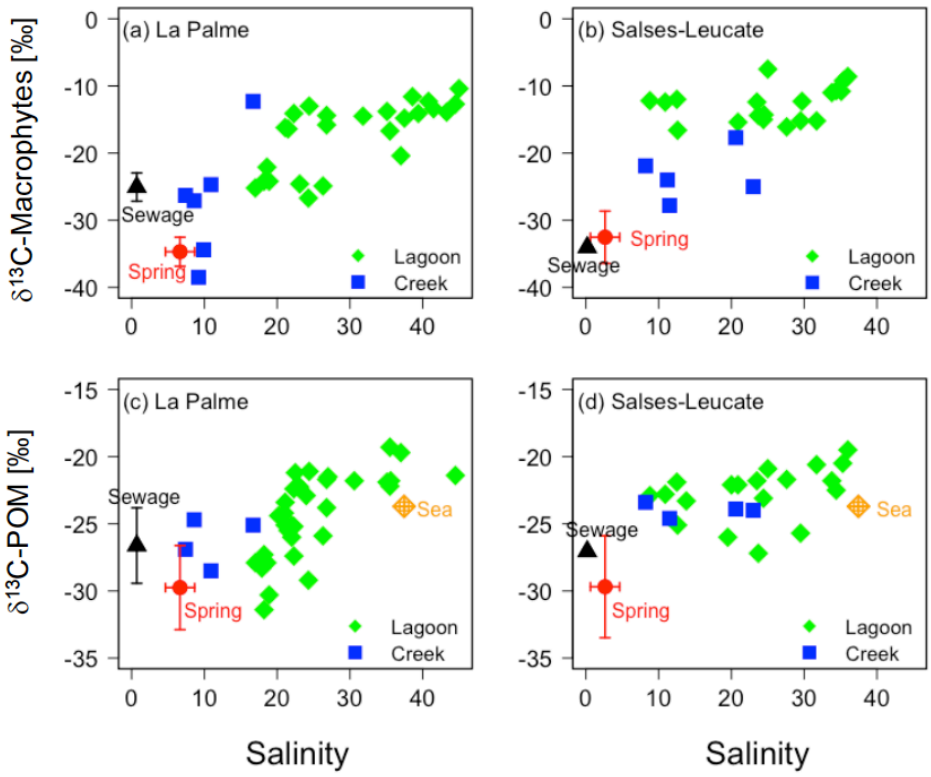

Figure 3.7| The δ^{13}C of (a, b) macrophytes and (c, d) POM along the salinity gradient in La Palme and Salses-Leucate lagoons, respectively. Endmembers indicate the average δ^{13}C of primary producers in the sewage effluents (black triangle), springs (red circle) and seawater (orange diamond). The shown δ^{13}C data from primary producers are shown together for the four sampling campaigns. Note the scale difference for the y-axes.

3.3.5 Interspecific variations in isotopic signature in macrophytes

Comparison of $\delta^{15}N$ and $\delta^{13}C$ of macrophytes of individual species (*Ulva sp, Ruppia cirrhosa, Zostera noltii and Acetabularia acetabulum*) indicated low interspecific variation for both $\delta^{15}N$ (0.1 - 2.0‰) and $\delta^{13}C$ (0.4 - 4.5‰). Previous studies also report small differences in isotopic signatures of macrophytes among different species (Carlier et al. 2007; Derse et al. 2007). We therefore consider the pooled macrophyte isotope data in our interpretation.

3.4 Discussion

3.4.1 Processes affecting macrophyte and phytoplankton $\delta^{15}N$

3.4.1.1 Nitrogen concentrations in lagoons and sources

The non-linear decrease in NO_3^- concentrations with increasing salinity observed in both La Palme and Salses-Leucate lagoons indicates (a) a low salinity source term and (b) efficient NO_3^- removal along the salinity gradient (Fig 3.3a and b). Biological uptake is likely the main process removing NO_3^- from the lagoons (Liu et al. 2009). Denitrification, which is the only other relevant processes removing NO_3^- in aquatic systems, is unlikely to occur as surface water oxygen concentrations are close to (or above) saturation (9.3 ± 3.7 mg L^{-1} in La Palme lagoon; 8.5 ± 2.7 mg L^{-1} in Salses-Leucate lagoon) (Capone 2008; Leffler and Welker 2013).

Typical for coastal environments, NH_4^+ concentrations are 3-7 times higher in the sediment than in the overlying water due to mineralization of organic matter as well as dissimilatory nitrate reduction to ammonium (DNRA) (An and Gardner 2002; Kim et al. 2017). The inhibition of nitrification, due to anoxia in sediment, enhances this accumulation of NH_4^+ (Christensen et al. 2000), and these high NH_4^+ concentrations in sediment are available for remobilisation. In the karstic groundwater springs, sewage effluent and the lagoon, aerobic conditions inhibit NO_3^- conversion to NH_4^+ via DNRA (Christensen et al. 2000).

At salinity below 20 (La Palme lagoon) and 30 (Salses-Leucate lagoon), DIN:DIP ratios were mostly above the Redfield Ratio due to nitrogen-enriched inputs from groundwater springs and/or sewage effluents (Fig. 3.3e and f). This indicates that primary production is P-limited in low salinity parts of the lagoons, and N-limited for the more saline parts.

3.4.1.2 Nitrogen uptake and associated isotopic fractionation

Phytoplankton assimilates DIN from the water column (Bradley et al. 2010). Permanently submerged species take up nutrients almost exclusively at their leaves (Ruiz and Velasco 2009; Zhao et al. 2013). Uptake at leaves also accounts for about 80% of total nitrogen acquisition by non-permanently submerged phragmites (Lee and Dunton 1999). The majority of the macrophytes analysed herein are permanently submerged species, with some samples collected close to the banks including a small number of phragmites specimen. Leaf samples analysed in this study are thus assumed to source their nitrogen from the water column like phytoplankton.

Macrophytes can assimilate water column nitrogen even at very low concentrations (Lee and Dunton 1999). Isotope fractionation during uptake depends significantly on the availability of nitrogen, increasing with increasing nitrogen concentrations, and thus potentially altering isotopic signatures in particular at nitrogen-rich systems / locations (Fry 2003; Benson et al. 2008). The higher DIN:DIP ratios in the low salinity parts of both lagoons (above the Redfield ratios; Fig. 3.3) indicate that these systems are not N-limited, and thus isotopic fractionation may have occurred, resulting in lower $\delta^{15}N$ in primary producers relative to the isotopic ratios found in the water column.

Assuming that the $\delta^{15}N$ signature of the water column NO_3^- ($\delta^{15}N_{pool}$) is representative of the signature taken up by the primary producers, the $\delta^{15}N$ signature of the primary producers ($\delta^{15}N_{prod}$) can be expressed as:

$$\delta^{15}N_{prod} = \delta^{15}NO_{3\,pool}^{-} - \varepsilon_{prod} \quad (3.2)$$

where ε_{prod} represents the fractionation factor associated with NO_3^- uptake (Fry 2003). We constrain the effect of fractionation by estimating ε_{prod} for macrophytes and phytoplankton using concurrently collected $\delta^{15}N$ in primary producers and in the water column from the groundwater sources where highest nutrient concentrations are found and thus maximum ε_{prod} for this system are expected (Evans 2001; Cohen and Bradham 2010). Furthermore, groundwater has a relatively constant nitrogen isotopic signature. The primary producers are thus permanently in contact with the same type of water making these sites reliable 'reference' stations.

Maximum fractionation factors calculated for all sampling campaigns in the 3 different springs (1 in La Palme lagoon and 2 in Salses-Leucate lagoon) were 4.7‰ and 1.4‰ for macrophytes and phytoplankton, respectively. These values are close to the fractionation factor of macrophytes from spring-fed rivers (1.9 to 3.6‰; Brabandere et al. 2007) and that of phytoplankton (1‰; Montoya and McCarthy 1995). Maximum fractionation factors observed for aquatic macrophytes are on the order of 5‰ (Altabet and Francois 1994; Kohzu et al. 2008). We thus assume that isotopic fractionation during nitrogen uptake by primary producers will be considerably lower than 5‰ in the lagoons where DIN concentrations are significantly lower.

A fully quantitative analysis of relative contributions of sources would require a detailed knowledge of the relationship of fractionation as a function of nutrient concentration and the potential spatial variability of macrophytes and phytoplankton species with salinity (Brabandere et al. 2007). Nitrogen isotope data from lagoon water is not available due to low nitrogen concentrations in the studied near-natural lagoons. This prevents us thus from being able to construct a full isotopic balance in lagoon water and presents an important limitation of our approach, which is likely to be encountered in many natural oligotrophic ecosystems. In order to fully quantify the nutrient transfer to primary producers, the nutrient concentration would have to be measured quasi-continuously because the fractionation factor depends on the concentration at the time of uptake, which cannot be assumed to be constant over the lifetime of the organisms in most lagoon ecosystems. These limitations do not exist in the same

way in eutrophied systems with relatively constant isotopic signatures.

Finally, the relative contribution of the three different sources supplying nitrogen to support primary producers growth (karstic groundwater discharge, advective porewater fluxes and sewage effluent) cannot be identified by using only the signatures of one stable isotope (i.e. $\delta^{15}N$). Important conclusions can nevertheless be drawn on the relative contributions of different endmembers.

3.4.1.3 Nitrogen sources for primary producers

Generally, the $\delta^{15}N$ of macrophytes and phytoplankton closely match the nitrogen isotopic signatures of the karstic groundwater and porewater sources, with some exceptions (Fig. 3.8). $\delta^{15}N$ in macrophytes slightly below source signatures was observed in La Palme lagoon in June 2016 and is consistent with a small fractionation effect during groundwater-borne nitrogen uptake. Overall, at fractionation below 5‰, macrophytes and phytoplankton must have sourced the majority of their nitrogen from fresh karstic groundwater and/or porewater fluxes.

The $\delta^{15}N\text{-}NO_3^-$ of the karstic groundwater and the $\delta^{15}N$-DIN (mainly NH_4^+) of porewater are relatively close to each other in La Palme lagoon (Fig. 3.8a), making it difficult to differentiate the relative contributions from these two sources from their isotope signature alone in this lagoon. In Salses-Leucate lagoon however, karstic groundwater and porewater are differentiated isotopically (Fig. 3.8b).

In Salses-Leucate lagoon, those samples collected closer to the groundwater springs typically have signatures close to or below the $\delta^{15}N$ signature of karstic groundwater (macrophytes in June 2016 and POM in June 2017; Fig. 3.8b), suggesting that at these locations, primary producers' uptake their nitrogen predominantly from the karstic groundwater. The influence of karstic groundwater inputs into this lagoon is restricted to the area close to the karstic springs, due to smaller inflow from karstic groundwater (inflow of karstic discharge estimated to account for ca. 0.008% of lagoon volume per day; Fleury

et al. (2007)), larger size and the better connection with the ocean, as shown by the salinity distribution (Fig. 3.2b). Similarly, the isotope signatures indicate a minor role of karstic groundwater in nitrogen supply, suggesting that primary producers in this large lagoon source most of their nitrogen from the porewater source. The isotope data from La Palme lagoon corroborates overall the relatively larger impact of karstic groundwater in primary producers, mainly due to the larger groundwater inflow relative to the lagoon size (ca. 1% of lagoon volume per day) compared to Salses-Leucate lagoon and the restricted exchange with the sea, as also indicated by the salinity distribution (Fig. 3.1a; Stieglitz et al. 2013). The contrasting hydrodynamic conditions in La Palme and Salses-Leucate lagoons explain thus the differences of isotopic signatures in the primary producers from these two lagoons.

Porewaters and sewage effluent are sources of NH_4^+ to the lagoons. These two sources can easily be differentiated by their nitrogen signatures, with porewater $\delta^{15}N\text{-}NH_4^+$ at 7.1 ± 3.3‰ in La Palme lagoon and 6.4 ± 2.1‰ in Salses-Leucate lagoon significantly lower than in sewage effluent (30.6‰ in La Palme lagoon and 28.3‰ in Salses-Leucate lagoon). The nitrogen signatures in primary producers in both lagoons reflect closely the $\delta^{15}N\text{-}NH_4^+$ of porewater most of the time (Fig. 3.8). Porewater fluxes often represent a major source of dissolved inorganic nitrogen to coastal environments, including lagoons, bays, estuaries and ocean basins (e.g. Kroeger et al. 2007; Street et al. 2008; Rodellas et al. 2015; Sadat-Noori et al. 2016). The dynamics of this input can vary significantly according to the hydraulic conditions, tidal forcing and the distance of the fresh and saline mixing zone from the shore (Taniguchi et al. 2006; Sadat-Noori et al. 2016).

The high NH_4^+ fluxes from porewater fluxes (Rodellas et al. 2018) combined with our isotopic signature data indicate that porewater fluxes are major source of NH_4^+. The volumetrically large contribution of nitrogen in the form of NH_4^+ has important implications for lagoon primary production, because phytoplankton and macrophytes preferentially take up NH_4^+ over NO_3^- due to reduced energetic costs (Lotze and Schramm 2000; Middelburg and Nieuwenhuize 2000; Cohen and Fong 2005). Uptake of NO_3^- is more energetically demanding, because it

requires the synthesis of NO_3^- and NO_2^- reductases and associative active transport systems (Syrett 1981).

Both La Palme and Salses-Leucate lagoons are shallow, allowing proliferous macrophytes to develop within the euphotic zone (> 60% dense macrophyte cover; IFREMER 2014). In such coastal lagoons, nutrients are efficiently incorporated into macrophytes biomass. In both lagoons, N/P ratios are relatively high in comparison to the Redfield ratio (Fig. 3.3). In La Palme lagoon, N/P ratios above the Redfield ratio in the low-salinity areas indicate influence of new nitrogen inputs (mainly NO_3^-) from the karstic groundwater, while high N/P ratio at mid-salinity in Salses-Leucate are a result of inputs of (regenerated) porewater NH_4^+. Whilst nitrogen is often a limiting factor in coastal systems, this is not the case in these lagoons due to the inputs of nitrogen from karstic groundwater and porewater fluxes. Groundwater inputs are thus particularly important in coastal lagoons like La Palme and Salses-Leucate lagoons where surface inputs are negligible.

High $\delta^{15}N$ signatures in macrophytes collected in La Palme lagoon in June 2017 (above 8‰; when NO_3^- concentration at the outlet of the sewage was exceptionally high; see below) and in phytoplankton (POM) in November 2016 in Salses-Leucate lagoon (Fig. 3.8) suggest major contributions from sewage effluent to support primary production during these periods. High signatures in La Palme lagoon in June 2017 coincide with the summer season, which is the main tourist season in the region, resulting in an increase in local population and thus, presumably, in the amount of sewage effluent. Indeed, during this period, an unusually high NO_3^- concentration was measured in the sewage effluent (522.4 µmol L^{-1}). This suggests that nitrogen fluxes from sewage effluent are higher in this season, and thus the uptake of sewage-driven nitrogen is likely more available for primary producers. Whereas NH_4^+ volatilization could have contributed to increasing the $\delta^{15}N$ of the remaining N pool resulting in ^{15}N enrichment of the macrophytes (Kendall et al. 2007), they alone do not explain the high $\delta^{15}N$ of the lagoon macrophytes in June 2017. NH_4^+ volatilization occurs under alkaline condition and high temperature, which are not found in either lagoon (Capone 2008; Das Gupta et al. 2016). Similarly, phytoplankton collected

at the outlet of the sewage treatment plants has elevated $\delta^{15}N$ signatures, also suggesting that it assimilated the ^{15}N-enriched nitrogen of the treated wastewater (Fig. 3.6c and d).

When excluding the exceptional high values in June 2017, the $\delta^{15}N$ signature of macrophytes fluctuate overall within a small range, particularly for Salses-Leucate lagoon (e.g. 2.1 to 7‰ in Salses-Leucate lagoon), whereas that of phytoplankton showed larger variability (e.g. -1.8 to 9.9‰ in Salses-Leucate lagoon) (Fig. 3.6), suggesting that macrophytes are better time-integrative measures of nitrogen input than phytoplankton (Dudley and Shima 2010). Similar observations were reported in estuaries by Cole et al. (2005). With a short life span (from a few days to a week) and large mobility of phytoplankton, its nitrogen signature will change at the short-term scale of hydrological events (Cloern et al. 2002). In contrast, (rooted) macrophytes integrate the isotopic signatures of the nitrogen sources over their longer lifetime, which usually ranges from 15 days to 160 days (Hemminga et al. 1999; Marbà et al. 2006). Their signatures represent thus a proxy of the longer-term average source signatures (Lepoint et al. 2004; Derse et al. 2007).

The different timescales of nutrient integration into macrophytes and phytoplankton allow assessing the temporal variability of nutrient inputs. Nitrogen supplied to the lagoon several weeks before the collection of samples cannot be 'tracked' in phytoplankton samples, but it is integrated in macrophyte records. For instance, the relatively higher $\delta^{15}N$ signatures in macrophytes than in phytoplankton in La Palme lagoon in June 2017 indicates a high nutrient supply from sewage effluent for several weeks before the sampling campaign, which must have ceased some days before the sampling campaign for it not to be reflected in the corresponding phytoplankton record (Fig. 3.8a). Similarly, the high $\delta^{15}N$ signature in phytoplankton in Salses-Leucate lagoon (November 2016), which is not recorded in macrophyte signatures, may indicate only recent sewage input that has not (yet) affected macrophyte signatures (Fig. 3.8b).

Overall, the combination of $\delta^{15}N$ records in long-lived macrophytes and short-lived phytoplankton provides insights into the dynamics of nitrogen input and

primary production in coastal ecosystems. This approach is a particularly useful additional tool in groundwater studies, where commonly large uncertainties in quantifying nitrogen fluxes (see section 3.2.1) result in uncertain evaluation of the 'true' impact of groundwater-derived nutrient fluxes on coastal ecosystems.

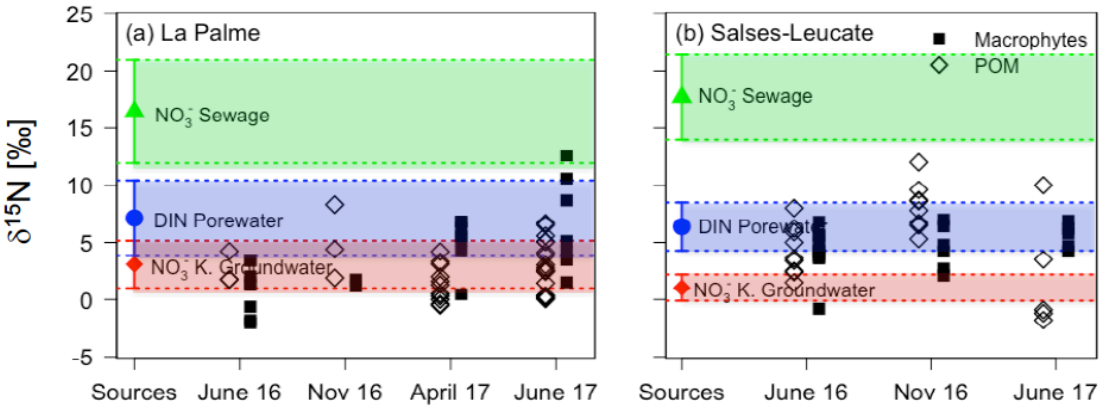

Figure 3.8| The $\delta^{15}N$ of macrophytes and POM (phytoplankton) in (a) La Palme and (b) Salses-Leucate lagoons, together with the isotopic signatures measured in inorganic nitrogen dissolved in water from the three identified sources. The nitrogen isotopic signatures are measured values and thus are not corrected for fractionation.

3.4.1.4 Contribution of different nitrogen sources

As noted above, the lack of an accurate characterization of fractionation factors and the identification of three major nitrogen sources prevents a fully quantitative assessment of the relative contribution of nitrogen sources. However, a qualitative assessment of the relevance of groundwater and porewater fluxes as a nitrogen source to primary producers (relative to sewage inputs) can be obtained by treating both advective water fluxes as a single source (groundwater+porewater). Indeed, the nitrogen isotopic signatures of the groundwater and porewater were relatively close to each other, particularly in La Palme lagoon. The contribution of the groundwater+porewater source can be estimated using the isotope mixing equation (Phillips and Gregg 2003):

$$\delta^{15}N_{pp} = f \times \delta^{15}N_{gw+por} + (1-f) \times \delta^{15}N_{sew} \qquad (3.3)$$

where f corresponds to the fraction of groundwater+porewater source, $\delta^{15}N_{pp}$ represents the nitrogen isotopic signatures in the primary producers and $\delta^{15}N_{gw+por}$ and N_{sew} are the nitrogen isotopic signatures of the groundwater+porewater and sewage endmembers, respectively. Assuming a fractionation factor of 2.5‰ during the nitrogen uptake (see section 3.4.1.2), the relative contribution of the groundwater+porewater source can be constrained by assuming that this source is exclusively dominated by the nitrogen signature of either karstic groundwater or porewater advection. The combination of groundwater and porewater fluxes would supply 76-100% and 60-94% of the nitrogen used to support primary producer growth in La Palme and Salses-Leucate lagoons, respectively. The remaining percentage accounts for the contribution of nitrogen from the sewage effluent. This qualitative assessment confirms that primary producers in both lagoons sourced most of their nitrogen from groundwater or porewater fluxes.

3.4.2 Macrophyte and phytoplankton carbon uptake and isotope signature

3.4.2.1 Inorganic carbon sources and signature

The role of groundwater and porewater fluxes as sources of DIC has previously been documented (Santos et al. 2012b; Atkins et al. 2013), constituting a major component of the carbon cycling in coastal ecosystems (Cai et al. 2003). The carbon isotope data in this study indicates that groundwater processes also play a major role in the carbon dynamics of Mediterranean lagoons.

The δ^{13}C-DIC values increase with increasing salinity in both lagoons and indicate binary and conservative mixing between a low salinity - low δ^{13}C-DIC source (karstic groundwater) and a high salinity - high δ^{13}C-DIC source (marine / seawater in equilibrium with the atmosphere with respect to DIC) (Fig. 3.5). However, some outliers in the relationship between the δ^{13}C of DIC and salinity indicate that other processes may play minor role. For instance, DIC inputs from porewater fluxes influence the δ^{13}C-DIC signatures in lagoon waters (see below), uptake by primary producers increases the isotopic signatures of DIC due to

preferential uptake of $^{12}CO_2$ over $^{13}CO_2$, and in contrast, respiration decreases the δ^{13}C-DIC due to input of lighter isotopes (Chanton and Lewis 1999).

Whereas the relationship between δ^{13}C-DIC and salinity in both lagoons suggests binary mixing between karstic groundwater and seawater, porewater is also likely an important source of DIC, given the mineralization of deposited organic matter in sediments and the high porewater fluxes of water and dissolved nutrients (Rodellas et al. 2018). Indeed, both the distribution of NH_4^+ concentrations in lagoon waters (Fig. 3.3c and d) and the high NH_4^+ measured in porewaters supports an important mineralization of organic matter and the potential transfer of mineralization products into the water column.

Considering the DIC excess (relative to overlying lagoon waters) concentrations in porewaters from La Palme lagoon measured in a concurrent study (600 - 1400 μmol L^{-1}; C. Monnin, unpublished data) and the estimated porewaters flows ((42 – 89) × 10^3 m^3 d^{-1}; Rodellas et al. 2018), DIC fluxes driven by porewater fluxes is on the order of (20 – 120) × 10^3 m^3 d^{-1}. These inputs are comparable to the DIC fluxes supplied by karstic groundwater discharge to La Palme lagoon, which are (20 – 170) × 10^3 m^3 d^{-1} as derived from karstic groundwater flows ((3 – 25) × 10^3 m^3 d^{-1}; Rodellas et al. 2018) and DIC concentrations in the karstic spring (5900 ± 800 μmol L^{-1}; C. Monnin, unpublished data). However, at the absence of porewater δ^{13}C-DIC data, we cannot fully determine the influence of porewater on the carbon uptake by primary producers.

Finally, porewater DIC should have isotope signature similar to the organic matter source deposited to sediments (Aller et al. 2008; Pozzato et al. 2018) and its carbon signatures are highly variable because of methanogenesis (LaZerte 1981). Decomposed macrophytes and particulate organic matter are the main components of organic matter in lagoon sediments (Garzon-Garcia et al. 2017), Because δ^{13}C in macrophytes and particulate organic matter varies with salinity (Fig. 3.7), the δ^{13}C-DIC in porewater is also likely to vary with salinity (thus a not-constant endmember), making it difficult to trace porewater δ^{13}C-DIC in the lagoon waters.

Whilst isotope data itself does not allow the differentiation of DIC contributions of groundwater and sewage input due to their similar signature, sewage contributions is commonly considered negligible in the carbon budget in coastal systems (unlike its role in the nitrogen budget) (Dudley and Shima 2010; Tseng et al. 2016). Therefore, overall, our results suggest that karstic groundwater, porewater fluxes and seawater are the major sources of DIC in the studied lagoons.

3.4.2.2 DIC uptake by primary producers

Like for nitrogen, the DIC uptake by macrophytes occurs mainly through the leaves, and root contributions are considered insignificant (Hemminga and Mateo 1996; Enoch H. Z. and Olesen J. M. 2006). Primary producers sampled in this study are thus assumed to source also most of their inorganic carbon from the water column. Our results show overall low carbon signatures in primary producers located close to the karstic groundwater springs and high signatures from the marine parts, indicating different DIC sources (Fig. 3.7). The low $\delta^{13}C$ in macrophytes and phytoplankton (POM) sampled in the groundwater springs suggests that they incorporate groundwater-derived DIC, which is depleted in ^{13}C due to the mineralization of organic matter in the karstic springs (Fig. 3.7).

Due to the smaller size of La Palme lagoon and relatively larger groundwater inflow and more restricted exchange with the ocean in comparison with Salses-Leucate lagoon, the relative impact of karstic groundwater is greater than in the larger, better-mixed Salses-Leucate lagoon (Stieglitz et al. 2013). The larger size of Salses-Leucate lagoon facilitates a more efficient lagoon water-atmosphere exchange due to larger wind fetch (Stieglitz et al. 2013). This is mirrored in the primary producers' carbon isotope signatures, indicating an overall greater assimilation of carbon of marine (atmospheric) origin in Salses-Leucate lagoon than in La Palme lagoon (Fig. 3.7b and c).

DIC is considered a major control on the $\delta^{13}C$ of the primary producers (Lin et al. 1991). $\delta^{13}C$ in macrophytes and phytoplankton increase with increasing $\delta^{13}C$-DIC in both lagoons (Fig. 3.9), similar to previously reported relationships in

coastal bay (Chanton and Lewis 1999) and lakes (LaZerte and Szalados 1982). However, a 1:1 relationship between the δ^{13}C-DIC and the δ^{13}C-primary producers is not observed. This is likely due to isotopic fractionation, although additional sources of carbon could also affect this relationship. Previous estimations of isotopic fractionation associated with inorganic carbon uptake are around 12‰ and 20‰ for macrophytes and phytoplankton, respectively (LaZerte and Szalados 1982; Chanton and Lewis 1999). These estimations are in good agreement with the fractionation factors derived in our study by applying the previously described approach (section 3.4.1.2) to carbon signatures along the salinity gradients (16.7 ± 5.4‰ for macrophytes and 20.6 ± 3.0‰ for phytoplankton in La Palme lagoon; 14.8 ± 6.0‰ for macrophytes and 20.3 ± 3.3‰ for phytoplankton in Salses-Leucate lagoon). Fractionation thus explains the majority of the difference between the carbon signatures of DIC and primary producers and the lack of a 1:1 relationship. Assimilation of atmospheric CO_2 during emersion as additional source of carbon for macrophytes can be excluded here because macrophytes are rarely to never exposed in the studied lagoons (tidal effects are negligible) (Hemminga & Mateo, 1996).

The estimated fractionation factor during DIC uptake by concurrently analysing the δ^{13}C in water and primary producers of the karstic groundwater spring is 21.3 ± 3.4‰ for phytoplankton. Relatively constant carbon isotopic signatures are expected (and measured) in the groundwater spring, and thus we can assume that the δ^{13}C-DIC of the water column is representative of the signature taken up by the primary producers for this sample. A fractionation factor can also be estimated for the primary producers in the coastal Mediterranean Sea station (sea endmember), where δ^{13}C-DIC in water can also be assumed constant (unlike the rest of the lagoon). For the sea endmember, it is 24.5 ± 2.1‰, which is slightly higher than in the groundwater endmember. This indicates that fractionation may be controlled by salinity, with fractionation being smaller at low salinities (groundwater) and greater at high salinity (sea), as previously reported by Chanton and Lewis (1999). This difference in fractionation may result from a change in phytoplankton species with salinity (e.g. Lionard et al. 2005). A quantitative estimation of groundwater versus porewater contributions

on the DIC uptake by primary producers cannot be made from the isotopic signature alone, but our indirect flux estimation (from water flow multiplied by endmember concentration) indicated contributions from both groundwater and porewater as sources of DIC to coastal lagoons.

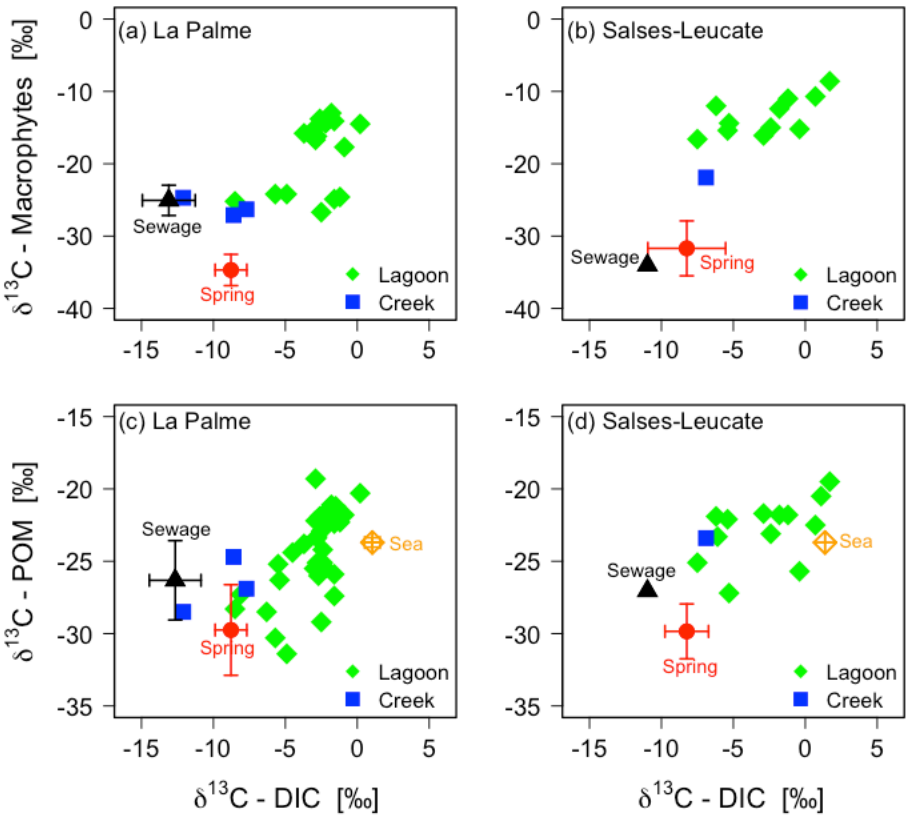

Figure 3.9| The $\delta^{13}C$ of Macrophytes (a, b) and POM (c, d) versus $\delta^{13}C$-DIC in lagoon water from La Palme and Salses-Leucate lagoons, respectively. Endmembers indicate the average $\delta^{13}C$ of primary producers in the sewage effluents (black triangle), springs (red circle) and seawater (orange diamond). $\delta^{13}C$ data from primary producers in the lagoons (green diamond) and the creeks (blue square) are shown together for the four sampling campaigns. Note the scale difference on the y-axes.

3.5 Conclusion

This study provides direct evidence for the role of karstic groundwater and porewater fluxes in sustaining primary production in the studied coastal lagoons. The combined nitrogen isotopic signatures in macrophytes and phytoplankton demonstrate that karstic groundwater and porewater fluxes are

the main sources of inorganic nitrogen assimilated by primary producers in La Palme and Salses-Leucate lagoons. Sewage effluents contribute, however, locally to the nitrogen input at times when sewage nitrogen concentrations are particularly high. Nitrogen isotope signatures in macrophytes represents long-term average source signatures while those of phytoplankton indicate recent variations in inputs.

The distinct signatures of carbon stable isotope in low-salinity karstic groundwater and seawater in the studied lagoons allowed us to differentiate between these two sources of dissolved inorganic carbon. The low carbon signatures from karstic groundwater were traced in primary producers collected in the low salinity parts of the lagoon, revealing the influence of groundwater inputs as a source of carbon to support primary production. Conversely, high signatures from the marine inorganic carbon were traced in primary producers located in the marine parts of the lagoons.

Combination of nitrogen and carbon stable isotope signatures in both short-lived and long-lived primary producers allows tracing nitrogen and carbon sources from groundwater and advective porewater sustaining primary production in coastal ecosystems on the timescales of their lifespan. Furthermore, the impact of karstic groundwater sustaining primary production is greater in the small La Palme lagoon due to larger fresh karstic groundwater inflow and the restricted exchange with the open sea, while in Salses-Leucate lagoon (larger lagoon), the karstic groundwater influence is limited to the areas close to the sources.

– Chapter 4 –

Enhanced growth rate of the Mediterranean mussel in a coastal lagoon driven by groundwater inflow

This chapter is based on:

Aladin Andrisoa, Franck Lartaud, Valentí Rodellas, Ingrid Neveu, Thomas C. Stieglitz. Enhanced growth rates of the Mediterranean mussels in a coastal lagoon driven by groundwater inflow. Accepted in *Frontiers in Marine Science*.

4.1 Introduction

In the Mediterranean Sea, which is an oligotrophic basin characterized by limited surface water inputs, groundwater discharge is a major source of nutrients to coastal systems and may thus affect the primary production in the ecosystems (Herrera-Silveira 1998; Basterretxea et al. 2010; Tovar-Sánchez et al. 2014; Rodellas et al. 2015). However, the impacts of groundwater discharge are not limited to nutrient loading: a wide range of organisms also respond to changes in water salinity, light penetration into water column, pH and turbulence (Short and Burdick 1996; Troccoli-Ghinaglia et al. 2010; Lee et al. 2017). For example, groundwater input has been demonstrated to increase meiofauna diversity (Encarnação et al. 2015) and the abundance and body size of Mediterranean mussels (Piló et al. 2018) in Olhos de Agua beach in Portugal, and enhance species richness, abundance and biomass of fishes and invertebrates in Japanese coastal waters, where high groundwater-borne nutrient concentrations have been reported (Hata et al. 2016; Utsunomiya et al. 2017). Conversely, groundwater discharge reduces coral species diversity in coastal systems due to lower salinity (Lirman et al. 2003; Amato et al. 2016). While some studies document the effect of groundwater discharge on primary producers in coastal ecosystems (e.g. Herrera-Silveira 1998; Charette et al. 2001; Andrisoa et al. 2019), the impact of groundwater discharge on the growth of animals such as mussels and fish species remains largely unstudied (Hata et al. 2016; Piló et al. 2018).

In this study, we assess the effects of groundwater discharge on the growth of the Mediterranean mussel (Mytilus galloprovincialis), which is a commercially important species in the Mediterranean region. Typical for bivalves, mussels sequentially deposit new shell layers during their growth. The shell growth patterns are controlled by both environmental and physiological factors such as temperature, salinity, food availability, tides, day/night cycles and biological clocks (Evans 1972; Richardson 1988; Jones et al. 1989; Sato 1997; Schöne et al. 2004). We here investigate the variations in growth rate and condition index (tissue dry weight / shell dry weight) of mussels growing in the groundwater-fed

Salses-Leucate lagoon (France) and examine the role of environmental parameters in mussel growth in this natural environment.

4.2 Materials and Methods

4.2.1 Study sites

Salses-Leucate lagoon is located on the southwestern French Mediterranean coast. The region experiences rainfall during fall and spring (500 mm per year) with little rain during summer, and is characterized by strong northwesterly winds, regularly exceeding 10 m s^{-1}, which play an important role in the hydrodynamics of the lagoon (e.g. Stieglitz et al. 2013; Rodellas et al. 2018).

Groundwater discharges directly into the lagoon from two karstic springs, Font Estramar and Font Dame, with mean water flows of 3.0×10^5 m^3 d^{-1} and 2.0×10^5 m^3 d^{-1}, respectively (Fleury et al. 2007) (Fig. 4.1). The lagoon is permanently connected with the Mediterranean Sea by three large artificial openings in the eastern part of the lagoon, through which lagoon water efficiently exchanges on a continuous basis. A recent study showed that nutrient inputs driven by the discharge of the two karstic springs are the main source of nitrogen for primary producers in the western basin (Andrisoa et al. 2019). A few small intermittent streams deliver freshwater to the lagoon from the catchment area only during high-rainfall periods.

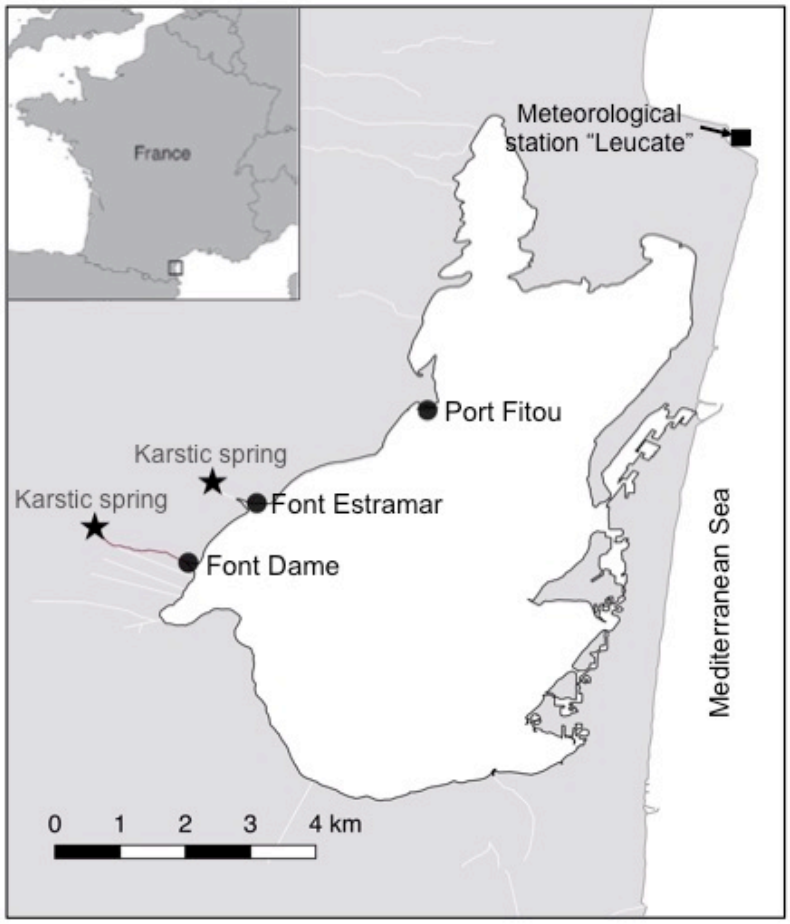

Figure 4.1| Salses-Leucate lagoon location on the French Mediterranean coastline. The groundwater-influenced sites (Font Dame and Font Estramar) and control site (Port Fitou) are shown, as well as the groundwater springs and the meteorological station.

4.2.2 Installation of mussel cages and monitoring of environmental parameters

Three different locations in the western basin of Salses-Leucate lagoon were selected to evaluate the influence of groundwater inputs on mussel growth: two groundwater-influenced sites, located close to the karstic springs of Font Dame and Font Estramar, respectively, and a control site (Port Fitou) far from the groundwater sources and representative for average lagoon conditions (Fig. 4.1). At each location, thirty to sixty (naturally present) specimens of Mediterranean mussels *Mytilus galloprovincialis* were collected on 10 October 2016 at Font Dame and Font Estramar sites and 17 February 2017 at Port Fitou (Table 4.1; Fig. 4.2a). The initially selected lagoon control sites (i.e. deep cages) were not appropriate due to large salinity variability, requiring a new control site (Port

Fitou) installed only four month after the beginning of the experiments. New specimens were collected on 27 June 2017 at Font Dame sites but not at Font Estramar sites. Shell length of each individual was measured and specimens were immersed in a calcein solution of 150 mg/L for one hour (Fig. 4.2b). The fluorescent marker calcein is incorporated into growing calcium carbonate structures (Moran 2000), and used for identification and measurement of growth of various calcifying species (Mahé et al. 2010; Lartaud et al. 2013; Nedoncelle et al. 2013). Sodium bicarbonate (105 g) was added to the solution to adjust the pH to 8.2 and to enhance the solubility of calcein. After shell marking, the calcein-marked mussels were returned to their original location by placing them in cages (25 cm x 12 cm). At a mean water depth of ca. 70 cm at both Font Dame and Font Estramar sites, cages were installed at 50 cm (surface cage) and 20 cm (bottom cage) above the bottom, experiencing different conditions in the periodically stratified water column due to fresh groundwater inflow (Fig. 4.2c). One cage was installed at Port Fitou (vertical homogeneity of the water column). As the mussels were returned to their respective original habitat, it is reasonable to assume that they tolerate the environmental conditions and that growth is not affected by the experimental setup. The calcein-marked mussels were periodically sampled from the cages between November 2016 and January 2018 (Table 4.1).

CTD loggers (Solinst LTC Levelogger and NKE S2T600) were installed with all the mussel cages at the three sites to monitor temperature, salinity and water level variations (Fig. 4.2d). Water level was corrected for atmospheric pressure. Loggers were protected with copper mesh to avoid biofouling of the sensors, and were regularly cleaned (once every 1-2 months). Precipitation, wind and atmospheric pressure data at the nearby meteorological station “Leucate” were extracted from the French meteorological service (Météo France).

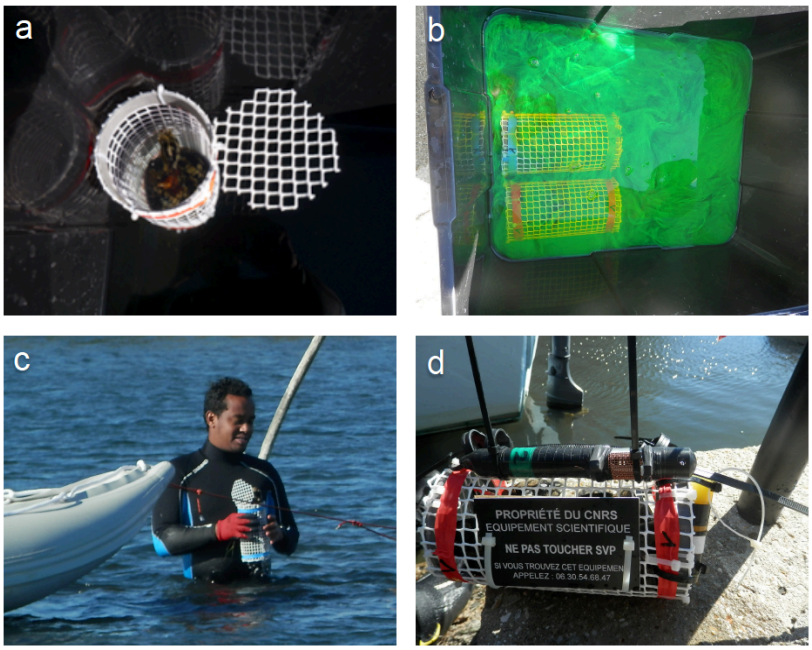

Figure 4.2| (a) Mussels collected from the lagoon, (b) calcein marking, (c) cage installation and (d) cage with CTD loggers.

Table 4.1| The shell length mean (Mean ± SD) and range (Min-Max), and the number (n) of mussels installed / collected from the cages with collection date from the different stations in Salses-Leucate lagoon: FDS: Font Dame Surface, FDD: Font Dame Deep, FES: Font Estramar Surface, FED: Font Estramar Deep and PF: Port Fitou.

	Date	FDS	FDD	FES	FED	PF
Installation	10/10/2016	49 ± 16 (21-78, n=30)	58 ± 8 (43-79, n=29)	51 ± 11 (22-67, n=40)	38 ± 6 (22-52, n=76)	
	17/02/2017	-	-	-	-	58 ± 6 (46-78, n=33)
	27/06/2017	40 ± 11 (20-82, n=63)	46 ± 10 (29-80, n=30)	-	-	-
Collection	24/11/16	59 ± 10 (49-77, n=6)	66 ± 11 (55-82, n=5)	56 ± 4 (51-61, n=5)	47 ± 3 (44-51, n=6)	-
	14/01/17	63 ± 7 (54-74, n=6)	63 ± 6 (53-71, n=7)	56 ± 11 (27-69, n=10)	39 ± 3 (36-42, n=10)	-
	27/03/17	59 ± 7 (52-70, n=5)	61 ± 5 (53-67, n=6)	56 ± 4 (51-60, n=6)	44 ± 3 (41-49, n=7)	63 ± 8 (57-77, n=7)
	27/06/17	52 ± 10 (38-68, n=15)	-	-	-	65 ± 7 (56-70, n=10))
	29/11/17	54 ± 13 (37-82, n=15))	57 ± 13 (49-81, n=8)	-	-	63 ± 4 (57-67, n=5))
	29/01/18	43 ± 4 (38-50, n=10)	53 ± 10 (39-66, n=5)	-	-	60 ± 11 (46-79, n=10)

4.2.3 Sample preparation

In the laboratory, mussel samples were cleaned to remove all epibionts and other attached organisms. The shell total length was measured along the maximum growth axis using a calliper. The shells were carefully opened and tissues removed. The shell and the flesh of each individual were dried at 60°C overnight and weighted separately.

For the sclerochronological analysis, the right valve of each shell was cut along the maximum growth axis and perpendicular to the growth lines with a Buehler Isomet low-speed saw, using a 0.3 mm thick diamond wafering blade (Fig. 4.3a). The section was mounted on a glass slide using Epoxy Araldite 2020 resin (Fig. 4.3b). A thin section (0.8 mm) of shell was cut along the maximum growth axis, ground with 80, 180, 400 and 800 SiC grit, polished with 3, 1 and 0.3 µm Al_2O_3 powder and rinsed with deionized water following the protocol in Nedoncelle et al. (2013). In order to resolve growth patterns in the shells (Fig. 4.3c), polished sections were etched in a Mutvei's solution composed of 500 mL 1% acetic acid, 500 mL 25% glutaraldehyde, and 5 g alcian blue powder for 1 h at 37-40°C (Schöne et al. 2005a) (Fig. 4.3d). Etched samples were immediately rinsed with deionized water and dried.

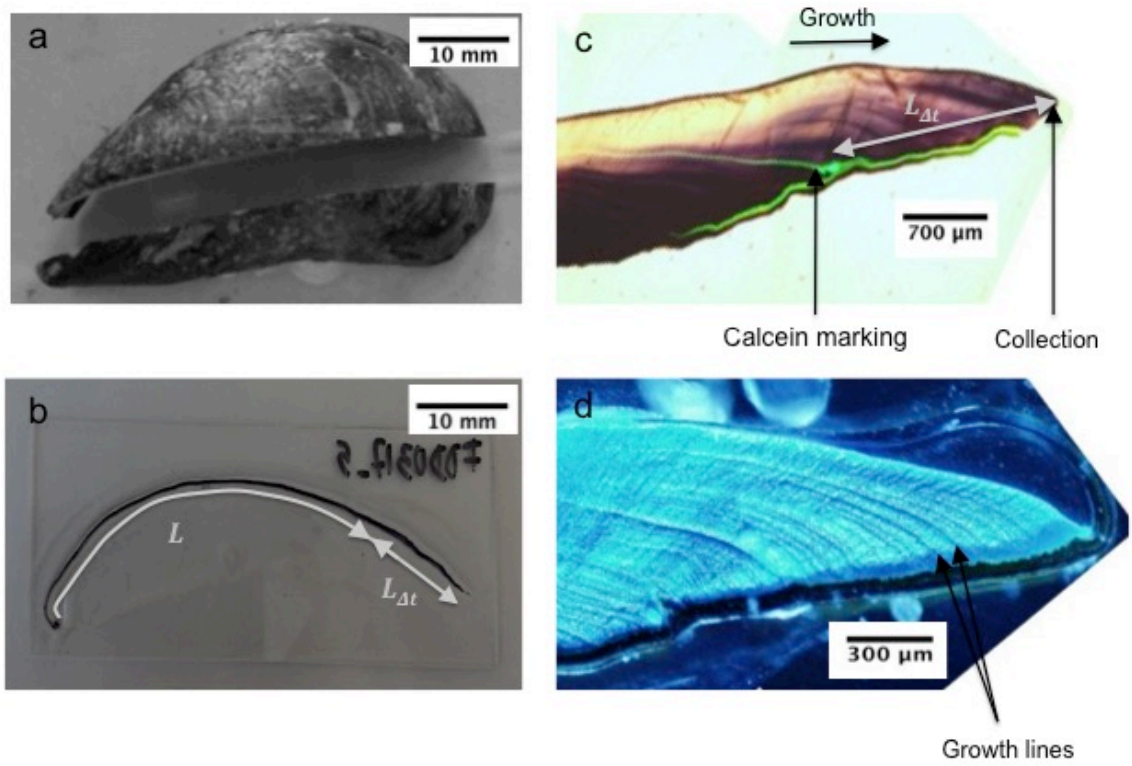

Figure 4.3| (a) Mussel section along the maximum growth axis, (b), section mounted on glass slide showing the shell length ($L_t = L + L_{\Delta t}$), (c) shell under natural light showing the calcein marking and (d) the shell under fluorescent light showing growth increments.

4.2.4 Condition Index

The condition index (C.I.) is defined as the ratio between the flesh (tissue) dry weight and the shell dry weight (Eq. 4.1). This index is commonly used to assess the health and the quality of the mussel for scientific and commercial purposes (Lucas and Beninger 1985; Yildiz et al. 2006; Peharda et al. 2007). It is particularly important in quality assessment and marketing value of bivalves – the higher the proportion of tissue, the better the commercial value (Župan and Šarić 2014).

$$C.I. = \frac{Tissue\ dry\ weight}{Shell\ dry\ weight}\ x\ 100 \qquad (4.1)$$

4.2.5 Growth analyses

In order to identify the growth lines marked with calcein, the cross-sections (on the glass slide) were viewed under epifluorescent microscope at magnification 4X (OLYMPUS BX61) and digitized with an OLYMPUS DP 72 camera at the Observatoire Oceanologique de Banyuls-sur-Mer, France (BIOPIC platform). Mutvei-treated sections were analyzed under reflecting light using the same microscope and camera. Growth analyses were carried out on mounted photographs using image processing software Adobe Photoshop and Image J. The distance between the calcein mark and the ventral edge of the shell ($L_{\Delta t}$) was measured to allow an estimation of the growth rate during the period held in the cages (Fig. 4.3c). The number of growth increments was counted to estimate the growth periodicity. The width of growth increments was measured to assess the relation between growth and environmental parameters. In some cases, the growth pattern was not well revealed by the Mutvei etching, which may lead to an underestimation of growth increments and an overestimation of the increment width (Nedoncelle et al. 2013). We focused our analysis on the shells with clear growth increments. The periodicities in shell growth were estimated by Fast Fourier Transform (FFT) (Welch 1967; Walker 1996).

4.2.6 Growth curves

The growth rate of individual mussels was modelled using the Von Bertalanffy growth equation as described in Nedoncelle et al. (2013):

$$L_t = L_\infty(1 - exp^{[-K(t-t_0)]}) \qquad (4.2)$$

where L_t is the shell total length (mm), measured along the maximal growth axis (Fig. 4.3b); L_∞ is the asymptotic theoretical shell length (mm); K represents the growth coefficient (year^{-1}); and t_0 is the time constant obtained from the minimum size at mussel settlement (L_0) (L_0 and t_0 are assumed to be zero in our calculations; Ramón et al. 2007). For each individual, L_t was measured and the shell portion $L_{\Delta t}$ determined from the distance between the calcein mark and the end of the shell (Fig. 4.3b).

The linear regression between the total shell length (L_t) and L allows to define the Ford-Walford *y*-intercept a and regression slope b used to calculate the Von Bertalanffy parameters K and L_∞ (Nedoncelle et al. 2013):

$$L_t = a + b * L \quad (4.3)$$

$$K = -\ln(b)/\Delta t \quad (4.4)$$

$$L_\infty = a/(1-b) \quad (4.5)$$

The growths of mussels from different sites were compared using commonly used indices of growth performance: the phi-prime index (φ') and the index P, calculated from the Von Bertalanffy growth parameters K and L_∞ (e.g. Brey 1999; Ragonese et al. 2012):

$$\varphi' = \log_{10}(K) + 2 * \log_{10}(L_\infty) \quad (4.7)$$

$$P = \log_{10}(K * L_\infty) \quad (4.8)$$

4.2.7 Statistical analyses

Data normality and homogeneity of variances were tested with Shapiro-Wilk and Levene's tests, respectively. All statistical analyses were considered at α=0.05 level. Analysis of Variance (one-way ANOVA) was used to assess the differences in condition indices between sites Font Dame Surface, Font Dame Deep, Font Estramar Surface, Font Estramar Deep and Port Fitou. We used t-test statistics to determine if there were significant differences in condition indices, growth rates, salinity and water temperature between groundwater-influenced sites (Font Dame Surface, Font Dame Deep, Font Estramar Surface, Font Estramar Deep, which were pooled together for this comparison) and the control site (Port Fitou). The differences between surface cages (Font Dame Surface and Font Estramar Surface) and bottom cages (Font Dame Deep and Font Estramar Deep) were also tested using t-test statistics.

4.3 Results

4.3.1 Condition index

The average condition indices estimated from the sampled mussels during the study period were 8.8 ± 2.3% (n=50) at Font Dame Surface, 9.9 ± 2.3% (n=26) at Font Dame Deep, 9.5 ± 3.3% (n=20) at Font Estramar Surface, 8.8 ± 2.2% (n=23) at Font Estramar Deep and 5.8 ± 1.4% (n=30) at Port Fitou. The condition index varied significantly between sites (ANOVA: $F = 5.32$, $p<0.05$) with significantly higher indices at the groundwater-influenced sites over the control site (t-test: $t = 5.93$, $p<0.05$) (Fig. 4.4a).

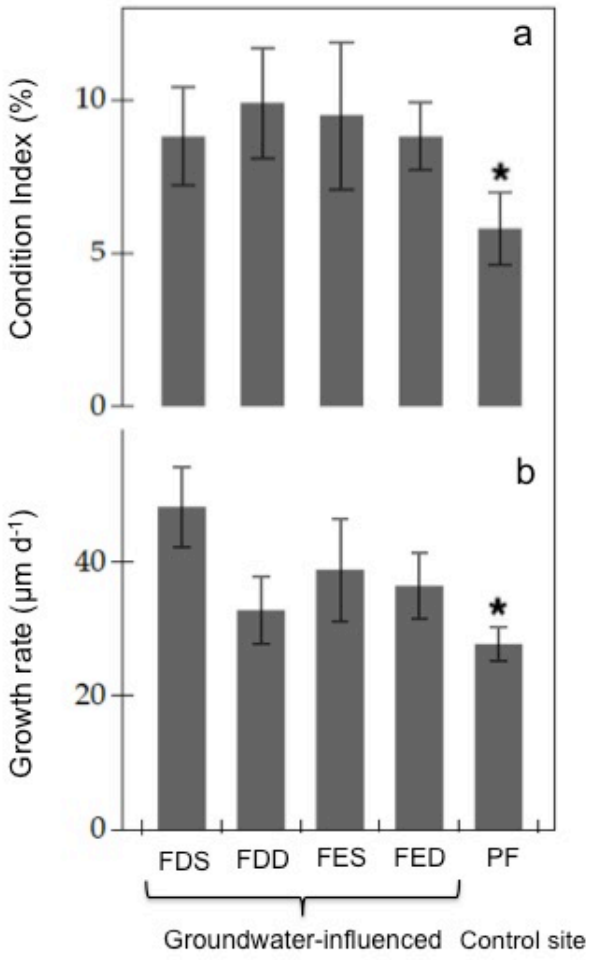

Figure 4.4| (a) Mean (± SD) condition indices and (b) growth rate in groundwater-influenced sites (FDS: Font Dame Surface, FDD: Font Dame Deep, FES: Font Estramar Surface and FED: Font Estramar Deep) and the control site (PF: Port Fitou) in Salses-Leucate lagoon. The asterisk indicates that p is less than 0.05 for the Student's t-test between groundwater-influenced sites and control site (condition index: groundwater influenced-sites n=119, control site n=30, t-test, t=5.93, p<0.05; growth rate: groundwater influenced-sites n=74, control site n=8, t-test, t=5.24, p<0.05).

4.3.2 Shell growth rate

The mean growth rates for sampled mussels were 48.2 ± 6.0 μm d^{-1} (n=31) at Font Dame Surface, 32.8 ± 5.0 μm d^{-1} (n=17) at Font Dame Deep, 38.8 ± 7.7 μm d^{-1} (n=13) at Font Estramar Surface, 36.4 ± 5.0 μm d^{-1} (n=13) at Font Estramar Deep and 27.7 ± 2.5 μm d^{-1} (n=8) at Port Fitou (Fig. 4.4b). Similar to the condition index, the growth rate of mussels from the groundwater-influenced sites (mean = 40.9 ± 9.2 μm d^{-1}) was significantly higher than that of the control site (27.7 ± 2.5 μm d^{-1}) (t-test: $t = 5.24$, $p<0.05$). At the groundwater-influenced sites (Font Dame and Font Estramar), the growth rates were significantly higher for the mussels from the surface than those from the bottom (t-test: $t = 3.97$, $p<0.05$) with the highest rate observed at Font Dame Surface.

4.3.3 Growth curves

The Von Bertalanffy growth curves derived from *M. galloprovincialis* collected in Salses-Leucate lagoon at the groundwater-influenced sites (combined data from Font Dame Surface, Font Dame Deep, Font Estramar Surface and Font Estramar Deep; n=79, size range = 26.5 - 81.5 mm) and at the control site (n=11, size range = 56.0 - 68.0 mm) are presented in Fig. 4.5, together with curves obtained for the same species growing at other coastal Mediterranean sites. Overall, the growth rates of *M. galloprovincialis* from Salses-Leucate lagoon (groundwater-influenced sites: K = 0.54, L_∞ = 75.0 mm; control site: K = 0.46, L_∞ = 63.9 mm) are among the highest reported for this species in the Mediterranean region, particularly for the groundwater-influenced sites (Table 4.2; Fig. 4.5). As commonly observed, the results indicated a fast growth rate at a younger age and a decrease in growth rates as the shell approaches its maximum size (Fig. 4.5). Individuals collected from the groundwater-influenced sites showed higher total growth rates than individual from the control site. For instance, after three years, mussels from the groundwater-influenced sites reached 60 mm while those from the control site reached only 48 mm. Furthermore, the growth performance indices at the groundwater influenced sites (φ' = 3.48, P = 1.61) and the control site (φ' = 3.27, P = 1.47) were also among the highest reported to date for this species in the Mediterranean region (Table 4.2).

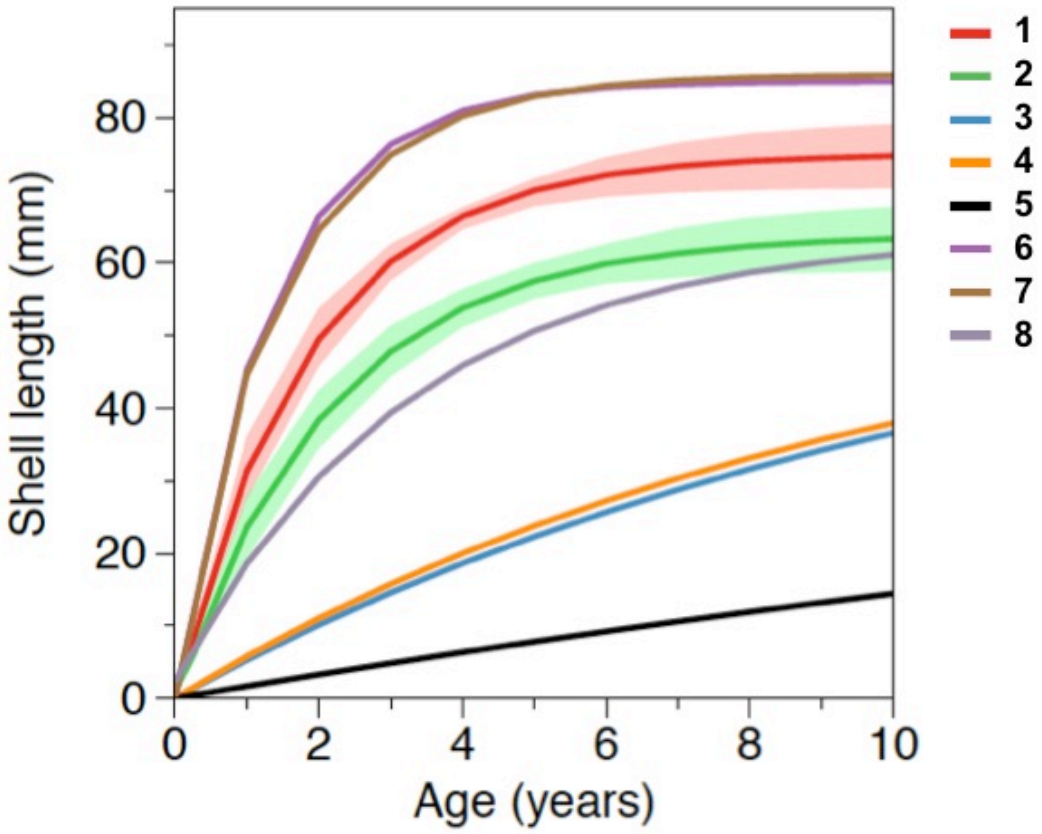

Figure 4.5| Von Bertalanffy growth curves of *Mytilus galloprovincialis* from the groundwater-influenced sites and the control site in Salses-Leucate lagoon and from other coastal systems in the Mediterranean region with **1**: groundwater-influenced sites in this study (K=0.54, L_∞=75.0); **2**: control site in this study (K=0.46, L_∞=63.9); **3**: semi-enclosed basin in Italy (K=0.09, L_∞=62.1, Posa and Tursi 1991); **4**: coastal basin in Italy (K=0.10, L_∞=58.7, Posa and Tursi 1991); **5**: coastal bay in Italy (K=0.03, L_∞=51.3, Sarà et al. 2012); **6**: coastal bay in Spain (K=0.76, L_∞=85.0, Ramón et al. 2007), **7**: coastal lagoon in Italy (K=0.66, L_∞=85.9, Ceccherelli and Rossi 1984) and **8**: coastal area in Algeria (K=0.31, L_∞=64.0, Abada-Boujemaa Y. M. 1996). Shaded areas represent the standard deviations of data obtained in the present study.

Table 4.2| The Von Bertalanffy growth parameters and the growth performance indices values of *M. galloprovincialis* from this study and other coastal systems in the Mediterranean region.

References	Sites	K	L_∞ (mm)	φ'	P
This study	GW-influenced sites	0.54	75.0	3.48	1.61
	Control site	0.46	63.9	3.27	1.47
Posa and Tursi 1991	Semi-enclosed basin, Italy	0.09	62.1	2.54	0.75
	Coastal basin, Italy	0.10	58.7	2.54	0.77
Sarà et al. 2012	Coastal bay, Italy	0.03	51.3	1.90	0.19
Ramón et al. 2007	Coastal bay, Spain	0.76	85.0	3.74	1.81
Cerccherelli and Rossi 1984	Coastal lagoon, Italy	0.66	85.9	3.69	1.75
Abada-Boujemaa M. 1996	Coastal area, Algeria	0.31	64.0	3.10	1.30

4.3.4 Growth increments

Mussels growing in Salses-Leucate lagoon formed growth increment with daily (circadian) rhythm. Among the shells showing clear growth pattern, the average number of increments were 0.9 ± 0.2 (n=17), 0.7 ± 0.1 (n=15), 0.8 ± 0.2 (n=9), 0.8 ± 0.1 (n=9) and 0.7 ± 0.1 (n=6) per day in Font Dame Surface, Font Dame Deep, Font Estramar Surface, Font Estramar Deep and Port Fitou, respectively. For instance, a mussel collected at Font Estramar Surface formed 93 growth increments during 96 days. The number of increments was consistently lower than the number of days.

Sclerochronological profiles showed a large variability in increment width for a given shell. The periodicities in increments width were estimated by Fast Fourier Transform (FFT) analyses. The analyzed shells exhibited similar patterns and, as an example, three shells (one each site) are presented in Fig. 4.6. The FFT analyses revealed peaks at low frequency corresponding to periodicities of 12.7, 11.2 and 11.3 increments for the shells S1 (FDS0118-3), S2 (FDD0118-4) and S3 (PF0118-3), respectively. Considering the near-daily rhythm of the growth increment, the peaks correspond thus to a period of 11 - 13 days (near-

fortnightly period). The power spectrum for the three shells also showed peaks at high frequencies corresponding to the periods of approximately 3 and 5 days.

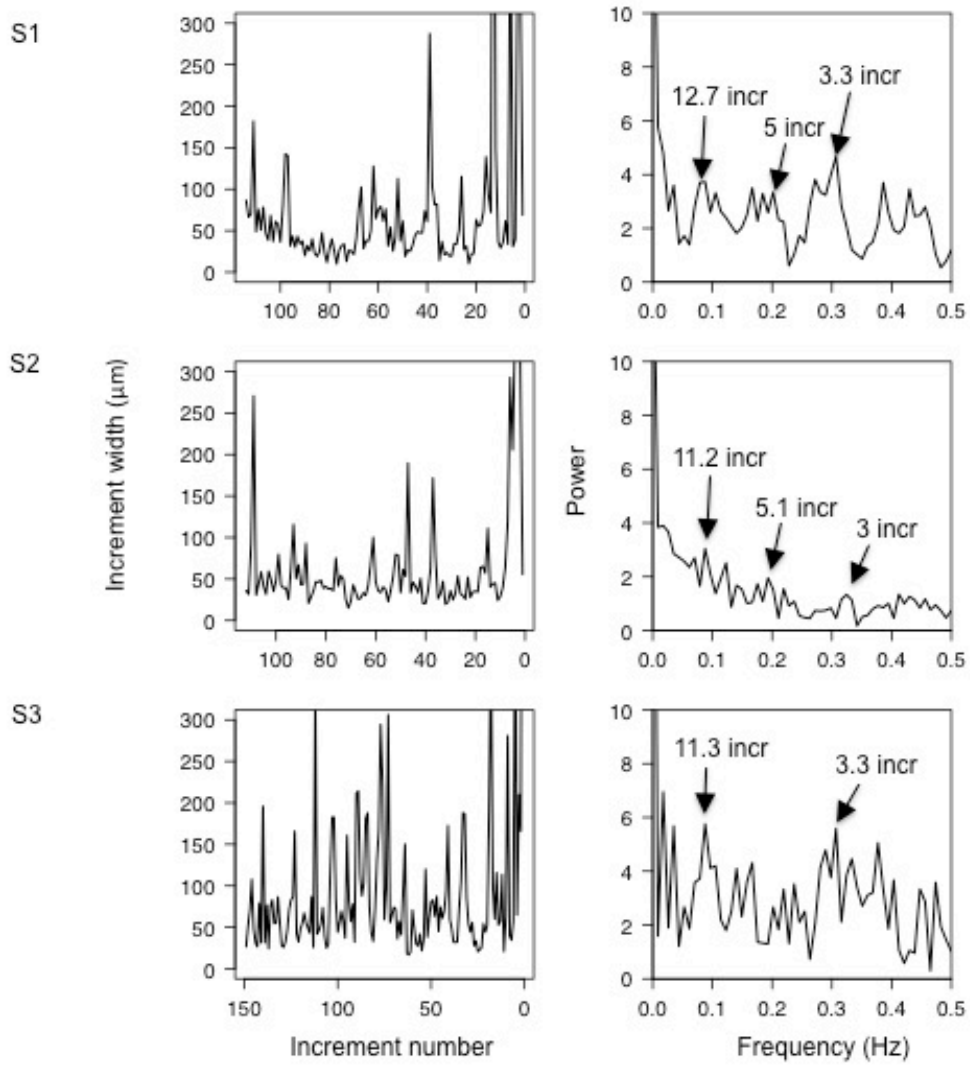

Figure 4.6| Left panel: increment number from the calcein mark (right side) to the collection (left side) for three representative *Mytilus galloprovincialis* shells S1 (FDS0118-3), S2 (FDD0118-4) and S3 (PF0118-3) between June 2017 and January 2018. Right panel: Fast Fourier Transform showing the periodicities of the increment width.

4.3.5 Environmental parameters

4.3.5.1 Time series variations

The daily precipitation in Salses-Leucate lagoon ranged between 0.0 and 70.2 mm with a maximum value recorded shortly after the calcein marking (13 October 2016) (Fig. 4.7a). High rainfall events coincided overall with high wind events and occurred chiefly between January and April. The region is characterized by frequent strong winds generally blowing from the northwest. Southeasterly winds also arrive from the Mediterranean Sea but they are less frequent. The wind speed recorded varied between 1.6 and 18.0 m s^{-1} with an average value of 5.8 ± 2.8 m s^{-1} (Fig. 4.7b).

Lagoon water levels at Font Dame, Font Estramar and Port Fitou showed similar patterns. They are principally controlled by precipitations as well as winds (Ladagnous and Le Bec 1997). The water level generally increased with increasing precipitation and wind speed (Fig. 4.7c). The average water levels were 0.7 ± 0.1, 0.8 ± 0.2 and 1.0 ± 0.1 m in Font Dame, Font Estramar and Port Fitou, respectively, indicating that the installed cages (at 0.2 and 0.5 m from the sediment-water interface) were rarely exposed.

The water temperature showed overall similar patterns at the study sites with seasonal minimum values observed in winter and maximum values in summer overlaid by daily variations (Fig. 4.7d). From February 2017 to January 2018 (data available at all sites), the water temperatures were significantly higher at groundwater-influenced sites (mean values in FDS = 18.1 ± 5.1, FDD = 18.1 ± 6.0, FES = 20.5 ± 4.8 and FED = 20.1 ± 5.1 °C) than at Port Fitou (mean = 17.3 ± 6.7 °C) (t-test: $t = 2.34$, $p<0.05$). Furthermore, for the total period of data collection (October 2016 – January 2018), the water temperatures were significantly higher at the surface (FDS = 16.7 ± 5.1 °C; FES = 16.5 ± 5.5 °C) than at the bottom (FDD = 16.5 ± 5.5 °C; FED = 15.8 ± 5.9 °C) (t-test: $t = 1.38$, $p<0.05$).

The salinity was highly variable at the groundwater-influenced sites (Font Dame and Font Estramar) and no clear pattern was observed (Fig. 4.7e), with salinity ranges of 9.0 - 35.8 (FDS), 7.4 - 44.4 (FDD), 10.2 - 36.8 (FES) and 10.0 - 40.7

(FED). In contrast, salinity in Port Fitou was relatively stable with seasonal values ranging between 26.2 and 41.8, showing small daily variations and a seasonal pattern with maximum values recorded at the end of summer (consistent with an increase of evaporation and a decrease of freshwater inputs). The salinity at Port Fitou was overall considerably higher than that observed at the groundwater-influenced sites, reflecting average lagoon conditions (t-test: $t = 37.95$, $p<0.05$).

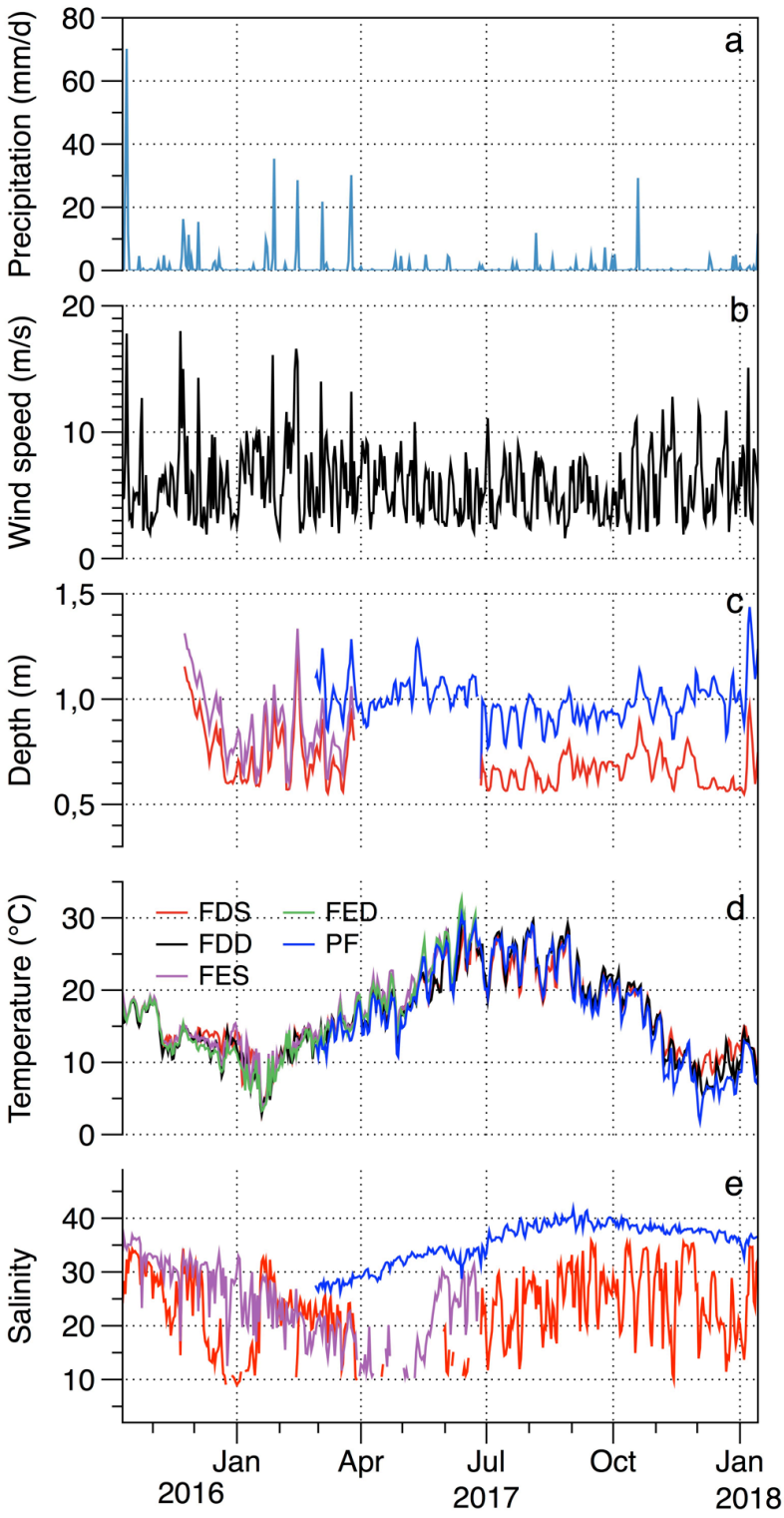

Figure 4.7| Temporal variations between October 2016 and January 2018 in (a) precipitation, (b) wind speed, (c) water depth, (d) temperature and (e) salinity in Salses-Leucate lagoon: Font Dame Surface (FDS), Font Dame Deep (FDD), Font Estramar Surface (FES), Font Estramar Deep (FED) and Port Fitou (PF). The salinity data shows large variability and presents similar seasonal pattern for surface and bottom cages. For clarity, we present the surface water salinity only.

4.3.5.2 Spectral analyses

At both groundwater-influenced sites, spectral analyses of parameters in bottom and surface waters showed similar patterns and periodicities, and thus here we present surface water data only. The FFT analyses of the temperature data showed overall well-defined peaks centered at 12 h, 1 day and 13 days for surface waters at the three study sites (Font Dame, Font Estramar and Port Fitou) except for Font Estramar at the low frequency (Fig. 4.8a, b and c). For salinity, peaks were also observed at 12 h, 1 day and 13 days for the site Font Dame while no clear peaks were observed at Font Estramar and Port Fitou (Fig. 4.8d, e and f). Periodicities of 12 h and 11 days were exhibited for the water depth at Font Dame and Port Fitou while at Font Estramar the water depth followed periodicities of 12 h and 24 h (Fig. 4.8g, h and i). The FFT analyses for the wind speed showed clear peaks at 1 day and 2.6 days (Fig. 4.8j)

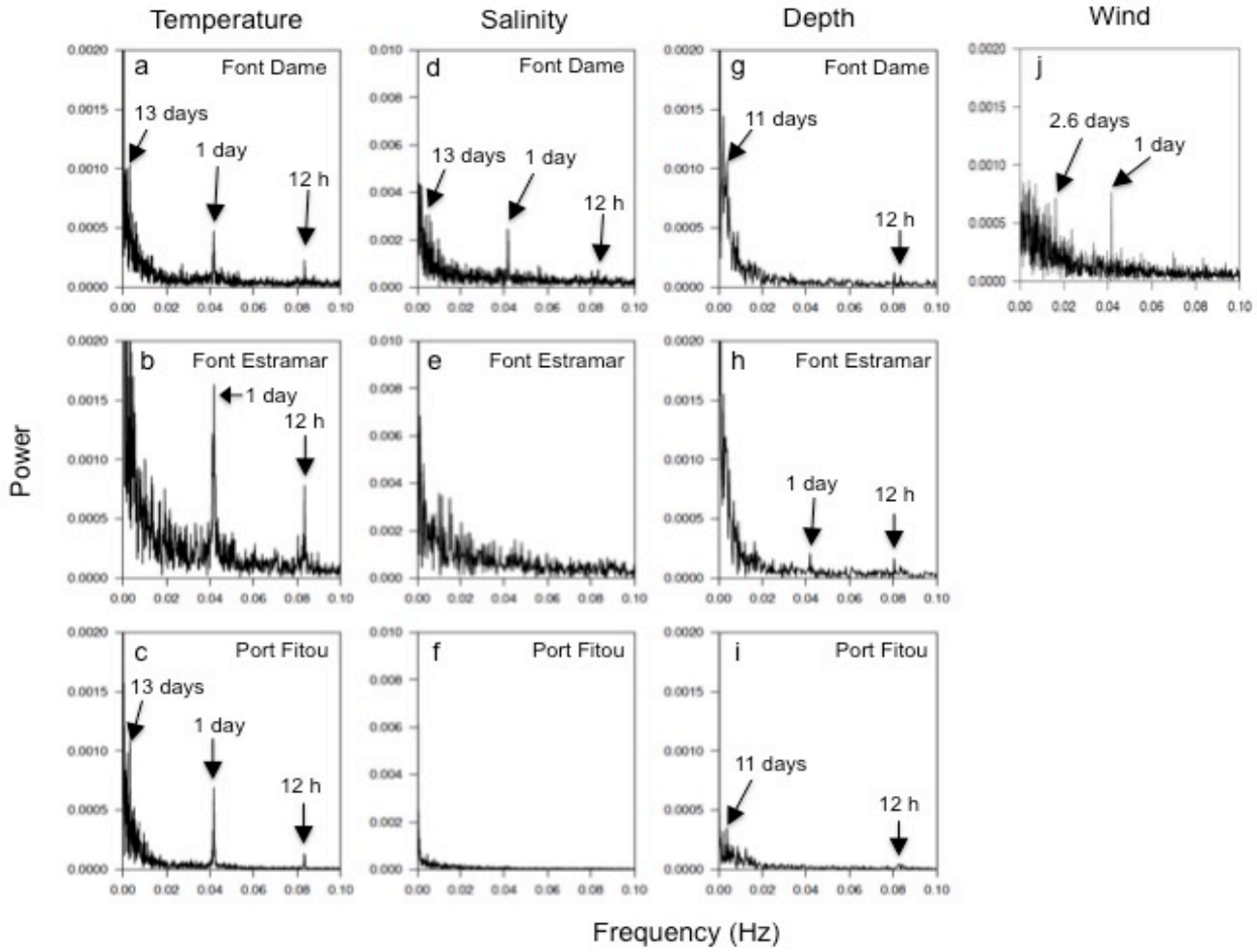

Figure 4.8| (a, b, c) Fast Fourier Transformations of the temperature, (d, e, f) salinity and (g, h, i) water depth at Font Dame (FD), Font Estramar (FE) and Port Fitou (PF), and (j) the wind speed at the study. Arrows indicate peaks of the power spectrum.

4.4 Discussion

4.4.1 Periodicity in shell growth and environmental influences

The growth increment count demonstrates that *M. galloprovincialis* in Salses-Leucate lagoon forms growth increment on a near-daily basis (circadian rhythm). Generally, growth patterns reported in mytilid species refer rather to tidal cycles (Langton 1977; Richardson 1989; Buschbaum and Saier 2001; Zaldibar et al. 2004) and circa-tidal periodicity has been observed in several bivalves (Pannella and Macclintock 1968; Evans 1972; Richardson 1988; Schöne et al. 2003c; Miyaji et al. 2007; Connor and Gracey 2011). For instance, Richardson (1989) showed that *M. edulis* growing under tidally submerged conditions exhibits a clearly defined growth pattern coinciding with the number of emersions. In Salses-Leucate lagoon, tidal variations are relatively small (< 0.05 m) as a consequence of the small tidal cycles in the Mediterranean Sea and the restricted exchange between the lagoon and sea, and thus tidal cycles have a negligible influence on mussel growth patterns. The circadian rhythm observed in mussels from Salses-Leucate lagoon has been reported in other bivalve mollusks (Pannella and Macclintock 1968; Richardson 1988; Parsons et al. 1993; Chauvaud et al. 2005), and is often related to cycles governed by biological clocks (Pittendrigh and Daan 1976; Schöne 2008; Connor and Gracey 2011). The biology of most organisms is closely related to the changes in their environmental conditions, which often present clear daily patterns of, mainly, temperature and light. As a consequence, bivalves and other organisms have developed behavioral and physiological daily patterns (Connor and Gracey 2011). As commonly observed in coastal environments, temperature, salinity, water depth and wind speed variations in Salses-Leucate lagoon exhibit daily periodicity, suggesting that these environmental factors contribute to the daily pattern of mussel growth in the lagoon.

Although the growth pattern is oriented toward a daily pattern, the number of growth increments counted in the shell was generally slightly lower than the number of days, suggesting that either growth halts during some part of the study period or that the growth pattern was not well revealed by the Mutvei

etching, resulting in a potential underestimation of the number of growth increments (Nedoncelle et al. 2013). Similar observations have been reported previously for *Arctica islandica* (Witbaard et al. 1994; Schöne et al. 2005b), *Pecten maximus* (Chauvaud et al. 2005) and *Phacosoma japonicum* (Tanabe 2007). They observed that the number of growth increment formed during a limited interval of time is (sometimes significantly) lower than the number of days (or tides) at the study sites. Winter growth cessation is indeed common in bivalves (Jones and Quitmyer 1996; Tanabe 2007; Okaniwa et al. 2010), because the production of shell carbonate ceases below species-specific growth temperature thresholds. For instance, *Margaritifera margaritifera* in northern Sweden stops producing shell carbonate below 5°C (Schöne 2008) while *M. galloprovincialis* from Tokyo Bay, Japan, stops growing or barely grows for water temperature between 8 and 14°C (Okaniwa et al. 2010). Growth cessation may also occur all year round as a result of an abrupt change in the environmental conditions due to strong wind events, drop in salinity and/or phytoplankton bloom (due to toxicity or clogging of the gill system) (Page and Hubbard 1987; Chauvaud et al. 1998; Schöne 2008; Okaniwa et al. 2010). The observed discrepancy in days and growth increments in this study is small in comparison to those observed at many other sites, likely due to the comparatively stable environmental conditions in the lagoon, but nevertheless suggests that the conditions temporarily cause either a complete cessation of growth during specific days or a desynchronization in the circadian rhythm of growth increment deposition (Chauvaud et al. 2005).

Aside from the (near-) daily cycles, the spectral analysis of the increment width shows spectral peaks at frequencies corresponding to periods of 11 - 13 days (Fig. 4.6). The temperature, salinity and water depth patterns also exhibit periodicity of approximately 11 - 13 days, suggesting a spring-neap cycle influence on the growth of *M. galloprovincialis* in Salses-Leucate lagoon. Tidal patterns in (non-lagoonal) bivalves are widespread and are expressed by thin increments altering with groups of relatively thick ones, forming periodic pattern of 13 - 14 days, corresponding to the fortnightly spring-neap tide cycles (Evans 1972; Richardson 1989; Miyaji et al. 2007), and suggested to be related to

valve activity and/or current velocity changes modifying the food availability (Clark 2005; Lartaud et al. 2010a; Tran et al. 2011). Whilst spring-neap cycles can affect groundwater discharge rate in tidal systems (e.g. Kim and Hwang 2002; Taniguchi et al. 2002; Sieyes et al. 2008), this is unlikely the case in Salses-Leucate lagoon due to the quasi-negligible tidal amplitude. However, spring-neap cycles are likely affecting the exchange between the lagoon and the Mediterranean Sea (Sylaios et al. 2006), and may therefore play a role in controlling the temperature, salinity, water depth and eventually the nutrient supply in Salses-Leucate lagoon.

The origin of the periodicity of approximately 3 and 5 days in the increment growth remains uncertain (Fig. 4.6). It may be related to frequent wind events, which show a periodicity of 2.6 days (close to the 3 - 5 days periodicities of the growth increments), and thus drive the circulation within the lagoon and exchange with the sea, thereby controlling environmental factors in the lagoon (Fig. 4.7). For instance, southeasterly winds favour the input of seawater in the lagoon while northwesterly winds reduce its input. Furthermore, wind-driven circulation of lagoon water through sediments is recognized as an important source of nutrient in coastal lagoons (Rodellas et al. 2018). This 'wind-driven' nutrient supply may increase phytoplankton abundance, which in turn may control mussel growth, albeit with a small temporal lag governed by primary production timescales.

4.4.2 Growth of *M. galloprovincialis* in the Mediterranean region

The Von Bertalanffy curves show that the growth rates of *M. galloprovincialis* from Salses-Leucate lagoon are among the highest rates recorded for this species in the Mediterranean region (Fig. 4.5). This clearly indicates that Salses-Leucate lagoon is well suitable for the growth of *M. galloprovincialis*. The time required to grow to a length of 30 mm (ca. 1 year) is significantly shorter than that reported for the same species from the coastal bay of Mare Grande and the semi-enclosed basin of Mare Piccolo (Italy) of approximately 7 years (Posa and Tursi 1991) or longer in the Gulf of Castellammare (Sarà et al. 2012). The growth rates of *M. galloprovincialis* observed in this study (particularly from the groundwater-

influenced sites) are only a little below those reported from the coastal lagoon of Sacca di Scardovari on the Adriatic coast (Ceccherelli and Rossi 1984) and Fangar Bay in Spain (Ramón et al. 2007). The Sacca di Scardovari lagoon and Fangar Bay are both located at the mouth of big rivers (Po River and Ebro River, respectively), and thus these areas are likely receiving nutrient inputs from rivers. Moreover, these areas are well known for agricultural activities, which may also be a relevant source of nutrients (Busch 2013; Di Giuseppe et al. 2014). Despite the seasonal variations in water temperature in Salses-Leucate lagoon, the water temperature ranges (Median=16.0ºC, Q1=12.3ºC and Q3=20.4°C) includes the optimal temperature range for growth of *M. galloprovincialis* (17 – 20°C) (Blanchette et al. 2007).

4.4.3 Role of groundwater discharge

M. galloprovincialis at the groundwater influenced sites shows higher growth rate and condition index compared to that of the control site, suggesting that groundwater influenced sites are favourable for their growth (Fig. 4.4 & 4.5). Three compounding effects of groundwater inputs to coastal areas can explain the differences between mussel growth at groundwater-influenced and non-influenced sites, i.e. groundwater-driven variations in i) temperature, ii) nutrient availability and iii) salinity.

i) Despite the seasonal variations of water temperature in the lagoon (Fig. 4.7d), the average water temperature at the groundwater-influenced sites is significantly higher than the temperature at the control site. Since temperatures in groundwater sources are relatively constant throughout the year (17 – 19°C), groundwater inputs in winter (when lagoon waters temperatures 'elsewhere' are below 10°C) produce an increase of lagoon water temperatures at the groundwater-influenced sites. The higher growth rate and condition index observed at the groundwater-influenced sites may thus (at least in part) be related to this groundwater-driven increase in temperature (Schöne et al. 2002, 2005b).

ii) In addition to water temperature, food availability is a major factor controlling shell growth and condition indices. Bivalve growth increases with increasing phytoplankton abundance (Page and Hubbard 1987; Sato 1997), with food availability controlling 64 to 70% of the variation in growth of *M. galloprovincialis* (His et al. 1989). Sato (1997) demonstrated that growth of bivalve *Phacosoma japonica* in Ariake Bay (Japan) is also primarily influenced by food availability. High phytoplankton abundance has been directly linked to groundwater input in several costal systems worldwide (Valiela et al. 1990; McClelland et al. 1997; Herrera-Silveira 1998). A recent study demonstrates that groundwater discharge from Font Dame and Font Estramar sustains primary production of the lagoon investigated here (Andrisoa et al. 2019). Indeed, the concentrations of particulate organic nitrogen in Salses-Leucate lagoon (which is dominated by phytoplankton in this lagoon; (Carlier et al. 2009)), are higher in groundwater-influenced sites (62 ± 40 µg N L^{-1}) than in the control site (52.8 ± 21.9 µg N L^{-1}) (A. Andrisoa, unpublished data). The high nutrient concentrations driven by groundwater inputs likely favour phytoplankton growth at the groundwater-influenced sites, which is readily available for mussel growth at these sites.

iii) Groundwater from Font Dame and Font Estramar discharges substantial amounts of freshwater into Salses-Leucate lagoon, considerably affecting the salinity at the groundwater-influenced sites. Salinity is one of the dominant environmental factors controlling growth. Generally, *M. galloprovincialis* exhibits highest growth at salinity 35 (His et al. 1989). Typical responses of mussels to lower salinity include reduced feeding activity, slower growth and valve closure (Navarro 1988; Riisgård et al. 2012). For example, due to low salinities in the Baltic Sea (salinity between 6 and 8 in the northern part), mussels are dwarfed in this area (Kautsky 1982; Vuorinen et al. 2002). Similarly, Riisgård et al. (2012) showed that mussels growing at salinity 10 have slower growth rates than those growing at salinity 30. However, acclimation to reduced salinities may take place, and mussels are able to adjust growth at changing salinities (Davenport 1979; Qiu et al. 2002). The higher mussel growth rates measured at the groundwater-influenced sites despite lower salinity suggest that mussels

growing there are either acclimated to low salinity environments or that salinity has a less important effect on mussel growth compared to temperature and food availability in this lagoonal environment. Also note that salinity at the groundwater-influenced sites is highly variable (Fig. 4.7e), which may cause stress to the animals. Many bivalves can tolerate small changes in salinity, but salinity outside their acceptable range may negatively affect their growth (Peteiro et al. 2018).

It should be noted that due to sampling constraints (see methods), specimens from different sites were not sampled for exactly the same periods. This could have implications for our results since both growth rates and condition indices highly reflect species reproductive dynamics. Growth rates and condition indices are generally lower during the resting phase (usually from November to February) and higher during gonad maturation and ripening (from April to October) (e.g. Karayücel and Ye 2010; Vural et al. 2015). Mussels from Font Dame and Port Fitou were studied throughout almost a year, thus covering the different phases of the reproductive cycle, therefore the comparison between groundwater-influenced and control sites must be considered robust. However, specimens from Font Estramar site were monitored from October 2016 to late March 2017 only, and therefore biased towards winter months. Considering the expected lower growth rates in winter periods, the results obtained from the groundwater-influenced site Font Estramar are likely an underestimation of mussel growth rate and condition index in the annual cycle. Further, mussels at the control site Port Fitou were naturally present in a narrower range size than at the groundwater sites, potentially biasing the results. A transplantation of specimen from other sites to cover the same size distribution would likely have introduced an unknown, potentially large bias. Despite these experimental limitations, mussel growth rates and condition indices at groundwater influenced sites are significantly higher than those estimated at control site.

The growth rates of mussels in the upper (shallower) cages are slightly higher than those of bottom cages (Fig. 4.4b). Despite the shallow water depth (≈0.8 m), the water column at the groundwater-influenced sites is generally stratified

(except during wind events). The upper cages are relatively more influenced by lower-density groundwater inputs (mean salinity FDS = 21.8 ± 7.1; FES = 24.3 ± 7.0) in comparison to the bottom cages (mean salinity FDD= 27.6 ± 6.5; FED = 27.2 ± 6.1). Thus, temperatures and nutrient concentrations are expected to be higher in surface waters than in bottom waters as a consequence of groundwater inputs, favouring mussel growth rates in the upper cages. The high light availability and temperatures driven by direct solar radiation in surface waters may also favour phytoplankton and thus mussel growth. Higher growth rate of mussels in surface waters than in deeper layers has previously been reported and attributed either to differences in temperature (Fuentes et al. 2000) or the high availability of phytoplankton (Page and Hubbard 1987). In addition, the lower growth rates observed in the bottom cages may partially result from siltation. Sediment resuspension occurs often in the study area due to frequent wind events and may explain in part the difference in growth observed between upper and lower cages. Silts and clay can clog the gills of mussels, interfere with filter feeding and affect indirectly by reducing light availability for phytoplankton, inhibiting the growth of bivalves (Bricelj et al. 1984; Box and Mossa 1999).

4.4.4 Economic implications

The Mediterranean mussel (*M. galloprovincialis)* is a highly valuable commercial species. The world production of mussels from aquaculture reach an annual value of 1.2 million tons corresponding to an economic value of over 500 million U.S dollars (Okumuş et al. 2014). About 80.000 tons are produced annually in France (Župan and Šarić 2014), and in Thau lagoon (a neighboring site on the French Mediterranean coast), annual mussel production is estimated at 5.400 tons (Gangnery et al. 2004). In particular the competitive price compared to other bivalves makes mussels a sought after seafood (Orban et al. 2002). However, in recent years, the production of mussel is levelling off due to reduced number of suitable coastal sites for high productivity mussel farming, as consequences of human activities (Cataudella et al. 2015). The results of this study clearly show that coastal sites influenced by groundwater inputs represent

ideal environments for mussel growth (and thus potential mussel farming), resulting in higher growth rates (1.5 cm yr^{-1}) and condition index. Higher condition index indicates high quality of a marketed product, i.e. better health status and fatness, especially during the periods of gonad maturation and ripening. Mussel aquaculture is traditionally placed in coastal waters with large primary productivity (e.g. Peharda et al. 2007). Results from this study suggest that groundwater-influenced sites can offer environmental conditions well suited for mussel aquaculture, and therefore, it may be economically profitable to farm mussels in groundwater-influenced areas.

4.5 Conclusion

This study showed that *M. galloprovincialis* in Salses-Leucate lagoon produce circadian (daily rhythm) shell growth increments and have amongst the highest growth rates to date reported for the Mediterranean region. In Salses-Leucate lagoon, mussels from groundwater-influenced sites have higher growth rate and condition index compared to those from a control site (chiefly influenced by seawater), demonstrating that groundwater inflows are favourable for mussel growth. Groundwater discharging to coastal areas is characterized by relatively constant temperatures and is an important source of nutrients, providing thus significant food resources to filter feeders like mussels. This study indicates that higher temperature and food availability associated with groundwater inputs may explain the fast growth rate of *M. galloprovincialis* at groundwater-influenced sites in Salses-Leucate lagoon, and thus provides direct evidence for the 'downstream' ecological impacts of groundwater discharge on this commercially important species.

Identifying suitable sites for profitable production is a considerable challenge in mussel aquaculture. Groundwater-influenced sites are suitable sites for mussel farming, particularly in oligotrophic waters like the Mediterranean Sea. In addition to its increasingly recognized ecological role, this study suggests that groundwater inputs to coastal areas can have non-negligible economic effects on fisheries products in coastal socio-ecosystems.

– Chapter 5 –

Conclusion and perspectives

5.1 Conclusion

This PhD thesis aims at contributing to closing the gap of fundamental understanding of the role groundwater flows play in the functioning and vulnerability of coastal lagoonal ecosystems. While a great amount of works has been and continuous to be undertaken on many aspects of ecosystem functioning, anthropogenic and climate impacts on coastal lagoons, the role groundwater plays in their ecosystem functioning has not received much attention to date. The objective of this thesis is therefore to provide evidence on the 'downstream' ecological role of groundwater discharges in coastal lagoons. This study was conducted in La Palme and Salses-Leucate lagoons located on the French Mediterranean coastline to: 1) to quantify the fluxes of nutrients associated with groundwater discharge and recirculation flow; 2) to assess the role of groundwater discharge and porewater fluxes in supporting primary production; and 3) to evaluate the effects of groundwater discharge in the growth of the Mediterranean mussels. The different chapters of this thesis (Chapters 2-4) address these tasks as summarized below:

5.1.1 Quantification of nutrient fluxes from groundwater discharge and recirculation (Chapter 2)

This study evaluates the fluxes of nutrients driven by groundwater discharge and lagoon water recirculation into La Palme lagoon (France; Mediterranean Sea). Porewater nutrient profiles show that porewater NH_4^+ and PO_4^{3-} concentrations are significantly enriched relative to lagoon waters with concentrations generally increasing with depth. However, NO_3^- concentrations in porewaters are comparable to those measured in surface waters while they are significantly higher in the karstic groundwater and in the sewage effluent than in lagoon waters and the concentrations decrease with increasing salinity. The fluxes of NO_3^-, NH_4^+ and PO_4^{3-} from terrestrial groundwater and recirculation through sediments are assessed using concurrent water and radon mass balances. The comparison of nutrient fluxes from different sources in La Palme lagoon (karstic groundwater, recirculation, diffusion from sediments, sewage effluent and atmospheric deposition) reveals that the recirculation of lagoon

water through sediments is the main source of NH_4^+ (1900-5500 mol d^{-1}) and PO_4^{3-} (22-71 mol d^{-1}) while karstic groundwater is the main source of NO_3^- (200-1200 mol d^{-1}) to La Palme lagoon. This highlights the important role of groundwater processes as a major conveyor of dissolved nutrients to coastal ecosystems and the need of better understanding on their ecological implications to properly constrain the functioning and vulnerability of coastal lagoon ecosystems.

5.1.2 Role of groundwater discharge and porewater fluxes in supporting primary production (Chapter 3)

In order to provide evidence on the 'downstream' ecological implication of groundwater processes in coastal systems, in this study we assess the role groundwater discharge and porewater fluxes in supporting primary production in La Palme and Salses-Leucate lagoons by investigating the nitrogen ($\delta^{15}N$) and carbon $\delta^{13}C$ stable isotopes in macrophyte and phytoplankton. The $\delta^{15}N$ in macrophytes and phytoplankton reflect predominantly the nitrogen isotopic signatures of the karstic groundwater and porewater sources, indicating that the karstic groundwater and porewater fluxes are the main sources of inorganic nitrogen assimilated by primary producers in La Palme and Salses-Leucate lagoons. Sewage effluents contribute, however, locally to the nitrogen input at times of exceptionally high nitrogen concentrations. The nitrogen isotope signatures reveal also that macrophytes are better time-integrative measures of nitrogen input compared to phytoplankton. Macrophytes integrate the isotopic signatures of the nitrogen sources over their longer lifetime while nitrogen signatures in phytoplankton change at short-time scale due to their short life span. Moreover, the increased $\delta^{13}C$-DIC with increasing salinity indicates a binary conservative mixing between a low salinity - low $\delta^{13}C$-DIC source (karstic groundwater) and a high salinity - high $\delta^{13}C$-DIC source (seawater). Porewater is also an important source of DIC, given the mineralization of deposited organic matter in sediments and the high DIC flux from porewater. Therefore, carbon isotopic signatures in macrophytes and phytoplankton suggest that karstic groundwater, porewater fluxes and seawater are likely the main sources of inorganic carbon to primary producers in La Palme and Salses-Leucate lagoons.

The impact of karstic groundwater sustaining primary production is greater in the small La Palme lagoon due to larger fresh karstic groundwater inflow and the restricted exchange with the open sea. However in the larger Salses-Leucate lagoon, the karstic groundwater influence is limited to the areas close to the sources. The hydrology of the two studied lagoons controls the ecological implications of the groundwater discharge as revealed by the isotope signatures.

5.1.3 Effects of groundwater discharge in the growth of the Mediterranean mussels (Chapter 4)

In this study, we evaluate the impacts of groundwater discharge in the growth of the Mediterranean mussels *Mytilus galloprovincialis* by investigating the variation in growth rate and condition index of mussels (tissue weight / shell weight) growing in and outside groundwater-influence in Salses-Leucate lagoon (France). Mussels in Salses-Leucate lagoon produce growth increments on a near-daily basis (circadian rhythm) in their shell as opposed to semi-diurnal increments in tidally influenced systems. Mussels from groundwater-influenced sites have higher growth rate and condition index compared to those from a control site (chiefly influenced by seawater), demonstrating that groundwater inflows are favourable for mussel growth. Groundwater discharging to coastal areas is characterized by relatively constant temperatures and is an important source of nutrients, providing thus significant food resources to filter feeders like mussels. This study indicates that higher temperature and food availability associated with groundwater inputs may explain the fast growth rate of *Mytilus galloprovincialis* in groundwater-influenced sites in Salses-Leucate lagoon, and thus provides direct evidence for the 'downstream' ecological impacts of groundwater discharge on this commercially important species.

Identifying suitable sites for profitable production is a considerable challenge in mussel aquaculture. Groundwater-influenced sites are suitable sites for mussel farming, particularly in oligotrophic waters like the Mediterranean Sea. In addition to its more and more recognized ecological role, this study suggests that groundwater inputs to coastal areas can have non-negligible economical effects in coastal socio-ecosystems.

5.2 Research perspectives

From the research presented in this thesis, a number of perspectives for further research are evident.

This study provides evidence on the importance of stable isotope approach in assessing the transfer of DIN and DIC from groundwater and porewater fluxes to primary producers in two oligotrophic coastal lagoons (La Palme and Salses-Leucate lagoons). Porewater fluxes (recirculation) should occur in every lagoon (but depends on sediment types), thus likely an important source of nitrogen and carbon for primary producers. However, the study only represents a snapshot of the French Mediterranean coastal lagoons. In order to better understand the impact of groundwater processes on primary production on regional scale, the same approach should be applied to other coastal lagoons with different characteristics (e.g. eutrophic lagoons, large surface inputs, different land use in the catchment areas…).

Our study on the quantification of nutrient fluxes demonstrated the importance of lagoon water recirculation as main the source of NH_4^+ and the stable isotope approach reveals that porewater NH_4^+ is a main source of inorganic nitrogen to primary producers. Despite this important role that porewater NH_4^+ plays on the ecological functioning of coastal lagoons, the origin of the NH_4^+ in sediment is still unclear. While referred as porewater-driven NH_4^+, they could be originally supplied by other sources. Therefore, understanding the origin of porewater NH_4^+ in coastal lagoons should be considered in future researches. It would be thus interesting to conduct an enrichment experiments (i.e. additions of compounds artificially enriched in the rare heavy isotope to a natural system) to provide an instantaneous view on the fate and transformation processes of NH_4^+ in the sediment. Similar considerations apply to P, Si and other nutrients.

Nutrient concentrations in karstic groundwater sources are elevated due to important nutrient loading in the regional karstic aquifers. Changes in land use practises over the past decades have resulted in a considerable variability of nutrient input into groundwater reservoirs with time. As groundwater has great transit times of some decades, there is thus a time lag between this input of

nutrients to a groundwater reservoir and the subsequent discharge to coastal waters. To better understand the delayed response of groundwater discharge to past land-use changes and its ecological implications, there is therefore a need to determine the groundwater age and its relation with groundwater nutrient load.

Our study on stable isotopes ascertains the important role of groundwater discharge and porewater fluxes can play in supporting primary production in coastal lagoons under influence of groundwater inflow. Indeed, we demonstrated the transfer of inorganic nitrogen and carbon from groundwater discharge and porewater fluxes to primary producers. The next step is to assess the effects of groundwater discharge and porewater flows through a bottom-up support to higher trophic levels of the lagoonal food web. This is required to fully understand the ecological implications in coastal lagoon ecosystems. To this effect, we are currently working with a Japanese team in collaboration with IFREMER Sète to study the impact of groundwater inflow on primary producers, oysters and fishes in Thau lagoon.

Although we studied the effects of groundwater discharge on growth of Mediterranean mussels in Salses-Leucate, our approach was solely based on the growth rate and condition index. Analysing the nitrogen and carbon signatures in the mussel tissue is the next step to determine the source of nitrogen and carbon for these mussels. Moreover, the geochemical properties within the mussel shells provide information on the temporal changes of environmental factors. For instance, oxygen isotopic signatures in shells have been shown to be reliable proxy for changes in water temperature and salinity (Schöne et al. 2003b; Lartaud et al. 2010b). Therefore, reconstructing the temporal variations of lagoon salinity throughout the lifetime of the animal using the oxygen isotope signature and the element ratio Mg/Ca embedded in the shell is an important direction for future research. This research will improve our understanding on the relationship between shell growth and groundwater inflow.

References

Abada-Boujemaa Y. M. 1996. Cinétique, croissance, production et composition biochimique des deux bivalves mytilidés: Perna perna (.) et Mytilus galloprovincialis (Lmk) du littoral algérois. Muséum National d'Histoire Naturelle.

Adyasari, D., T. Oehler, N. Afiati, and N. Moosdorf. 2018. Groundwater nutrient inputs into an urbanized tropical estuary system in Indonesia. Sci. Total Environ. **627**: 1066–1079. doi:10.1016/j.scitotenv.2018.01.281

Alin, S. R., and T. C. Johnson. 2007. Carbon cycling in large lakes of the world: A synthesis of production, burial, and lake-atmosphere exchange estimates: CARBON CYCLING IN LARGE LAKES. Glob. Biogeochem. Cycles **21**: n/a-n/a. doi:10.1029/2006GB002881

Alin, S., S. Siedlecki, B. Hales, and others. 2012. Coastal Carbon Synthesis for the Continental Shelf of the North American Pacific Coast (NAPC): Preliminary Results. 19.

Allègre, C. J., P. Louvat, J. Gaillardet, L. Meynadier, S. Rad, and F. Capmas. 2010. The fundamental role of island arc weathering in the oceanic Sr isotope budget. Earth Planet. Sci. Lett. **292**: 51–56. doi:10.1016/j.epsl.2010.01.019

Aller, R. C., N. E. Blair, and G. J. Brunskill. 2008. Early diagenetic cycling, incineration, and burial of sedimentary organic carbon in the central Gulf of Papua (Papua New Guinea). J. Geophys. Res. Earth Surf. **113**: F01S09. doi:10.1029/2006JF000689

Altabet, M. A., and R. Francois. 1994. Sedimentary nitrogen isotopic ratio as a recorder for surface ocean nitrate utilization. Glob. Biogeochem. Cycles **8**: 103–116. doi:10.1029/93GB03396

Amato, D. W., J. M. Bishop, C. R. Glenn, H. Dulai, and C. M. Smith. 2016. Impact of Submarine Groundwater Discharge on Marine Water Quality and Reef Biota of Maui. PLOS ONE **11**: e0165825. doi:10.1371/journal.pone.0165825

Aminot, A., and R. Kérouel. 2007. Dosage automatique des nutriments dans les eaux marines: méthodes en flux continu, Editions Quae.

An, S., and W. S. Gardner. 2002. Dissimilatory nitrate reduction to ammonium (DNRA) as a nitrogen link, versus denitrification as a sink in a shallow estuary (Laguna Madre/Baffin Bay, Texas). Mar. Ecol. Prog. Ser. **237**: 41–50.

Andrisoa, A., T. C. Stieglitz, V. Rodellas, and P. Raimbault. 2019. Primary production in coastal lagoons supported by groundwater discharge and

porewater fluxes inferred from nitrogen and carbon isotope signatures. Mar. Chem. doi:10.1016/j.marchem.2019.03.003

Anschutz, P., G. Chaillou, and P. Lecroart. 2007. Phosphorus diagenesis in sediment of the Thau Lagoon. Estuar. Coast. Shelf Sci. **72**: 447–456. doi:10.1016/j.ecss.2006.11.012

Anschutz, P., C. Charbonnier, J. Deborde, L. Deirmendjian, D. Poirier, A. Mouret, D. Buquet, and P. Lecroart. 2016. Terrestrial groundwater and nutrient discharge along the 240-km-long Aquitanian coast. Mar. Chem. **185**: 38–47. doi:10.1016/j.marchem.2016.04.002

Anschutz, P., T. Smith, A. Mouret, J. Deborde, S. Bujan, D. Poirier, and P. Lecroart. 2009. Tidal sands as biogeochemical reactors. Estuar. Coast. Shelf Sci. **84**: 84–90. doi:10.1016/j.ecss.2009.06.015

Anthony, A., J. Atwood, P. August, and others. 2009. Coastal lagoons and climate change: ecological and social ramifications in US Atlantic and Gulf coast ecosystems. Ecol. Soc. **14**.

Anthony, K., S. R. Connolly, and B. L. Willis. 2002. Comparative analysis of energy allocation to tissue and skeletal growth in corals. Limnol. Oceanogr. **47**: 1417–1429.

Aravena, R., M. L. Evans, and J. A. Cherry. 1993. Stable Isotopes of Oxygen and Nitrogen in Source Identification of Nitrate from Septic Systems. Ground Water **31**: 180–186. doi:10.1111/j.1745-6584.1993.tb01809.x

Atekwana, E. A., and D. K. Krishnamurthy. 1998. Seasonal Varia-tions of Dissolved Inorganic Carbon and A130 of Surface Waters: Application of a Modified Gas Evolution Technique. J. Hydrol. 205z265-278.

Atkins, M. L., I. R. Santos, S. Ruiz-Halpern, and D. T. Maher. 2013. Carbon dioxide dynamics driven by groundwater discharge in a coastal floodplain creek. J. Hydrol. **493**: 30–42. doi:10.1016/j.jhydrol.2013.04.008

Barnes, R. S. K. 1980. Coastal Lagoons, CUP Archive.

Barros, G. V., L. A. Martinelli, T. M. Oliveira Novais, J. P. H. B. Ometto, and G. M. Zuppi. 2010. Stable isotopes of bulk organic matter to trace carbon and nitrogen dynamics in an estuarine ecosystem in Babitonga Bay (Santa Catarina, Brazil). Sci. Total Environ. **408**: 2226–2232. doi:10.1016/j.scitotenv.2010.01.060

Basterretxea, G., A. Tovar-Sanchez, A. J. Beck, and others. 2010. Submarine groundwater discharge to the coastal environment of a Mediterranean island (Majorca, Spain): ecosystem and biogeochemical significance. Ecosystems **13**: 629–643.

Beck, A. J., J. P. Rapaglia, J. K. Cochran, and H. J. Bokuniewicz. 2007. Radium mass-balance in Jamaica Bay, NY: Evidence for a substantial flux of submarine groundwater. Mar. Chem. **106**: 419–441. doi:10.1016/j.marchem.2007.03.008

Bejannin, S., P. van Beek, T. Stieglitz, M. Souhaut, and J. Tamborski. 2017. Combining airborne thermal infrared images and radium isotopes to study submarine groundwater discharge along the French Mediterranean coastline. J. Hydrol. Reg. Stud. **13**: 72–90. doi:10.1016/j.ejrh.2017.08.001

Benson, E. R., J. M. O'Neil, and W. C. Dennison. 2008. Using the aquatic macrophyte Vallisneria americana (wild celery) as a nutrient bioindicator. Hydrobiologia **596**: 187–196. doi:10.1007/s10750-007-9095-0

Bernard, R. J., B. Mortazavi, L. Wang, A. C. Ortmann, H. MacIntyre, and W. C. Burnett. 2014. Benthic nutrient fluxes and limited denitrification in a sub-tropical groundwater-influenced coastal lagoon. Mar. Ecol. Prog. Ser. **504**: 13–26. doi:10.3354/meps10783

Beusen, A. H. W., A. L. M. Dekkers, A. F. Bouwman, W. Ludwig, and J. Harrison. 2005. Estimation of global river transport of sediments and associated particulate C, N, and P: RIVER EXPORT OF PARTICULATE MATTER. Glob. Biogeochem. Cycles **19**: n/a-n/a. doi:10.1029/2005GB002453

Blanchette, C. A., B. Helmuth, and S. D. Gaines. 2007. Spatial patterns of growth in the mussel, Mytilus californianus, across a major oceanographic and biogeographic boundary at Point Conception, California, USA. J. Exp. Mar. Biol. Ecol. **340**: 126–148. doi:10.1016/j.jembe.2006.09.022

Bopp, L., C. L. Quéré, M. Heimann, A. C. Manning, and P. Monfray. 2002. Climate-induced oceanic oxygen fluxes: Implications for the contemporary carbon budget. Glob. Biogeochem. Cycles **16**: 6-1-6–13. doi:10.1029/2001GB001445

Boschker, H. T. S., J. C. Kromkamp, and J. J. Middelburg. 2005. Biomarker and carbon isotopic constraints on bacterial and algal community structure and functioning in a turbid, tidal estuary. Limnol. Oceanogr. **50**: 70–80.

Boudouresque, C. F., and M. Verlaque. 2002. Biological pollution in the Mediterranean Sea: invasive versus introduced macrophytes. Mar. Pollut. Bull. **44**: 32–38. doi:10.1016/S0025-326X(01)00150-3

Box, J. B., and J. Mossa. 1999. Sediment, Land Use, and Freshwater Mussels: Prospects and Problems. J. North Am. Benthol. Soc. **18**: 99–117. doi:10.2307/1468011

Brabandere, L. D., T. K. Frazer, and J. P. Montoya. 2007. Stable nitrogen isotope ratios of macrophytes and associated periphyton along a nitrate gradient

in two subtropical, spring-fed streams. Freshw. Biol. **52**: 1564–1575. doi:10.1111/j.1365-2427.2007.01788.x

Bradley, P. B., M. P. Sanderson, M. E. Frischer, J. Brofft, M. G. Booth, L. J. Kerkhof, and D. A. Bronk. 2010. Inorganic and organic nitrogen uptake by phytoplankton and heterotrophic bacteria in the stratified Mid-Atlantic Bight. Estuar. Coast. Shelf Sci. **88**: 429–441. doi:10.1016/j.ecss.2010.02.001

Brey, T. 1999. Growth performance and mortality in aquatic macrobenthic invertebrates. Adv. Mar. Biol. **35**: 153–243.

Bricelj, V. M., R. E. Malouf, and C. de Quillfeldt. 1984. Growth of juvenile <Emphasis Type="Italic">Mercenaria mercenaria</Emphasis> and the effect of resuspended bottom sediments. Mar. Biol. **84**: 167–173. doi:10.1007/BF00393001

Brito, A. C., A. Newton, P. Tett, and T. F. Fernandes. 2012. How will shallow coastal lagoons respond to climate change? A modelling investigation. Estuar. Coast. Shelf Sci. **112**: 98–104. doi:10.1016/j.ecss.2011.09.002

Brochier, F., and E. Ramieri. 2001. Climate Change Impacts on the Mediterranean Coastal Zones. SSRN Scholarly Paper ID 277549. ID 277549 Social Science Research Network.

Brunet, F., D. Gaiero, J. L. Probst, P. J. Depetris, F. Gauthier Lafaye, and P. Stille. 2005. δ^{13} C tracing of dissolved inorganic carbon sources in Patagonian rivers (Argentina). Hydrol. Process. **19**: 3321–3344. doi:10.1002/hyp.5973

Bruno, D. O., and E. M. Acha. 2015. Winds vs. tides: factors ruling the recruitment of larval and juvenile fishes into a micro-tidal and shallow choked lagoon (Argentina). Environ. Biol. Fishes **98**: 1449–1458. doi:10.1007/s10641-014-0371-3

Burnett, W. C., P. K. Aggarwal, A. Aureli, and others. 2006. Quantifying submarine groundwater discharge in the coastal zone via multiple methods. Sci. Total Environ. **367**: 498–543. doi:10.1016/j.scitotenv.2006.05.009

Burnett, W. C., H. Bokuniewicz, M. Huettel, W. S. Moore, and M. Taniguchi. 2003. Groundwater and Pore Water Inputs to the Coastal Zone. Biogeochemistry **66**: 3–33.

Burnett, W. C., and H. Dulaiova. 2003. Estimating the dynamics of groundwater input into the coastal zone via continuous radon-222 measurements. J. Environ. Radioact. **69**: 21–35. doi:10.1016/S0265-931X(03)00084-5

Burnett, W. C., R. Peterson, W. S. Moore, and J. de Oliveira. 2008. Radon and radium isotopes as tracers of submarine groundwater discharge – Results

from the Ubatuba, Brazil SGD assessment intercomparison. Estuar. Coast. Shelf Sci. **76**: 501–511. doi:10.1016/j.ecss.2007.07.027

Busch, J. A. 2013. Phytoplankton dynamics and bio-optical variables associated with Harmful Algal Blooms in aquaculture zones,.

Buschbaum, C., and B. Saier. 2001. Growth of the mussel Mytilus edulis L. in the Wadden Sea affected by tidal emergence and barnacle epibionts. J. Sea Res. **45**: 27–36. doi:10.1016/S1385-1101(00)00061-7

Cable, J. E., and J. B. Martin. 2008. In situ evaluation of nearshore marine and fresh pore water transport into Flamengo Bay, Brazil. Estuar. Coast. Shelf Sci. **76**: 473–483. doi:10.1016/j.ecss.2007.07.045

Cai, W.-J., Y. Wang, J. Krest, and W. S. Moore. 2003. The geochemistry of dissolved inorganic carbon in a surficial groundwater aquifer in North Inlet, South Carolina, and the carbon fluxes to the coastal ocean. Geochim. Cosmochim. Acta **67**: 631–639. doi:10.1016/S0016-7037(02)01167-5

Capone, D. G. 1988. BENTHIC NITROGEN FIXATION, p. 105–137. *In* Nitrogen in the Marine Environment. Elsevier.

Capone, D. G. 2008. Nitrogen in the marine environment, Elsevier.

Carlier, A., P. Riera, J. Amouroux, J. Bodiou, M. Desmalades, and A. Grémare. 2009. Spatial heterogeneity in the food web of a heavily modified Mediterranean coastal lagoon: stable isotope evidence. Aquat. Biol. **5**: 167–179. doi:10.3354/ab00147

Carlier, A., P. Riera, J.-M. Amouroux, J.-Y. Bodiou, K. Escoubeyrou, M. Desmalades, J. Caparros, and A. Grémare. 2007. A seasonal survey of the food web in the Lapalme Lagoon (northwestern Mediterranean) assessed by carbon and nitrogen stable isotope analysis. Estuar. Coast. Shelf Sci. **73**: 299–315. doi:10.1016/j.ecss.2007.01.012

Castel, J., P. Caumette, and R. Herbert. 1996. Eutrophication gradients in coastal lagoons as exemplified by the Bassin d'Arcachon and the Étang du Prévost. Hydrobiologia **329**: ix–xxviii.

Cataudella, S., D. Crosetti, F. Massa, General Fisheries Commission for the Mediterranean (Food and Agriculture Organization of the United Nations), and Food and Agriculture Organization of the United Nations. 2015. Mediterranean coastal lagoons: sustainable management and interactions among aquaculture, capture fisheries and the environment,.

Caumette, P., J. Castel, and R. Herbert, eds. 1996. Coastal Lagoon Eutrophication and ANaerobic Processes (C.L.E.AN.), Springer Netherlands.

Ceccherelli, V. U., and R. Rossi. 1984. Settlement, growth and production of the mussel Mytilus galloprovincialis. Mar. Ecol. Prog. Ser. Oldendorf **16**: 173–184.

Cerdà-Domènech, M., V. Rodellas, A. Folch, and J. Garcia-Orellana. 2017. Constraining the temporal variations of Ra isotopes and Rn in the groundwater end-member: Implications for derived SGD estimates. Sci. Total Environ. **595**: 849–857. doi:10.1016/j.scitotenv.2017.03.005

Chanton, J. P., and F. G. Lewis. 1999. Plankton and Dissolved Inorganic Carbon Isotopic Composition in a River-Dominated Estuary: Apalachicola Bay, Florida. Estuaries **22**: 575. doi:10.2307/1353045

Chappuis Eglantine, Seriñá Vanesa, Martí Eugènia, Ballesteros Enric, and Gacia Esperança. 2017. Decrypting stable-isotope (δ13C and δ15N) variability in aquatic plants. Freshw. Biol. **62**: 1807–1818. doi:10.1111/fwb.12996

Charette, M. A., and M. C. Allen. 2006. Precision Ground Water Sampling in Coastal Aquifers Using a Direct-Push, Shielded-Screen Well-Point System. Groundw. Monit. Remediat. **26**: 87–93. doi:10.1111/j.1745-6592.2006.00076.x

Charette, M. A., K. O. Buesseler, and J. E. Andrews. 2001. Utility of radium isotopes for evaluating the input and transport of groundwater-derived nitrogen to a Cape Cod estuary. Limnol. Oceanogr. **46**: 465–470.

Charette1, M. A., and K. O. Buesseler. 2004. Submarine groundwater discharge of nutrients and copper to an urban subestuary of Chesapeake Bay (Elizabeth River). Limnol. Oceanogr. **49**: 376–385. doi:10.4319/lo.2004.49.2.0376

Chauvaud, L., A. Lorrain, R. B. Dunbar, Y.-M. Paulet, G. Thouzeau, F. Jean, J.-M. Guarini, and D. Mucciarone. 2005. Shell of the Great Scallop *Pecten maximus* as a high-frequency archive of paleoenvironmental changes: GREAT SCALLOP PECTEN MAXIMUS. Geochem. Geophys. Geosystems **6**: n/a-n/a. doi:10.1029/2004GC000890

Chauvaud, L., G. Thouzeau, and Y.-M. Paulet. 1998. Effects of environmental factors on the daily growth rate of Pecten maximus juveniles in the Bay of Brest (France). J. Exp. Mar. Biol. Ecol. **227**: 83–111. doi:10.1016/S0022-0981(97)00263-3

Chauvet, C. 1988. Manuel sur l'aménagement des pêches dans les lagunes côtières: la bordigue méditerranéenne, Food & Agriculture Org.

Cho, H.-M., G. Kim, E. Y. Kwon, N. Moosdorf, J. Garcia-Orellana, and I. R. Santos. 2018. Radium tracing nutrient inputs through submarine groundwater discharge in the global ocean. Sci. Rep. **8**: 2439. doi:10.1038/s41598-018-20806-2

Christensen, P. B., S. Rysgaard, N. P. Sloth, T. Dalsgaard, and S. Schw\a erter. 2000. Sediment mineralization, nutrient fluxes, denitrification and dissimilatory nitrate reduction to ammonium in an estuarine fjord with sea cage trout farms. Aquat. Microb. Ecol. **21**: 73–84.

Christensen, P. B., and J. Sørensen. 1986. Temporal Variation of Denitrification Activity in Plant-Covered, Littoral Sediment from Lake Hampen, Denmark. Appl Env. Microbiol **51**: 1174–1179.

Christensen, P. B., and J. Sørensen. 1988. Denitrification in sediment of lowland streams: Regional and seasonal variation in Gelbæk and Rabis Bæk, Denmark. FEMS Microbiol. Ecol. **4**: 335–344. doi:10.1111/j.1574-6968.1988.tb02700.x

Church, J. A., and N. J. White. 2006. A 20th century acceleration in global sea-level rise. Geophys. Res. Lett. **33**. doi:10.1029/2005GL024826

Clark, G. R. 2005. Daily growth lines in some living Pectens (Mollusca: Bivalvia), and some applications in a fossil relative: Time and tide will tell. Palaeogeogr. Palaeoclimatol. Palaeoecol. **228**: 26–42. doi:10.1016/j.palaeo.2005.03.044

Cloern, J. E., E. A. Canuel, and D. Harris. 2002. Stable carbon and nitrogen isotope composition of aquatic and terrestrial plants of the San Francisco Bay estuarine system. Limnol. Oceanogr. **47**: 713–729.

Cockenpot, S., C. Claude, and O. Radakovitch. 2015. Estimation of air–water gas exchange coefficient in a shallow lagoon based on 222 Rn mass balance. J. Environ. Radioact. **143**: 58–69. doi:10.1016/j.jenvrad.2015.02.007

Cohen, R. A., and A. M. Bradham. 2010. Uptake of stable N isotopes by Myriophyllum spicatum is not selective. Aquat. Bot. **92**: 227–232. doi:10.1016/j.aquabot.2009.12.005

Cohen, R. A., and P. Fong. 2005. EXPERIMENTAL EVIDENCE SUPPORTS THE USE OF δ15N CONTENT OF THE OPPORTUNISTIC GREEN MACROALGA ENTEROMORPHA INTESTINALIS (CHLOROPHYTA) TO DETERMINE NITROGEN SOURCES TO ESTUARIES1: MACROALGAL N ISOTOPIC FRACTIONATION. J. Phycol. **41**: 287–293. doi:10.1111/j.1529-8817.2005.04022.x

Cole, M. L., K. D. Kroeger, J. W. McClelland, and I. Valiela. 2005. Macrophytes as indicators of land-derived wastewater: Application of a δ^{15} N method in aquatic systems: MACROPHYTES AS INDICATORS OF WASTEWATER. Water Resour. Res. **41**: n/a-n/a. doi:10.1029/2004WR003269

Cole, M. L., K. D. Kroeger, J. W. Mcclelland, and I. Valiela. 2006. Effects of Watershed Land use on Nitrogen Concentrations and δ15 Nitrogen in

Groundwater. Biogeochemistry **77**: 199–215. doi:10.1007/s10533-005-1036-2

Conley, D. J., J. Carstensen, G. Ærtebjerg, P. B. Christensen, T. Dalsgaard, J. L. S. Hansen, and A. B. Josefson. 2007. Long-Term Changes and Impacts of Hypoxia in Danish Coastal Waters. Ecol. Appl. **17**: S165–S184.

Connor, K. M., and A. Y. Gracey. 2011. Circadian cycles are the dominant transcriptional rhythm in the intertidal mussel Mytilus californianus. Proc. Natl. Acad. Sci. U. S. A. **108**: 16110–16115. doi:10.1073/pnas.1111076108

Cook, P. G., S. Lamontagne, D. Berhane, and J. F. Clark. 2006. Quantifying groundwater discharge to Cockburn River, southeastern Australia, using dissolved gas tracers ^{222}Rn and SF_6: GROUNDWATER DISCHARGE TO THE COCKBURN. Water Resour. Res. **42**: n/a-n/a. doi:10.1029/2006WR004921

Cook, P. G., V. Rodellas, A. Andrisoa, and T. C. Stieglitz. 2018a. Exchange across the sediment-water interface quantified from porewater radon profiles. J. Hydrol. **559**: 873–883. doi:10.1016/j.jhydrol.2018.02.070

Cook, P. G., V. Rodellas, and T. C. Stieglitz. 2018b. Quantifying Surface Water, Porewater, and Groundwater Interactions Using Tracers: Tracer Fluxes, Water Fluxes, and End-member Concentrations. Water Resour. Res. **54**: 2452–2465. doi:10.1002/2017WR021780

Cook, P. G., C. Wood, T. White, C. T. Simmons, T. Fass, and P. Brunner. 2008. Groundwater inflow to a shallow, poorly-mixed wetland estimated from a mass balance of radon. J. Hydrol. **354**: 213–226. doi:10.1016/j.jhydrol.2008.03.016

Corbett, D. R., W. C. Burnett, P. H. Cable, and S. B. Clark. 1998. A multiple approach to the determination of radon fluxes from sediments. J. Radioanal. Nucl. Chem. **236**: 247–253.

Corbett, D. R., and J. E. Cable. 2003. Seepage Meters and Advective Transport in Coastal Environments: Comments on “Seepage Meters and Bernoulli’s Revenge” by E. A. Shinn, C. D. Reich, and T. D. Hickey. 2002. Estuaries 25:126-132. Estuaries **26**: 1383–1387. doi:10.1007/BF02803639

Crook, E. D., D. Potts, M. Rebolledo-Vieyra, L. Hernandez, and A. Paytan. 2012. Calcifying coral abundance near low-pH springs: implications for future ocean acidification. Coral Reefs **31**: 239–245. doi:10.1007/s00338-011-0839-y

Crusius, J., P. Berg, D. J. Koopmans, and L. Erban. 2008. Eddy correlation measurements of submarine groundwater discharge. Mar. Chem. **109**: 77–85. doi:10.1016/j.marchem.2007.12.004

Cyronak, T., I. R. Santos, D. V. Erler, and B. D. Eyre. 2013. Groundwater and porewater as major sources of alkalinity to a fringing coral reef lagoon (Muri Lagoon, Cook Islands). Biogeosciences **10**: 2467–2480. doi:10.5194/bg-10-2467-2013

Dailidienė, I., H. Baudler, B. Chubarenko, and S. Navrotskaya. 2011. Long term water level and surface temperature changes in the lagoons of the southern and eastern Baltic. Oceanologia **53**: 293–308. doi:10.5697/oc.53-1-TI.293

Danovaro, R., and A. Pusceddu. 2007. Biodiversity and ecosystem functioning in coastal lagoons: Does microbial diversity play any role? Estuar. Coast. Shelf Sci. **75**: 4–12. doi:10.1016/j.ecss.2007.02.030

Das Gupta, A., S. Sarkar, J. Singh, T. Saha, and A. K. Sil. 2016. Nitrogen dynamics of the aquatic system is an important driving force for efficient sewage purification in single pond natural treatment wetlands at East Kolkata Wetland. Chemosphere **164**: 576–584. doi:10.1016/j.chemosphere.2016.08.140

Davenport, J. 1979. The isolation response of mussels (Mytilus edulis L.) exposed to falling sea-water concentrations. J. Mar. Biol. Assoc. U. K. **59**: 123–132. doi:10.1017/S0025315400043423

De Brabandere, L., N. Brion, M. Elskens, W. Baeyens, and F. Dehairs. 2007. δ15N dynamics of ammonium and particulate nitrogen in a temperate eutrophic estuary. Biogeochemistry **82**: 1–14. doi:10.1007/s10533-006-9047-1

De Vittor, C., F. Relitti, M. Kralj, S. Covelli, and A. Emili. 2016. Oxygen, carbon, and nutrient exchanges at the sediment-water interface in the Mar Piccolo of Taranto (Ionian Sea, southern Italy). Environ. Sci. Pollut. Res. Int. **23**: 12566–12581. doi:10.1007/s11356-015-4999-0

De Wit, R. 2011. Biodiversity of Coastal Lagoon Ecosystems and Their Vulnerability to Global Change. Ecosyst. Biodivers. 14.

Deborde, J., P. Anschutz, I. Auby, C. Glé, M.-V. Commarieu, D. Maurer, P. Lecroart, and G. Abril. 2008. Role of tidal pumping on nutrient cycling in a temperate lagoon (Arcachon Bay, France). Mar. Chem. **109**: 98–114. doi:10.1016/j.marchem.2007.12.007

Derolez, V., J. Oheix, V. Ouisse, and others. 2015. Suivi estival des lagunes méditerranéennes françaises-Bilan des résultats 2014.

Derse, E., K. L. Knee, S. D. Wankel, C. Kendall, C. J. Berg, and A. Paytan. 2007. Identifying Sources of Nitrogen to Hanalei Bay, Kauai, Utilizing the Nitrogen Isotope Signature of Macroalgae. Environ. Sci. Technol. **41**: 5217–5223. doi:10.1021/es0700449

Deutsch, B., S. Forster, M. Wilhelm, J. W. Dippner, and M. Voss. 2010. Denitrification in sediments as a major nitrogen sink in the Baltic Sea: an extrapolation using sediment characteristics. Biogeosciences **7**: 3259–3271.

Devol, A. H. 2015. Denitrification, Anammox, and N2 Production in Marine Sediments. Annu. Rev. Mar. Sci. **7**: 403–423. doi:10.1146/annurev-marine-010213-135040

Di Giuseppe, D., G. Bianchini, L. Vittori Antisari, A. Martucci, C. Natali, and L. Beccaluva. 2014. Geochemical characterization and biomonitoring of reclaimed soils in the Po River Delta (Northern Italy): implications for the agricultural activities. Environ. Monit. Assess. **186**: 2925–2940. doi:10.1007/s10661-013-3590-8

Dimova, N. T., and W. C. Burnett. 2011. Evaluation of groundwater discharge into small lakes based on the temporal distribution of radon-222. Limnol. Oceanogr. **56**: 9. doi:10.4319/lo.2011.56.2.0486

Dore, M. H. I. 2005. Climate change and changes in global precipitation patterns: What do we know? Environ. Int. **31**: 1167–1181. doi:10.1016/j.envint.2005.03.004

Dorsett, A., J. Cherrier, J. B. Martin, and J. E. Cable. 2011. Assessing hydrologic and biogeochemical controls on pore-water dissolved inorganic carbon cycling in a subterranean estuary: A 14C and 13C mass balance approach. Mar. Chem. **127**: 76–89. doi:10.1016/j.marchem.2011.07.007

DREAL, D. 2010. DOCOB de l'Étang de la Palme.

Duck, R. W., and J. F. da Silva. 2012. Coastal lagoons and their evolution: A hydromorphological perspective. Estuar. Coast. Shelf Sci. **110**: 2–14. doi:10.1016/j.ecss.2012.03.007

Dudley, B. D., and J. S. Shima. 2010. Algal and invertebrate bioindicators detect sewage effluent along the coast of Titahi Bay, Wellington, New Zealand. N. Z. J. Mar. Freshw. Res. **44**: 39–51. doi:10.1080/00288331003641687

Dulaiova, H., R. Peterson, W. C. Burnett, and D. Lane-Smith. 2005. A multi-detector continuous monitor for assessment of 222 Rn in the coastal ocean. J. Radioanal. Nucl. Chem. **263**: 361–363.

Encarnação, J., F. Leitão, P. Range, D. Piló, M. A. Chícharo, and L. Chícharo. 2015. Local and temporal variations in near-shore macrobenthic communities associated with submarine groundwater discharges. Mar. Ecol. **36**: 926–941. doi:10.1111/maec.12186

Enoch H. Z., and Olesen J. M. 2006. Plant response to irrigation with water enriched with carbon dioxide. New Phytol. **125**: 249–258. doi:10.1111/j.1469-8137.1993.tb03880.x

Evans, J. W. 1972. Tidal Growth Increments in the Cockle Clinocardium nuttalli. Science **176**: 416–417. doi:10.1126/science.176.4033.416

Evans, R. D. 2001. Physiological mechanisms influencing plant nitrogen isotope composition. Trends Plant Sci. **6**: 121–126. doi:10.1016/S1360-1385(01)01889-1

Fiandrino, A., A. Giraud, S. Robin, and C. Pinatel. 2012. Validation d'une méthode d'estimation des volumes d'eau échangés entre la mer et les lagunes et définition d'indicateurs hydrodynamiques associés.

Fleury, P., M. Bakalowicz, and G. de Marsily. 2007. Submarine springs and coastal karst aquifers: A review. J. Hydrol. **339**: 79–92. doi:10.1016/j.jhydrol.2007.03.009

Fry, B. 2003. Steady state models of stable isotopic distributions. Isotopes Environ. Health Stud. **39**: 219–232. doi:10.1080/1025601031000108651

Fuentes, J., V. Gregorio, R. Giráldez, and J. Molares. 2000. Within-raft variability of the growth rate of mussels, Mytilus galloprovincialis, cultivated in the Rıa de Arousa (NW Spain). Aquaculture **189**: 39–52.

Gangnery, A., C. Bacher, and D. Buestel. 2004. Application of a population dynamics model to the Mediterranean mussel, Mytilus galloprovincialis, reared in Thau Lagoon (France). Aquaculture **229**: 289–313. doi:10.1016/S0044-8486(03)00360-0

Garcia-Solsona, E., J. Garcia-Orellana, P. Masqué, V. Rodellas, M. Mejías, B. Ballesteros, and J. A. Domínguez. 2010a. Groundwater and nutrient discharge through karstic coastal springs (<i>Castelló</i>, Spain). Biogeosciences **7**: 2625–2638. doi:10.5194/bg-7-2625-2010

Garcia-Solsona, E., J. Garcia-Orellana, P. Masqué, V. Rodellas, M. Mejías, B. Ballesteros, and J. A. Domínguez. 2010b. Groundwater and nutrient discharge through karstic coastal springs (*Castelló*, Spain). Biogeosciences **7**: 2625–2638. doi:10.5194/bg-7-2625-2010

Garzon-Garcia, A., J. P. Laceby, J. M. Olley, and S. E. Bunn. 2017. Differentiating the sources of fine sediment, organic matter and nitrogen in a subtropical Australian catchment. Sci. Total Environ. **575**: 1384–1394. doi:10.1016/j.scitotenv.2016.09.219

Gilfedder, B. S., S. Frei, H. Hofmann, and I. Cartwright. 2015. Groundwater discharge to wetlands driven by storm and flood events: Quantification using continuous Radon-222 and electrical conductivity measurements and dynamic mass-balance modelling. Geochim. Cosmochim. Acta **165**: 161–177. doi:10.1016/j.gca.2015.05.037

Gillikin, D. P., A. Lorrain, S. Bouillon, P. Willenz, and F. Dehairs. 2006. Stable carbon isotopic composition of Mytilus edulis shells: relation to

metabolism, salinity, δ13CDIC and phytoplankton. Org. Geochem. **37**: 1371–1382. doi:10.1016/j.orggeochem.2006.03.008

Goñi, M. A., and I. R. Gardner. 2003. Seasonal Dynamics in Dissolved Organic Carbon Concentrations in a Coastal Water-Table Aquifer at the Forest-Marsh Interface. Aquat. Geochem. **9**: 209–232. doi:10.1023/B:AQUA.0000022955.82700.ed

Gonneea, M. E., A. E. Mulligan, and M. A. Charette. 2013. Seasonal cycles in radium and barium within a subterranean estuary: Implications for groundwater derived chemical fluxes to surface waters. Geochim. Cosmochim. Acta **119**: 164–177. doi:10.1016/j.gca.2013.05.034

Hammond, D. E., P. Giordani, W. M. Berelson, and R. Poletti. 1999. Diagenesis of carbon and nutrients and benthic exchange in sediments of the Northern Adriatic Sea. Mar. Chem. **66**: 53–79. doi:10.1016/S0304-4203(99)00024-9

Hansen, J., M. Sato, R. Ruedy, K. Lo, D. W. Lea, and M. Medina-Elizade. 2006. Global temperature change. Proc. Natl. Acad. Sci. **103**: 14288–14293. doi:10.1073/pnas.0606291103

Hansen, J. W., J. W. Udy, C. J. Perry, W. C. Dennison, and B. A. Lomstein. 2000. Effect of the seagrass Zostera capricorni on sediment microbial processes. Mar. Ecol. Prog. Ser. 83–96.

Hata, M., R. Sugimoto, M. Hori, T. Tomiyama, and J. Shoji. 2016. Occurrence, distribution and prey items of juvenile marbled sole Pseudopleuronectes yokohamae around a submarine groundwater seepage on a tidal flat in southwestern Japan. J. Sea Res. **111**: 47–53. doi:10.1016/j.seares.2016.01.009

Hellings, L., F. Dehairs, S. Van Damme, and W. Baeyens. 2001. Dissolved inorganic carbon in a highly polluted estuary (the Scheldt). Limnol. Oceanogr. **46**: 1406–1414. doi:10.4319/lo.2001.46.6.1406

Hemminga, M. A., N. Marba, and J. Stapel. 1999. Leaf nutrient resorption, leaf lifespan and the retention of nutrients in seagrass systems. Aquat. Bot. **65**: 141–158.

Hemminga, M., and M. Mateo. 1996. Stable carbon isotopes in seagrasses:variability in ratios and use in ecological studies. Mar. Ecol. Prog. Ser. **140**: 285–298. doi:10.3354/meps140285

Herbert, R. A. 1999. Nitrogen cycling in coastal marine ecosystems. FEMS Microbiol. Rev. **23**: 563–590.

Hernández-López, J., V. F. Camacho-Ibar, A. Macías-Tapia, K. J. McGlathery, L. W. Daesslé, and J. M. Sandoval-Gil. 2017. Benthic nitrogen fixation in Zostera

marina meadows in an upwelling-influenced coastal lagoon. Cienc. Mar. **43**: 35–53.

Hernández-Terrones, L., M. Rebolledo-Vieyra, M. Merino-Ibarra, M. Soto, A. Le-Cossec, and E. Monroy-Ríos. 2011. Groundwater Pollution in a Karstic Region (NE Yucatan): Baseline Nutrient Content and Flux to Coastal Ecosystems. Water. Air. Soil Pollut. **218**: 517–528. doi:10.1007/s11270-010-0664-x

Herrera-Silveira, J. A. 1998. Nutrient-phytoplankton production relationships in a groundwater-influenced tropical coastal lagoon. Aquat. Ecosyst. Health Manag. **1**: 373–385.

His, E., R. Robert, and A. Dinet. 1989. Combined effects of temperature and salinity on fed and starved larvae of the mediterranean mussel Mytilus galloprovincialis and the Japanese oyster Crassostrea gigas. Mar. Biol. **100**: 455–463. doi:10.1007/BF00394822

Holliday, D., T. C. Stieglitz, P. V. Ridd, and W. W. Read. 2007. Geological controls and tidal forcing of submarine groundwater discharge from a confined aquifer in a coastal sand dune system. J. Geophys. Res. Oceans **112**: 1–10. doi:http://dx.doi.org/10.1029/2006JC003580

Holmes, R. M., A. Aminot, R. Kérouel, B. A. Hooker, and B. J. Peterson. 1999. A simple and precise method for measuring ammonium in marine and freshwater ecosystems. Can. J. Fish. Aquat. Sci. **56**: 1801–1808.

Holmes, R. M., J. W. McClelland, D. M. Sigman, B. Fry, and B. J. Peterson. 1998. Measuring 15N–NH 4+ in marine, estuarine and fresh waters: An adaptation of the ammonia diffusion method for samples with low ammonium concentrations. Mar. Chem. **60**: 235–243.

Hong, Y., M. Li, and J. Gu. 2009. [Bacterial anaerobic ammonia oxidation (Anammox) in the marine nitrogen cycle--a review]. Wei Sheng Wu Xue Bao **49**: 281–286.

Huettel, M., P. Berg, and J. E. Kostka. 2014. Benthic Exchange and Biogeochemical Cycling in Permeable Sediments. Annu. Rev. Mar. Sci. **6**: 23–51. doi:10.1146/annurev-marine-051413-012706

Hwang, D.-W., G. Kim, Y.-W. Lee, and H.-S. Yang. 2005. Estimating submarine inputs of groundwater and nutrients to a coastal bay using radium isotopes. Mar. Chem. **96**: 61–71. doi:10.1016/j.marchem.2004.11.002

IFREMER. 2003. Réseau de Suivi Lagunaire du Languedoc-Rouissillon: 4 - Etang de La Palme, Sète France.

IFREMER. 2005. Réseau de Suivi Lagunaire du Languedoc-Rouissillon: Bilan des résultats 2004. Rapport RSL.

IFREMER. 2010. Construction d'un outil permettant d'estimer les charges en azote et phosphite admissible en milieu lagunaire.

IFREMER. 2014. Réseau de Suivi Lagunaire du Languedoc-Roussillon. Bilan des résultats 2013.

Inglett, P. W., and K. R. Reddy. 2006. Investigating the use of macrophyte stable C and N isotopic ratios as indicators of wetland eutrophication: Patterns in the P-affected Everglades. Limnol. Oceanogr. **51**: 2380–2387. doi:10.4319/lo.2006.51.5.2380

Jauzein, C., D. Couet, T. Blasco, and R. Lemée. 2017. Uptake of dissolved inorganic and organic nitrogen by the benthic toxic dinoflagellate Ostreopsis cf. ovata. Harmful Algae **65**: 9–18. doi:10.1016/j.hal.2017.04.005

Ji, T., J. Du, W. S. Moore, G. Zhang, N. Su, and J. Zhang. 2013. Nutrient inputs to a Lagoon through submarine groundwater discharge: The case of Laoye Lagoon, Hainan, China. J. Mar. Syst. **111–112**: 253–262. doi:10.1016/j.jmarsys.2012.11.007

Johannes, R. 1980. The Ecological Significance of the Submarine Discharge of Groundwater. Mar. Ecol. Prog. Ser. **3**: 365–373. doi:10.3354/meps003365

Johnson, A. G., C. R. Glenn, W. C. Burnett, R. N. Peterson, and P. G. Lucey. 2008. Aerial infrared imaging reveals large nutrient-rich groundwater inputs to the ocean. Geophys. Res. Lett. **35**: L15606. doi:10.1029/2008GL034574

Jones, D. S., M. A. Arthur, and D. J. Allard. 1989. Sclerochronological records of temperature and growth from shells of Mercenaria mercenaria from Narragansett Bay, Rhode Island. Mar. Biol. **102**: 225–234.

Jones, D. S., and I. R. Quitmyer. 1996. Marking Time with Bivalve Shells: Oxygen Isotopes and Season of Annual Increment Formation. PALAIOS **11**: 340–346. doi:10.2307/3515244

Karayücel, S., and M. Ye. 2010. Growth and Production of Raft Cultivated Mediterranean Mussel (Mytilus galloprovincialis Lamarck, 1819) in Sinop, Black Sea. 9.

Kautsky, N. 1982. Growth and size structure in a baltic Mytilus edulis population. Mar. Biol. **68**: 117–133. doi:10.1007/BF00397599

Kelly, J. L., C. R. Glenn, and P. G. Lucey. 2013. High-resolution aerial infrared mapping of groundwater discharge to the coastal ocean. Limnol. Oceanogr. Methods **11**: 262–277. doi:10.4319/lom.2013.11.262

Kemp, W. M., R. L. Wetzel, W. R. Boynton, C. F. D'Elia, and J. C. Stevenson. 1982. NITROGEN CYCLING AND ESTUARINE INTERFACES: SOME CURRENT CONCEPTS AND RESEARCH DIRECTIONS, p. 209–230. *In* V.S. Kennedy [ed.], Estuarine Comparisons. Academic Press.

Kendall, C. 2015. Resources on Isotopes. Delta **16**: 6.

Kendall, C., and R. Aravena. 2000. Nitrate Isotopes in Groundwater Systems, p. 261–297. *In* Environmental Tracers in Subsurface Hydrology. Springer, Boston, MA.

Kendall, C., E. M. Elliott, and S. D. Wankel. 2007. Tracing anthropogenic inputs of nitrogen to ecosystems. Stable Isot. Ecol. Environ. Sci. **2**: 375–449.

Kennish, M. J., and H. W. Paerl, eds. 2010. Coastal lagoons: critical habitats of environmental change, CRC.

Kessler, A. J., R. N. Glud, M. B. Cardenas, M. Larsen, M. F. Bourke, and P. L. M. Cook. 2012. Quantifying denitrification in rippled permeable sands through combined flume experiments and modeling. Limnol. Oceanogr. **57**: 1217–1232. doi:10.4319/lo.2012.57.4.1217

Kim, G., and D.-W. Hwang. 2002. Tidal pumping of groundwater into the coastal ocean revealed from submarine 222Rn and CH4 monitoring. Geophys. Res. Lett. **29**: 23-1-23–4. doi:10.1029/2002GL015093

Kim, H., K. Lee, D.-I. Lim, and others. 2017. Widespread Anthropogenic Nitrogen in Northwestern Pacific Ocean Sediment. Environ. Sci. Technol. **51**: 6044–6052. doi:10.1021/acs.est.6b05316

Kirkwood, D. S. 1992. Stability of solutions of nutrient salts during storage. Mar. Chem. **38**: 151–164.

Kjerfve, B. 1994. Coastal Lagoon Processes, Elsevier.

Knee, K. L., and A. Paytan. 2011. Submarine Groundwater Discharge, p. 205–233. *In* Treatise on Estuarine and Coastal Science. Elsevier.

Knee, K. L., J. H. Street, E. E. Grossman>, A. B. Boehm, and A. Paytan. 2010. Nutrient inputs to the coastal ocean from submarine groundwater discharge in a groundwater-dominated system: Relation to land use (Kona coast, Hawaii, U.S.A.). Limnol. Oceanogr. **55**: 1105–1122. doi:10.4319/lo.2010.55.3.1105

Kohzu, A., T. Miyajima, I. Tayasu, and others. 2008. Use of Stable Nitrogen Isotope Signatures of Riparian Macrophytes As an Indicator of Anthropogenic N Inputs to River Ecosystems. Environ. Sci. Technol. **42**: 7837–7841. doi:10.1021/es801113k

Koike, I., and A. Hattori. 1978. Denitrification and ammonia formation in anaerobic coastal sediments. Appl. Environ. Microbiol. **35**: 278–282.

Kotwicki, L., K. Grzelak, M. Czub, O. Dellwig, T. Gentz, B. Szymczycha, and M. E. Böttcher. 2014. Submarine groundwater discharge to the Baltic coastal zone: Impacts on the meiofaunal community. J. Mar. Syst. **129**: 118–126. doi:10.1016/j.jmarsys.2013.06.009

Kremer, J. N., A. Reischauer, and C. D'Avanzo. 2003. Estuary-specific variation in the air-water gas exchange coefficient for oxygen. Estuaries **26**: 829–836. doi:10.1007/BF02803341

Kroeger, K. D., and M. A. Charette. 2008. Nitrogen biogeochemistry of submarine groundwater discharge. Limnol. Oceanogr. **53**: 10251039. doi:10.4319/lo.2008.53.3.1025

Kroeger, K. D., P. W. Swarzenski, W. J. Greenwood, and C. Reich. 2007. Submarine groundwater discharge to Tampa Bay: Nutrient fluxes and biogeochemistry of the coastal aquifer. Mar. Chem. **104**: 85–97. doi:10.1016/j.marchem.2006.10.012

Kwon, H. K., H. Kang, Y. H. Oh, S. R. Park, and G. Kim. 2017. Green tide development associated with submarine groundwater discharge in a coastal harbor, Jeju, Korea. Sci. Rep. **7**. doi:10.1038/s41598-017-06711-0

Lacoste, é, P. Raimbault, M. Harmelin-Vivien, and N. Gaertner-Mazouni. 2016. Trophic relationships between the farmed pearl oyster Pinctada margaritifera and its epibionts revealed by stable isotopes and feeding experiments. Aquac. Environ. Interact. **8**: 55–66. doi:10.3354/aei00157

Ladagnous, H., and C. Le Bec. 1997. Lagune de Salses-Leucate. I-Analyse bibliographique.

Lakhdar, R., M. Soussi, M. H. Ben Ismail, and A. M'Rabet. 2006. A Mediterranean Holocene restricted coastal lagoon under arid climate: Case of the sedimentary record of Sabkha Boujmel (SE Tunisia). Palaeogeogr. Palaeoclimatol. Palaeoecol. **241**: 177–191. doi:10.1016/j.palaeo.2006.02.014

Lam, P., G. Lavik, M. M. Jensen, and others. 2009. Revising the nitrogen cycle in the Peruvian oxygen minimum zone. Proc. Natl. Acad. Sci. U. S. A. **106**: 4752–4757. doi:10.1073/pnas.0812444106

Langton, R. W. 1977. Digestive rhythms in the mussel Mytilus edulis. Mar. Biol. **41**: 53–58. doi:10.1007/BF00390581

Lartaud, F., L. Chauvaud, J. Richard, A. Toulot, C. Bollinger, L. Testut, and Y.-M. Paulet. 2010a. Experimental growth pattern calibration of Antarctic scallop shells (Adamussium colbecki, Smith 1902) to provide a biogenic archive of high-resolution records of environmental and climatic changes. J. Exp. Mar. Biol. Ecol. **393**: 158–167. doi:10.1016/j.jembe.2010.07.016

Lartaud, F., L. Emmanuel, M. de Rafelis, M. Ropert, N. Labourdette, C. A. Richardson, and M. Renard. 2010b. A latitudinal gradient of seasonal temperature variation recorded in oyster shells from the coastal waters of France and The Netherlands. Facies **56**: 13–25. doi:10.1007/s10347-009-0196-2

Lartaud, F., S. Pareige, M. de Rafelis, and others. 2013. A new approach for assessing cold-water coral growth in situ using fluorescent calcein staining. Aquat. Living Resour. **26**: 187–196. doi:10.1051/alr/2012029

Lassauque, J., G. Lepoint, T. Thibaut, P. Francour, and A. Meinesz. 2010. Tracing sewage and natural freshwater input in a Northwest Mediterranean bay: Evidence obtained from isotopic ratios in marine organisms. Mar. Pollut. Bull. **60**: 843–851. doi:10.1016/j.marpolbul.2010.01.008

LaZerte, B. D. 1981. The relationship between total dissolved carbon dioxide and its stable carbon isotope ratio in aquatic sediments. Geochim. Cosmochim. Acta **45**: 647–656. doi:10.1016/0016-7037(81)90039-9

LaZerte, B. D., and J. E. Szalados. 1982. Stable carbon isotope ratio of submerged freshwater macrophytes1,1: Carbon ratio of macrophytes. Limnol. Oceanogr. **27**: 413–418. doi:10.4319/lo.1982.27.3.0413

Le Fur, I., R. De Wit, M. Plus, J. Oheix, V. Derolez, M. Simier, N. Malet, and V. Ouisse. 2019. Re-oligotrophication trajectories of macrophyte assemblages in Mediterranean coastal lagoons based on 17-year time-series. Mar. Ecol. Prog. Ser. **608**: 13–32. doi:10.3354/meps12814

Lee, E., D. Shin, S. P. Hyun, K.-S. Ko, H. S. Moon, D.-C. Koh, K. Ha, and B.-Y. Kim. 2017. Periodic change in coastal microbial community structure associated with submarine groundwater discharge and tidal fluctuation. Limnol. Oceanogr. **62**: 437–451. doi:10.1002/lno.10433

Lee, K.-S., and K. H. Dunton. 1999. Inorganic nitrogen acquisition in the seagrass Thalassia testudinum: Development of a whole-plant nitrogen budget. Limnol. Oceanogr. **44**: 1204–1215.

Leffler, A. J., and J. M. Welker. 2013. Long-term increases in snow pack elevate leaf N and photosynthesis in Salix arctica : responses to a snow fence experiment in the High Arctic of NW Greenland. Environ. Res. Lett. **8**: 025023. doi:10.1088/1748-9326/8/2/025023

Lepoint, G., P. Dauby, and S. Gobert. 2004. Applications of C and N stable isotopes to ecological and environmental studies in seagrass ecosystems. Mar. Pollut. Bull. **49**: 887–891. doi:10.1016/j.marpolbul.2004.07.005

Lepoint, G., F. Nyssen, S. Gobert, P. Dauby, and J.-M. Bouquegneau. 2000. Relative impact of a seagrass bed and its adjacent epilithic algal community in consumer diets. Mar. Biol. **136**: 513–518. doi:10.1007/s002270050711

Li, S.-L., C.-Q. Liu, J. Li, Y.-C. Lang, H. Ding, and L. Li. 2010. Geochemistry of dissolved inorganic carbon and carbonate weathering in a small typical karstic catchment of Southwest China: Isotopic and chemical constraints. Chem. Geol. **277**: 301–309. doi:10.1016/j.chemgeo.2010.08.013

Li, Y.-H., and S. Gregory. 1974. Diffusion of ions in sea water and in deep-sea sediments. Geochim. Cosmochim. Acta **38**: 703–714. doi:10.1016/0016-7037(74)90145-8

Lin, G., T. Banks, and L. da S. L. O. R. Sternberg. 1991. Variation in δ13C values for the seagrass Thalassia testudinum and its relations to mangrove carbon. Aquat. Bot. **40**: 333–341. doi:10.1016/0304-3770(91)90079-K

Lionard, M., K. Muylaert, D. V. Gansbeke, and W. Vyverman. 2005. Influence of changes in salinity and light intensity on growth of phytoplankton communities from the Schelde river and estuary (Belgium/The Netherlands). Hydrobiologia **540**: 105–115. doi:10.1007/s10750-004-7123-x

Lirman, D., B. Orlando, S. Maciá, D. Manzello, L. Kaufman, P. Biber, and T. Jones. 2003. Coral communities of Biscayne Bay, Florida and adjacent offshore areas: diversity, abundance, distribution, and environmental correlates. Aquat. Conserv. Mar. Freshw. Ecosyst. **13**: 121–135. doi:10.1002/aqc.552

Liu, Q., M. Dai, W. Chen, C.-A. Huh, G. Wang, Q. Li, and M. A. Charette. 2012. How significant is submarine groundwater discharge and its associated dissolved inorganic carbon in a river-dominated shelf system? Biogeosciences **9**: 1777–1795. doi:10.5194/bg-9-1777-2012

Liu, X., Z. Yu, X. Song, and X. Cao. 2009. The nitrogen isotopic composition of dissolved nitrate in the Yangtze River (Changjiang) estuary, China. Estuar. Coast. Shelf Sci. **85**: 641–650. doi:10.1016/j.ecss.2009.09.017

Lotze, H. K., and W. Schramm. 2000. Ecophysiological traits explain species dominance patterns in macroalgal blooms. J. Phycol. **36**: 287–295. doi:10.1046/j.1529-8817.2000.99109.x

Loureiro, S., A. Newton, and J. Icely. 2006. Boundary conditions for the European Water Framework Directive in the Ria Formosa lagoon, Portugal (physico-chemical and phytoplankton quality elements). Estuar. Coast. Shelf Sci. **67**: 382–398. doi:10.1016/j.ecss.2005.11.029

Lucas, A., and P. G. Beninger. 1985. The use of physiological condition indices in marine bivalve aquaculture. Aquaculture **44**: 187–200. doi:10.1016/0044-8486(85)90243-1

Macintosh, D. J. 1994. Chapter 14 Aquaculture in Coastal Lagoons, p. 401–442. *In* B. Kjerfve [ed.], Elsevier Oceanography Series. Elsevier.

MacIntyre, S., R. Wanninkhof, and J. P. Chanton. 1995. Trace gas exchange across the air-sea interface in fresh water and coastal marine environments. Blackwell Sci. Ltd Camb. MA 52–97.

Madsen, T. V., and N. Cedergreen. 2002. Sources of nutrients to rooted submerged macrophytes growing in a nutrient-rich stream. Freshw. Biol. **47**: 283–291.

Mahé, K., E. Bellamy, F. Lartaud, and M. de Rafélis. 2010. Calcein and manganese experiments for marking the shell of the common cockle (Cerastoderma edule): tidal rhythm validation of increments formation. Aquat. Living Resour. **23**: 239–245. doi:10.1051/alr/2010025

Maher, D. T., I. R. Santos, L. Golsby-Smith, J. Gleeson, and B. D. Eyre. 2013. Groundwater-derived dissolved inorganic and organic carbon exports from a mangrove tidal creek: The missing mangrove carbon sink? Limnol. Oceanogr. **58**: 475–488. doi:10.4319/lo.2013.58.2.0475

Malta, E. -jan, T. Y. Stigter, A. Pacheco, A. C. Dill, D. Tavares, and R. Santos. 2017. Effects of External Nutrient Sources and Extreme Weather Events on the Nutrient Budget of a Southern European Coastal Lagoon. Estuaries Coasts **40**: 419–436. doi:10.1007/s12237-016-0150-9

Marbà, N., M. A. Hemminga, and C. M. Duarte. 2006. Resource translocation within seagrass clones: allometric scaling to plant size and productivity. Oecologia **150**: 362–372. doi:10.1007/s00442-006-0524-y

Markaki, Z., M. D. Loÿe-Pilot, K. Violaki, L. Benyahya, and N. Mihalopoulos. 2010. Variability of atmospheric deposition of dissolved nitrogen and phosphorus in the Mediterranean and possible link to the anomalous seawater N/P ratio. Mar. Chem. **120**: 187–194. doi:10.1016/j.marchem.2008.10.005

Martens, C. S., G. W. Kipphut, and J. V. Klump. 1980. Sediment-Water Chemical Exchange in the Coastal Zone Traced by in situ Radon-222 Flux Measurements. Science **208**: 285–288. doi:10.1126/science.208.4441.285

Martin, J. B., J. E. Cable, J. Jaeger, K. Hartl, and C. G. Smith. 2006. Thermal and chemical evidence for rapid water exchange across the sediment-water interface by bioirrigation in the Indian River Lagoon, Florida. Limnol. Oceanogr. **51**: 1332–1341. doi:10.4319/lo.2006.51.3.1332

Martínez-Soto, M. C., A. Tovar-Sánchez, D. Sánchez-Quiles, V. Rodellas, J. Garcia-Orellana, and G. Basterretxea. 2016. Seasonal variation and sources of dissolved trace metals in Maó Harbour, Minorca Island. Sci. Total Environ. **565**: 191–199. doi:10.1016/j.scitotenv.2016.03.244

McClelland, J. W., and I. Valiela. 1998. Linking nitrogen in estuarine producers to land-derived sources. Limnol. Oceanogr. **43**: 577–585. doi:10.4319/lo.1998.43.4.0577

McClelland, J. W., I. Valiela, and R. H. Michener. 1997. Nitrogen-stable isotope signatures in estuarine food webs: a record of increasing urbanization in coastal watersheds. Limnol. Oceanogr. **42**: 930–937.

McCoy, C. A., and D. R. Corbett. 2009. Review of submarine groundwater discharge (SGD) in coastal zones of the Southeast and Gulf Coast regions of the United States with management implications. J. Environ. Manage. **90**: 644–651. doi:10.1016/j.jenvman.2008.03.002

McGlathery, K. J., N. Risgaard-Petersen, and P. B. Christensen. 1998. Temporal and spatial variation in nitrogen fixation activity in the eelgrass Zostera marina rhizosphere. Mar. Ecol. Prog. Ser. 245–258.

Mesnage, V., and B. Picot. 1995. The distribution of phosphate in sediments and its relation with eutrophication of a Mediterranean coastal lagoon. Hydrobiologia **297**: 29–41. doi:10.1007/BF00033499

Middelburg, J. ., and J. Nieuwenhuize. 2001. Nitrogen Isotope Tracing of Dissolved Inorganic Nitrogen Behaviour in Tidal Estuaries. Estuar. Coast. Shelf Sci. **53**: 385–391. doi:10.1006/ecss.2001.0805

Middelburg, J. J., and L. A. Levin. 2009. Coastal hypoxia and sediment biogeochemistry. Biogeosciences **6**: 1273–1293. doi:https://doi.org/10.5194/bg-6-1273-2009

Middelburg, J. J., and J. Nieuwenhuize. 2000. Uptake of dissolved inorganic nitrogen in turbid, tidal estuaries. Mar. Ecol. Prog. Ser. **192**: 79–88.

Miller, D. C., and W. J. Ullman. 2004. Ecological Consequences of Ground Water Discharge to Delaware Bay, United States. Groundwater **42**: 959–970. doi:10.1111/j.1745-6584.2004.tb02635.x

Miththapala, S. 2013. Lagoons and estuaries, IUCN.

Miyaji, T., K. Tanabe, and B. R. Schöne. 2007. Environmental controls on daily shell growth of Phacosoma japonicum (Bivalvia: Veneridae) from Japan. Mar. Ecol. Prog. Ser. **336**: 141–150.

Miyajima, T., Y. Miyajima, Y. T. Hanba, K. Yoshii, T. Koitabashi, and E. Wada. 1995. Determining the stable isotope ratio of total dissolved inorganic carbon in lake water by GC/C/IIRMS. Limnol. Oceanogr. **40**: 994–1000. doi:10.4319/lo.1995.40.5.0994

Montoya, J. P., and J. J. McCarthy. 1995. Isotopic fractionation during nitrate uptake by phytoplankton grown in continuous culture. J. Plankton Res. **17**: 439–464. doi:10.1093/plankt/17.3.439

Moore, W. S. 1999. The subterranean estuary: a reaction zone of ground water and sea water. Mar. Chem. **65**: 111–125.

Moore, W. S. 2010. The Effect of Submarine Groundwater Discharge on the Ocean. Annu. Rev. Mar. Sci. **2**: 59–88. doi:10.1146/annurev-marine-120308-081019

Moore, W. S., and D. F. Reid. 1973. Extraction of radium from natural waters using manganese-impregnated acrylic fibers. J. Geophys. Res. **78**: 8880–8886. doi:10.1029/JC078i036p08880

Moran, A. L. 2000. Calcein as a marker in experimental studies newly-hatched gastropods. Mar. Biol. **137**: 893–898.

Morin, G. P., N. Vigier, and A. Verney-Carron. 2015. Enhanced dissolution of basaltic glass in brackish waters: Impact on biogeochemical cycles. Earth Planet. Sci. Lett. **417**: 1–8. doi:10.1016/j.epsl.2015.02.005

Navarro, J. M. 1988. The effects of salinity on the physiological ecology of Choromytilus chorus (Molina, 1782)(Bivalvia: Mytilidae). J. Exp. Mar. Biol. Ecol. **122**: 19–33.

Nedoncelle, K., F. Lartaud, M. de Rafelis, S. Boulila, and N. Le Bris. 2013. A new method for high-resolution bivalve growth rate studies in hydrothermal environments. Mar. Biol. **160**: 1427–1439. doi:10.1007/s00227-013-2195-7

Newton, A., J. Icely, S. Cristina, and others. 2014. An overview of ecological status, vulnerability and future perspectives of European large shallow, semi-enclosed coastal systems, lagoons and transitional waters. Estuar. Coast. Shelf Sci. **140**: 95–122. doi:10.1016/j.ecss.2013.05.023

Ni, Z., L. Zhang, S. Yu, and others. 2017. The porewater nutrient and heavy metal characteristics in sediment cores and their benthic fluxes in Daya Bay, South China. Mar. Pollut. Bull. **124**: 547–554. doi:10.1016/j.marpolbul.2017.07.069

Niencheski, L. F. H., H. L. Windom, W. S. Moore, and R. A. Jahnke. 2007. Submarine groundwater discharge of nutrients to the ocean along a coastal lagoon barrier, Southern Brazil. Mar. Chem. **106**: 546–561. doi:10.1016/j.marchem.2007.06.004

Nixon, S. W. 1995. Coastal marine eutrophication: A definition, social causes, and future concerns. Ophelia **41**: 199–219. doi:10.1080/00785236.1995.10422044

Null, K. A., N. T. Dimova, K. L. Knee, B. K. Esser, P. W. Swarzenski, M. J. Singleton, M. Stacey, and A. Paytan. 2012. Submarine Groundwater Discharge-Derived Nutrient Loads to San Francisco Bay: Implications to Future Ecosystem Changes. Estuaries Coasts **35**: 1299–1315. doi:10.1007/s12237-012-9526-7

Okaniwa, N., T. Miyaji, T. Sasaki, and K. Tanabe. 2010. Shell growth and reproductive cycle of the Mediterranean mussel Mytilus galloprovincialis in Tokyo Bay, Japan: relationship with environmental conditions. Plankton Benthos Res. **5**: 214–220.

Okumuş, İ., N. Başçinar, and M. Özkan. 2014. The Effects of Phytoplankton Concentration, Size of Mussel and Water Temperature on Feed Consumption and Filtration Rate of the Mediterranean Mussel (Mytilus galloprovincialis Lmk). Turk. J. Zool. **26**: 167–172.

Omnes, P., G. Slawyk, N. Garcia, and P. Bonin. 1996. Evidence of denitrification and nitrate ammonification in the River Rhone plume (northwestern Mediterranean Sea). Mar. Ecol. Prog. Ser. **141**: 275–281.

Orban, E., G. Di Lena, T. Nevigato, I. Casini, A. Marzetti, and R. Caproni. 2002. Seasonal changes in meat content, condition index and chemical composition of mussels (Mytilus galloprovincialis) cultured in two different Italian sites. Food Chem. **77**: 57–65.

Orpin, A. R., P. V. Ridd, and L. K. Stewart. 1999. Assessment of the relative importance of major sediment transport mechanisms in the central Great Barrier Reef lagoon. Aust. J. Earth Sci. **46**: 883–896. doi:10.1046/j.1440-0952.1999.00751.x

Ouisse, V., P. Riera, A. Migné, C. Leroux, and D. Davoult. 2011. Freshwater seepages and ephemeral macroalgae proliferation in an intertidal bay: I Effect on benthic community structure and food web. Estuar. Coast. Shelf Sci. **91**: 272–281. doi:10.1016/j.ecss.2010.10.034

Page, H. M., and D. M. Hubbard. 1987. Temporal and spatial patterns of growth in mussels Mytilus edulis on an offshore platform: relationships to water temperature and food availability. J. Exp. Mar. Biol. Ecol. **111**: 159–179. doi:10.1016/0022-0981(87)90053-0

Pannella, G., and C. Macclintock. 1968. Biological and environmental rhythms reflected in molluscan shell growth. J. Paleontol. **42**: 64–80. doi:10.1017/S0022336000061655

Parsons, G. J., S. M. C. Robinson, J. C. Roff, and M. J. Dadswell. 1993. Daily Growth Rates as Indicated by Valve Ridges in Postlarval Giant Scallop (Placopecten magellanicus) (Bivalvia: Pectinidae). Can. J. Fish. Aquat. Sci. **50**: 456–464. doi:10.1139/f93-053

Pasqueron De Fommervault, O., F. D'Ortenzio, A. Mangin, and others. 2015. Seasonal variability of nutrient concentrations in the Mediterranean Sea: Contribution of Bio-Argo floats. J. Geophys. Res. Oceans **120**: 8528–8550. doi:10.1002/2015JC011103

Patriquin, D., and R. Knowles. 1972. Nitrogen fixation in the rhizosphere of marine angiosperms. Mar. Biol. **16**: 49–58.

Paulsen, R. J., C. F. Smith, D. O'Rourke, and T.-F. Wong. 2001. Development and Evaluation of an Ultrasonic Ground Water Seepage Meter. Groundwater **39**: 904–911. doi:10.1111/j.1745-6584.2001.tb02478.x

Peharda, M., I. Župan, L. Bavčević, A. Frankić, and T. Klanjšček. 2007. Growth and condition index of mussel Mytilus galloprovincialis in experimental integrated aquaculture. Aquac. Res. **0**: 071119223248006-??? doi:10.1111/j.1365-2109.2007.01840.x

Peng, T.-H., T. Takahashi, and W. S. Broecker. 1974. Surface radon measurements in the North Pacific Ocean station Papa. J. Geophys. Res. **79**: 1772–1780. doi:10.1029/JC079i012p01772

Penman, H. L. 1948. Natural evaporation from open water, hare soil and grass. Proc. R. Soc. Lond. Ser. Math. Phys. Sci. **193**: 120–145.

Pérez-Ruzafa, A., C. Marcos, and I. M. Pérez-Ruzafa. 2011. Mediterranean coastal lagoons in an ecosystem and aquatic resources management context. Phys. Chem. Earth Parts ABC **36**: 160–166. doi:10.1016/j.pce.2010.04.013

Peteiro, L. G., S. A. Woodin, D. S. Wethey, D. Costas-Costas, A. Martínez-Casal, C. Olabarria, and E. Vázquez. 2018. Responses to salinity stress in bivalves: Evidence of ontogenetic changes in energetic physiology on Cerastoderma edule. Sci. Rep. **8**: 8329.

Phillips, D. L., and J. W. Gregg. 2003. Source partitioning using stable isotopes: coping with too many sources. Oecologia **136**: 261–269. doi:10.1007/s00442-003-1218-3

Piló, D., A. B. Barbosa, M. A. Teodósio, and others. 2018. Are submarine groundwater discharges affecting the structure and physiological status of rocky intertidal communities? Mar. Environ. Res. **136**: 158–173. doi:10.1016/j.marenvres.2018.02.013

Pittendrigh, C. S., and S. Daan. 1976. A functional analysis of circadian pacemakers in nocturnal rodents. J. Comp. Physiol. **106**: 333–355. doi:10.1007/BF01417860

PNRNM. 2016. Observatoire des étangs. Parc Nat. Régional Narbonnaise En Méditerranée.

Posa, D., and A. Tursi. 1991. Growth Models of Mytilus galloprovincialis Lamarck on the Mar Grande and on the Mar Piccolo of Taranto (Southern Italy). Stat. Appl. **3**: 135–143.

Povinec, P. P., H. Bokuniewicz, W. C. Burnett, and others. 2008. Isotope tracing of submarine groundwater discharge offshore Ubatuba, Brazil: results of the

IAEA–UNESCO SGD project. J. Environ. Radioact. **99**: 1596–1610. doi:10.1016/j.jenvrad.2008.06.010

Pozzato, L., J. Rassmann, B. Lansard, J.-P. Dumoulin, P. van Breugel, and C. Rabouille. 2018. Origin of remineralized organic matter in sediments from the Rhone River prodelta (NW Mediterranean) traced by Δ14C and δ13C signatures of pore water DIC. Prog. Oceanogr. **163**: 112–122. doi:10.1016/j.pocean.2017.05.008

Prakash, R., K. Srinivasamoorthy, S. Gopinath, and K. Saravanan. 2018. Measurement of submarine groundwater discharge using diverse methods in Coleroon Estuary, Tamil Nadu, India. Appl. Water Sci. **8**: 13. doi:10.1007/s13201-018-0659-0

Precht, E., and M. Huettel. 2003. Advective pore-water exchange driven by surface gravity waves and its ecological implications. Limnol. Oceanogr. **48**: 1674–1684. doi:10.4319/lo.2003.48.4.1674

Purvaja, R., R. Ramesh, A. K. Ray, and T. Rixen. 2008. Nitrogen cycling: A review of the processes, transformations and fluxes in coastal ecosystems. Curr. Sci. **94**: 1419–1438.

Qiu, J.-W., R. Tremblay, and E. Bourget. 2002. Ontogenetic changes in hyposaline tolerance in the mussels Mytilus edulis and M. trossulus: implications for distribution. Mar. Ecol. Prog. Ser. **228**: 143–152. doi:10.3354/meps228143

Ragonese, S., S. Vitale, S. Mazzola, E. Pagliarino, and M. L. Bianchini. 2012. Behavior of some growth performance indexes for exploited Mediterranean hake. Acta Adriat. Int. J. Mar. Sci. **53**: 105–123.

Rahman, S., J. J. Tamborski, M. A. Charette, and J. K. Cochran. 2019. Dissolved silica in the subterranean estuary and the impact of submarine groundwater discharge on the global marine silica budget. Mar. Chem. **208**: 29–42. doi:10.1016/j.marchem.2018.11.006

Raimbault, P., N. Garcia, and F. Cerutti. 2008. Distribution of inorganic and organic nutrients in the South Pacific Ocean- evidence for long-term accumulation of organic matter in nitrogen-depleted waters. Biogeosciences **5**: 281–298.

Raimbault, P., G. Slawyk, B. Boudjellal, and others. 1999. Carbon and nitrogen uptake and export in the equatorial Pacific at 150°W: Evidence of an efficient regenerated production cycle. J. Geophys. Res. Oceans **104**: 3341–3356. doi:10.1029/1998JC900004

Ramón, M., M. Fernández, and E. Galimany. 2007. Development of mussel (Mytilus galloprovincialis) seed from two different origins in a semi-

enclosed Mediterranean Bay (N.E. Spain). Aquaculture **264**: 148–159. doi:10.1016/j.aquaculture.2006.11.014

Rao, A. M. F., M. J. McCarthy, W. S. Gardner, and R. A. Jahnke. 2008. Respiration and denitrification in permeable continental shelf deposits on the South Atlantic Bight: N2:Ar and isotope pairing measurements in sediment column experiments. Cont. Shelf Res. **28**: 602–613. doi:10.1016/j.csr.2007.11.007

Raven, J. A., A. M. Johnston, J. E. Kübler, and others. 2002. Mechanistic interpretation of carbon isotope discrimination by marine macroalgae and seagrasses. Funct. Plant Biol. **29**: 355–378.

Richardson, C. A. 1988. TIDALLY PRODUCED GROWTH BANDS IN THE SUBTIDAL BIVALVE SPISULA SUBTRUNCATA (DA COSTA). J. Molluscan Stud. **54**: 71–82. doi:10.1093/mollus/54.1.71

Richardson, C. A. 1989. An Analysis of the Microgrowth Bands in the Shell of the Common Mussel Mytilus Edulis. J. Mar. Biol. Assoc. U. K. **69**: 477–491. doi:10.1017/S0025315400029544

Rigaud, S., O. Radakovitch, R.-M. Couture, B. Deflandre, D. Cossa, C. Garnier, and J.-M. Garnier. 2013. Mobility and fluxes of trace elements and nutrients at the sediment–water interface of a lagoon under contrasting water column oxygenation conditions. Appl. Geochem. **31**: 35–51. doi:10.1016/j.apgeochem.2012.12.003

Riisgård, H. U., L. Bøttiger, and D. Pleissner. 2012. Effect of Salinity on Growth of Mussels, Mytilus edulis, with Special Reference to Great Belt (Denmark). Open J. Mar. Sci. **02**: 167. doi:10.4236/ojms.2012.24020

Rodellas, V., J. Garcia-Orellana, E. Garcia-Solsona, P. Masqué, J. A. Domínguez, B. J. Ballesteros, M. Mejías, and M. Zarroca. 2012. Quantifying groundwater discharge from different sources into a Mediterranean wetland by using 222Rn and Ra isotopes. J. Hydrol. **466–467**: 11–22. doi:10.1016/j.jhydrol.2012.07.005

Rodellas, V., J. Garcia-Orellana, P. Masqué, M. Feldman, and Y. Weinstein. 2015. Submarine groundwater discharge as a major source of nutrients to the Mediterranean Sea. Proc. Natl. Acad. Sci. **112**: 3926–3930. doi:10.1073/pnas.1419049112

Rodellas, V., J. Garcia-Orellana, A. Tovar-Sánchez, G. Basterretxea, J. M. López-Garcia, D. Sánchez-Quiles, E. Garcia-Solsona, and P. Masqué. 2014a. Submarine groundwater discharge as a source of nutrients and trace metals in a Mediterranean bay (Palma Beach, Balearic Islands). Mar. Chem. **160**: 56–66. doi:10.1016/j.marchem.2014.01.007

Rodellas, V., J. Garcia-Orellana, A. Tovar-Sánchez, G. Basterretxea, J. M. López-Garcia, D. Sánchez-Quiles, E. Garcia-Solsona, and P. Masqué. 2014b. Submarine groundwater discharge as a source of nutrients and trace metals in a Mediterranean bay (Palma Beach, Balearic Islands). Mar. Chem. **160**: 56–66. doi:10.1016/j.marchem.2014.01.007

Rodellas, V., J. Garcia-Orellana, G. Trezzi, P. Masqué, T. C. Stieglitz, H. Bokuniewicz, J. K. Cochran, and E. Berdalet. 2017. Using the radium quartet to quantify submarine groundwater discharge and porewater exchange. Geochim. Cosmochim. Acta **196**: 58–73. doi:10.1016/j.gca.2016.09.016

Rodellas, V., T. C. Stieglitz, A. Andrisoa, P. G. Cook, P. Raimbault, J. J. Tamborski, P. van Beek, and O. Radakovitch. 2018. Groundwater-driven nutrient inputs to coastal lagoons: The relevance of lagoon water recirculation as a conveyor of dissolved nutrients. Sci. Total Environ. **642**: 764–780. doi:10.1016/j.scitotenv.2018.06.095

Roskosch, A., N. Hette, M. Hupfer, and J. Lewandowski. 2012. Alteration of Chironomus plumosus ventilation activity and bioirrigation-mediated benthic fluxes by changes in temperature, oxygen concentration, and seasonal variations. Freshw. Sci. **31**: 269–281. doi:10.1899/11-043.1

Ruiz, M., and J. Velasco. 2009. Nutrient Bioaccumulation in Phragmites australis: Management Tool for Reduction of Pollution in the Mar Menor. Water. Air. Soil Pollut. **205**: 173. doi:10.1007/s11270-009-0064-2

Sadat-Noori, M., I. R. Santos, D. R. Tait, and D. T. Maher. 2016. Fresh meteoric versus recirculated saline groundwater nutrient inputs into a subtropical estuary. Sci. Total Environ. **566–567**: 1440–1453. doi:10.1016/j.scitotenv.2016.06.008

Santiago, L. S., K. Silvera, J. L. Andrade, and T. E. Dawson. 2017. Functional strategies of tropical dry forest plants in relation to growth form and isotopic composition. Environ. Res. Lett. **12**: 115006. doi:10.1088/1748-9326/aa8959

Santos, I. R., K. R. Bryan, C. A. Pilditch, and D. R. Tait. 2014. Influence of porewater exchange on nutrient dynamics in two New Zealand estuarine intertidal flats. Mar. Chem. **167**: 57–70. doi:10.1016/j.marchem.2014.04.006

Santos, I. R., W. C. Burnett, T. Dittmar, I. G. N. A. Suryaputra, and J. Chanton. 2009. Tidal pumping drives nutrient and dissolved organic matter dynamics in a Gulf of Mexico subterranean estuary. Geochim. Cosmochim. Acta **73**: 1325–1339. doi:10.1016/j.gca.2008.11.029

Santos, I. R., B. D. Eyre, and M. Huettel. 2012a. The driving forces of porewater and groundwater flow in permeable coastal sediments: A review. Estuar. Coast. Shelf Sci. **98**: 1–15. doi:10.1016/j.ecss.2011.10.024

Santos, I. R., D. T. Maher, and B. D. Eyre. 2012b. Coupling Automated Radon and Carbon Dioxide Measurements in Coastal Waters. Environ. Sci. Technol. **46**: 7685–7691. doi:10.1021/es301961b

Santos, I. R., F. Niencheski, W. Burnett, and others. 2008. Tracing anthropogenically driven groundwater discharge into a coastal lagoon from southern Brazil. J. Hydrol. **353**: 275–293. doi:10.1016/j.jhydrol.2008.02.010

Santos Isaac R., Cook Perran L. M., Rogers Louissa, Weys Jason de, and Eyre Bradley D. 2012. The "salt wedge pump": Convection-driven pore-water exchange as a source of dissolved organic and inorganic carbon and nitrogen to an estuary. Limnol. Oceanogr. **57**: 1415–1426. doi:10.4319/lo.2012.57.5.1415

Sarà, G., G. K. Reid, A. Rinaldi, V. Palmeri, M. Troell, and S. A. L. M. Kooijman. 2012. Growth and reproductive simulation of candidate shellfish species at fish cages in the Southern Mediterranean: Dynamic Energy Budget (DEB) modelling for integrated multi-trophic aquaculture. Aquaculture **324–325**: 259–266. doi:10.1016/j.aquaculture.2011.10.042

Sato, S. 1997. Shell microgrowth patterns of bivalves reflecting seasonal change in phytoplankton abundance. Paleontol. Res. **1**: 260–266.

Schöne, B. ., K. . Flessa, D. . Dettman, and D. . Goodwin. 2003a. Upstream dams and downstream clams: growth rates of bivalve mollusks unveil impact of river management on estuarine ecosystems (Colorado River Delta, Mexico). Estuar. Coast. Shelf Sci. **58**: 715–726. doi:10.1016/S0272-7714(03)00175-6

Schöne, B. R. 2008. The curse of physiology—challenges and opportunities in the interpretation of geochemical data from mollusk shells. Geo-Mar. Lett. **28**: 269–285. doi:10.1007/s00367-008-0114-6

Schöne, B. R., E. Dunca, J. Fiebig, and M. Pfeiffer. 2005a. Mutvei's solution: An ideal agent for resolving microgrowth structures of biogenic carbonates. Palaeogeogr. Palaeoclimatol. Palaeoecol. **228**: 149–166. doi:10.1016/j.palaeo.2005.03.054

Schöne, B. R., A. D. Freyre Castro, J. Fiebig, S. D. Houk, W. Oschmann, and I. Kröncke. 2004. Sea surface water temperatures over the period 1884–1983 reconstructed from oxygen isotope ratios of a bivalve mollusk shell (Arctica islandica, southern North Sea). Palaeogeogr. Palaeoclimatol. Palaeoecol. **212**: 215–232. doi:10.1016/j.palaeo.2004.05.024

Schöne, B. R., D. H. Goodwin, K. W. Flessa, D. L. Dettman, and P. D. Roopnarine. 2002. Sclerochronology and growth of the bivalve mollusks Chione (Chionista) fluctifraga and C. (Chionista) cortezi in the northern Gulf of California, Mexico. Veliger **45**: 45–54.

Schöne, B. R., S. D. Houk, A. D. Freyre Castro, J. Fiebig, W. Oschmann, I. Kroncke, W. Dreyer, and F. Gosselck. 2005b. Daily Growth Rates in Shells of Arctica islandica: Assessing Sub-seasonal Environmental Controls on a Long-lived Bivalve Mollusk. PALAIOS **20**: 78–92. doi:10.2110/palo.2003.p03-101

Schöne, B., K. Tanabe, D. L. Dettman, and S. Sato. 2003b. Environmental controls on shell growth rates and δ18O of the shallow-marine bivalve mollusk Phacosoma japonicum in Japan. Mar. Biol. **142**: 473–485.

Schöne, B., K. Tanabe, D. Dettman, and S. Sato. 2003c. Environmental controls on shell growth rates and δ18O of the shallow-marine bivalve mollusk Phacosoma japonicum in Japan. Mar. Biol. **142**: 473–485. doi:10.1007/s00227-002-0970-y

Schubert, M., A. Paschke, D. Bednorz, W. Bürkin, and T. Stieglitz. 2012a. Kinetics of the Water/Air Phase Transition of Radon and Its Implication on Detection of Radon-in-Water Concentrations: Practical Assessment of Different On-Site Radon Extraction Methods. Environ. Sci. Technol. **46**: 8945–8951. doi:10.1021/es3019463

Schubert, M., A. Paschke, E. Lieberman, and W. C. Burnett. 2012b. Air–Water Partitioning of ^{222} Rn and its Dependence on Water Temperature and Salinity. Environ. Sci. Technol. **46**: 3905–3911. doi:10.1021/es204680n

Schwarzenbach, R. P., P. M. Gschwend, and D. M. Imboden. 2002. Environmental Organic Chemistry, John Wiley & Sons.

Sekulic, B. 1996. Balance of Average Annual Fresh Water Inflow into the Adriatic Sea. Int. J. Water Resour. Dev. **12**: 89–98. doi:10.1080/713672198

Sholkovitz, E., C. Herbold, and M. Charette. 2003. An automated dye-dilution based seepage meter for the time-series measurement of submarine groundwater discharge. Limnol. Oceanogr. Methods **1**: 16–28. doi:10.4319/lom.2003.1.16

Short, F. T., and D. M. Burdick. 1996. Quantifying eelgrass habitat loss in relation to housing development and nitrogen loading in Waquoit Bay, Massachusetts. Estuaries **19**: 730–739. doi:10.2307/1352532

Sieyes, N. R. de, K. M. Yamahara, B. A. Layton, E. H. Joyce, and A. B. Boehm. 2008. Submarine discharge of nutrient-enriched fresh groundwater at Stinson Beach, California is enhanced during neap tides. Limnol. Oceanogr. **53**: 1434–1445. doi:10.4319/lo.2008.53.4.1434

Sigman, D. M., M. A. Altabet, R. Michener, D. C. McCorkle, B. Fry, and R. M. Holmes. 1997. Natural abundance-level measurement of the nitrogen isotopic composition of oceanic nitrate: an adaptation of the ammonia diffusion method. Mar. Chem. **57**: 227–242.

Siokou-Frangou, I., U. Christaki, M. G. Mazzocchi, M. Montresor, M. Ribera d'Alcalá, D. Vaqué, and A. Zingone. 2010. Plankton in the open Mediterranean Sea: a review. Biogeosciences **7**: 1543–1586. doi:https://doi.org/10.5194/bg-7-1543-2010

Slomp, C. P., and P. Van Cappellen. 2004. Nutrient inputs to the coastal ocean through submarine groundwater discharge: controls and potential impact. J. Hydrol. **295**: 64–86. doi:10.1016/j.jhydrol.2004.02.018

Smith, C. G., J. E. Cable, J. B. Martin, and M. Roy. 2008. Evaluating the source and seasonality of submarine groundwater discharge using a radon-222 pore water transport model. Earth Planet. Sci. Lett. **273**: 312–322. doi:10.1016/j.epsl.2008.06.043

Sospedra, J., L. F. H. Niencheski, S. Falco, C. F. F. Andrade, K. K. Attisano, and M. Rodilla. 2018. Identifying the main sources of silicate in coastal waters of the Southern Gulf of Valencia (Western Mediterranean Sea). Oceanologia **60**: 52–64. doi:10.1016/j.oceano.2017.07.004

Stachowicz, J. J., J. R. Terwin, R. B. Whitlatch, and R. W. Osman. 2002. Linking climate change and biological invasions: Ocean warming facilitates nonindigenous species invasions. Proc. Natl. Acad. Sci. **99**: 15497–15500. doi:10.1073/pnas.242437499

Stieglitz, T. 2005. Submarine groundwater discharge into the near-shore zone of the Great Barrier Reef, Australia. Mar. Pollut. Bull. **51**: 51–59. doi:10.1016/j.marpolbul.2004.10.055

Stieglitz, T. C., P. van Beek, M. Souhaut, and P. G. Cook. 2013. Karstic groundwater discharge and seawater recirculation through sediments in shallow coastal Mediterranean lagoons, determined from water, salt and radon budgets. Mar. Chem. **156**: 73–84. doi:10.1016/j.marchem.2013.05.005

Stieglitz, T. C., P. G. Cook, and W. C. Burnett. 2010. Inferring coastal processes from regional-scale mapping of 222Radon and salinity: examples from the Great Barrier Reef, Australia. J. Environ. Radioact. **101**: 544–552. doi:10.1016/j.jenvrad.2009.11.012

Stieglitz, T., M. Taniguchi, and S. Neylon. 2008. Spatial variability of submarine groundwater discharge, Ubatuba, Brazil. Estuar. Coast. Shelf Sci. **76**: 493–500. doi:10.1016/j.ecss.2007.07.038

Street, J. H., K. L. Knee, E. E. Grossman, and A. Paytan. 2008. Submarine groundwater discharge and nutrient addition to the coastal zone and

coral reefs of leeward Hawai'i. Mar. Chem. **109**: 355–376. doi:10.1016/j.marchem.2007.08.009

Sundareshwar, P. V., J. T. Morris, E. K. Koepfler, and B. Fornwalt. 2003. Phosphorus Limitation of Coastal Ecosystem Processes. Science **299**: 563–565. doi:10.1126/science.1079100

Sylaios, G. K., V. A. Tsihrintzis, C. Akratos, and K. Haralambidou. 2006. Quantification of water, salt and nutrient exchange processes at the mouth of a Mediterranean coastal lagoon. Environ. Monit. Assess. **119**: 275–301. doi:10.1007/s10661-005-9026-3

Syrett, P. J. 1981. Nitrogen metabolism of microalgae. Can. Bull. Fish. Aquat. Sci.

Szymczycha, B., and J. Pempkowiak. 2015. The Role of Submarine Groundwater Discharge as Material Source to the Baltic Sea, Springer.

Tabari, H., and P. Willems. 2018. Seasonally varying footprint of climate change on precipitation in the Middle East. Sci. Rep. **8**: 4435. doi:10.1038/s41598-018-22795-8

Tait, D. R., D. V. Erler, I. R. Santos, T. J. Cyronak, U. Morgenstern, and B. D. Eyre. 2014. The influence of groundwater inputs and age on nutrient dynamics in a coral reef lagoon. Mar. Chem. **166**: 36–47. doi:10.1016/j.marchem.2014.08.004

Tamborski, J., S. Bejannin, J. Garcia-Orellana, and others. 2018. A comparison between water circulation and terrestrially-driven dissolved silica fluxes to the Mediterranean Sea traced using radium isotopes. Geochim. Cosmochim. Acta **238**: 496–515. doi:10.1016/j.gca.2018.07.022

Tamborski, J. J., J. K. Cochran, and H. J. Bokuniewicz. 2017. Submarine groundwater discharge driven nitrogen fluxes to Long Island Sound, NY: Terrestrial vs. marine sources. Geochim. Cosmochim. Acta **218**: 40–57. doi:10.1016/j.gca.2017.09.003

Tamborski, J. J., A. D. Rogers, H. J. Bokuniewicz, J. K. Cochran, and C. R. Young. 2015. Identification and quantification of diffuse fresh submarine groundwater discharge via airborne thermal infrared remote sensing. Remote Sens. Environ. **171**: 202–217. doi:10.1016/j.rse.2015.10.010

Tanabe, K. 2007. Age and growth rate determinations of an intertidal bivalve, Phacosoma japonicum, using internal shell increments. Lethaia **21**: 231–241. doi:10.1111/j.1502-3931.1988.tb02075.x

Taniguchi, M., W. C. Burnett, J. E. Cable, and J. V. Turner. 2002. Investigation of submarine groundwater discharge. Hydrol. Process. **16**: 2115–2129. doi:10.1002/hyp.1145

Taniguchi, M., and Y. Fukuo. 1993. Continuous Measurements of Ground-Water Seepage Using an Automatic Seepage Meter. Groundwater **31**: 675–679. doi:10.1111/j.1745-6584.1993.tb00601.x

Taniguchi, M., T. Ishitobi, and J. Shimada. 2006. Dynamics of submarine groundwater discharge and freshwater-seawater interface. J. Geophys. Res. Oceans **111**. doi:10.1029/2005JC002924

Tomanek, null, and null Somero. 1999. Evolutionary and acclimation-induced variation in the heat-shock responses of congeneric marine snails (genus Tegula) from different thermal habitats: implications for limits of thermotolerance and biogeography. J. Exp. Biol. **202**: 2925–2936.

Tovar-Sánchez, A., G. Basterretxea, V. Rodellas, and others. 2014. Contribution of Groundwater Discharge to the Coastal Dissolved Nutrients and Trace Metal Concentrations in Majorca Island: Karstic vs Detrital Systems. Environ. Sci. Technol. **48**: 11819–11827. doi:10.1021/es502958t

Tran, D., A. Nadau, G. Durrieu, P. Ciret, J.-P. Parisot, and J.-C. Massabuau. 2011. Field chronobiology of a molluscan bivalve: how the moon and sun cycles interact to drive oyster activity rhythms. Chronobiol. Int. **28**: 307–317. doi:10.3109/07420528.2011.565897

Tréguer, P. J., and C. L. De La Rocha. 2013. The World Ocean Silica Cycle. Annu. Rev. Mar. Sci. **5**: 477–501. doi:10.1146/annurev-marine-121211-172346

Trezzi, G., J. Garcia-Orellana, J. Santos-Echeandía, V. Rodellas, E. Garcia-Solsona, G. Garcia-Fernandez, and P. Masqué. 2016. The influence of a metal-enriched mining waste deposit on submarine groundwater discharge to the coastal sea. Mar. Chem. **178**: 35–45. doi:10.1016/j.marchem.2015.12.004

Troccoli-Ghinaglia, L., J. A. Herrera-Silveira, F. A. Comín, and J. R. Díaz-Ramos. 2010. Phytoplankton community variations in tropical coastal area affected where submarine groundwater occurs. Cont. Shelf Res. **30**: 2082–2091. doi:10.1016/j.csr.2010.10.009

Trommer, G., A. Leynaert, C. Klein, A. Naegelen, and B. Beker. 2013. Phytoplankton phosphorus limitation in a North Atlantic coastal ecosystem not predicted by nutrient load. J. Plankton Res. **35**: 1207–1219. doi:10.1093/plankt/fbt070

Tseng, L. Y., A. K. Robinson, X. Zhang, and others. 2016. Identification of Preferential Paths of Fossil Carbon within Water Resource Recovery Facilities via Radiocarbon Analysis. Environ. Sci. Technol. **50**: 12166–12178. doi:10.1021/acs.est.6b02731

Ullman, W. J., and R. C. Aller. 1982. Diffusion coefficients in nearshore marine sediments1. Limnol. Oceanogr. **27**: 552–556. doi:10.4319/lo.1982.27.3.0552

Utsunomiya, T., M. Hata, R. Sugimoto, and others. 2017. Higher species richness and abundance of fish and benthic invertebrates around submarine groundwater discharge in Obama Bay, Japan. J. Hydrol. Reg. Stud. **11**: 139–146. doi:10.1016/j.ejrh.2015.11.012

Valiela, I., and J. E. Costa. 1988. Eutrophication of Buttermilk Bay, a Cape Cod coastal embayment: concentrations of nutrients and watershed nutrient budgets. Environ. Manage. **12**: 539–553.

Valiela, I., J. Costa, K. Foreman, J. M. Teal, B. Howes, and D. Aubrey. 1990a. Transport of groundwater-borne nutrients from watersheds and their effects on coastal waters. Biogeochemistry **10**: 177–197.

Valiela, I., J. Costa, K. Foreman, J. M. Teal, B. Howes, and D. Aubrey. 1990b. Transport of groundwater-borne nutrients from watersheds and their effects on coastal waters. Biogeochemistry **10**: 177–197.

Valiela, I., K. Foreman, M. LaMontagne, and others. 1992. Couplings of watersheds and coastal waters: sources and consequences of nutrient enrichment in Waquoit Bay, Massachusetts. Estuaries **15**: 443–457.

Viaroli, P., M. Bartoli, G. Giordani, M. Naldi, S. Orfanidis, and J. M. Zaldivar. 2008. Community shifts, alternative stable states, biogeochemical controls and feedbacks in eutrophic coastal lagoons: a brief overview. Aquat. Conserv. Mar. Freshw. Ecosyst. **18**: S105–S117. doi:10.1002/aqc.956

Vizzini, S., and A. Mazzola. 2003. Seasonal variations in the stable carbon and nitrogen isotope ratios (13C/12C and 15N/14N) of primary producers and consumers in a western Mediterranean coastal lagoon. Mar. Biol. **142**: 1009–1018. doi:10.1007/s00227-003-1027-6

Vizzini, S., B. Savona, M. Caruso, A. Savona, and A. Mazzola. 2005. Analysis of stable carbon and nitrogen isotopes as a tool for assessing the environmental impact of aquaculture: a case study from the western Mediterranean. Aquac. Int. **13**: 157–165. doi:10.1007/s10499-004-9023-5

Voss, M., A. Baker, S. E. Cornell, and others. 2011. Nitrogen processes in coastal and marine ecosystems. Eur. Nitrogen Assess. Sources Eff. Policy Perspect. 147–176.

Vuorinen, I., A. E. Antsulevich, and N. V. Maximovich. 2002. Spatial distribution and growth of the common mussel Mytilus edulis L. in the archipelago of SW-Finland, northern Baltic Sea. Boreal Environ. Res. **7**: 41–52.

Vural, P., H. Yildiz, and S. Acarli. 2015. Growth and survival performances of Mediterranean mussel (Mytilus galloprovincialis, Lamarck, 1819) on different depths in Cardak lagoon, Dardanelles. 6.

Walker, J. 1996. Fast Fourier Transforms. CRC Press.

Wang, H., M. Dai, J. Liu, and others. 2016. Eutrophication-Driven Hypoxia in the East China Sea off the Changjiang Estuary. Environ. Sci. Technol. **50**: 2255–2263. doi:10.1021/acs.est.5b06211

Wanninkhof, R. 2014. Relationship between wind speed and gas exchange over the ocean revisited. Limnol. Oceanogr. Methods **12**: 351–362. doi:10.4319/lom.2014.12.351

Weinstein, Y., Y. Yechieli, Y. Shalem, W. C. Burnett, P. W. Swarzenski, and B. Herut. 2011. What Is the Role of Fresh Groundwater and Recirculated Seawater in Conveying Nutrients to the Coastal Ocean? Environ. Sci. Technol. **45**: 5195–5200. doi:10.1021/es104394r

Welch, P. 1967. The use of fast Fourier transform for the estimation of power spectra: A method based on time averaging over short, modified periodograms. IEEE Trans. Audio Electroacoustics **15**: 70–73. doi:10.1109/TAU.1967.1161901

Welsh, D. T. 2000. Nitrogen fixation in seagrass meadows: regulation, plant–bacteria interactions and significance to primary productivity. Ecol. Lett. **3**: 58–71.

Wilke, M., and H. Boutière. 2000. Synthèse générale du fonctionnement hydrobiologique de l'étang de La Palme. CEH Perpignan Fr.

Wilson, J., and C. Rocha. 2012. Regional scale assessment of Submarine Groundwater Discharge in Ireland combining medium resolution satellite imagery and geochemical tracing techniques. Remote Sens. Environ. **119**: 21–34. doi:10.1016/j.rse.2011.11.018

Witbaard, R., M. I. Jenness, K. Van Der Borg, and G. Ganssen. 1994. Verification of annual growth increments in Arctica islandica L. from the North Sea by means of oxygen and carbon isotopes. Neth. J. Sea Res. **33**: 91–101. doi:10.1016/0077-7579(94)90054-X

Yang, T., S.-Y. Jiang, J.-H. Yang, G. Lu, N.-Y. Wu, J. Liu, and D.-H. Chen. 2008. Dissolved inorganic carbon (DIC) and its carbon isotopic composition in sediment pore waters from the Shenhu area, northern South China Sea. J. Oceanogr. **64**: 303–310. doi:10.1007/s10872-008-0024-2

Yildiz, H., Palaz, Mustafa, and Bulut, Musa. 2006. Condition indices of Mediterranean Mussels growing on suspended ropes in Dardanelles. J. Food Technol. 221–224.

Zaldibar, B., I. Cancio, and I. Marigómez. 2004. Circatidal variation in epithelial cell proliferation in the mussel digestive gland and stomach. Cell Tissue Res. **318**: 395–402. doi:10.1007/s00441-004-0960-0

Zalewski, M. 2002. Ecohydrology—the use of ecological and hydrological processes for sustainable management of water resources / Ecohydrologie—la prise en compte de processus écologiques et hydrologiques pour la gestion durable des ressources en eau. Hydrol. Sci. J. **47**: 823–832. doi:10.1080/02626660209492986

Zhao, Y., X. Xia, and Z. Yang. 2013. Growth and nutrient accumulation of Phragmites australis in relation to water level variation and nutrient loadings in a shallow lake. J. Environ. Sci. **25**: 16–25. doi:10.1016/S1001-0742(12)60004-7

Zheng, Z.-L. 2009. Carbon and nitrogen nutrient balance signaling in plants. Plant Signal. Behav. **4**: 584–591. doi:10.4161/psb.4.7.8540

Zieman, J. C., S. A. Macko, and A. L. Mills. 1984. Role of Seagrasses and Mangroves in Estuarine Food Webs: Temporal and Spatial Changes in Stable Isotope Composition and Amino Acid Content During Decomposition. Bull. Mar. Sci. **35**: 380–392.

Župan, I., and Šarić. 2014. Growth and condition index – two important factors in mussel farming. Meso Prvi Hrvat. Časopis O Mesu **XVI**: 275, 255–278, 259.